



UNIVERSITAT_{DE}
BARCELONA

Functional analysis of a phloem cysteine protease in *Arabidopsis thaliana*

Eugenia Pitsili



Aquesta tesi doctoral està subjecta a la llicència **Reconeixement- NoComercial – Compartir Igual 4.0. Espanya de Creative Commons.**

Esta tesis doctoral está sujeta a la licencia **Reconocimiento - NoComercial – Compartir Igual 4.0. España de Creative Commons.**

This doctoral thesis is licensed under the **Creative Commons Attribution-NonCommercial-ShareAlike 4.0. Spain License.**

UNIVERSITAT DE BARCELONA

FACULTAT DE FARMÀCIA I CIÈNCIES DE L'ALIMENTACIÓ

(Supervisor : Núria Sánchez Coll)

Functional analysis of a phloem cysteine
protease in *Arabidopsis thaliana*

Eugenia Pitsili

Barcelona, September 2021

UNIVERSITAT DE BARCELONA

FACULTAT DE FARMÀCIA I CIÈNCIES DE L'ALIMENTACIÓ

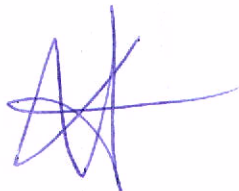
PROGRAMA DE DOCTORAT: BIOTEKNOLOGIA

Functional analysis of a phloem
cysteine protease in *Arabidopsis*
thaliana

Memòria presentada per Eugenia Pitsili per optar al títol de doctor per la
Universitat de Barcelona

Directora de la tesis

Núria Sánchez Coll



Tutor de la tesis

Marc Valls i Matheu



Doctoranda

Eugenia Pitsili



Acknowledgments

So I have finally finished the PhD after 4 (almost 5) years, years that seem to have passed extremely fast... years that changed my life, make me more mature as a person and as a scientist. 4 years that I was doing what I really love most importantly, I travelled, I meet new people, I gain new experiences, I got depressed, happy, stressed, angry, laughed with my heart, I had failures and success. There were times that I was disappointed, others that I was just tired but above all I had amazing moments of happiness. This time in my life that I was thinking it was going to be hard and difficult, it turned out to be the best so far. For all these I owe a lot to many people that I would like to thank.

To Marc and Nuria

The fact that I am standing here now, I owe it to Nuria that gave me the opportunity to accomplish this thesis. Thank you for trusting me and helping me in my good days but also when things were not "smooth". Along with Marc, you have been both mentors and tutors in this journey, helping us day by day to find our way and learn how to be confident, to speak our mind and be patient.

To Biobact lab

I don't know how I can thank you enough for being there for me. We spend so much time together every day ended up seeing you more than my actual family. Joselito, thank you for showing me how to do co-IPs, giving me useful ideas when I was stuck and improve my taste in food! I will never forget your dedication to find the best burger in Barcelona and your exceptional cheesecake and pizzas. Nerea with the amazing dresses, I am so glad another girl came in the lab and I was not alone with the boys, thank you for all your help, for the conversations, for making us think about the environment. Roger, my dear hacker! Without you I would be crying in front of the computer screen. You helped me see that is not my enemy! I am grateful for all the help that you also gave me apart from the programming part, for collecting seeds and taking care of my plants when I was abandoning them and most importantly for supporting me. Such a loving character! Weiqi, it was a pleasure to meet you, working next to you, learning about the Chinese food and culture. You are my favourite to tease, you know that! Ben, Fernando you are the seniors that are remaining, take care of the rest! Sofia, Jenna, Alvaro, Marta, Joel also I am extremely I have the opportunity to spend time with you and laugh as much as possible! All the students that spend a short or a long time next to me, I hope you learned something as I learned from you how to be a better supervisor (Thank you Laia, Joana and Alex). For

the newest people in the lab that we didn't have the time to interact that much, I will say to do their best to keep the bonds of the people, it's a real strength to have them!

To ex-members of the lab

These people! My people! With some we spend less and with some more time together working. Some finished the PhD a few months ago and I am so proud of you. I am grateful that I met you, I can say that I consider your friendship a great gift and I am not sad that we are not all together anymore because wherever you will go I know I have a friend there to visit! Marina, Saul, Marc, Anurag, Alex I will try my best to do this trip with all of you in India. We started a tradition and it has to continue. Pau, especially you, thank you for everything, for being my best friend, for having this weird incredible mind, for supporting me. I love you all! Ujjal, Liang Li, Liang Y., it was a fantastic journey, thank you for being there and sharing moments and experiences with me. I will always remember you and I wish we will meet again. Good luck in whatever you decide to do.

CRAG friends

During these years I met a lot of people, coming and going, CRAG was always changing. I want to specially thank my girls, Ornella, Bea and Aida for being my friends in these years. I will not forget the beers after work, the video calls during the COVID confinement, the coffees to discuss and complain, the breakfasts! The most adorable person ever met, Salva, my friend with a thousand faces! What to thank you for first I don't know, I love you! Also Jorge Fung, thank you for showing me your loving side, for being my friend, for the countless invitations to see you, I will come I promise! Luis Galliego, what a scientist, what a professional, what a problem solver! Nacho kamilopardali, you are a wonderful person and friend, I have learned so many things from you, thank you for being next door, it was a pleasure listening to your loud voice as I am sure you could listen mine. I cannot exclude here my friends on the second floor, Vicky, Miguel, Miguelon and mi flor Rosa! You are amazing, we shared so many nice things together, barbeques, beers, our worries, our happiness! Special thanks also to Juan, Fidel and Ivan that are the people always willing to go for a beer after work that made my life so much easier!

All the people that we interacted and were there for small and big things, for helping in their own way, for even making the environment friendly, is important to keep the good mood to be able to pass this time of our lives. Also I would like to thank the people from CRAG services, from greenhouse to technical support, the HR and the people in the entrance for all the help and the chats that we were having. Keep up the good work!

I think is essential to include here the colleagues from my two stays in Zurich in Antia's laboratory. It was very critical the time that I had there, thank you for your help, your advice, your propositions. Bojan, Tiago, Elizabeth and Anna especially that we interacted more, I

hope we will see each other again and I wish you all the best. Specially I would like to mention Antia, who accepted me in her lab, gave me the opportunity to learn from her and make comments for the project. It was really valuable and I am extremely grateful.

I am also grateful to people that we collaborated and exchange material. Michael Holdsworth, Fabien Nogué, Sergi Munné, Pitter Huesgen and the laboratory of Van Breusegem.

My friends at home

I cannot forget at this point all my friends from Greece (and not only) that are next to me all these years. Babis, Sasa, Aris and many many more, we have taken different paths but I am grateful for all your support to whatever I am doing no matter how far we are. Ilectra, my best friend, my sister, I am extremely happy that we managed to find a date for your wedding to suit all of us! I wouldn't miss it for the world. You are my butterfly, my soul mate!

My family

A huge part of what I am today and where I have been I owe it to my parents and my sister. They grew me to be an independent person, learn how to believe in myself, be strong in every step that I took. They showed me that is very important to chase your dreams, respect the others, be grateful for what you have and never betray your principals and success will come with effort. I thank them because they made sacrifices to be able to offer me the education that I had (and is not a short period!), they were there every single time in happy and sad moments although in distance we were apart, they supported me mentally always. My family is the centre point for me, thank you for the unconditional love.

David...David is a chapter in my life that although he is not in favour of expressing feelings I cannot exclude a special thanks to him. We walked this path together, you were there holding my hand in this journey, receiving all these changes in my mood. I am sorry for my difficult character and thank you for not giving up on me.

At last, this thesis is devoted to my baby girl, Kari. She was my light, my life, my friend. The only thing she was interested in, was sleeping, eating, playing with the ball and make me happy. I thank her because she showed me that happiness is hidden in simple small little moments. I would trade the world to have you again next to me.

Synopsis

Metacaspases are a family of cysteine proteases found in lower eukaryotes and plants. They are considered to be distant relatives of caspases, present only in animals. The role of metacaspases is quite diverse, from developmental processes involved in tissue formation, to responses against pathogens and other environmental stresses. For some members of the family there is ongoing research regarding their function and possible substrates and for some others they have not been characterized.

In this study we attempted to functionally analyse *Arabidopsis thaliana* metacaspase 3 (MC3), an uncharacterized metacaspase which was found to be expressed in the vascular tissue. We considered that the best way to address this challenge was to use a reverse genetics approach in combination with proteomic analysis. In Chapter 2, we specifically identified the exact localization of the transcript and the protein *in planta*, we generated mutant plants using the CRISPR/Cas9 technology and we analysed their growth in basal conditions. Moreover, we performed a whole proteome analysis for different tissues and we attempted to identify candidate substrates by N-termini analysis. In Chapter 3, we delved into multiple stresses testing how plants with over-accumulation or lack of MC3 responded to stress conditions, since multiple proteins related to stress responses came up from the proteomic study.

In Chapter 2 we generated reporter lines to specify the exact localization of the gene expression. MC3 was found specifically expressed in the phloem vascular tissue. Furthermore, translational fusion to fluorescent proteins verified the same pattern for protein localization. Using multiple mutant lines, we performed an analysis of the phenotypes caused from the absence, malfunction or overexpression of the putative protease in the development of the plant. Overall growth and formation of the vascular tissue in particular, were not affected when plants were grown upon standard growth conditions. From previous studies, MC1 reporter lines exhibited expression in the stele in almost every developmental stage and MC4 has a high and ubiquitous expression in most of the tissues.

Double mutants were generated in order to exclude the possibility of functional redundancy and we showed that under normal conditions the overall growth of these plants remained similar to wild-type plants. Finally, we checked the total proteome of the plants to compare the differentially abundant proteins in different expression backgrounds. Overall, the analysis demonstrated that root tissue of MC3 overexpressor lines showed differential accumulation of stress related proteins, specifically osmotic and hypoxic related.

Metacaspases have been shown to participate amongst others, in the plant responses to biotic and abiotic stresses. In Chapter 3 we analyzed whether MC3 had a role in responses to different environmental stresses. We found that MC3 function is associated with drought stress, since plants overaccumulating MC3 were able to survive more and performed better under low water availability conditions. Moreover, compared to wild-type plants, *mc3* mutant appeared less sensitive to ABA, which is one of the hormones orchestrating drought responses. Considering that the vasculature plays a very important role in facilitating ABA signalling, we investigated vascular formation upon osmotic stress in plants with altered MC3 levels. Overexpressor lines showed a faster formation of the vascular tissue under osmotic stress conditions than wild type plants. Finally, we observed that in conditions of low oxygen concentrations, the excessive amount of MC3 can also be beneficial for plant survival. Additional stresses were tested in order to detect if MC3 function was specific of osmotic unbalances. Plants were not affected of the presence or absence of MC3 upon light and temperature altered conditions, neither upon infection with a vascular pathogen. In conclusion, we reported that metacaspase 3 is a phloem-specific metacaspase which contributes to drought tolerance possibly due to enhanced metaphloem vascular differentiation upon osmotic stress conditions.

Contents

Synopsis	9
Abbreviations	15
Chapter 1: General Introduction	
The world of Proteases- Cysteine proteases.....	19
Metacaspase Family	20
A. Arabidopsis metacaspases	22
B. Metacaspases in other species.....	25
Programmed Cell Death in Plant Development (dPCD)	27
Vascular tissues: The Phloem	30
A. Phloem Proteases.....	32
B. Developmental formation of phloem in Arabidopsis roots	34
A.1 Terminal differentiation of SEs	37
A.2 Supporting Companion Cells.....	41
Objectives	43
Chapter 2: Characterization of MC3 cysteine protease function in plant development	
Summary.....	47
Metacaspase 3 is a Type I metacaspase from <i>A. thaliana</i>	49
Localization of MC3 in the phloem vascular tissue.....	50
MC3 has a phloem specific gene expression pattern	50
MC3 protein is localized in the cytoplasm of the phloem vascular tissue..	54
Activation of the protease.....	58
Generation of mutants for the MC3 functional analysis	61
Different approaches to obtain <i>mc3</i> mutant lines.....	61

Redundancy with phloem proteases and metacaspase family proteins.....	63
Phenotypical Characterization of <i>mc3</i> mutants.....	68
Flowering time is not affected in <i>mc3</i> mutant plants.....	71
MC3 does not severely affect phloem formation.....	74
Proteome Analysis	79
Proteome Composition Analysis in Leaf tissue.....	80
N-terminome analysis	86
Proteomic Analysis in root tissue	90

Chapter 3: Identifying the role of metacaspase 3 upon environmental stresses

Summary	97
Promoter analysis shows transcription factor (TF) binding motifs related to stress responses	99
MC3 function upon Abiotic Stresses	103
Heat stress	103
Hypoxia	106
Drought.....	111
ABA sensitivity is reduced in <i>mc3</i> knock-out plants.....	116
Stress Responses related to ABA.....	125
Vascular formation occurs earlier upon osmotic stress in plants over-accumulating MC3	130

Chapter 4: General Discussion

Overview of the thesis.....	135
A metacaspase specifically localized in the phloem vascular tissue	135
A new role for metacaspases in osmotic stress conditions	139

MC3 overexpression leads to pre-mature metaphloem development upon osmotic stress	142
Over-accumulation of MC3 might enhance plant performance upon various stresses	144
Conclusions	149
Materials and Methods	
Generation of Genetic tools	153
DNA and RNA Analysis.....	158
Protein Analysis	161
Proteomics analysis	163
Imaging.....	166
Phenotyping Under Normal Conditions.....	167
Phenotyping Under Stress Conditions	169
Hormone Quantification	173
Statistical Analysis	173
Resumen en castellano	175
References	177
Annex	
PART 1	209
PART 2.....	211

Abbreviations

MC: Metacaspase
VPE: Vacuolar Processing Enzymes
PLCP: Papain Like Cysteine Protease
PCD: Programmed Cell Death
dPCD: Developmentally controlled PCD
ePCD: Environmentally triggered PCD
ER: Endoplasmic reticulum
GFP: Green fluorescent protein
PLCPs: Papain-like cysteine proteases
ROS: Reactive Oxygen Species
TE: Tracheary elements
SE: Sieve elements
PSE: Protophloem Sieve element
MSE: Metaphloem Sieve element
PPP: Protophloem Pericycle Pole
SP: Sieve Plate
PD: Plasmodesmata
QC: Quiescent centre
CC: Companion cells
SCW: Secondary Cell Wall
SAM: Shoot Apical Meristem
RAM: Root Apical Meristem
CA: Catalytic inactive
HR: Hypersensitive Response
TF: Transcription factor
Wt: Wild Type
OE: Overexpressor
ABA: Absisic Acid
GA: Gibberellic Acid
BR: Brassinosteroids
MS: Mass spectrometry

LC: Liquid chromatography

PTM: Post Translational Modification

LD: Long Day

SD: Short Day

PR: Primary Root

LR: Lateral Root

CHAPTER 1

General Introduction

Introduction

The world of Proteases- Cysteine proteases

Proteolytic enzymes encompass a large group with diversity in biochemical and regulatory characteristics. The protease superfamily is responsible for a variety of biological processes with proteases present from lower (virus, bacteria, and parasite) to higher organisms (animals). Proteases cleave protein substrates into smaller fragments by catalysing the hydrolysis of peptide bonds. These bonds can be either internal for endopeptidases, C-terminal (carboxypeptidases) or N- terminal (aminopeptidases) for exopeptidases (Barrett 1994). Due to the lack of substrate knowledge, the way to classify proteases is according to their catalytic site. In MEROPS they are distributed in five main catalytic classes: cysteine (C) proteases, serine (S) proteases, aspartic (A) proteases, threonine (T) proteases and metalloproteases (M) (Rawlings et al., 2018). Additionally, the database has subdivided the proteases into families and clans according to relationships formed through evolution. The Arabidopsis genome encodes over 800 proteases, which are distributed over almost 60 families (Van Der Hoorn 2008).

Proteolysis in plants affects many processes in development and in responses to variable environmental stimuli, being also crucial in keeping the cellular protein homeostasis and recycling of resources. Apart from the role of proteases in maturation of proteins and massive degradation, they also have important functions in signalling pathways by processing signalling molecules (Buono et al., 2019; Balakireva and Zamyatnin 2019; Liu et al., 2018; Salguero-Linares and Coll 2019). Cysteine proteases are named as mentioned above, from the common cysteine residue in their catalytic active site but regarding structure, they are quite diverse. In plants, they can be divided in 5 clans which is an evidence of divergent evolution. As an example, clans CA and CE contain proteases with a papain-like fold, whereas clan CD proteases have a caspase-like fold. Their function is spread in many different processes throughout plant

life, from programmed cell death in development and disease to regulation of tissue architectures and senescence.

The term proteolytic cascade refers to a biological event characterized by proteases that activate other proteases by processing. The tight regulation of their activation can be achieved with post-translational modifications, as they are in most of the cases produced as a zymogen. The N- or C-terminal inhibitory prodomain prevent premature activity of the proteases. Prodomains also contribute to the folding of the proteases (Bryan 2002) and often contain signals for subcellular targeting (Huete-Pérez et al., 1999). To be activated, they can perform auto cleavage in cis or trans, or another upstream protease from the same or completely different family is responsible to catalytically activate them. Most of the cysteine proteases show an enhanced activity under acidic pH (Jerala et al., 1998; Meyer et al., 2016; Zauner et al., 2018). These proteolytic signaling cascades are happening quickly and multiply the signal, taking advantage of constitutively expressed and highly selective proteases. Proteolytic cascades are common in the animal kingdom whereas in plants is quite elusive (Paulus and Van der Hoorn 2019).

Metacaspase Family

Metacaspases are a family of cysteine proteases found only in plants, fungi and protozoa. Along with orthocaspases, they were identified as containing a caspase- like fold structure (Klemenčič and Funk 2018a; Uren et al. 2000) that classifies them in the CD clan of cysteine proteases (Minina et al., 2017). The broad phylogenetic distribution of metacaspases and paracaspases across distinct kingdoms of life and the large variation of their biochemical and structural features complicate their classification. Recently, a universal nomenclature was proposed in the scientific community that unifies the way that are represented (Minina et al. 2020). Like animal caspases, metacaspases also have a catalytic histidine- cysteine dyad with the cysteine residue to function as the nucleophilic component for hydrolysis of the substrate peptide bond. They also contain the same hemoglobinase fold of caspases which gives them some structural

similarities. However, close structural comparison between these two families brought into light many differences that reveal different modes of action (Chang and Yang 2000; McLuskey and Mottram 2015; Watanabe and Lam 2005). The basic differences can be summarized in four main points:

- a) The substrate sequence preference is different. Caspases cleave after Aspartic acid residues (Earnshaw et al., 1999) and metacaspases show preference for cleavage after the basic residues Lysine and Arginine (Minina et al., 2017; Salvesen et al., 2016; Vercammen et al., 2004; Watanabe and Lam 2005).
- b) Caspase inhibitors have been used to block metacaspase enzymatic activity but not successfully and metacaspases failed to cleave caspases substrates.
- c) Metacaspases due to their structure function as monomers compare to the dimerization that has been observed in caspases (Salvesen et al., 2016).
- d) Most of the metacaspases have shown dependency on Ca^{2+} for their activation (exception of AtMC9) (Bozhkov et al. 2005; Vercammen et al. 2004; Watanabe and Lam 2005, 2011; Zhu et al. 2020).

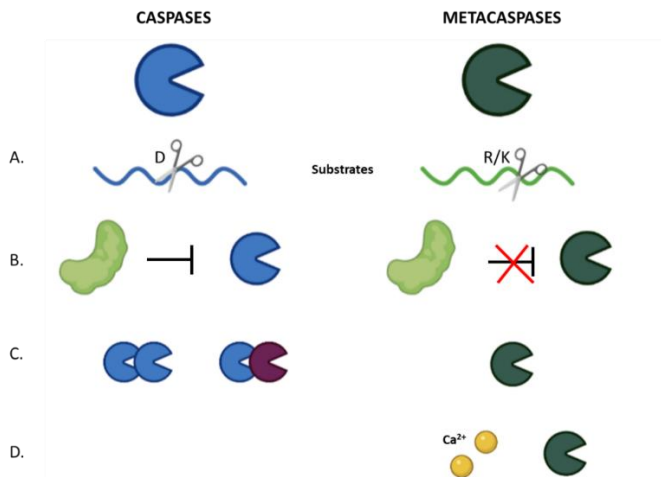


Figure 1.1: Basic differences between caspase and metacaspase family. Amino acids indicated: D Aspartic Acid, R Arginine, K Lysine.

The metacaspase family can be divided in 3 subgroups according to their structural arrangement their domains: Type I, II and III. Type I metacaspases contain the conserved p20 and p10 catalytic domains similar to caspases but also an additional N- terminal prodomain with proline or glutamate- rich repeat and in some cases a zinc- finger motif which is lacking from type II metacaspases. Type II metacaspases lack the N-terminal prodomain and have an extended linker region of ~150 aa between the catalytic p20 and p10 domains (Vercammen et al. 2004). Type III metacaspases are quite different, bearing only the p20 and p10 domains but in reverse position with p20 to be in the C –terminal (Choi and Berges 2013; Klemenčič and Funk 2018b). Type I can be found from Proteobacteria to plants, type II are more restricted in plants and algae and type III have been identified in haptophyta, cryptophyta and heterokontophyta (including diatoms). All types seem to depend on calcium for their function with some exceptions like *Arabidopsis AtMC9* that has a pH rather than a calcium dependent activity (Klemenčič and Funk 2019; Watanabe and Lam 2011; Zhang and Lam 2011). Alteration of pH intracellularly and increase of Ca^{2+} is a common consequence of stress conditions which can explain the fulfilment of the conditions needed to activate metacaspases. In type II MCs the higher Ca^{2+} concentration promotes their activation by cleavage between the p20 and p10 domain in the linker region while in some type I MCs the prodomain must be cleaved for protein activation (Coll et al., 2010, 2014; Hander et al., 2019; Vercammen et al., 2004). In yeast it has been shown that the prodomain of type-I metacaspases is important for formation of protein aggregates (Lee et al. 2010). Like caspases, metacaspases and paracaspases are multifunctional proteins regulating diverse biological phenomena, such as aging, immunity, proteostasis, and programmed cell death (PCD) (Minina et al., 2017; Tsiatsiani et al., 2011).

A. *Arabidopsis* metacaspases

In the model plant *Arabidopsis thaliana*, 9 metacaspases have been identified; *AtMC1-3*, which are type I and *AtMC4-9*, which are type II (Uren et al. 2000). According to the new established nomenclature they are *AtMCA-1a* to

AtMCA-1c (type I) and *AtMCA-11a* to *AtMCA-11f* (type II) (Minina et al. 2020). Although we are aware of this new system of nomenclature for the rest of the thesis to avoid confusion, we will follow the previous system. In the Arabidopsis genome, all three type I MCs are dispersed in different chromosomes but type II are all clustered in Chr.1 apart from *MC9* that is located in Chr.5. The sequence similarity among the members of the family is not high, with the highest score between *MC4* and *MC7* that share 55-72% and are thought to be created from gene duplication. The most distant of all is *MC9* that shares 37% identity with the rest type II MCs. Differences are also observed in the way the genome sequence is organised in introns and exons and the numbers vary from zero introns in *MC9* to 4 in all type I MCs.

Transcripts for these nine Arabidopsis MC genes are expressed at different levels in various tissues and developmental stages and their role is quite distinct throughout the plant life. *MC1* and *MC2* have been shown to display antagonistic roles in regulating the hypersensitive response (HR) triggered by pathogens. Under normal conditions *MC1* is kept inactive by the protease inhibitor Serpin 1 (Coll et al., 2010; Lema Asqui et al., 2018). Furthermore, *MC1* accumulates in protein aggregates, which indicates a potential role in aggregate clearance (Coll et al., 2014). A recent study from (Hander et al. 2019) showed that *MC4* is present in the cell cytosol as a zymogen and is activated upon calcium flux due to plasma membrane rupture after wounding. The Ca^{2+} results in the auto cleavage of the protease which subsequently cleaves the PROPEP1 to form the functional peptide PEP. Pep1 can be transported through the damaged plasma membrane to the extracellular space, bind to the BAK1-PEPR1/2 receptor complex and transmit the signal to the surrounding cells to activate defence responses. Another MC that is triggered upon abiotic stress conditions is *AtMC8* that shows upregulation upon UV light and hydrogen peroxide, methyl viologen and other stress induction factors (He et al., 2008; Tang et al., 2016).

MC9 participates in a totally different concept of PCD as a final step of a differentiation process. Expression analysis showed that *MC9* is present in cotyledons cells, protoxylem, root cap, tracheary elements and petals prior abscission (Bollhöner et al., 2012; Tsiatsiani et al., 2013). It is responsible for the post mortem clearance of TE to form the empty tube-like structure of the xylem

Introduction

vascular tissue. The mechanism that MC9 degrades the cytosolic compounds of the TEs is not known. The metacaspase is coordinated with other proteases function such as Xylem Cysteine Protease 2 (XCP2) which can be processed from MC9 *in vitro* (Tsiatsiani et al., 2013). *In vivo* this cleavage is not yet proved. Another important function is the prevention of ectopic cell death in non-vascular tissues by downregulating autophagy in dying TEs and regulating the balance between the peptides KRATOS and BIA that can restrict or enhance respectively the ectopic cell death in neighbouring cells (Bollhöner et al., 2013; Escamez et al., 2016; 2019). For most of the Arabidopsis metacaspase family, the substrates are still unknown. Until now it is known as mentioned above, PROPEP1 is cleaved by MC4 and MC9 cleaves PEPCK1. In the study of MC9 degradome by (Tsiatsiani et al. 2013) the identification of MC9-dependent PEPCK1 proteolysis indicated its involvement in gluconeogenesis and in seed development. MC9 has also been shown to mediate PCD activation in leaf tissues through cleavage of the GRI propeptide to produce a mature smaller peptide in the apoplast, which then binds to and activates a receptor kinase on the plasma membrane, although GRI didn't appear in the degradome study (Wrzaczek et al. 2014). The level of specificity between the metacaspase and the substrate cleavage is upon discussion. (Shen et al., 2019) tested the potential cleavage of PROPEP peptides from all 9 metacaspases in protoplasts and discovered that all of type II in a higher or lower degree can process them. They obtained with CRISPR-Cas technology a quadruplet mutant, *mc4/5/6/7*, which showed immunodeficiency phenotypes upon *Botrytis cinerea* infection but still shows some residual processing for the PROPEP peptides.

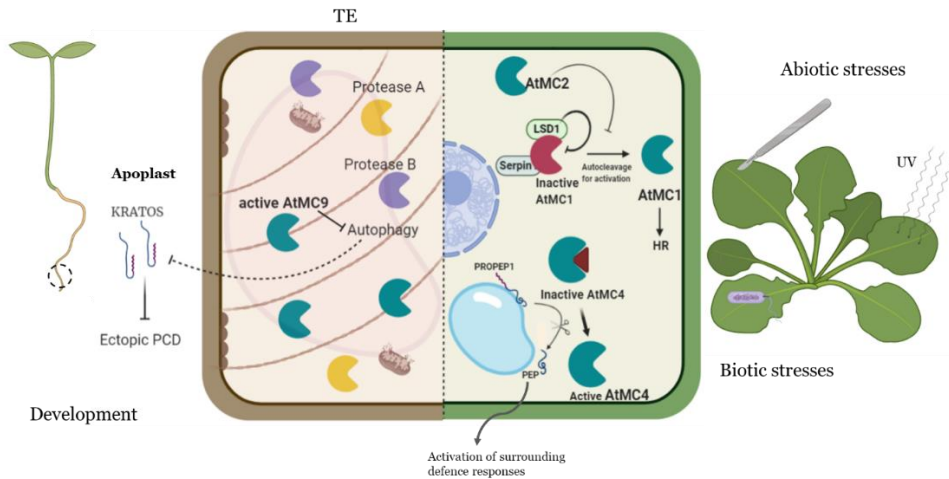


Figure 1.2: Schematic representation of metacaspase function in various conditions proven *in vivo*, during *Arabidopsis* plant life. Left, TE in phase of post mortem clearance where many proteases get activated to degrade the cytoplasm, among them MC9 that also has a role in preventing ectopic cell death by downregulating autophagy. Right, upon pathogen attack, MC1 is released from a complex of negative regulators and promotes cell death and HR. MC2 acts as a negative regulator of the process. In case of tissue wounding, MC4 gets activated by Ca^{2+} influx, processing PROPEP1 into PEP peptide that gets secreted and activates defence responses in the surrounding tissue.

B. Metacaspases in other species

The roles of metacaspases have also been studied in yeast, model plants and many economically important crops. Overall, the role of metacaspases have not been clarified yet, there is increasing evidence that they are involved in PCD initiation or execution under difference conditions. A great number of them is functional upon stress conditions, to ensure that homeostasis is kept.

Yca1 from yeast (*Saccharomyces cerevisiae*) was the first metacaspase to show multifunctional capabilities. Apart from the regulation of cell death upon stress conditions, is also responsible for the degradation of aggregates and the cell cycle regulation (Guaragnella et al., 2010; Madeo et al., 2002). In Norway spruce (*Picea abies*), the type II metacaspase MclI-PA proteolytic activity is essential for the nuclear degradation during developmental PCD for *P. abies*

Introduction

embryo suspensor. Knock down mutants of the protease resulted in increased cell proliferative activity and lack of suspensor differentiation (Bozhkov et al. 2005). Similar to AtMC9, McII-PA pathway seem to be linked with autophagy which has a cell auto protective role (Minina et al. 2013). Two poplar metacaspases, PttMC13 and PttMC14, upon activation participate in xylem corpse clearance after vacuolar collision but are not essential for the initiation of the PCD, as has been shown for AtMC9 (Bollhöner et al. 2018).

The specific roles of different types of metacaspases in plant resistance to pathogens are largely unknown. Numerous studies focusing on different plant species have proved the relation of this family to plant defence mechanisms and resistance, although the molecular mechanism underlying this process is still obscure. In wheat, metacaspase TaMCA4 plays an important role in PCD induced by the fungal pathogen *Puccinia striiformis f.sp. tritici* (Wang et al. 2012), CaMC9 from pepper (*Capsicum annuum*), an homologue of AtMC9 acts as a positive regulator of cell death upon infection by *Xanthomonas campestris pv. Vesicatoria* (Kim et al, 2013), VvMC2 and VvMC5 from grapevine are upregulated upon infection with *Plasmopara viticola*, executing PCD (Gong et al. 2019). Upon infection of *Nicotiana benthamiana* with *Colletotrichum destructivum*, NbMCA1 seem to have role in degradation of virulence factors of the pathogen, processing of pro-protein involved in stress responses and eliminating damaged proteins created during stress (Hao et al, 2007). The tomato (*Solanum lycopersicum*) type II *LeMCA1* gene is upregulated after *B. cinerea* infection (Hoerberichts et al., 2003). In maize leaves, ozone treatment and aging resulted in significantly enhanced expression of type II metacaspases, suggesting their crucial role in leaf response to abiotic stress and age-mediated senescence (Ahmad et al. 2012). A recent study for maize metacaspases using mostly a heterologous expression system in *N. benthamiana*, showed that ZmMC1 and ZmMC2 negatively regulate the NLR Rp1-D21 mediated HR, a function that shows similarity with AtMC2 activity (Luan et al. 2021). Another important finding came from a study of diatom metacaspases, which shows that PtMC5 (type III) is only activated by Ca²⁺ and ROS in two cysteine residues, the catalytic C259 and C202. The second, when oxidised forms a disulphide bond with the first and acts as an enhancer of the protease activity to induce PCD (Graff van Creveld et al., 2018).

These reports clearly suggested the possible roles of metacaspases during growth, development and several biotic or abiotic stress-related responses in plants by regulating PCD. Over the past few years many studies have been published, trying to identify metacaspases in more species and define their phylogenetic relationship. Since the homologues may show different function depending on the species studied, it is recommended to study each protease in the original species and try to obtain gain and loss of function mutants. Our knowledge on the activation mechanism and regulation of metacaspases remains scattered. However, substrate identification both *in vivo* and *in vitro* could definitely help to address better their role in PCD.

Programmed Cell Death in Plant Development (dPCD)

Developmentally controlled PCD occurs throughout the whole plant life to facilitate vegetative and reproductive stages of development (Beers 1997). A great number of tissues undergo a terminal differentiation program in which often dPCD is involved as a final step in order to be properly formed and functional. During vegetative development, cell death occurs to facilitate plants to grow, for example in the formation of empty xylem vessels from tracheary elements to disperse effectively water and minerals. Another example of vegetative PCD is the elimination of cells from the lateral root cap, shaping aerenchyma tissue as well as organ abscission (Escamez & Tuominen, 2014; Farage-Barhom et al., 2008; Kumpf & Nowack, 2015; L. Liu & Fan, 2013). The acquisition of the leaf shape and size in some plant species requires PCD to sculpt structures (Gunawardena 2008). Furthermore, in order to reproduce successfully and germinate, plants need to selectively remove numerous cells involved in many steps of the reproductive process. The formation of gametophytes, the degeneration of tapetum layer in the anther layer when is no longer needed, the proper transmission of the sperm cells into the floral stigma and self-

Introduction

incompatibility during fertilization require cell clearance in a tightly controlled manner (Bosch & Franklin-Tong, 2018; Daneva et al., 2016; Rogers 2006; Wilkins et al., 2015). Seed development is another essential process for the development of the plant and PCD facilitates the embryo to emerge from the seed coat and subsequently provide nutrients that are released from the endosperm (Domínguez & Cejudo, 2014; Smertenko & Bozhkov, 2014).

In animals, the types of cell death regarding patterns and morphological characteristics have been well defined (Galluzzi et al., 2018), whereas in the plant kingdom there is an ongoing discussion about the way of classification and whether the similarities that can be found are comparable to animals. Developmental PCD has been classified from (Van Doorn et al., 2011) as vacuolar type of cell death. Vacuolar type cell death combines characteristics from autophagy process and the action of many hydrolases released from disintegrating vacuoles. The signal that triggers the initiation of the process is usually hormones (Ueda et al., 2015; Kunikowska et al., 2013; Trobacher, 2009) although the information available regarding their exact connection is not clear. Plant hormones comprise a very important part of the plant response against biotic and abiotic stresses as well as of the growth and development machinery (Gray 2004; He et al., 2018; Milhinhos and Miguel 2013). Subsequently, a network of transcription factors is activated and modulate the response of the plant in a coordinated manner (Cubría-Radio and Nowack 2019). Once cell death is triggered, multiple cellular signals are involved to secure the integration of the process, such as reactive oxygen species (ROS), calcium fluxes and cytoplasmic acidification (Huysmans et al., 2017). PCD execution occurs when lytic enzymes are released and degradation processes take place. The vacuole is critical for the release of lytic enzymes that start the degradation of cellular compartments (Van Durme & Nowack, 2016; Hara-Nishimura & Hatsugai, 2011; Hara-Nishimura et al., 2005). The cytoskeleton is reorganized and permeabilization of plasma membrane and nuclear envelope occurs (Smertenko and Franklin-Tong 2011). Mitochondria get swollen, nucleases perform DNA fragmentation and in the end of the process, *post mortem* clearance takes place. The clearance of the dead cell is not considered part of the cell death procedure rather than a following process. Depending on the cell type, cell clearance can be complete or partial,

and persistent corpses of specific cells accomplish vital functions in the plant body (Escamez and Tuominen 2014; Fendrych et al., 2014).

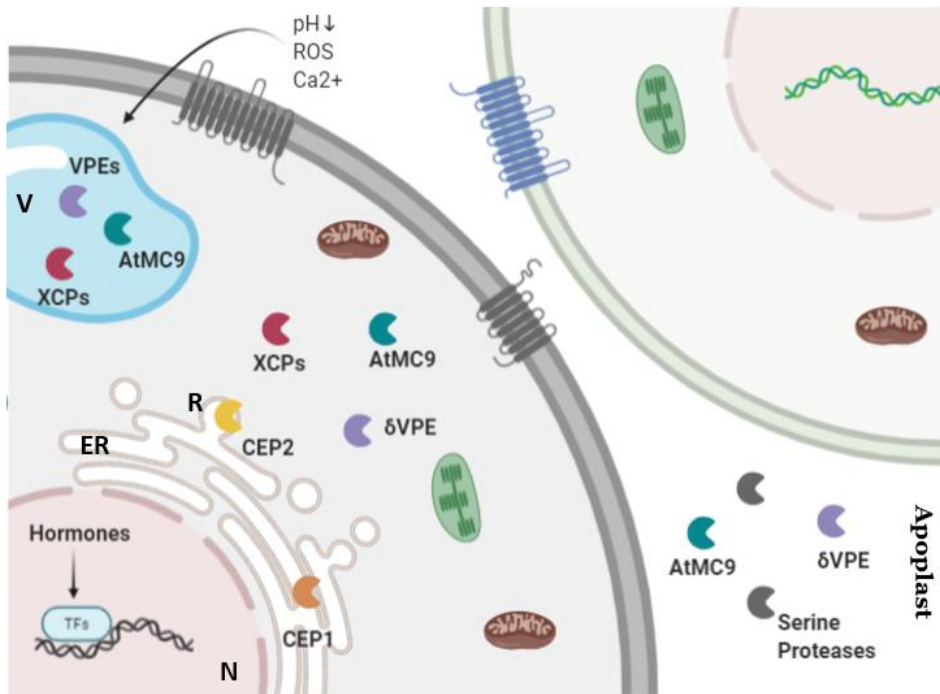


Figure 1.3: Schematic presentation of dPCD-associated proteases from Arabidopsis, with known or predicted subcellular localization. Before activation, the majority dPCD-associated proteases accumulate as inactive zymogen or in specific subcellular compartments. Storage spaces can be the vacuole, the ER and ER-derived vesicles. Once PCD is primarily triggered from hormonal signals, Ca signaling, ROS accumulation and decrease in the p H give the signal for the PCD initiation. Collision of the cellular compartments leads to release of these proteases into the same compartments as their targets. Abbreviations are: V for Vacuole, N for Nucleus, ER for Endoplasmic reticulum, R for Ricinosome.

Caspases are considered to be the key regulators of animal cell death. During plant cell death, papain-like Cys proteases (PLCPs) (Liu et al., 2018) vacuolar processing enzymes (VPEs) along with MCs (Bozhkov et al. 2005; Suarez et al. 2004) are responsible for elimination of organelles such as plastids, ribosomes, ER membranes and peroxisomes. An example of multiple proteases participating in terminal differentiation including dPCD is the formation of TEs. In

Arabidopsis, xylem cysteine peptidase 1 (XCP1) and XCP2 from PLCP family, along with AtMC9 are involved in post mortem clearance, since the triple mutant *atmc9/xcp1/xcp2* didn't show disruption of the vasculature development but delay in the evacuation of the cytoplasmic content (Avci et al., 2008; Bollhöner et al., 2013; Escamez et al., 2016). Additionally, the PLCP CEP1 was shown that affects the SCW deposition as well as PCD and *cep1* plants have delayed growth and less number of xylem cells (Han et al. 2019). CEP1 is also expressed in multiple tissues such as the suspensor cells and the anther's tapetum, prior to PCD events (Zhang et al., 2014; Zhou et al., 2016). VPE enzymes are cysteine proteases sharing enzymatic but not structural characteristic with animal caspases. The Arabidopsis genome encodes four different *VPE* genes, with δ *VPE* being specifically expressed in the inner integument of the seed coat and subcellularly form aggregates between the cell wall and plasma membrane of shrinking integument cells (Nakaune 2005). In the δ *vpe-1* mutant, PCD characterized by nuclear degradation and cellular breakdown is delayed whereas germination or dormancy were not affected. In tomato, five *VPE* genes, named *SIVPE1* to *SIVPE5*, were found to be expressed in the seed coat. However, even with the downregulation of all five *SIVPEs* by RNAi, the seed coat is able to differentiate normally (Ariizumi et al. 2011).

Absence of phenotype in single knock out mutants is a common phenomenon which make it difficult to clarify the mode of action and the function of a protein. The most reasonable explanation is the genetic and functional redundancy that plant proteases show. As described previously there are numerous protease families with many representatives to ensure that in every process will continue without disruption if one enzyme is absent or defective.

Vascular tissues: The Phloem

For plants as multicellular organisms that don't have the ability to move in their environment, it was mandatory to evolve in such a way that they could take advantage as much as possible from their surroundings. A major step in plant colonization is the creation of an efficient vascular tissue, which allowed

Chapter 1

them to develop organs in the most beneficial position but still keep an effective communication among them (Niklas and Newman 2013). Furthermore, the vascular system provides mechanical support and gives shape to the plant. The delivery of multiple necessary resources to the various plant organs had to be conducted from tube shaped tissues, effective in intercellular communication. For this long distance transportation system there are two types of tissues which comprise the vasculature (Lucas et al., 2013): xylem, which transports water and minerals provided from the soil from the root to the upper tissues and phloem, which transports photosynthetic products, hormone signals and amino acids from source to sink organs (Van Bel 2003; Pittermann 2010; Raven 2003). Through these tissues, plants are able to communicate and coordinate their growth and their responses to biotic or abiotic stresses as well. Xylem and phloem vessels are highly specialized cells sharing some common characteristics such as modified cell walls, degraded nucleus and cytoplasm and simplified structure, although they undergo a separate differentiation program which leads to fundamental structural differences. From simpler plant forms of life to the most evolved that are the angiosperms, phloem cells lost gradually most of the cell compartments during the differentiation that forms the functional pipeline. In animals, the blood circulation is supported by the heart that functions as a pump, whereas in plants the transport takes place in case of xylem by osmosis and in case of the phloem by hydrostatic pressure (Oparka et al., 1994, Geiger 1975).

Vascular tissues are not comprised by only one type of cell. Xylem contains the tracheary elements that conduct the water transport and xylem fiber cells. In phloem, there are the sieve elements (SE) that transport the photo assimilates and the neighbouring companion cells (CCs) that function as "nurse" cells. Parenchyma cells exist in both vascular tissues to provide mechanical support. In the root and shoot apical meristem (RAM, SAM) stem cells differentiate into various cell types that comprise the root and the shoot respectively, while still regenerate in order to maintain themselves (Weigel and Jürgens 2002). The vasculature meristem descent from the SAM and RAM and adds cells to the vascular tissues. Therefore, procambial and cambial cells are considered as vascular stem cells (Hirakawa et al., 2010; Miyashima et al., 2013). Constant communication between vascular stem cells is required to keep the balance in

the differentiated cells (Campbell et al., 2016; Hirakawa et al., 2010; Hirakawa et al., 2011; Lehesranta et al., 2010).

A. Phloem Proteases

Proteins found in mature sieve elements are originated either from companion cells and then get transported in the vascular or from the immature SEs before the enucleation. Regarding the second case, these particular proteins require high stability characteristics to survive the differentiation process. Translation occurring in mature sieve elements is highly improbable, since ribosomes have never been observed in mature SEs. The structure and the position of the tissue are limitation factors for its study, especially in a proteomic level. Attempts performed by some researchers, used the whole vascular or phloem sap exudates (reviewed by Carella et al., 2016). The basic impediment is to differentiate the SEs from the surrounding CCs and ensure that the phloem sap contains proteins only from one cell type. In Arabidopsis phloem, many TFs and some signalling peptides that participate in the developmental formation of the tissue, have been identified so far. In contrast, the proteases that may participate in the terminal differentiation process remain completely unidentified. Additionally, little is known about the proteases responsible for the cleavage of peptide signalling molecules or their post translational modifications.

Transcriptomic experiments show expression of proteases specifically in the vasculature tissues or the cambium (Zhao et al., 2005). Upregulated in phloem tissue were five proteases in total, belonging to different families. The higher expression showed metacaspase *MC3*, followed by two serine proteases, *SBT4.12* and *SBT4.5*. Two aspartic proteases, *At1g62290* and *At4g33490*, show lower but tissue-specific expression. From the above proteases only the serine-like subtilase *SBT4.12* has been localized in the root steel and characterized as one of the possible upstream regulators of the IDA peptide which has a role in flowering time, a signal that travels through the phloem (Kuroha et al., 2009; Schardon et al., 2016). CLE peptides are a family of signalling peptides that regulate root development and although the proteins responsible for their

processing are not known, chemical studies with multiple protease inhibitors show that aspartate, cysteine, serine and metalloproteases are capable of cleaving them (Ni and Clark 2006). In 2005, Rautengarten *et al.* performed a large scale analysis of T-DNA insertion mutants for all the serine proteases belonging to the S8 family but no conclusions were obtained for their function in the vasculature tissue due to absence of distinguishable phenotypes. Redundancy of the family is one factor that can explain the normal development of the plant. Metacaspases seem to be expressed widely in the plant but *MC3* as shown from transcriptomic data, has a specific expression in companion cells of the phloem tissue yet the role of the protease remains unstudied (Otero *et al.* 2021; Zhang *et al.*, 2008). In *Tritium aestivum* the type II metacaspase *TaeMCAII*, was shown to be upregulated in SE undergoing differentiation and shift localization from cytoplasm to the cell wall at the final stage of the cell content degradation (Zhang *et al.*, 2017). To unravel the proteases' function an important obstacle must be overcome, which is not only the intra- family but also inter- family redundancy. Between families, small molecules of protease inhibitors have been used, but the lack of specificity make them a much needed primary tool to be used in combination with reverse genetic experiments. Multiple knock-out mutants for the majority of the vascular-associated proteases could also contribute to determine to which extent redundancy occurs, and what is the role of each member of the family. Furthermore, another method in order to capture the bigger picture for SE proteomic composition, would be to isolate large amounts of protoplasts from SEs and perform proteomic analysis but the high turgor pressure they maintain and cytoskeletal structure make the sieve elements extremely fragile once are removed from the protective cell wall. A novel culture system that gives the ability to mesophyll cells to trans- differentiate into xylem, phloem and CCs (VISUAL, VISUAL- CC) depending the hormone supply, is a promising option and proteomic studies have already appeared using it (Breda *et al.*, 2017; Kondo *et al.*, 2015, 2016; Tamaki *et al.*, 2020).

B. Developmental formation of phloem in Arabidopsis roots

The Arabidopsis root meristem is located at the root tip and consists of a stem cell niche. The niche contains the quiescent centre (QC) which are usually four cells mitotically inactive and the surrounding stem cells which are divided to give the rest of the tissues (Dolan et al. 1993). The root is organised in 4 zones according to the growth state of the cells: The meristematic zone is directly upon the QC where cells coming from their precursors stem cells, are divided and obtain their identity, followed by the transition zone where cells establish their differentiation pattern according to the tissue that they belong. Further up, in the elongation zone cells are growing and gaining size to enter at last in the differentiation zone where all tissues are formed (Ishikawa and Evans 1995). For each cell type the transition from cell division to differentiation zone is slightly different. Due to the importance of the phloem, it is the first differentiated tissue after 18-23 cells from the QC whereas the surrounding cells are formed later. For example, the cortex cells enter the elongation zone after 30 cells in 5d old seedlings and xylem differentiates in much late stages when root hair formation begins (Dello Iorio et al., 2007; Truernit et al., 2012).

The root vasculature is composed of two phloem poles positioned opposite to each other surrounding the xylem pole in the centre of the root. Each phloem pole has two different but crucially connected cell types: the sieve elements, which perform the actual transportation, and the companion cells, which provide essential metabolic functions for the differentiated sieve elements that lack a nucleus. Each phloem pole's SE and CCs derive from different single stem cells. The first division of the stem vascular cell is anticlinal followed by two periclinal divisions that give rise to proto- and meta- phloem SEs respectively (Mahonen et al., 2000). Protophloem is the first form of phloem tissue that differentiates close to the root tip being responsible for the distribution of photo assimilates and growth factors and metaphloem is created from the second cell of the periclinal division but differentiates and replaces protophloem further up. From that point on, cells divide several times anticlinal before entering the special differentiation

program that makes phloem functional (De Rybel et al., 2016). According to the transcriptome present in the protophloem cells from the QC to the enucleation point, seven groups of cells can be assembled: (I) “stem cell”, cell in position 1 (II) “transit amplifying”, cells in position 2-9, (III) “transitioning”, cells in position 8-11 (IV) “early differentiating”, cells in position 10-15, (V) “late differentiating”, cells in position 16-17 (VI) “very late differentiating - NEN4-like”, cells in position 18-19, VII “enucleating”, cell in position 19 (Roszak et al., 2021). The identity of CCs is fully completed with a delay of 2-3 cells compared to protophloem, although recently was shown that in earlier stages of development, CCs and PSE maintain a plasticity and can switch identities in order to ensure the correct formation of the vasculature in case of PSE misidentification (Gujas et al., 2020). Positional information is very important to the configuration of cell identity, since many surrounding cell types share partially common transcriptomes (Otero et al. 2021).

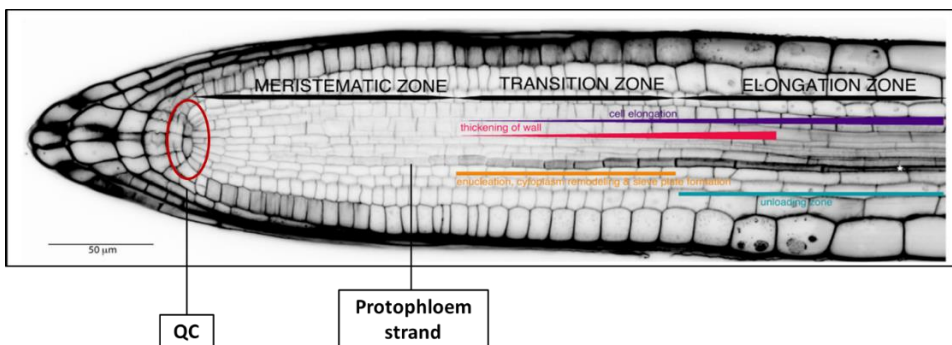


Figure 1.4: Overview of the Arabidopsis root meristem zones. Starting from the QC and expanding till the elongation zone. Differentiation zone is further up, not present in the figure. Indicated are also in a spatio-temporal way, the events that lead to the protophloem sieve element differentiation (cell file marked by white asterisk). Adapted from (Anne and Hardtke 2018).

In Arabidopsis, the embryo stage of 16 cells is the initiation developmental point in which the cell vascular identity is obtained from non-vascular precursors as shown recently by (Smit et al., 2020). Primarily, hormonal signalling determines the initial cell fate and regulates the pattern during the phloem formation. Auxin response through AUXIN RESPONSE FACTORS

(ARFs) is necessary but not sufficient to specify the cell identity. Cytokinin and brassinosteroids (BRs) have crucial roles in the cambium and precursor phloem cells respectively (De Rybel et al., 2016). BR receptor kinases, BRI1, BRL1 and BRL3, are constantly expressed in the developing tissues reassuring the correct patterning of phloem (Fàbregas et al., 2013) and act antagonistically with phloem-specific CLAVATA3/EMBRYO SURROUNDING REGION-RELATED 45 (CLE45) peptide signalling in roots. Sieve element differentiation is impaired in mutants that lack all three BR receptors although it is proposed that BRs have a more systemic impact in root growth, by controlling phloem driven signals (Graeff et al., 2020, 2021; Kang et al., 2017).

Mutant analyses have identified various genes involved in the formation of vascular tissues. In addition to upstream transcriptional regulators and signalling pathway components required for overall vascular morphogenesis, these screens have also identified factors that are specifically involved in phloem development. Transcriptomic analysis combined with VISUAL culture system, has facilitated the identification of many regulatory TFs. With this system was confirmed that BES1 and BZR1 promote redundantly bi-directional differentiation of procambial cells into xylem and phloem cells (Saito et al., 2018). *APL* was the first gene regulator identified to be specifically expressed in phloem precursor cells and is required for cell division and vascular identity (Bonke et al., 2003). In *bes1* CRISPR mutants *APL* was downregulated, suggesting that BES1 can positively regulating phloem differentiation upstream of *APL*. Similarly, NAC020 was proved to be an early, SE-specific NAC TF that potentially acts as a negative regulator of *APL* (Kondo et al., 2016). Using fluorescence-activated cell sorting (FACS) and subsequently single cell transcriptomics (Roszak et al., 2021) verified six PEAR transcription factors that positively regulate *APL* expression, whereas in a sextuple mutant *APL* expression was not detected. By CHIP-qPCR was also shown that the regulation is a result of a direct binding on the *APL* promoter region. Another target of *PEAR* genes appeared to be *PINEAPPLE*, a newly characterised DOF TF that seem to be important for the sucrose allocation within the root meristem in order seedlings to be able to turn to autotrophy (Otero et al., 2021).

OCTOPUS (OPS) and OCTOPUS-LIKE2 (OPL2) are membrane proteins of the same family expressed in precursor phloem cells before APL. In *ops* mutants, individual protophloem cells fail to differentiate and result in discontinuous phenotype (known as "gap") indicating disrupted phloem strand integrity, a phenotype that could be reversed by expression of GSK3-BIN2 which acts antagonistically in determine phloem identity (Anne et al., 2015). The effect of the double mutant *ops opl* is more severe than in the single ones, indicating functional redundancy (Ruiz Sola et al., 2017; Truernit et al., 2012). Similar phloem defects have been described in BREVIS RADIX (BRX) mutant, which is another mainly polar membrane located protein, target of ARF5 (MONOPTEROS) gene (Mouchel et al., 2006). These factors promote sieve element identity and help cells to maintain it, opposite to CLE45 peptide and BARELY ANY MERISTEM 3 (BAM3) receptor-like kinase function. The two pathways seem to keep the balance and the timing in cell specification (Depuydt et al., 2013). In addition, COTELYDON VASCULAR PATTERN2 (CVP2) acts upstream of OPS regulating the level of phosphatidylinositol-4,5-bisphosphate (PIP2). A double mutant of CVP2 and its homolog CVP2-like1 (CVL1) shows the "gap" phenotype, similar to the *ops* and *brx* mutants (Rodriguez-Villalon et al., 2015).

Apart from the VISUAL system, in the past three years many single-cell RNA-sequencing root studies have revolutionized our knowledge for individual cell types (indicative works from: Graeff et al., 2021; Ryu et al., 2019; Wendrich et al., 2020; Zhang et al., 2019). The combination of these techniques with multiple mutant analysis could offer enormous potential in unravelling the developmental programs of many root cell types and more specifically for phloem and xylem which are difficult tissues to work with due to their position in the plant.

A.1 Terminal differentiation of SEs

SEs undergo a unique differentiation process, during which most of the cellular components are partially distorted and rearranged, leaving free lumen space for the loading processes. Characteristic subcellular events are the

enucleation, fortification of the cell wall by callose deposition to withstand hydrostatic pressure, accumulation of P protein bodies and the establishment of sieve plates (SP) structures for intracellular communication (reviewed in Heo et al., 2017). After losing the nucleus, protophloem SEs immediately become part of the 'phloem unloading zone', accommodating the translocation of small molecules towards the entire root meristem starting from the neighbouring pericycle cells (Ross-Elliott et al. 2017).

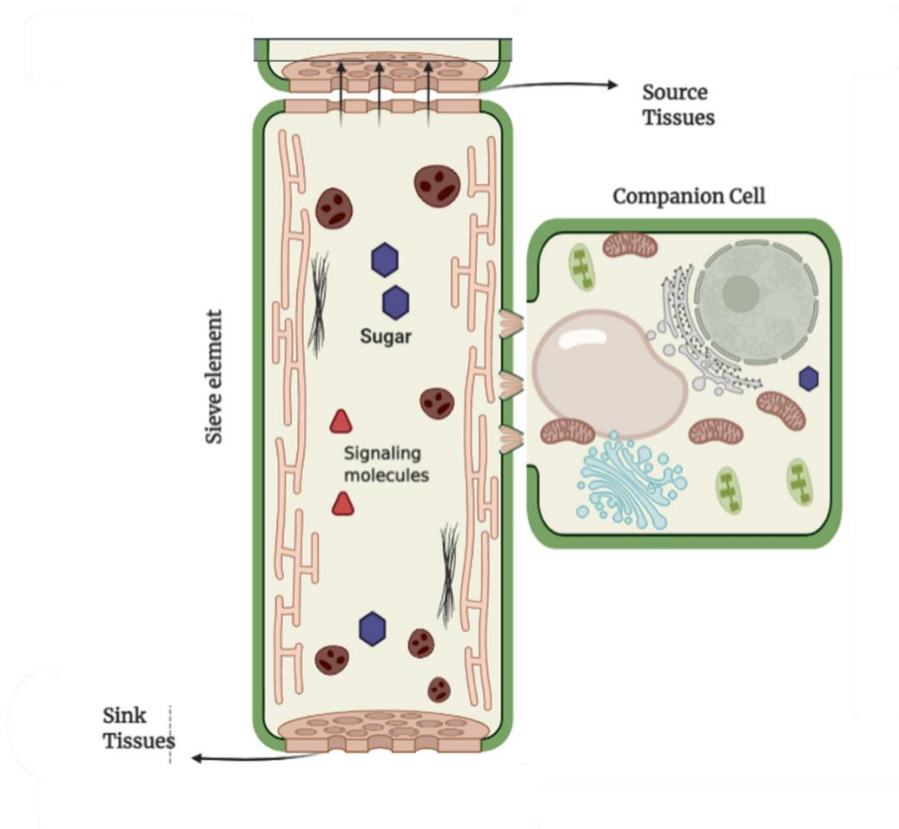


Figure 1.5: Schematic representation of the crucial relationship between CCs and SEs. Photoassimilates and signalling molecules are loaded from source tissues, through CCs to the phloem (differentiated proto- and meta-phloem cells) and travel to the sink tissues where they get unloaded. The unloading starts from the phloem pericycle cells. CCs have enlarged nucleus and numerous cytoplasmic organelles. The ER is full of ribosomes in contrast with the SEs, where is shrunk and translocated to the periphery. The cytoplasm of SEs is quite empty, organelles like chloroplasts, mitochondria and small lytic vacuoles exist close to the cell wall, along with P protein filaments.

Chapter 1

SE nuclear degradation is considered the peak moment of the differentiation and is marked by the deformation of the nucleus. First, the nuclear envelope becomes disorganized and the nucleus shrinks. During enucleation, the nuclear contents diffuse into the cytoplasm, where they get degraded, leaving behind a remnant of the nuclear envelope. The whole process is completed within 10 min. When the nucleus deforms, the nucleolus becomes fragmented. The mitochondria also gradually change shape during nuclear degradation, and the ER undergoes structural changes by making stacks, losing ribosomes and migrating towards cell periphery. No signs of a large central vacuole have been observed, but small lytic vacuoles were present before and after enucleation. Modified organelles such as the plastids and mitochondria are moving towards the cell wall (Furuta et al., 2014; Oparka & Turgeon, 1999; Sjölund, 1997; Truernit et al., 2012).

The molecular mechanism that is responsible for complete protophloem differentiation, nor the initial signal is still not completely known but it seems to be a cell autonomous process although the surrounding cells express simultaneously multiple genes forming a ring pattern to support the cells undergoing enucleation (Otero et al., 2021). Furuta et al., at 2014 showed that two members of the NAC TF family, NAC45/86, are expressed in differentiating SEs and in the phloem pole pericycle cells. ALTERED PHLOEM DEVELOPMENT (APL), a MYB TF, acts upstream controlling their expression. APL, as mentioned above, is a key regulator and promoter of SE differentiation since the *apl* loss-of-function mutant showed mixed identity of SE and TE cells and is seedling lethal (Bonke et al., 2003). NAC45/86 redundantly regulate the expression of NAC-DEPENDENT EXONUCLEASE 1, 2 and 4 (NENs) and control the translocation of NEN1 and 2 from the cytosol to the nucleus. The NAC–NEN pathway was shown to regulate nuclear degradation during SE differentiation. Similar to the *apl* mutant, a double knockout mutant, *nac45- nac86*, exhibited seedling lethality and nuclei was present in PSEs, while some cytoplasmic changes such as mitochondrial reshaping or callose deposition in the cell wall formation remained intact despite the connection that they seem to have with the upstream APL function. In *nen4* mutant seedlings, the root length was only slightly reduced and cytoplasmic clearance, nuclear envelope disorganization or

Introduction

organelle clustering occurred normally. The nuclear content was present although the shape was disturbed showing formed masses. In contrast with TE formation where several proteases are known to participate in *post mortem* clearance of the cell, in phloem until now no enzyme has been identified to degrade the cytoplasmic content. For both tissues the initiation of PCD in case of xylem and the special differentiation of phloem is remaining elusive.

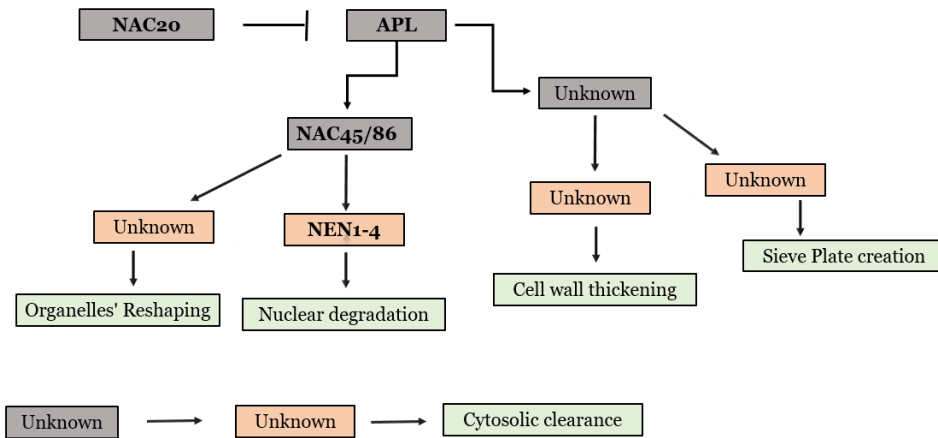


Figure 1.6: Known and unknown TFs and execution enzymes in the differentiation process of a phloem sieve element. With grey colour are highlighted the upstream TFs, with orange the execution enzymes such as NEN nucleases and with green colour are the individual events that result in the final form of the sieve phloem cell. Adapted from (Geldner 2014).

Choline levels are crucial for the proper transformation of PD into SPs, which depends on the expression of CHOLINE TRANSPORTER LIKE 1 (CHER1), a protein present in many cell types (Dettmer et al., 2014). However, the detailed cellular processes regulated by CHER1 and the choline level are not specified. Callose deposition by CALLOSE SYNTHASE 7 (CalS7) is also required for the formation of SPPs. CalS7 is specifically expressed in phloem tissue and knock out mutants failed to create multiple elaborate pores for functional SPs (Xie et al., 2011).

A.2 Supporting Companion Cells

In angiosperms, once SEs differentiate are heavily depended on the specialized CCs. Unlike SEs, which lose the nucleus and the majority of their organelles, CCs are characterized by their increased cellular density. A large nucleus and an increased number of ribosomes, mitochondria, ER, and plastids are observed in CCs (Oparka and Turgeon 1999). The main function of CCs is to support SEs and keep them viable. Apart from their role as nurses to the adjacent SE, they are responsible for many more activities for the plant growth from determining the flowering time by controlling the expression and transport of long sought florigen FT to the SAM, to defending the entry point for many pathogens that try to invade phloem tissue (Jaeger and Wigge 2007; Tsuwamoto and Harada 2011; Zhu et al., 2016). The CC function in leaves consists of loading photoassimilates into the SE but their role in the root still remains obscure.

Most of proteins found are related to transport events, confirming their importance in loading and unloading the phloem, such as Arabidopsis H⁺-ATPase isoform 3 (AHA3), a membrane proton pump (DeWitt and Sussman 1995), SUC2 which is a sucrose transporter (Gottwald et al., 2000). In leaf CCs the amino acid/ H⁺ symporter AAP2 (Zhang et al., 2010), the potassium channel KAT1 (Schachtman et al., 1992), the hexose uni- porters SWEET1 and SWEET4 (Chen et al., 2012) and the tonoplast peptide transporter PTR4/NPF8.4 (Weichert et al., 2012), are also specifically expressed. All the proteins mentioned above were also confirmed by (Kim et al. 2021) and separated from phloem SE in leaf tissue by single cell transcriptomics. The transcriptomic networks responsible for the differentiation of CCs initials are not yet determined but several proteins expressed in formed CCs are quite specific indicating that these cells have a unique proteome (reviewed by Otero et al., 2016).

CLAVATA 1 (CLV1) has been shown to be expressed in CCs and regulates the activity of the meristem and differentiation in the SAM. Additionally, many genes seem to have a specific expression in the PSE and after the differentiation to change their expression in CCs (reviewed by Otero et al., 2016). Examples are *APL* and *LATERAL ROOT DEVELOPMENT 3 (LRD3)* which is also

Introduction

important for the early phloem formation and the correct delivery of phloem content in long distant tissues (Ingram et al., 2011). Otero et al., 2021 dissected the phloem tissue trying to identify genes that are specifically expressed in each cell category, offering new insights in marker genes for PSE, MSE, CCs and PPP.

Objectives

The general objective of this study was to characterize the mode of action and the functional role of *Arabidopsis thaliana* metacaspase 3 (MC3).

To this end, the following specific objectives were proposed:

1. To determine the gene expression patterns of MC3 gene and localize the MC3 protein
2. To identify potential MC3 proteolytic substrates and changes occurring in the proteome caused by altered MC3 levels.
3. To investigate the role of MC3 during development of the plant by phenotypical analysis of the effects caused by altered MC3 levels.
4. To investigate the role of MC3 in stress responses by phenotypical analysis of the effects caused by altered MC3 levels when plants are challenged with a stress factor

CHAPTER 2

Characterization of MC3

cysteine protease function in

plant development

Results

Summary

Metacaspases are a family of cysteine proteases found in lower eukaryotes and plants. They are considered distant relatives of animal caspases. In *Arabidopsis thaliana*, the metacaspase family is composed by nine genes divided in two sub-groups depending on their domain architecture. Metacaspase 3 belongs to type I metacaspases and was found to be expressed in the vascular tissue and more specifically in the differentiating protophloem of the root and the supporting phloem companion cells. We used confocal microscopy to localize the protein at a subcellular level. Furthermore, we analysed the phenotype derived from absence or overexpression of the gene during plant development. Phloem tissue formation was also analysed with specific focus on the differentiation process of the protophloem cells and the formation of the vascular tissue. We also checked the hypothesis of functional redundancy with other proteases of the same family that appear to have overlapping expression pattern. We showed that under normal conditions the overall growth of the plant is not affected. Furthermore, we checked the total proteome of the plants to compare differences in protein abundance in different expression backgrounds and in different tissues. Overall, the analysis showed that the root tissue of the protein overexpressor is enriched in stress-related proteins, specifically osmotic and hypoxia-related, whereas in the leaf tissue the differences were not as clear.

Results

Metacaspase 3 is a Type I metacaspase from Arabidopsis

Metacaspases in Arabidopsis can be divided into two types regarding their domain architecture. Type I metacaspases have an N-terminal prodomain containing a proline-rich repeat motif and a zinc finger motif. Type II metacaspases lack such a prodomain but harbour a linker region between the putative large (p20) and small (p10) subunits. We analysed the sequence of MC3 to identify by similarity the conserved domains and the amino acids that are part of the catalytic dyad, which characterizes the family (Fig 2.1).

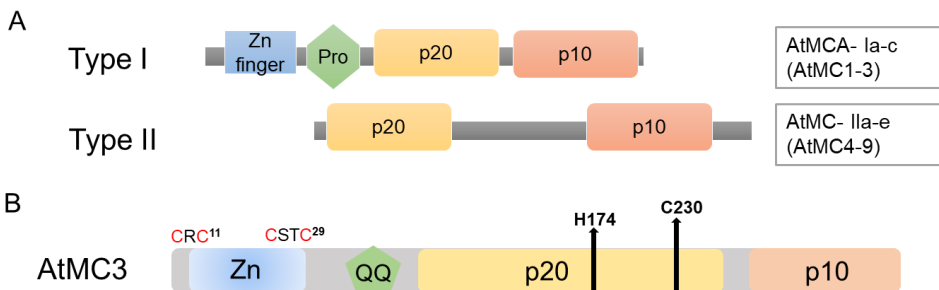


Figure 2.1: Protein structure of *Arabidopsis thaliana* metacaspase family (A) Schematic representation of the metacaspases protein domains in *A. thaliana*. (B) Protein domains of MC3 with indicative motifs.

In metacaspase 3, the prodomain contains a glutamine-rich region comparable to the proline-rich region that is appearing in the rest of Type I metacaspases (Vercammen et al. 2004). The polyQ motif is also present in the yeast metacaspase Yca1 and seem to be necessary for the formation of aggregates (Lee et al., 2010). Another difference with MC1 and MC2 is the fact that only one putative CXXC-type zinc finger structure is found in MC3 prodomain (position indicated at Fig 2.1B), similar to the lesion-simulating disease-1 protein (LSD1), a negative regulator of the hypersensitive response with homology to GATA type transcription factors. The second zinc finger motif, at position 11, is missing an amino acid to be complete. The catalytic residues are a Histidine (H) in position 174 and a Cysteine (C) in 230 of the p20 domain. The total predicted size of the protein that contains 362 amino acids (aa), is 40.49kD. The prodomain is 10.53 kD, p20 domain is 16.70 kD and p10 domain is 13.8 kD. Since MC1 is

Results

auto- cleaving the prodomain in order to be active (Lema et al., 2018), we hypothesized that MC3 might behave in a similar fashion, and contain conserved Arginine (R) residues indicating putative cleavage sites. According to the protein sequence and the comparison with MC1, there is an R in position 91 that could be processed in order to remove the prodomain for the activation of the protein.

Localization of MC3 in the phloem vascular tissue

MC3 has a phloem specific gene expression pattern

To identify the expression of the *MC3* gene in Arabidopsis tissue, a genomic fragment of 1kb upstream of the CDS sequence that contain the promoter region was cloned and fused to β -glucuronidase GUS reporter system. Seedlings were collected after 4 and 7 days growing on MS media and analysed histochemically to detect GUS (Fig 2.2).

In Figure 2.2A the expression of *pMC3:GUS* in 4 days-old seedlings is shown. Promoter activity starts close to the root tip but it is largely absent in the meristematic zone. Seedlings are showing expression throughout the whole vascular tissue in root, hypocotyl and cotyledons. Furthermore, when 7 or 12 days-old seedlings were used (Figure 2.2B, 2.3A), the expression was also detected in the first true leaves of the rosette which were emerged. Looking into more details in the root tissue, it is clear the expression in the two strands of the vascular tissue (Figure 2.3B).

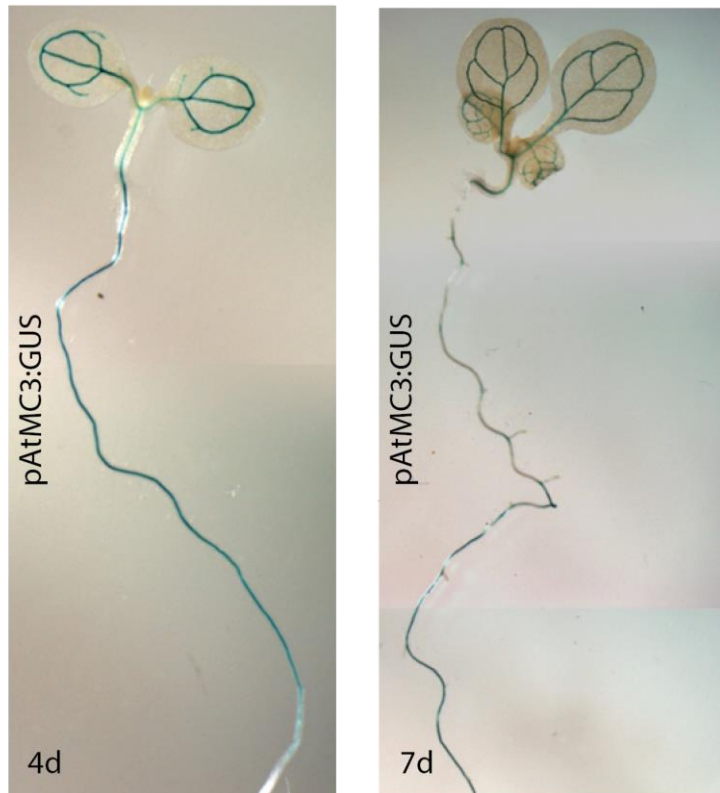


Figure 2.2: Expression of *MC3* in Arabidopsis roots. Histochemical GUS staining of transgenic Arabidopsis lines expressing GUS fusions under control of the *MC3* endogenous promoter. Expression profile of *MC3* in the whole seedling of 4 and 7 days-old seedlings. (Pictures were taken from Planas M., “Caracterització de la metacaspasa-3 (AtMC3) en els processos de desenvolupament i resposta a patogen”, TFG thesis, University of Barcelona, 2014).

Results

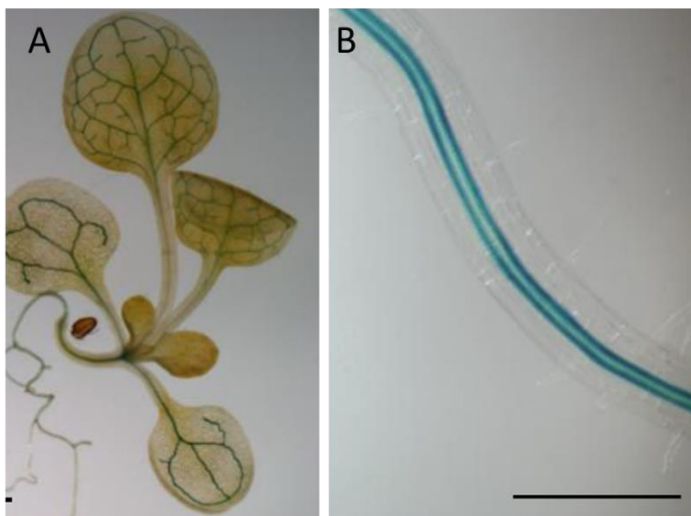


Figure 2.3: Expression of *MC3* in Arabidopsis. Histochemical GUS staining of transgenic Arabidopsis lines expressing GUS fusions under control of the *MC3* endogenous promoter. Expression profile of *MC3* in the (A) whole seedling of 12 and (B) root vasculature of 4 days-old seedlings. (Pictures were taken from Planas M., "Caracterització de la metacaspasa-3 (*AtMC3*) en els processos de desenvolupament i resposta a pathogen", TFG thesis, University of Barcelona, 2014).

To analyse the expression pattern of *MC3* at a more detailed cellular level the same promoter sequence was fused to Venus fluorescent protein targeted to the nucleus and visualized under confocal microscope. Roots of 7-day-old seedlings were analysed showing that the expression was companion cell-specific, identified from their elongated nuclei to support the enucleated sieve elements in the whole root (Fig 2.4). The next step was to determine the site at the CCs where *MC3* expression started taking place. Remarkably, when the meristematic zone was analysed with propidium iodide (PI) staining, expression was detected also in the three protophloem cells that are entering the enucleation process (Fig 2.4). In the root, PI staining allows to distinguish phloem due to the fortified secondary cell walls that sieve elements have during differentiation. Calcofluor White Staining was also used, since it binds with non-cellulose and chitin contained in the plant cell walls. After the enucleation, the expression is changing to the pericycle cells that have more round nuclei and CCs. This pattern is quite common for genes that have been shown to have a function in phloem

development such as *APL*, *NAC45/86* (Bonke et al., 2003; Furuta et al., 2014). CCs, pericycle and protophloem cells are derived from different precursor cells but all are considered part of the vasculature. In the XZ-image three to four spots of VENUS signal are visible and correspond to the CCs when the stack was taken in the elongation zone and only two that corresponds to the proto- phloem poles were seen when the stack was taken in the meristematic zone (Fig 2.4).

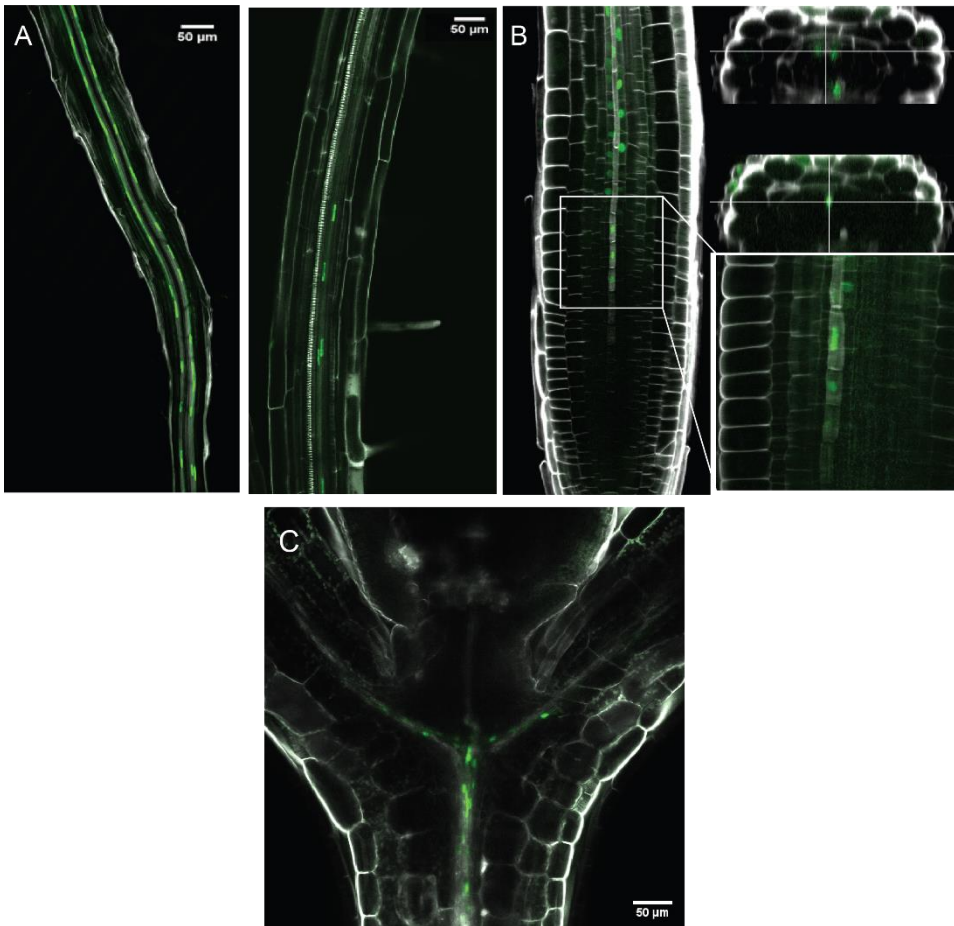


Figure 2.4: Expression pattern of *MC3* monitored with *pMC3:NLS-3XVenus* construct in promoter marker line. Nuclear-localized mVENUS signals (green) are co-visualized with propidium iodide or calcofluor staining. Pictures were taken in different root zones, differentiation (A) and meristematic (B) and in the hypocotyl area (C). Top right picture presents orthogonal views of the differentiated (upper) and non-differentiated

Results

(lower) vascular. Below is a magnification of the vasculature tissue from the meristematic zone picture. Scale bar, 50 μ m.

Recent advances in single-cell gene expression studies have contributed to the understanding of transcriptional regulation in dynamic development processes and highly heterogeneous cell populations such as the Arabidopsis root. Root cells are highly heterogeneous, even within a single cell type. In order to confirm the specificity of the gene expression found for *MC3*, an *in silico* analysis was performed using available online datasets from previous publications. All the data found, confirmed the specific phloem expression of *MC3* in both root and leaf vasculature as shown in Table 1.

Table1: *MC3* gene expression from single cell or cell sorting transcriptome sequencing data.

Publication	MC3 presence	Tissue
(Ryu et al., 2019)	+	Phloem, LRC
(Zhang et al., 2019)	+	Phloem
(Shulse et al. 2019)	+	Phloem
(Brady et al. 2007)	+	Sieve elements, CCs
(Kim et al. 2021)	+	Companion Cells
(Otero et al. 2021)	+	Sieve elements, CCs

MC3 protein is localized in the cytoplasm of the phloem vascular tissue

The Arabidopsis metacaspase family has been attributed many different roles throughout the plant life, with quite diverse tissue-localization and conditions necessary for their function. To reveal the localization of MC3 protein in the plant, the full length CDS sequence was fused to green fluorescent protein (GFP), under

the control of a 2 kb fragment of the endogenous promoter upstream from the start codon (*pMC3:MC3-GFP*). CDS was used as plants transformed with the constructs containing the genomic sequence did not show detectable MC3 protein levels. Localization of the protein fusions was analysed in the T3 homozygous stable plants grown for 6-7 days in MS media. Similar to gene expression, protein expression was also very specific for the companion cells of the phloem tissue and appeared to localize mostly in the cytosol (Fig 2.5A and B). The same expression pattern was detected in cotyledons (Fig 2.6). Lines with the predicted cysteine catalytic site of MC3 mutated to an alanine were also generated and analysed (*pMC3:MC3-C230A-GFP*) to identify possible differences due to an inactive catalytic centre. As shown in Figure 2.5C, the catalytic cysteine did not seem to affect the localization of the protein since it also localized in the cytosol as in the active version.

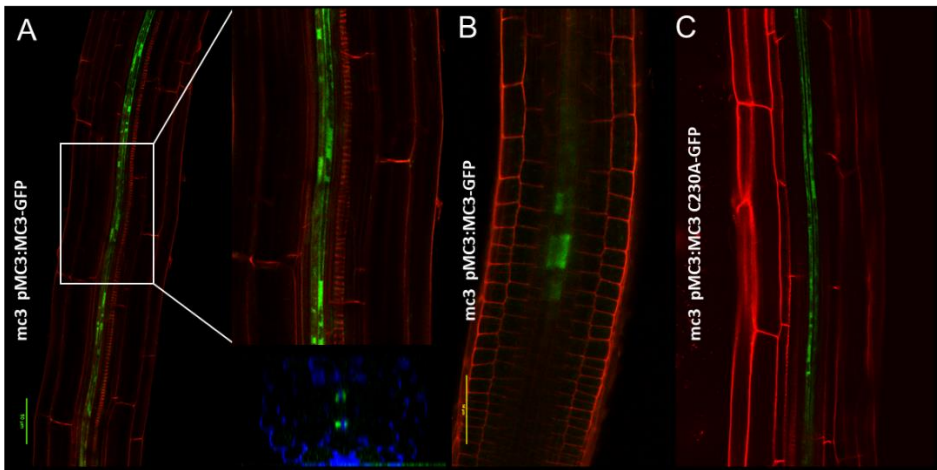


Figure 2.5: Expression pattern of MC3 protein. Translational fusion of *MC3-GFP* under its native promoter was monitored by confocal microscopy. Pictures were taken in two different root zones. (A) Differentiation zone of the root and a radial view from the top. (B) Meristematic zone. (C) Translational fusion of catalytically inactive *MC3 C230A-GFP* under its native promoter. Differentiation zone was visualized. The GFP green fluorescent signal was co-visualized with propidium iodide (PI, grey). Scale bar, 50 μm.

Results

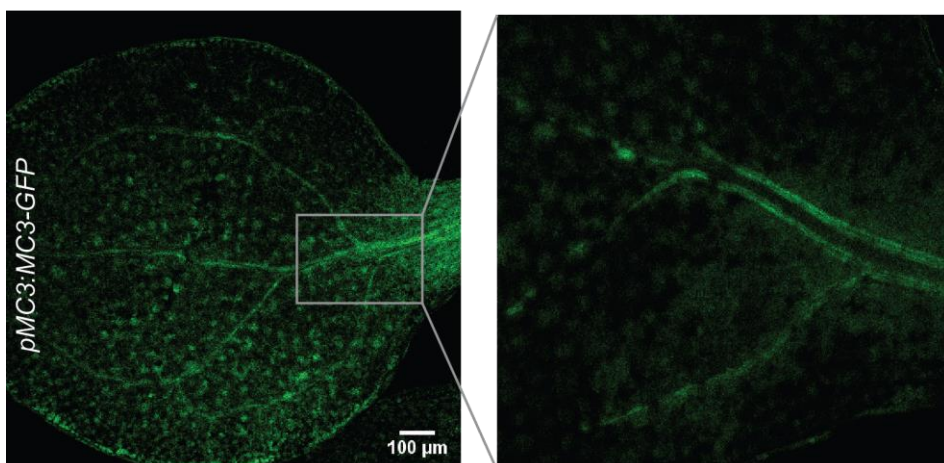


Figure 2.6: Expression pattern of MC3 protein in cotyledons. Translational fusion of *MC3-GFP* under its native promoter was monitored. Pictures were taken in cotyledons of 7-days old seedlings.

At the subcellular level, *MC3* seems to be expressed and evenly distributed throughout the cytoplasm of the cell. *MC3* overexpressing lines under the *UBQ10* constitutive promoter were also generated both to increase the amount of the *MC3* protein in the plant and to determine whether overexpression had an effect on the plant. The transgene was introduced to both *Col-0* and *mc3* #13.3 CRISPR background (see below the section describing generation of *MC3* mutants). Analysis of the overexpressing lines shows a localization pattern extended to the whole root tissue with an enhanced expression in the vascular tissue as expected from the *pMC3:MC3-GFP* line (Fig 2.7A, C). Differences with the overexpressed catalytic inactive form of the protein in terms of localization were also not observed. Interestingly, the *MC3* levels decrease when the overexpressing construct was introduced into an *mc3* mutant background and both the active (*MC3*) and putatively inactive (*MC3-C230A*) form shows protein aggregate formation. Focusing on the centre of the root tissue the expression could be detected more intensely in the protophloem sieve elements and the strand of surrounding CCs. Since the GFP was not detected in the differentiated phloem cells as the nucleus is absent, it is not likely that the protein can be transferred from the surrounding cells (Fig 2.7C, D).

Chapter 2

Focusing on the epidermal cells of the root that are bigger in size, conclusions were made regarding the subcellular localization. No signal was detected in the nucleus, nor in the vacuoles that appear as dark cycles occupying the largest part of the cell (Fig 2.7E, F). The differences observed depending on the background of the plant could be explained by the stabilization of the protease. In Col-0 plants the natural variant of the protease is present and could affect the overexpression of the transgene.

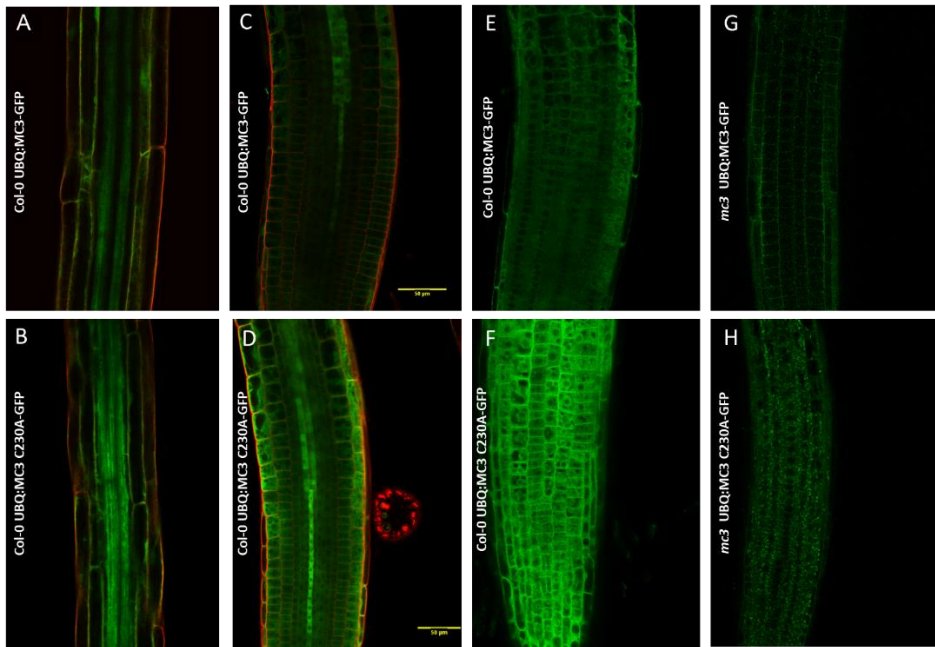


Figure 2.7: Expression pattern of MC3 overexpressor lines. (A), (B) Differentiation zone of the root. Upper panel (A) shows the active version of the protease and the lower one (B) is the catalytic inactive form. (C), (D) Protein expression in the root tip focused in the vascular tissue and the adjacent cell layers. (E), (F) Meristematic zone of the root: View of the epidermal cell layer. (G), (H) Expression pattern in the *mc3* mutant background. Meristematic zone of the root: View of the epidermal cell layer. Scale bar 50μm. Stain with PI.

Activation of the protease

In *Arabidopsis* it has been shown that type I metacaspases are behaving quite different regarding the necessity of the prodomain removal. MC1 can be auto-cleaved and the catalytic cysteine is necessary for the process of the zymogen and the activation of the protease. On the other hand, MC2 does not need to be processed to function in the suppression of HR (Coll et al., 2010). From type II metacaspases, only MC4 and 9 have been thoroughly studied. (Vercammen et al., at 2004) obtained recombinant type II metacaspases in bacteria, and showed that autocatalytic processing is depending on a defined catalytic cysteine which results in the formation of p20-like and p10-like fragments. Recently it has also been shown that Ca^{2+} influx is necessary for the activation of MC4, which takes place upon wounding (Hander et al. 2019; Zhu et al. 2020).

To determine the protease properties of MC3 and its cleavage pattern we used the *Nicotiana benthamiana* system for transient expression. Over-expressing MC3 constructs were transiently expressed in *N. benthamiana* leaves and protein extracts were immunoblotted with anti- GFP antibody. Interestingly, two bands appeared at 70kD and a lower one at 60-65 kD. The size of the two bands correspond in the full length of the protein including the fluorescent tag and probably an N-terminally cleaved version, as has been shown for MC1 (Lema et al., 2018). We observed that there is signal also in lower molecular weight (MW), multiple bands around 25-30kD. Bands were present in both active and inactive form (Fig 2.8A). The most intense band could correspond to cleaved GFP (27kD). The remaining bands could correspond to additional cleaved MC3 fragments or could be unspecific background.

Considering that *N. benthamiana* possesses its own set of metacaspases and additional proteases that could process MC3 unspecifically, we analysed by immunoblot stable over-expression of the protein variants in *Arabidopsis* transgenic lines (wild-type and *mc3* mutant background). We observed that when the endogenous version of the protease is present in the plant, we were able to detect a band that corresponds to the full-length protein with GFP tag (70 Kd) and two additional bands with slightly reduced MW (above 60kD). Furthermore, more

bands were present with lower molecular weight (MW), around 45kD (orange arrow in Fig 2.8B) but also a band at 25kD that corresponds most likely to free GFP. These multiple bands could indicate cleavage sites for the activation of the protease, although it does not seem to be dependent on the catalytic cysteine since the catalytic inactive form of MC3 has the same pattern of protein bands (Fig 2.8B).

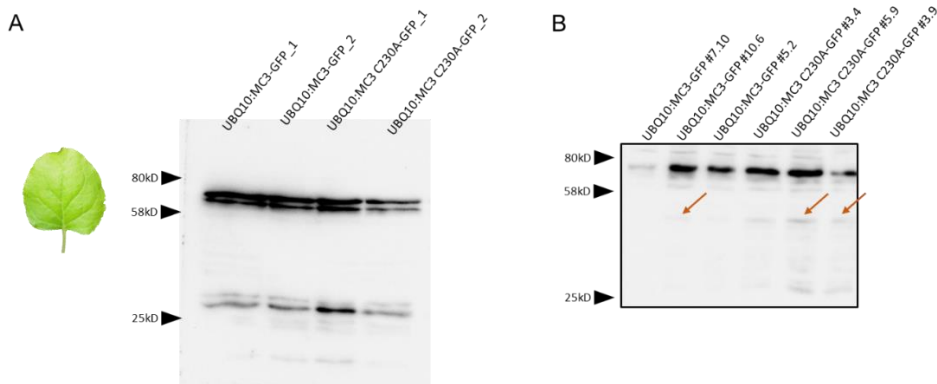


Figure 2.8: MC3 processing in *Nicotiana benthamiana* and *Arabidopsis*. (A) Immunoblot for samples collected from transient expression in *N. benthamiana* plants for *UBQ10:MC3* and *UBQ10:MC3 C230A* constructs. (B) Immunoblot using anti-GFP antibodies of three independent *UBQ10:MC3* T3 lines and three *UBQ10:MC3 C230A* lines in wild-type background.

To exclude that the natural version of MC3 in wild-type plants could perform part of the cleavage in the overexpressor lines, we analysed the cleavage pattern in *mc3* mutant background for lines carrying the transgene under the endogenous promoter. Due to the specificity of the localization of MC3, detection of protein levels by WB in transgenic lines containing constructs with native promoter can be challenging. The abundance of the protein is very low and the signal is diluted especially in leaf samples, considering the phloem-specific localization of the protein. For this reason, we tried to maximize the ratio of vascular/total tissue by collecting 7d old seedlings to perform protein extraction for these lines. Indeed, MC3 could be detected in the 70kD along with the lower band at 60kD, similar to the overexpressor lines when the exposure time increases. In addition to this, the bands corresponding to 30 and 35kD are present

Results

and there are more even below 25kD. Furthermore, the band at 45kD is also present. Mutation of the putative catalytic site did not have an effect on the cleavage pattern, confirming previous observations that indicate that MC3 is not self-processed (Fig 2.9). Unspecific bands do not appear when wild-type plants were used as control, demonstrating that the bands observed are most likely cleavage products from MC3 processing (Fig 2.9B).

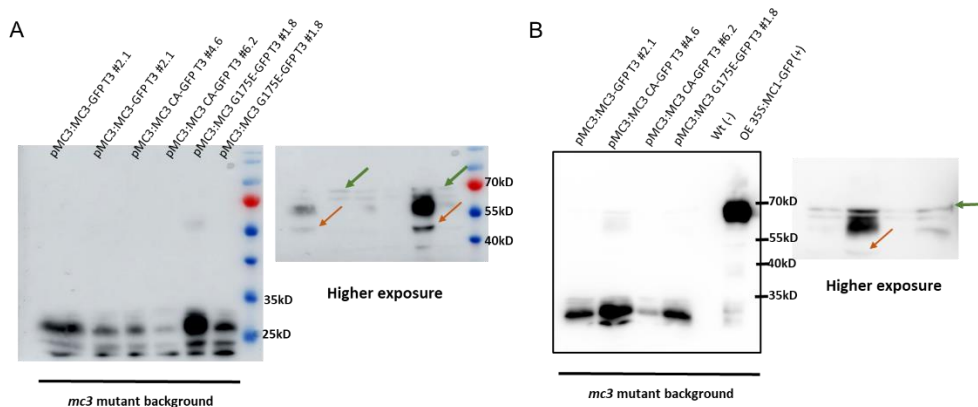


Figure 2.9: The predicted catalytic cysteine is not necessary for MC3 processing. (A) Immunoblot using anti-GFP antibodies of two independent *mc3* pMC3:MC3 T3 lines compared with homozygous *mc3* pMC3:MC3 C230A and *mc3* pMC3:MC3 G175E lines. (B) Immunoblot using anti-GFP antibodies of independent *mc3* pMC3:MC3 T3 lines compared with homozygous *mc3* pMC3:MC3 C230A and *mc3* pMC3:MC3 G175E lines including an overexpressor line of MC1 as positive and wild-type extracted proteins as negative controls.

To conclude, MC3 seems to be cleaved in multiple sites. From our results we can still not conclude which of the different forms of the protein is the active version and/or relevant for the MC3 function. However, our results clearly demonstrate that MC3 is not auto-processed from the predicted catalytic cysteine at position 230, revealing a mode of action that differs from previously characterized metacaspases in plants. Moreover, the mutation of the TILLING version didn't interfere with cleavage events since the pattern of bands observed was identical to the rest lines (TILLING mutant is described in the following section).

Generation of mutants for the MC3 functional analysis

Different approaches to obtain *mc3* mutant lines

To study the function of the protein, two different methods were followed to generate mutant versions. First, a TILLING (Targeting Induced Local Lesions in Genomes) strategy was used where the use of reverse-genetics provides an allelic series of induced point mutations in genes of interest. High-throughput TILLING allows the rapid and low-cost discovery of induced point mutations in populations of chemically mutagenized individuals (Till et al., 2003). The mutation obtained is leading to a single amino acid substitution in position 175 in the proximity of the catalytic histidine. The change is from glycine (Gly) which is ideal for accommodating changes in the polypeptide chain, to glutamic acid (Glu) which is negatively charged and has higher molecular weight (Fig 2.10A). Therefore, the mutation could potentially affect the enzyme in a kinetic level for proteolysis since the surrounding amino acids could either interfere with the active site or affecting the proper folding of the protein domains. To understand the changes in the protein structure, three dimensional models can be useful tools. SWISS-MODEL homology-based structure prediction (Biasini et al., 2014) was used to generate a predicted tertiary structure for the wild type MC3 and the TILLING version of the protein (*mc3* G175E). It is important to mention that the structure prediction might not be directly translated to the actual structure of the protein and therefore it should be tested *in vivo* to be verified any potential interference.

Results

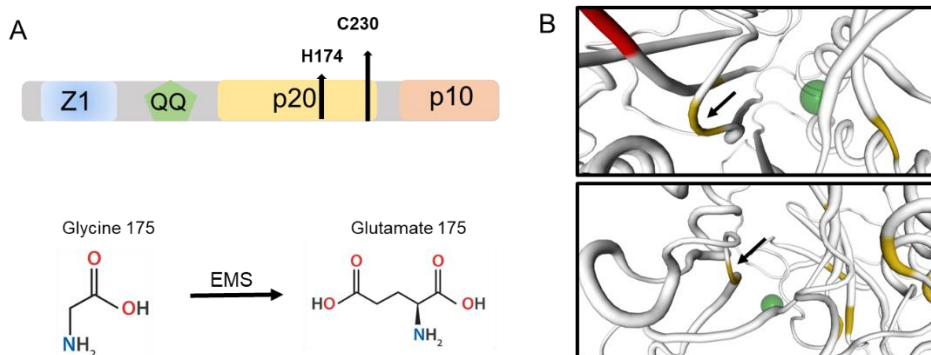


Figure 2.10: 3D analysis of TILLING mutant. (A) Amino acid substitution in the WT version. (B) Top: Prediction for the WT sequence from SWISS-MODEL. In the picture, Cys residues are highlighted by yellow color and a green ball is present where His is located. The Cys 230 is shown by a black arrow. The picture is focused on the catalytic active site (WT; upper panel, *mc3-TIL*; lower panel), highlighting the potential interference of GLU-175 in the catalytic dyad of MC3 G175E and changes in the total protein structure.

Once the mutant is obtained, several backcrosses to wild-type plants are necessary to eliminate background mutations. Homozygous mutants from the M5 generation of backcrosses were used to identify if the phenotypes due to the amino acid substitution in the *MC3* gene. In addition, complementation lines were obtained by transforming a wild-type version of the gene into the mutant background.

In parallel, CRISPR/Cas9 genome editing technology was employed to create specific mutations in the gene of interest (Fauser et al., 2014). The advantage of CRISPR compared to other gene editing methods relies in the fact that the mutations occur in a more controlled way since the targeted sequence is defined. It can cause different point mutations but also deletion of multiple fragments. In this study multiple homozygous lines were obtained with different CRISPR mutations, in which Cas9 had been removed. Two of them were selected to continue with the analysis.

The *mc3* #6.10 mutant possesses a one base insertion, two nucleotides after the triplet that codes for the catalytic cysteine resulting in the appearance of a premature stop codon due to a frameshift at position 236 aa (Fig 2.11). On the other hand, *mc3* #13.3 and #27.1 mutants have deletions of 763 bases spanning

Results

proteases, first a bibliographic analysis was conducted to identify proteases that are co- expressed with MC3 in the phloem. The number of proteases that are upregulated in vascular tissues and especially in phloem is not clear and only a few predicted proteases have been found in phloem sap studies. Lately with single cell sequencing we are beginning to have more detailed information for the expression patterns. Determining the extent to which redundancy obscures the functions of individual proteases within vascular tissues is a challenging task, especially in Arabidopsis that the vascular tissue has limited size. According to a transcriptome study performed some years ago (Zhao et al., 2005) some proteases were found to be upregulated only in the phloem, two subtilases (SBT4.12, SBT4.1), two aspartyl proteases (PASPA2, *At4g33490*) and the metacaspase MC3. Some proteases were also found to be upregulated in phloem and surrounding non-vascular tissue and these too may be important for phloem function. For example, ASPG-1 has been shown to confer drought avoidance when overexpressed by enhancing sensitivity of guard cells to ABA (Yao et al., 2012). From these proteins, four potential candidates were chosen to analyse the differential expression in the *mc3* background separate in the roots and the cotyledons of 7-days old seedlings. The ASPG-1, the cysteine protease At3g45310, which seems to be expressed ubiquitously in the root; the subtilisin-like serine protease SBT4.12 (*At5g59090*), which is involved in stress responses and specifically expressed in the stele (Kuroha et al., 2009; Meyer et al., 2016; Otero et al., 2021). As shown in Figure 2.12B, there is no significant differences in the transcriptional levels of these proteases when MC3 is absent from the plant.

Chapter 2

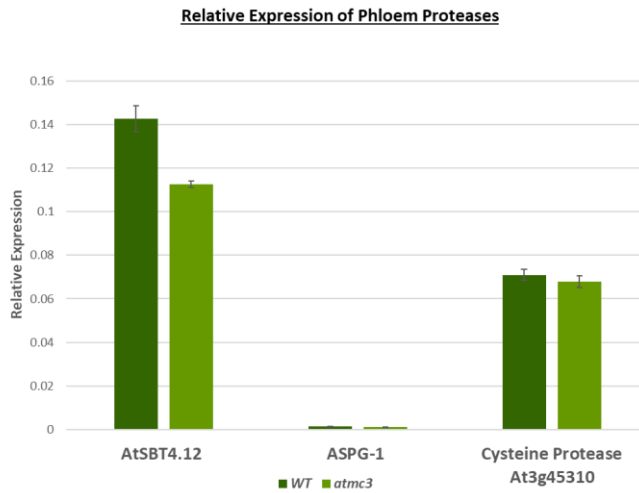


Figure 2.12: Analysis of the proteases co- expressed with MC3 in the phloem tissue. Relative expression analysis of the proteases expressed in the vascular. Roots of 7-days old seedlings were collected. Total RNAs were isolated and reverse-transcribed into cDNAs, which were used for quantitative PCR with primers corresponding to specific regions of *STB4.12*, *ASPG-1* and *At3g45310*. Data are means (\pm SE) of three biological replicates. Significant differences from wild-type within each treatment were determined by Student's t-test: $P < 0.05$.

The rest of metacaspases were also analysed to identify if there is compensatory transcriptional regulation within the family members due to MC3 absence. It has been shown that some of the metacaspases can also have expression patterns in the vascular tissue and that could lead to high redundancy levels. We first decided to analyse the relative expression for all the different metacaspases in the *mc3* mutant which did not show significant changes in the expression levels between *mc3* and wild-type plants. In the mutant plant the levels of *MC3* were also analysed and it was confirmed the absence of expression in the CRISPR line (Fig 2.13). Since metacaspases are regulated by other proteases for activation and

Results

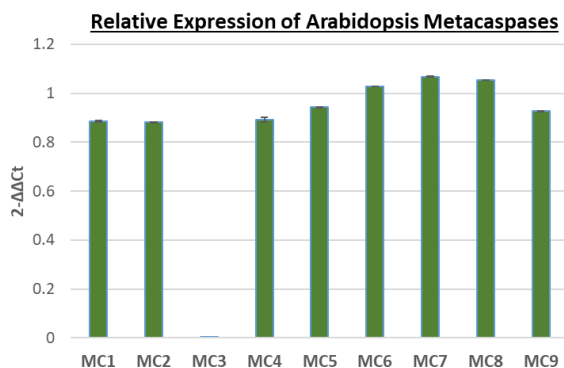


Figure 2.13: Analysis of the metacaspases co-expressed with *MC3*. Relative expression analysis of the 9 metacaspases. Roots of 7-days old seedlings were collected from Wt Col-0 and *mc3* mutant plants. Total RNAs were isolated and reverse-transcribed into cDNAs, which were used for quantitative PCR. Data are means (\pm SE) of three biological replicates. Significant differences from wild-type within each sample were determined by Student's t-test: $P < 0.05$.

some of them need processing to change from the zymogen into the active state, it is possible that the regulation occurs at the translational and not transcriptional level.

Interestingly, we found that MC1-GFP under the control of its endogenous promoter can be detected in the root and the signal is stronger around the vascular tissue (Fig 2.14). This result is more clear in the differentiation zone but also can be visible in the root tip. In addition, MC1 is visible in the last cell before enucleation with a change and an enhanced signal in the differentiated companion cells. The similar localization pattern of MC1 and MC3 could lead to redundant function of the two type I metacaspases. Double mutant of combinations for MC1, MC3, MC4 were created to continue with phenotypical characterization of the *mc3* mutant. MC4 was included because of the ubiquitous expression that displays in the root. For MC1 and MC4 available individual T-DNA insertion lines (*mc4* mutant was kindly provided by Van Breusegem lab) were used to be crossed with the *mc3* #13.3 CRISPR mutant (all in Arabidopsis Col-0 background).

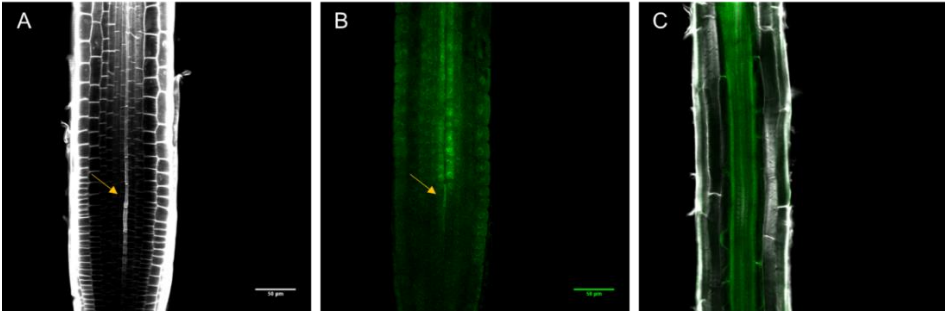


Figure 2.14: Expression pattern of MC1 protein. Translational fusion of MC1-GFP under native promoter (*mc1 pMC1:MC1-GFP*) was monitored by confocal microscopy. Pictures were taken in two different root zones, meristematic (A), (B) and differentiation (C). The GFP green fluorescent signal was co-visualized with calcofluor staining (grey) to reveal protophloem strands. In (A) and (B) are presented the channels separate for easier visualization and in (C) the channels are merged in a single image. Yellow arrows are indicating the last protophloem cell before enucleation. Scale bar, 50 μm .

Results

Phenotypical Characterization of *mc3* mutants

To further characterize the function of MC3 in the plant, general characteristics of the plant life were investigated. For this, the CRISPR mutant lines and complementation lines were compared to their wild-type and overexpressor lines of the protein. In the characterization the double mutants *mc1mc3* and *mc3mc4* were included as well as the TILLING *mc3* mutant. The more obvious macroscopic features of the plant shoot and inflorescences were checked. Seeds were germinated in MS- media and were transferred to soil after 9 days. At 21-days, the rosette leaves were studied. The *mc3* TILLING plant showed inhibited growth, which is reflected by the measured leaf area and the shapes of the leaves that are thinner and helical. The rest of the genotypes didn't show significant differences in their morphology and surface of the leaf area that reaches above 4 cm² for all of them. At 40 days the shoot heights were measured and only *mc3* TILLING (*mc3* G175E) showed a shorter shoot phenotype (Fig 2.15A). Overall, no significant differences were observed between Wt, overexpressor and

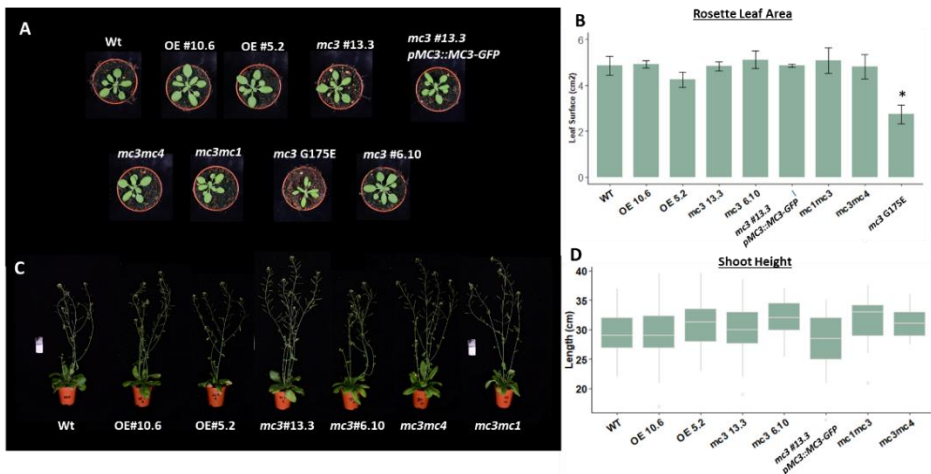


Figure 2.15: Plant phenotypes regarding development upon long day (LD) conditions. (A) Plants were photographed at 3-week-old stage to measure their rosette leaf area. The graph represents the mean value of the surface measured and error bars represent the SE (n>60). (B) Plants were photographed at 40 days. Graph represents the length of the shoot measured (n>40).

CRISPR mutants and surprisingly only the TILLING mutant was severely affected regarding the plant growth.

Furthermore, a phenotypical analysis of the reproductive structures was conducted. When investigating the single flowers from above, as seen in the upper row of Figure 2.16, both the double mutants and the *mc3 G175E* seem to have a more closed organization of the sepals, although presenting an already mature stigma. The *mc3 G175E* mutant showed an elongated and thick carpel with developed stigma visible, but the stamens were very short and not releasing pollen at this stage, whereas in the rest of the genotypes pollen grains were already released. In the third row of the figure there is a brief display of the developing siliques of the respective genotypes. They are presented from older siliques to younger fertilized floral organs, picked from the lower shoot upwards to the inflorescence. Clear differences in elongation were detected in the *mc3 G175E*, which were overall much shorter. When the siliques were opened (last row Fig 2.16), only approximately 1-5 developing seeds were found per silique and most ovules were aborted while the wild-type, CRISPR mutants, overexpressor line and double mutants were filled with seeds. These abortions could be explained by the absence of proper fertilization. Indeed, work with the TILLING mutant was challenging in terms of propagation because of two main reasons: (i) Seeds for experiments were a limiting factor as only little amounts of seeds could be collected per plant; and (ii) crossing with other plants had a low success rate, since the poor pollen quantity (pollen sacs were not dry) made the plant a difficult pollen donor. Altogether, these observations suggest that the self-fertilization in *mc3 G175E* is affected.

Results

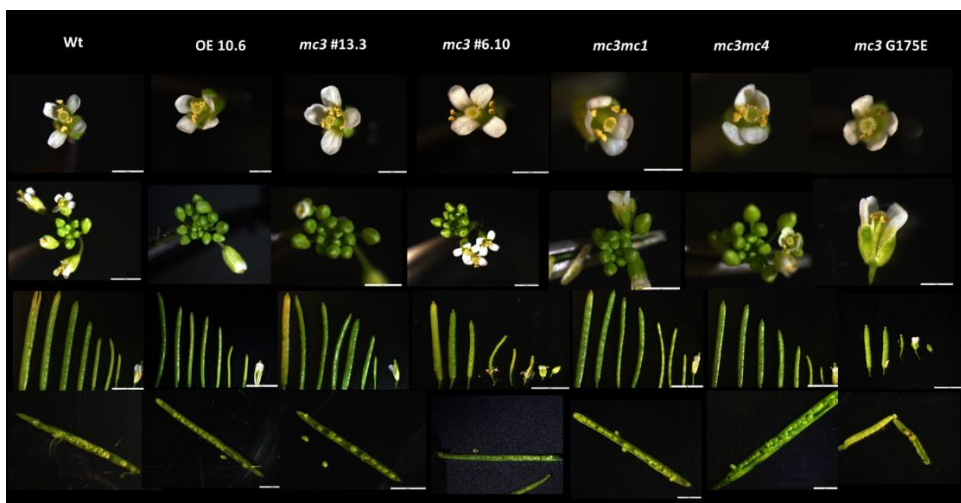


Figure 2.16: Inflorescence, flower and silique phenotypes. Top row shows a single flower from the top, followed by the view of the shoot tip in the middle row. In the third row the siliques are shown, as they develop from the fertilized stigma in younger flowers, displayed from older to younger stage from the left to the right. Bottom rows show opened siliques revealing seed content.

Regarding the macroscopic morphology of the plant, absence of metacaspase 3 in the CRISPR lines, overexpression or combination of two metacaspases absence did not seem to affect the plant development. On the other hand, the TILLING copy severely affected growth. The reason for the controversial phenotypes observed is hard to be determined. A possible explanation could be that in TILLING populations, background mutations are not easily eliminated and can affect another gene that is responsible for the phenotypes observed, despite the multiple backcrosses. In that case, the complemented line should remain affected. From the complementation lines (with *pMC3:MC3-GFP* construct) in the *mc3* G175E background, we obtained multiple lines. At T1 generation some plants have showed recovered phenotype and some kept having the phenotype of the TILLING. Since the complementation was not clear, we introduced the mutated version of the TILLING line of MC3 in the CRISPR background that is lacking MC3 (*mc3*#13.3) and analyse the phenotypes in these plants. The mutation G175E was also analysed in the heterozygous plants to determine if the mutation was dominant. As shown in Figure 2.17, the

heterozygous plants were like WT and the correct copy of the gene possibly contributed to complementation. Transformed CRISPR plants with the wild-type and the TILLING- G175E version were analysed in T2 generation and surprisingly the *mc3* G175 mutant phenotype was not reproduced. The conclusion was that a possible background mutation co- segregating with the one in MC3 could be responsible for the affected plant growth.

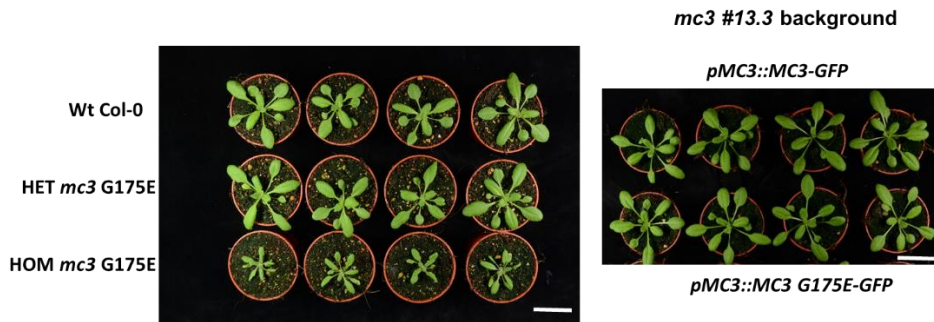


Figure 2.17: Phenotype of 3 week-old plants grown in LD conditions. Left panel shows wild-type plants, heterozygous and homozygous TILLING G175E mutants of MC3. Right panel shows T2 generation of CRISPR plants transformed with *pMC3::MC3-GFP* and *pMC3::MC3 G175E-GFP* constructs. Scale bar 4cm.

For the rest of the experiments of this thesis CRISPR mutants of the line #13.3 were used, as they are knock-out for MC3 (and referred to as *mc3* hereafter). The experiments that include the line #6.10 are indicated specifically.

Flowering time is not affected in *mc3* mutant plants

A crucial moment in the plant life is the decision for the time of flowering. The transition from the vegetative phase to flowering is considered one of the most tightly regulated developmental programs. During evolution, the time of flowering has been adapted to a range of environments to maximize reproductive success, seed production and fitness in general. The two main factors that control the process are the environmental signals and the internal gene pathways (Amasino 2010; Putterill et al., 2004). Plants can perceive light and temperature signals due to an internal core of genes, regulated by the circadian clock. Proteins

Results

of the clock can oscillate in a periodic 24 h waves and regulate their expression in a self- sustainable way.

The importance of the vascular tissue in the photoperiodic regulation of flowering is well known (Endo et al., 2014; Shim et al., 2017). A recent study by (Shimizu et al., 2015) confirmed the importance of the companion cells in the flowering timing control regarding LD or SD photoperiod, whereas the clock genes expressed in the epidermal layer have more crucial roles in regulating the hypocotyl length upon temperature signals. These results suggest that the circadian clock is responsible for different physiological responses depending on the tissue of expression. One of the most important molecules controlling flower regulation is FT (FLOWERING LOCUS T), which is regulated by the transcription factor CO (CONSTANS). FT is synthesized in the leaf companion cells and moves through phloem sieve elements to the shoot apical meristem (SAM) in order to initiate the flowering process. Responsible for the FT transport are two proteins, FTIP1, which is localized in the plasmodesmata and facilitates the movement from CCs to SE and NaKR1, which is responsible for the actual long distance movement of FT through sieve elements to the SAM (Abe et al., 2015; Liu et al., 2012; Song et al., 2015; Zhu et al., 2016).

Using DiURNAL online repository with gene expression data (<http://diurnal.mocklerlab.org>), *MC3* expression was shown to oscillate during the day independently from the photoperiod. The highest expression was detected in morning hours followed by a sudden reduction in the afternoon hours (Fig 2.18A). Regulation of hypocotyl elongation is a well- known response regulated by circadian clock. We wanted to test if the photoperiod and the light intensity affected the hypocotyl length in overexpressor and *mc3* compared to wild-type plants. Seedling were vernalized for 2 days and grown for 7 days in SD conditions in high and low light intensity, respectively. As shown in Figure 2.18B, the hypocotyl length depends on the condition used, but is not significantly affected depending on the genotype tested.

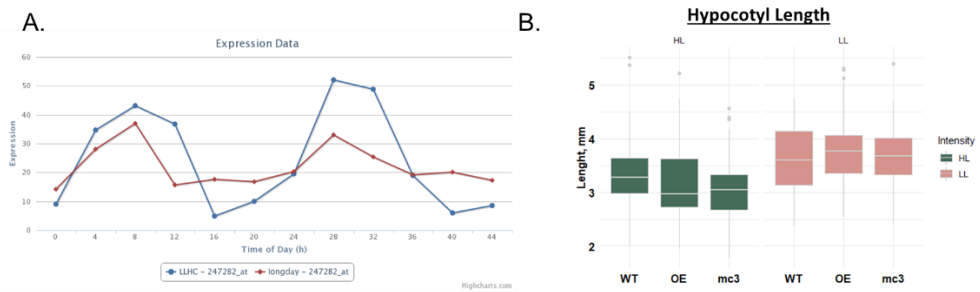


Figure 2.18: Circadian rhythms in *MC3* expression do not affect the hypocotyl length in SD photoperiod. (A) Expression data from DiURNAL. LLHC refers to continuous light (blue line) and LD- long day conditions (red line). (B) Seedlings were grown in SD conditions at 22°C for 7 days in High (HL) and Low (LL) light conditions. Boxplots are indicating the length of the hypocotyls of 7-days- old seedlings grown in SD (8h light/16h dark) conditions. HL stands for High Light intensity (170 $\mu\text{mol}/\text{m}^2/\text{s}$) and LL for Low Light intensity (50 $\mu\text{mol}/\text{m}^2/\text{s}$).

To investigate the putative connection between *MC3* and floral emergence, we analysed the transition from vegetative to flowering stage in all the different genotypes. Two different characteristics were used to determine the flowering time. First, the days that the plants needed to bolt or the first flower to appear and second, the number of the rosette leaves above 0.5 cm were counted the day of bolting/flowering. Our results showed that *mc3* plants reach the flowering stage earlier than the rest of the genotypes, although the total number of the rosette leaves is not different. The complementation of the *mc3* mutant plant with *MC3* under the endogenous promoter is able to bring the flowering time to wild-type levels, whereas overexpression of the protein did not affect the transition at all. Interestingly the double mutants *mc3mc1* and *mc3mc4* were the last to flower, also by not displaying significantly altered number of rosette leaves (Fig 2.19). That could indicate that although the developmental stage at which the plants are flowering is not different between the genotypes, but *mc3* reaches that stage earlier than the rest.

Results

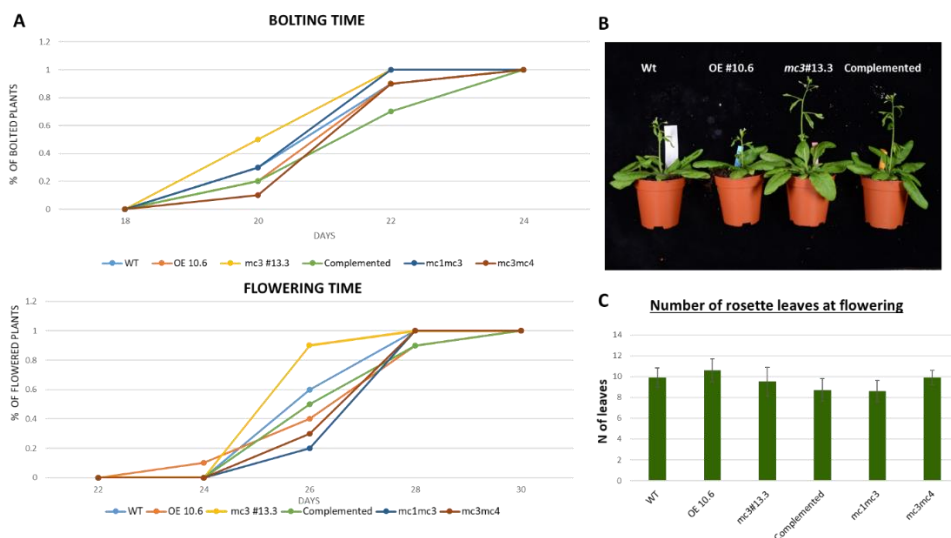


Figure 2.19: Analysis of the flowering time upon LD conditions. The experiment was repeated at least 3 times (N of plants >10 per replicate) with similar results. The graphs are representing a representative replicate. (A) Representation of the number of plants bolted (upper panel) and flowered (lower panel) over time. (B) Four-week-old plants of MC3 variant backgrounds, Wt, overexpressor, *mc3* and the complemented line (*mc3 pMC3:MC3-GFP*), grown in LD conditions. (C) Number of rosette leaves the day that the plants were counted as flowered.

MC3 does not severely affect phloem formation

Since MC3 showed a phloem-specific expression pattern, phloem formation was investigated in detail to detect phenotypes that could be caused by the absence of the protein. Reported phenotypes associated with incorrect phloem differentiation are among others, short roots, incomplete cotyledon venation pattern and gap cells appearing in the phloem strand (Gujas et al., 2017; Ruiz Sola et al., 2017; Wallner et al., 2017). Since phloem is responsible for the transport of photosynthetic products and signalling molecules, multiple changes in gene expression can be detected if the tissue is not properly functional (Bishopp et al., 2011; Yoo et al., 2013). Therefore, defects in phloem development can have a systemic adverse impact on the root meristem and root growth in general. In addition to gap cells phenotype, mutants of genes involved in phloem formation display defects in cell division and elongation during

Chapter 2

embryogenesis—cells divide in a position where they would normally undergo elongation (Truernit et al., 2012). Long-distance transport is also impaired, and auxin transport from fully differentiated SEs to immature SEs is affected as well, leading to a secondary phenotype in the meristem in which the division that gives rise to meta-/proto-phloem sieve elements occurs at a lower frequency (Rodriguez-Villalon et al., 2014). The increase in number of lateral roots observed in phloem-defective mutants has been attributed to the accumulation of auxin at higher regions due to the impaired long distance transport. Similar phenotypes have been reported in *brx*, *cvp2 cvl1*, and CLE45-treated roots (Depuydt et al., 2013; Rodriguez-Villalon et al., 2014; Scacchi et al., 2009).

First, the cotyledons venation pattern was investigated. Cleared cotyledons revealed the vascular vein structure. All genotypes checked showed a complete four loop pattern without disruptions of the vascular (Fig 2.20A). Also, root length was analysed to identify differences in the first days of development. Overexpression line and the *mc3* knock out mutant were the two lines with significantly longer roots in comparison to the rest of the genotypes that didn't show any difference. The complementation line of the *mc3* was, as expected, similar to wild-type plants. Lateral root (LR) formation was also analysed, measuring the number of visible LR emerging in wild-type, *mc3* and overexpressor lines. Three independent replicates of 7-days old seedling roots were measured under the stereoscope. No significant differences were detected among the lines (Fig 2.18D).

Results

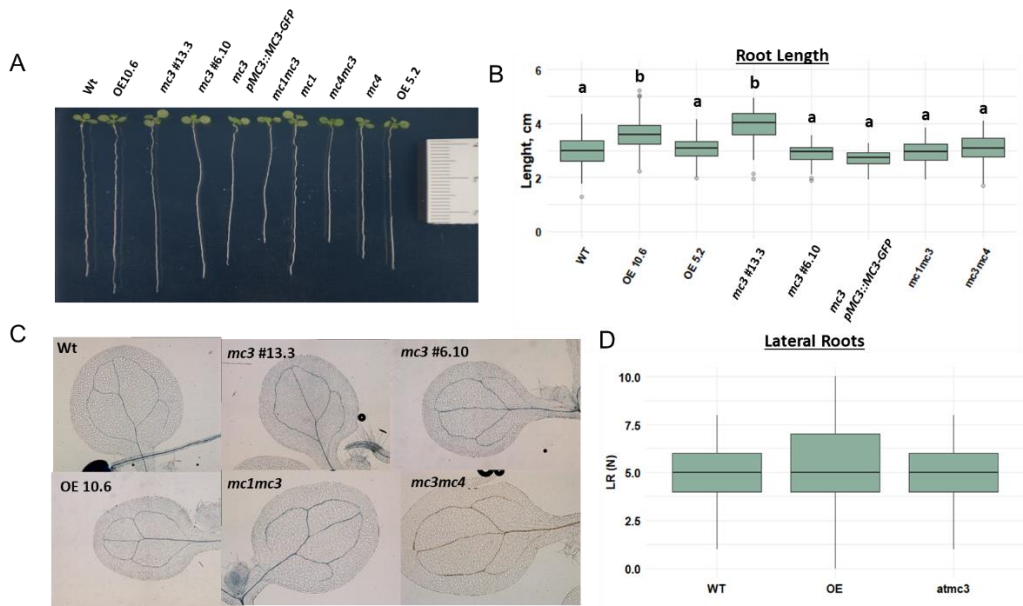


Figure 2.20: Phloem related phenotypes to detect developmental defects in the vascular formation. (A) Picture of 7-day-old seedlings of wild-type, two overexpressor lines, two CRISPR *mc3* mutants, *mc1mc3*, *mc3mc4* and the individuals *mc1* and *mc4*. Seedlings were grown in MS media under LD conditions. (B) Boxplots indicate the distribution of the 7-day old root length. (C) Cotyledon vein pattern comparing wild-type, overexpressor of MC3, double mutants and *mc3* single mutant. (D) Measurements of the amount of visible lateral roots for each genotype.

In the root of Arabidopsis, stem cells are organized in a stem-cell niche at the apex of the root meristem generating transit-amplifying cells, which undergo additional division in the proximal meristem and differentiate in the elongation/differentiation zone. For meristem maintenance, and therefore continuous root growth, the rate of cell differentiation must equal the rate of generation of new cells. This balance is maintained by the antagonistic effects of cytokinin, which promotes cell differentiation, and auxin, which promotes cell division. Cytokinin antagonizes auxin in a specific developmental domain (the vascular tissue transition zone) from where it controls the differentiation rate of all the other root tissues. Owing to a stereotyped division pattern, columns or files of

Chapter 2

cells develop, in which the spatial relationship of cells in a file reflects their age: younger cells lie near the root tip; older cells are higher up in the root. Therefore, all developmental stages are present in every root and anatomy reflects ontogeny. The Arabidopsis root can be viewed as a set of concentric cylinders: epidermis, cortex, endodermis and pericycle surrounding the vascular tissue in the middle of the root. The epidermis is made up of two different cell types, hair and non-hair, organized in contiguous cell files. The inner tissues are all composed of a single cell type (Benfey and Scheres 2000). Root meristem size can be measured as the number of meristematic cortex cells in a file extending from the QC to the first elongated cell excluded. The cortex is the best suitable tissue to count meristematic cells because it is composed of a single cell type and

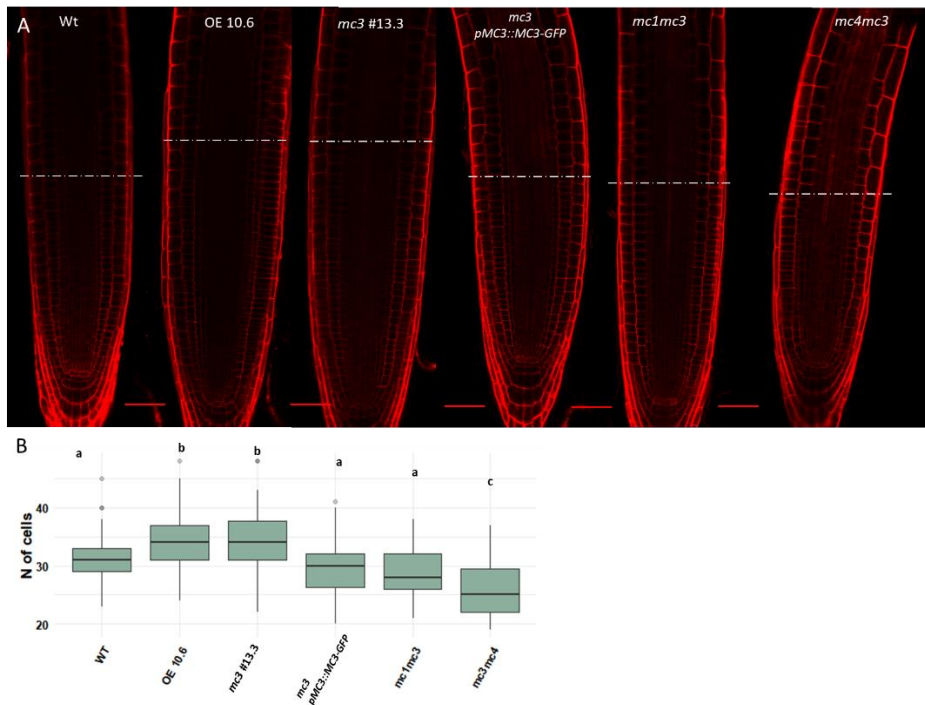


Figure 2.21: Meristem size in different MC3 backgrounds (A) Confocal images of 6-day-old wild-type, overexpressor, *mc3* mutant, complemented line and double mutants stained with PI. Arrows indicate the boundary between the proximal meristem and the elongation zone of the root. Scale bars: 50 μ m. (B) Meristem cell number at 6 days after germination. Four independent replicates were analysed (n of roots >20 per replicate).

Results

its cell number is constant between different roots. Inner tissues are difficult to count owing to their smaller size. To determine meristem size, 6-day-old seedlings were used for measurements. The overexpressor and the mutant showed a bigger meristematic zone with a difference of 4-5 cells compared to the wild-type (Fig 2.21), which may explain the longer size of the root that was observed in these lines.

From all the experiments performed, we concluded that MC3 does not cause any severe developmental phenotype related to phloem development. Taking into account the specificity of the protein expression and the fact that *mc9* mutant also does not display any developmental phenotype in the plant but was found to be responsible for the *post-mortem* tracheary element clearance to form xylem tissue (Bollhöner et al., 2013), we speculated that MC3 might have a specific role in the phloem terminal differentiation or in the identity of the phloem cell lines that requires additional experiments for detection. To be able to study the pattern of the formation, crosses between the *mc3* #13.3 and different PSE markers such as COTYLEDON VASCULAR PATTERN 2 (CVP2) and CC markers such as SUCROSE-PROTON SYMPORTER 2 (SUC2) were made. Homozygous for the mutation and the marker seedlings were grown in MS media for 6 days before confocal analysis and the marker line *pCVP2:NLS-Venus* or *pSUC2:GFP* were used as control. We didn't observe any defects in the progression of protophloem continuity, a notion confirmed by the continuous expression of the protophloem specific identity marker CVP2 or any defect that could lead to defects in transport from surrounding CCs as SUC2-GFP signal was distributed in the root tip (Fig 2.22).

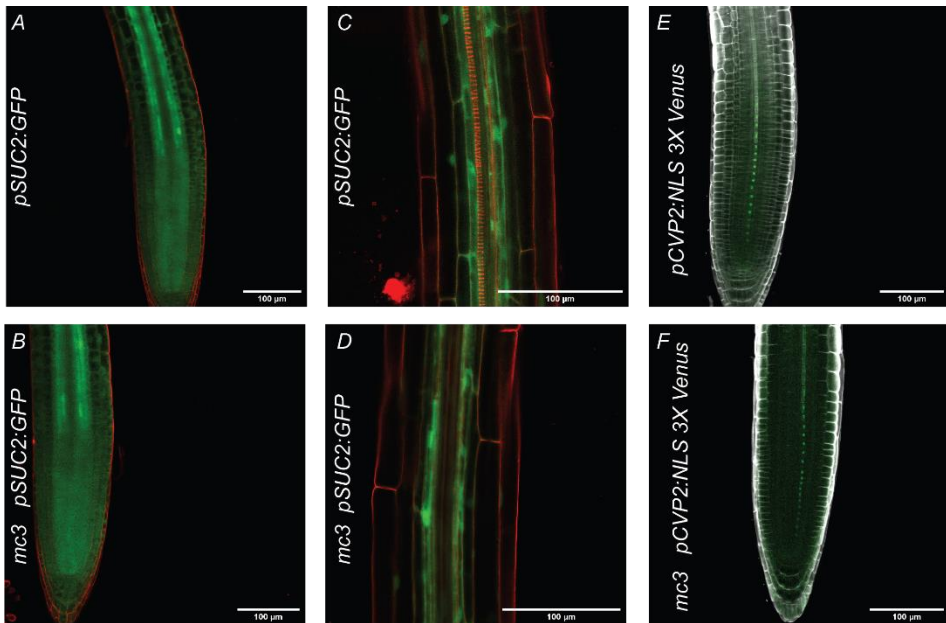


Figure 2.22: MC3 does not affect the identity of vascular cells. (A- D) 6-days old seedlings of marker line *pSUC2:GFP* and *mc3* mutant line crossed with the marker. PI staining, scale bar 1000μm. In (A) and (B) the root tips of 6-day-old seedlings of marker line are shown in (A) and the mutant crossed with the marker line in (B). In (C) the upper part of the root of the marker line is shown and (D) shows *mc3* crossed with the marker. (E), (F) Root tip from 6-day-old seedlings of marker line *pCVP2:NLS-3X Venus* (E) and *mc3* mutant line crossed with the marker (F). Calcofluor staining, scale bar 100 μm.

Proteome Analysis

Identifying the proteome of a group of cells or a tissue has always been a challenging process. With advanced technologies in recent years, several proteomic methodologies have been developed that can make possible to identify, characterize, and comparatively quantify the relative level of expression of proteins that are co-expressed.

Two different strategies can be followed to identify the composition and the dynamics of the proteome, called bottom-up and top-down approaches. In the bottom-up approach, commonly referred to as shotgun proteomics because of its similarity to shotgun sequencing as used in genomics (Claassen et al., 2012), a

Results

protease such as trypsin is used to cleave a protein mix, followed by fractionation by liquid chromatography (LC), and then Mass spectrometry (MS) analysis. Then the peptide identification algorithm reports a set of peptide-spectrum matches (PSMs) by searching the MS/MS spectra against a protein database. From these peptide identifications, the existence of proteins is detected with protein inference algorithms and the relative or absolute abundances of proteins are calculated with protein quantification approaches. (MS)- based shotgun proteomics is widely used to identify precursor proteins in a sample and quantify them. The disadvantages of the technique are that the homologous proteins or alternative splicing products can mislead the analysis. Also, during the experiments most of the PTM are lost, which makes it challenging for the protein identification. In the top-down approach, intact proteins are characterized by MS without previous proteolysis treatment. This type of approach although it provides larger sequence coverage, resolution of sequence ambiguities, and preservation of PTMs, however, is technically more challenging, so it is not widely used. Some of the shortcomings of the bottom-up approach have been overcome by the development of computational methods and use of data repositories to facilitate the identification of peptides. Technology advances are also implemented to reduce the time of the analysis. Recently it was shown that the use of gas separation instead of LC reduces significantly the time of peptide quantification (Meyer et al., 2020).

Since the phenotypical analysis did not show severe developmental defects in the plants described and MC3 is predicted to be a protease, which may affect the levels of the proteome, we analysed the protein abundance and changes caused depending on the levels of MC3 present. Also, substrate analysis techniques can provide useful insights into the role of a particular protease.

Proteome Composition Analysis in Leaf tissue

To understand better how the plant behaviour is affected by MC3 we wanted to get a global view of protein differential abundance. Ideally, phloem

Chapter 2

proteomes would have been analysed. We considered several techniques to enrich in phloem cells, but they all proved too challenging and/or did not yield sufficient protein levels for proteomic analyses. Therefore, we used leaf samples. Proteomes extracted from four biological replicates of leaf samples from 3-week old wild type, overexpressor and *mc3* knock out mutant plants were analysed. A label-free quantitative mass spectrometry was performed and allowed the identification of a total of 2970 proteins (Supplementary Table 1). This included MC3, which highly accumulated in the overexpressor line, but its abundance was below the detection limit in the wild-type and mutant line, as indicated by intensity-based absolute quantification (iBAQ) values. In the case of wild-type this could be explained by the tissue-specificity of the protein, which can lead to a reduction of the signal from CCs of the vasculature when the whole leaf sample is collected. The quantitative proteome analysis further indicated changes in proteome composition in MC3 transgenic plants, although only 225 of the 2970 quantified proteins exhibiting significant differences in abundance (ANOVA with T-test, p -value <0.05 , followed by Tukey's honest significance test). Because of the small number of significant protein differences, we decided to compare the genotypes pairwise. The proteins that came up statistically significant and with a fold change higher than 50% between the comparisons are showed in Table 2.

Results

Table 2: Proteins with a fold change higher that 50% between the comparisons, statistically significant. In the table is presented the gene name, the locus in the genome, fold change (FC) in the dual comparison performed and significance. In the last column is presented the biological function associated, according to TAIR database.

Gene names	Gene names (ordered locus)	T-test Signifi		T-test Signifi		T-test Signifi		Gene ontology (biological process)
		FC	oe_ko	FC	wt_ko	FC	oe_wt	
PNSL2	At1g14150	4.69 +		3.50 +		1.19		photosynthetic electron transport chain
T14P8.18	At1g02816	3.34 +		0.00		3.63 +		
F11M15.26	At1g51400	3.28 +		2.65		0.63		response to ozone, UVB, wounding
PAPP2C	At1g22280	2.97 +		0.00		1.66		protein dephosphorylation, red light signaling pathway
ECA4;ECA1	At1g07670	2.29 +		1.78 +		0.51 +		calcium ion transmembrane transport, transport, homeostasis
At5g16400	At5g16400	1.89 +		1.81 +		0.08		cell redox homeostasis, response to light intensity
AtMC3;MC3	At5g64240	1.88 +		0.00		2.46 +		
QEP37	At2g43950	1.64 +		0.00		1.05		cation transport
F23H11.27	At1g59960	1.56 +		0.00		1.61 +		
UREG	At2g34470	1.51 +		1.55 +		-0.04		nitrogen compound metabolic process, positive regulation of urease activity
F3C3.6	At1g32160	1.04 +		1.21		-0.18		
RPS29A	At3g43980	0.88 +		0.36		0.52		translation
At5g22580	At5g22580	0.87 +		0.68 +		0.19		
At1g27752	At1g27752	0.74 +		0.00		0.50		
At5g19860	At5g19860	0.71 +		0.63 +		0.09		
At2g27290	At2g27290	-0.90 +		-0.09		-0.82		
F27H5_130	At3g60340	-0.97 +		-0.35		0.00		
GAE1-6	At1g02000	-1.34 +		-0.25		0.00		carbohydrate metabolic process;cellular response to hypoxia;defense response to fungus, Gram negative bacteria
CML20	At3g50360	-1.55 +		-0.35		0.00		abscisic acid-activated signaling pathway involved in stomatal movemen
SMT2	At1g20330	-1.56 +		-0.46		-1.09		multidimensional cell growth;negative regulation of DNA endoreduplication ;xylem and phloem pattern specification
At3g15095	At3g15095	-3.43 +		-1.10		0.00		process;sterol biosynthetic process
AVA-P4	At1g19910	1.13		-2.74 +		3.87 +		photosystem II assembly
At1g32550	At1g32550	0.88		-2.10		2.98 +		
At3g43540	At3g43540	0.90		-1.25		2.15 +		
AtMC6	At1g79320	0.70		-0.24		0.94 +		
GLP1	At1g72610	-0.29		0.56		-0.85 +		
GASA1	At1g75750	-0.14		0.95 +		-1.09 +		gibberellic acid mediated signaling pathway, response to abscisic acid, response to brassinosteroid
RAD23C	At3g02540	-0.73		0.44		-1.17 +		proteasome-mediated ubiquitin-dependent protein catabolic process
RPS15D	At5g09510	-0.46		0.92		-1.38 +		ribosomal small subunit assembly
CML10	At2g41090	-0.63		0.84		-1.47 +		cellular response to hypoxia, cellular response to oxidative stress, regulation of L-ascorbic acid biosynthetic process
KIN2	At5g15970	0.00		1.55		-2.45 +		response to abscisic acid, response to osmotic stress, response to water deprivation
At2g43770	At2g43770	1.69		2.82 +		-1.13		
PAE12	At3g05910	0.00		2.39 +		-1.03		cell wall organization
At5g16400	At5g16400	1.89 +		1.81 +		0.08		cell redox homeostasis;response to light intensity
RABE1D;RABE1E	At3g09900	-0.19		-1.31 +		1.12		protein secretion;regulation of exocytosis
At2g25950	At2g25950	-0.47		-1.61 +		1.14		
At5g14120	At5g14120	-0.52		-2.14 +		1.62		
GDH2	At2g35120	-0.91		-2.82 +		1.91		glycine decarboxylation via glycine cleavage system

Comparison of overexpressor vs wild-type (Supplementary Table 3):

A protein that was found upregulated in both overexpressor and mutant lines in comparison to the wild-type plants is the plasma membrane V-ATPase (AVA-P4), which can have a role in signalling transport (Ratajczak 2000). Most of the differentially abundant proteins were of uncharacterized biological function. Significantly downregulated in the plants over-accumulating MC3 was KIN2 which responds to ABA and cold and reduces osmotic stress tolerance (Kurkela and Borg-franck 1992), but also CML10 which was found to be expressed quickly

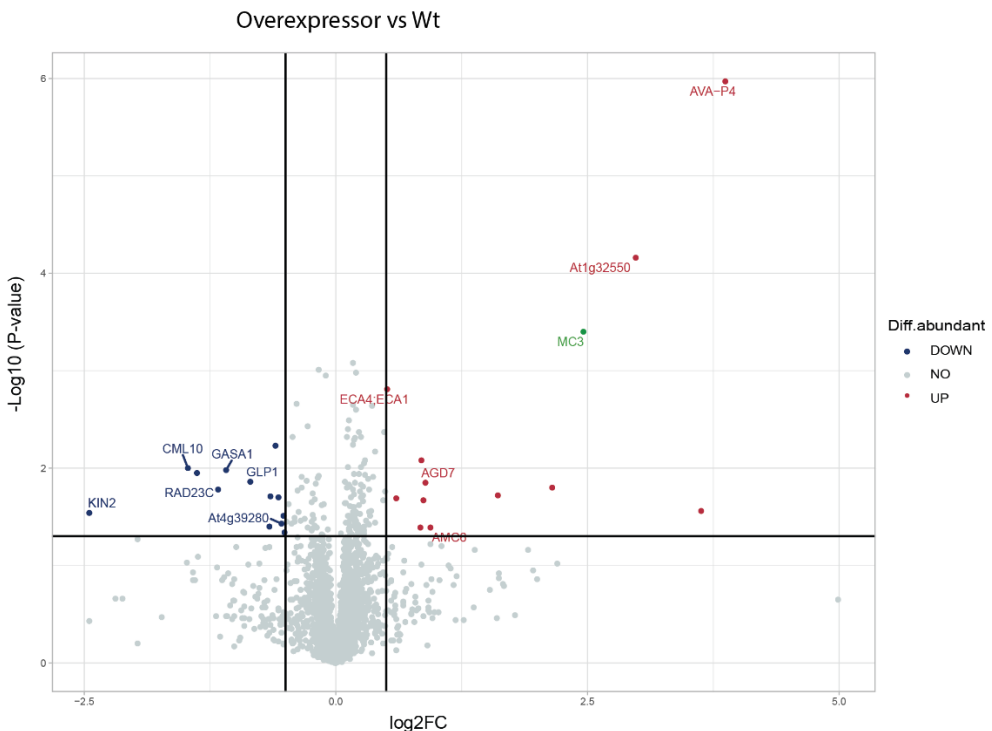


Figure 2.23: Identification of differentially abundant proteins in overexpressor compared with wild-type plants. Volcano plots shows the relation between the log₁₀ p-value and the log₂ fold change for the compared lines. Peptides with significantly reduced or increased abundance are considered those having $-\text{Log}_{10}(\text{P-value}) > 1.3$ and $\text{log}_2 \text{FC} < -0.55$ or > 0.55 respectively and are highlighted with blue and red colour.

following exposure of the plant to hypoxic conditions. CML10 might be also related to several responses for long-term persistent stresses (Cho et al., 2016).

Results

Another interesting downregulated protein is GASA1 that responds to hormones as ABA, GA and BRs (Bouquin et al., 2015).

Comparison overexpressor vs *mc3* mutant (Supplementary Table 2):

Upregulated proteins were divided in groups showing differential expression only in both overexpressor vs mutant and overexpressor vs Wt but not between mutant and Wt. That could be explained as differences observed because of very high upregulation of MC3. The second category includes proteins following a similar pattern of higher abundance in the comparisons attempted (Overexpressor>Wt, Overexpressor >*mc3* mutant, Wt> *mc3* mutant).

In this first category we found proteins with unknown function, but also PAPP2C which phosphorylates PIF3 in response to light stimuli (Phee et al., 2008), At2g43950 responsible for the chloroplast ion channels and At1g59960 an NADPH oxidoreductase. In the second category we found significant for the two comparisons the proteins PNSL2 which is a component of the chloroplast membrane and regulates the electron transport chain, ECA1; ECA4 which is responsible for protein trafficking and response to ion imbalances (Ca²⁺) (Nguyen et al., 2018) and At2g34470 for urea catabolism. From these proteins we could not conclude anything specific for the MC3 function.

On the other hand, downregulated in the overexpressor was the SMT2 protein, a sterol methyl transferase 2, which is one of the key enzymes of brassinosteroid biosynthesis in *Arabidopsis thaliana* (Chung et al. 2010). SMT2 has a crucial role in balancing the ratio of C28 (CR) and C29 sterols (sitosterol) (Schaeffer et al., 2001). *smt2* mutant showed discontinued vein cotyledon pattern. Additionally, CML20 is expressed in lower levels only in overexpressor line. Mutants of this protein exhibit enhanced sensitivity to ABA and increased drought tolerance (Wu et al., 2017). Finally, At3g15095 (Serine-Threonine kinase like protein) is responsible for the assembly of the photosystem II.

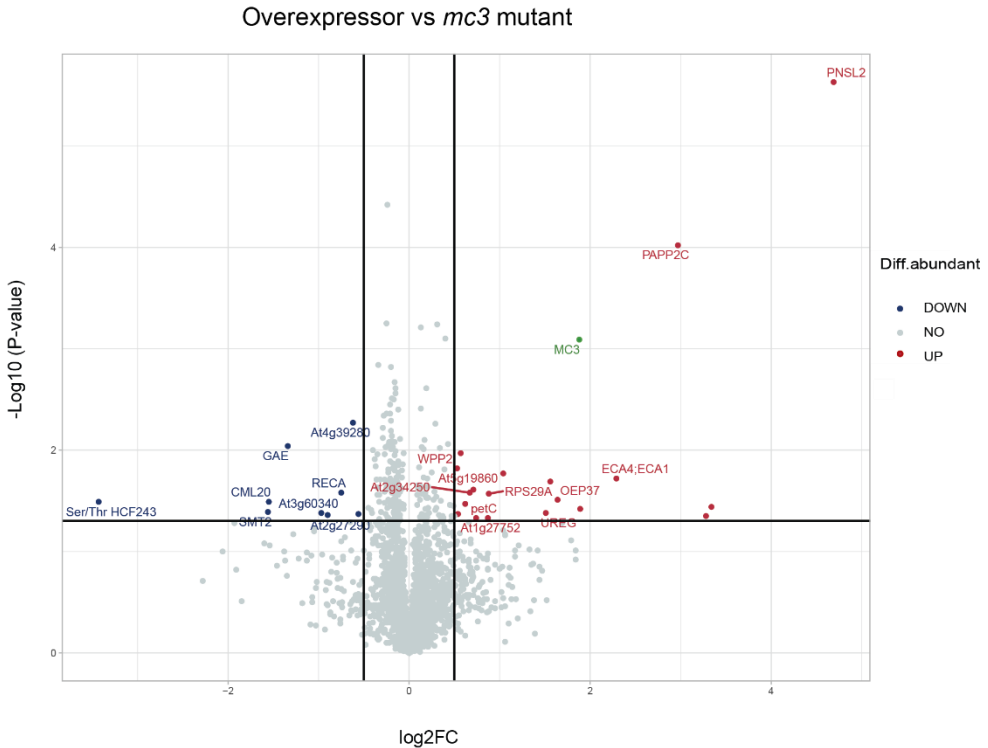


Figure 2.24: Identification of differentially abundant proteins in overexpressor compared with *mc3* mutant plants. Volcano plots shows the relation between the log₁₀ p-value and the log₂ fold change for the compared lines. Peptides with significantly reduced or increased abundance are considered those having $-\text{Log}_{10}(\text{P-value}) > 1.3$ and $\text{log}_2 \text{FC} < -0.55$ or > 0.55 respectively and are highlighted with blue and red colour.

Comparison wild-type- *mc3* mutant (Supplementary Table 4):

In the upregulated proteins we detected also the At2g34470 (UREG) for urea catabolism and GASA1. This is only upregulated in Wt and less expressed when MC3 is highly abundant or absent. ECA4 is also more expressed in overexpressor and Wt in contrast to the mutant and is important for the Ca²⁺ signals transport which can facilitate stress signals responses. Photosynthesis-related peptides were also upregulated. Finally, TRXF2 was also found upregulated, which is localized in the chloroplast and *trxf2* proteomic analysis showed defects in processes such as metabolism, photosynthesis and stress related responses. Importantly, ferredoxin NADPH was found to be negatively affected in the *trxf2*

Results

mutants, which is consistent with our results (Fernández-Trijueque et al., 2019). Downregulated proteins in the wild-type plants did not show any specific category of biological function.

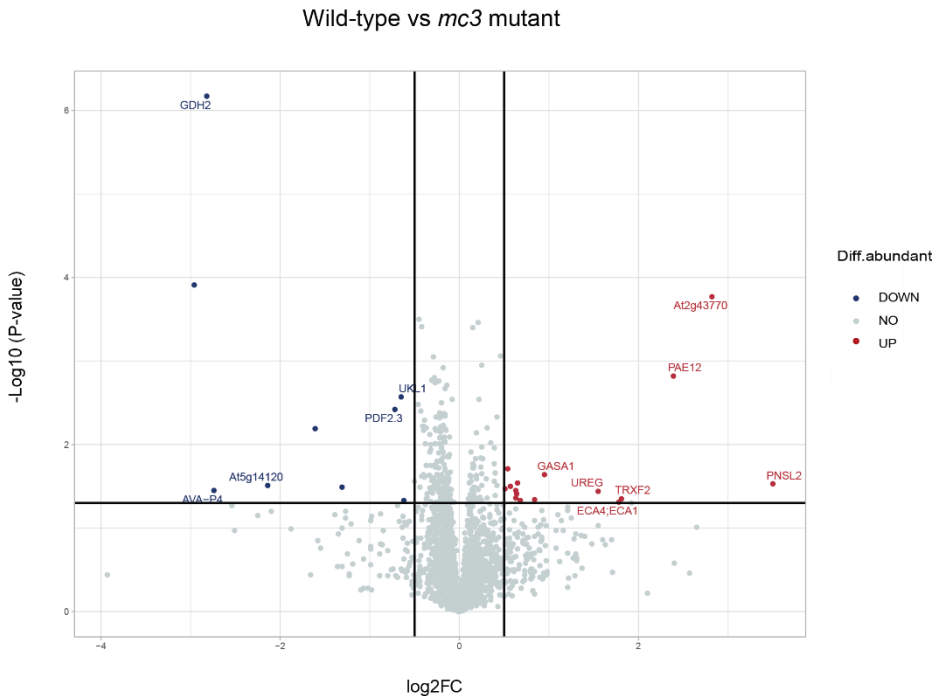


Figure 2.25: Identification of differentially abundant proteins in wild-type compared with *mc3* mutant plants. Volcano plots shows the relation between the log₁₀ p-value and the log₂ fold change for the compared lines. Peptides with significantly reduced or increased abundance are considered those having -Log₁₀ (P-value) > 1.3 and log₂ FC < -0.55 or > 0.55 respectively and are highlighted with blue and red colour.

N-terminome analysis

Proteases can be particularly challenging to study because of the high levels of redundancy among family members mentioned above. Despite the amount of proteases and proteolytic events discovered in plant species, only a few connections protease-substrate have been identified. Furthermore, many proteases are regulated at multiple levels, transcriptionally, translationally and post-translationally. To gain knowledge regarding the protease function,

Chapter 2

identification of the substrate is an important step. *In vitro* studies have managed to find and verify the responsible protease for a substrate cleavage using the correct treatments and controls (such as protease inhibitors) function to prove the connection. Unfortunately, not all the proteases are easily purified or secreted and *in vivo* analysis requires more different approaches to overcome the limitations such as overexpression, loss of function, specific inhibitors (Overall and Blobel 2007).

Targeted quantitative analysis of protein termini identifies precise cleavage sites in protease substrates with exquisite sensitivity and dynamic range in *in vitro* and *in vivo* systems. The most used strategies nowadays are the following approaches: COmbined FRActional DIagonal Chromatography (COFRADIC), Terminal Amine Isotopic Labeling of Substrates (TAILS) and High-efficiency Undecanal-based N-Termini EnRichment (HUNTER) (Canbay and auf dem Keller 2021; Kleifeld et al., 2010; Savickas et al., 2020; Staes et al., 2008; Weng et al., 2019). In contrast with most proteomic approaches, HUNTER is a proteomics technology that replaced precipitation-based protein purification by reversible high-efficiency binding to hydroxylated magnetic beads that allows a robust, sensitive and scalable method for the analysis of previously inaccessible microscale samples.

Here, this so-called N-terminome consisted of all peptides that possessed the mature protein N termini and the neo-N-termini that had been generated upon proteolysis by MC3. We analysed the *in vivo* N-terminome in leaves from 3-week old plants of wild-type, MC3 overexpressor line and loss-of-function *mc3* mutant plants using four independent replicates. By mass spectrometry were identified approximately 1600 N-terminal peptides, with 409 dimethylated peptides representing N termini with free α -amines *in vivo* (Supplementary Table 5).

From the peptides identified we examined those that fell into the non-canonical produced peptides and were dimethylated. The canonical peptides resulted from the analysis normally contain post-translational modifications (such as methionine cleavage from the N-termini of the protein), cleavage of signal peptides, alternative translation initiation sites and protein maturation events. The non-canonical peptides are those that will contain the substrate cleavage. In

Results

addition to this, acetylated peptides are most likely by-products of the treatments and the dimethylated are those which arise from proteolytic events (Perrar et al., 2019). To determine significantly altered protein termini abundance that may indicate differential cleavage between two genotypes, we excluded the acetylated peptides and focused only in the differences observed in the dimethylated ones. The threshold of important change in abundance was set at 0.6 log change (more than 60% abundance) and the peptides were filtered for this difference supported by a LIMMA-moderated t-test (P -value <0.05). Dual comparisons were again made to identify changes between different backgrounds and test consistency since we are looking for a possible substrate candidate.

Application of these criteria to compare plants with highest and lowest abundance of MC3 (overexpressor Vs mutant), identified only a few N-terminal peptides with significant changes (Fig 2.26 and Supplementary Table S6), most of them belonging to plastid proteins. Positional analysis showed that in all of them the amino-acid in P1 position was an R, which is the cleavage preference identified for metacaspases. The most visible and consistent difference found was GLU1, a ferredoxin dependent glutamate synthase that is expressed highly in leaves and more specifically in the phloem CCs-SEs complex as well as in the mesophyll. Recently it was shown that GLU1 helps the plant with iron deficiency (Cui et al., 2020). In our dataset this protein appeared in all the comparisons performed and was detected in higher levels in the *mc3* mutants, less in the wild-type plants and even less in the overexpressor. Regarding other peptides, At5g01260 is coding for a protein that was more abundant in the mutant in comparison to the overexpressor and has been associated with starch binding processes. In contrast, more peptides of the plastid protein *rbcL* were detected in the overexpressor, an indication that photosynthesis might be affected, although *rbcL* is also involved in ABA responses apart from photorespiration.

Chapter 2

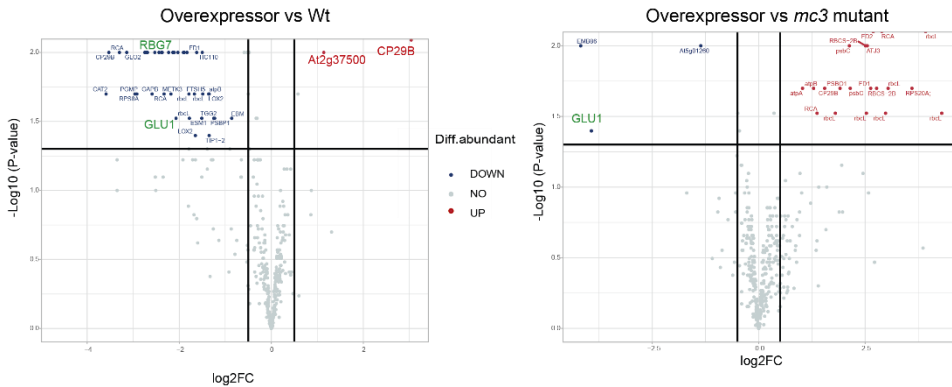


Figure 2.26: Identification of differentially abundant N-termini peptides in the different genotypes. Volcano plots shows the relation between the log₁₀ p-value and the log₂ fold change for the compared lines. Peptides with significantly reduced or increased abundance are considered those having -Log₁₀ (P-value)>1.5 and log₂ FC<-0.55 or >0.55 respectively and are highlighted with blue and red colour. With green colour letters are indicated the down-regulated peptides that they behave consistent in the dual comparisons.

In the comparisons between wild-type and mutant or overexpressor and wild-type (Fig 2.26, Supplementary Tables S7;8) the results were in the majority similar. A candidate-peptide that appeared significantly upregulated only in the wild-type is RBG7, which is related to stomatal movement and responses to osmotic stresses. Expressed highly in guard cells and subcellularly in the cytoplasm, is highly induced by cold environments. RBG7 seems to promote stomatal opening and reduce tolerance under salt and dehydration stress conditions, but promotes stomatal closing and thereby increases stress tolerance under conditions of cold tolerance (Kim et al., 2008). Surprisingly, most of the photosynthetic proteins from the plastids that were detected higher in the overexpressor when compared to the mutant, in this comparison show higher abundance in the wild type plants. Due to this inconsistency, we decided to consider these proteins as noise from the experimental execution. Higher abundant in the overexpressor we detected for CP29B which is a chloroplast RNA-binding protein. From transcriptomic and proteomic available data, it has been detected in phloem exudates and shows response to ABA signalling.

Results

Overall, the amount of N-terminal peptides detected was sufficient to consider the experiment valid, but the significant changes between the MC3 backgrounds did not provide any strong candidate to consider as a direct proteolytic cleavage mediated by the protease. Peptides that were more present in the overexpressor could appear because of higher cleavage events, hence the lack of MC3 leads to less peptide detection in the mutants. Most of these peptides though belong to proteins localized in the chloroplasts, which did not coincide with MC3 subcellular localization and could be a consequence of indirect changes in N-terminome.

Proteomic Analysis in root tissue

We tried to perform the same N-termini analysis taking only root samples of 7-days old seedlings in order to avoid masking the effect of the protease from the total amount of proteins that can be detected in leaf samples since the expression of MC3 is very specific for the CCs. Unfortunately, HUNTER did not provide robust results. On the other hand, a step before the final collection of N-termini, a sample was extracted from the analysis that allows efficiency calculations and detection of protein abundance in the different MC3 backgrounds. This sample is called preHUNTER and could provide information of total protein levels. The disadvantage of this analysis is that peptides should be labelled in order to be detected and we might have lost information. Therefore, this analysis cannot be considered as accurate as total quantitative proteomic analysis.

A similar approach was used to evaluate the resulting peptides as described before. From a total amount of 1072 proteins that were identified (Supplementary Table S9), same change threshold was applied in the dual comparisons, following T-test p-value analysis to discard non-significant differences. Taking into account the significant changes when comparing the overexpression line with mutant plants, a total of 27 proteins appeared (Fig 2.27 and Supplementary Table S10). The comparison of overexpressor with wild-type plants gave similar results (Fig 2.28 and Supplementary Table S9), which is an indication of consistency in the change of protein abundance when there is over-accumulation of MC3. Since,

Chapter 2

many of the proteins identified did not have any specific biological function described yet, we tried to focus on the functional groups that came up from the rest.

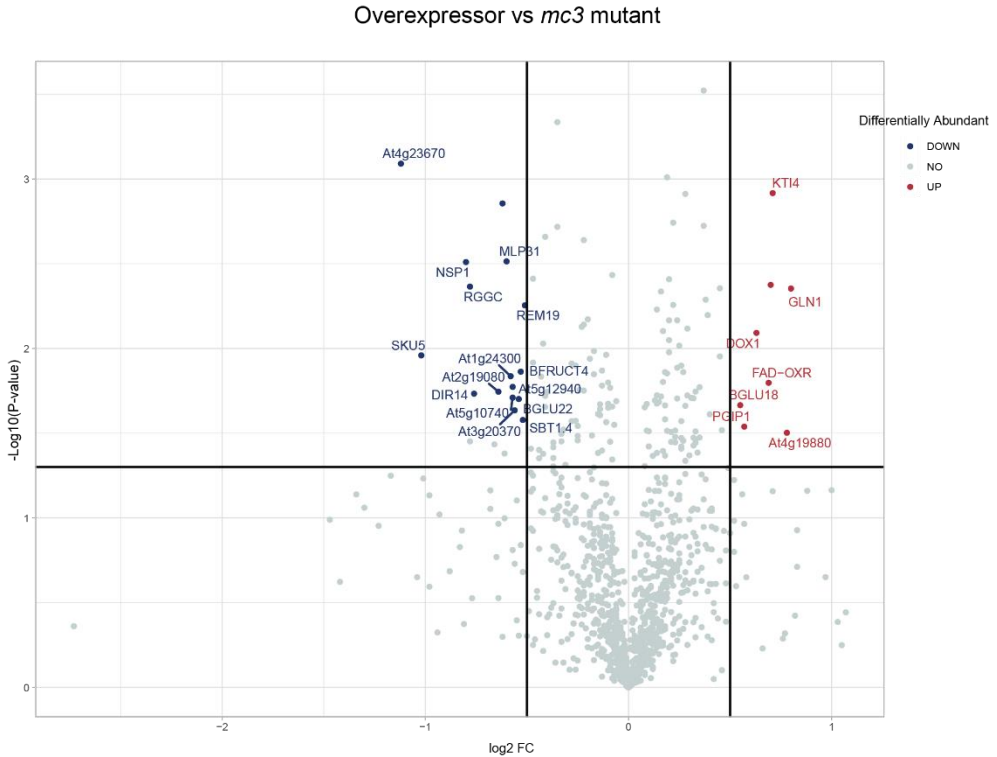


Figure 2.27: Identification of differentially abundant proteins in overexpressor compared with *mc3* mutant plant roots. Volcano plots shows the relation between the log₁₀ p-value and the log₂ fold change for the compared lines. Peptides with significantly reduced or increased abundance are considered those having $-\text{Log}_{10}(\text{P-value}) > 1.3$ and $\text{log}_2 \text{FC} < -0.55$ or > 0.55 respectively and are highlighted with blue and red colour.

Significantly downregulated in the overexpressor summarised from the two comparisons, are:

- A) Peroxidase proteins such as PER3, PER29 and PER45, which respond mostly to oxidative stress and catabolism of hydrogen peroxide. PER29 was recently identified as one of the five peroxidases essential for the formation of the Casparian strip (Rojas-Murcia et al., 2020).

Results

- B) Overexpressor roots also express less SKU5, a protein involved in the directional root tip growth by possibly regulating cell wall expansion (Sedbrook et al., 2002). Related to cell wall expansion is also CEL5 that was found downregulated in the overexpressor line compare to wild type plants.
- C) Furthermore, proteins related to ABA signalling such as BGLU22, BFRUCT4 affected. Both are directly activated by downstream signalling and specifically BFRUCT4 acts by closing the stomata upon ABA signalling (Chen et al., 2016). Interestingly we found the subtilase SBT1.4 (SASP) which has been associated to drought response to be less expressed in the overexpressor line. *sasp* mutants exhibit higher tolerance of the stress by modulating ABA signalling (Wang et al., 2018).

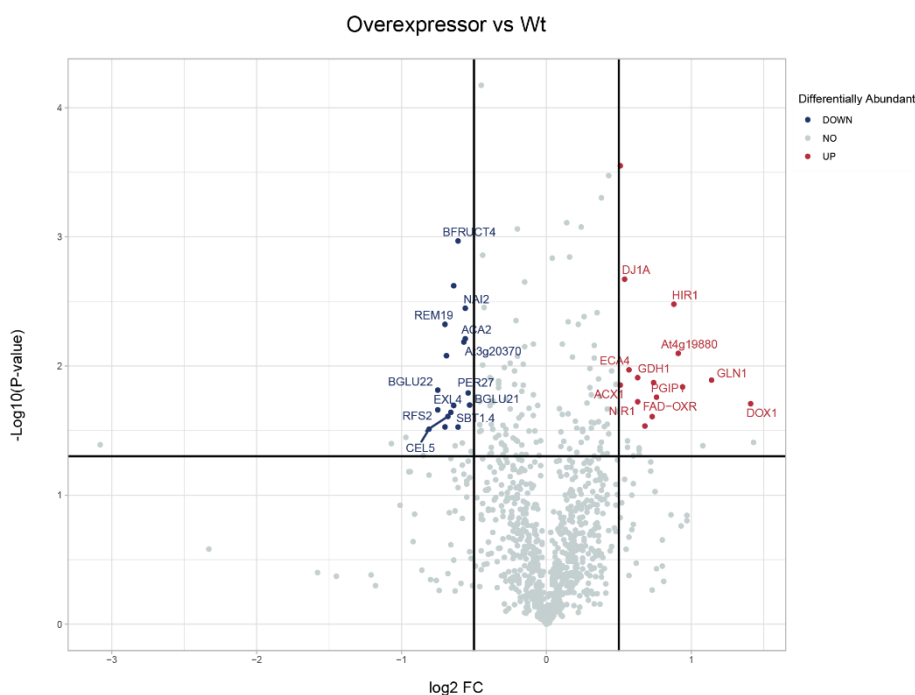


Figure 2.28: Identification of differentially abundant proteins in overexpressor compared with wild-type plant roots. Volcano plots shows the relation between the log₁₀ p-value and the log₂ fold change for the compared lines. Peptides with significantly reduced or increased abundance are considered those having $-\text{Log}_{10}(\text{P-value}) > 1.3$ and $\text{log}_2 \text{FC} < -0.55$ or > 0.55 respectively and are highlighted with blue and red colour.

Chapter 2

- D) NAI2 is a major component for the ER bodies formation and it has been reported that *nai2* mutants had increased growth and proline accumulation at low water potential (Kumar et al., 2015).

Upregulated appeared in the overexpressor line:

- A) Four proteins that positively regulate the response to hypoxia and oxidative stress (ACX1, At4g19880, FAD-OXR, DJ1A). ACX1 is also upregulated upon ABA (Ebeed et al., 2018). Also, DOX1 which is a cell death associated dioxygenase that has a protective role upon oxidative stress, responding to salicylic acid (SA) (De León et al., 2002).
- B) A glutamine synthetase (At1g6620, GLN1;2/ GSR2). GLN1;2 has a specific expression for the CCs of the phloem but didn't exhibit any phenotype upon abiotic stresses as did GLN1;1 (Lothier et al., 2011). Recent reports indicated that GLN1;2 is crucial for N assimilation of Arabidopsis plants grown in ample nitrate conditions (Guan et al., 2016)
- C) We identified BGLU18 for which the mutant line has shown less resistance to drought stress (Lee et al., 2006). BGLU enzymes depending on the tissue and the abiotic stress can be activated differently and catalyse different reactions with distinct substrates (Ahn et al., 2010).
- D) KTI4 is a protein involved in PCD responses and defence against bacterial pathogens. It has also shown that upon hydrogen peroxide upregulation.

We also performed a comparison of the wild-type/*mc3* mutant results only to detect differences derived from the absence of the protease. Filtering for the significant differentiated proteins (Supplementary Table 11), only two came up and CGEP was the one behaving opposite in the mutant and the overexpressor line. CGEP is an auto-catalytic serine peptidase, located mostly in the plastids. Comparative proteomics and genetic interactions show that CGEP is part of the chloroplast proteostasis network and is directly or indirectly involved in the regulation of starch metabolism (Bhuiyan et al., 2020). The *cgep* mutants grow

Results

similar to wild-type plants upon normal growth or high light and drought conditions.

To summarise, small differences were observed between absence and endogenous levels of MC3 which can be caused from redundancy by other proteases. On the contrary, over-accumulation of the protease results in an increase of many proteins related to hormone signalling, in the majority ABA, responses to stress conditions such as osmotic and oxidative stress were up- or down- regulated in abundance. From the results that we obtained, we hypothesised that it is possible that MC3 is having a role in stress responses.

CHAPTER 3

Identifying the role of metacaspase 3 upon environmental stresses

Results

Summary

Environmental stresses, such as low or high temperature, deficient or excessive water, high salinity, UV radiation and pathogens are hostile to plant growth and development, leading to great crop yield decrease worldwide. It is of great importance to study the plant responses and defence mechanisms against these stresses and their strategies of tolerance in order to strengthen crops against the increasing pressure of environmental changes due to climate change. The increasing food demands imposed by a growing population together with the crop yield losses are not sustainable for the future of the planet. Metacaspases have been shown to participate amongst others, in the plant responses to stresses.

In this part of the study we wanted to determine whether altering the levels of MC3 in the plant had any impact on environmental stress responses in the plant. Since the modulating the levels of MC3 did not cause any obvious developmental phenotype in the plant, and proteomic analysis of the different mutant and overexpressing lines showed a potential involvement of the protein in abiotic stress responses, we suspected that the protein could be involved in the response network that is activated when plants are under threat. We found that upon severe drought stress the overexpressor plants of metacaspase 3 survived more than the wild-type plants and *mc3* mutant plants behaved the opposite. The latter seemed less sensitive to ABA, the main hormone regulating the drought responses. We investigated formation of the vasculature upon osmotic stress and we found that the overexpressor lines were forming the metaphloem tissue earlier. In low oxygen conditions the excessive amount of MC3 contributed to plant survival. We also investigated the performance of mutant and overexpressing MC3 lines upon vascular pathogen infection and heat combined with light stress. The response was not altered in these conditions, which shows that MC3 was more specifically involved in stresses causing osmotic unbalance.

Results

Promoter analysis shows transcription factor (TF) binding motifs related to stress responses

The gene promoter region can provide information regarding the motifs present and the possible transcription factors (TFs) that could potentially bind to it. Transcriptional regulation is of great interest since TF are proteins that regulate and thus orchestrate plant growth and responses. However, defining the exact cis- regulatory elements that are functional in a promoter sequence is quite difficult and usually additional sites are present and should be taken into account. Multiple online tools have been developed to facilitate research and provide the most accurate possible analysis. The next step after identifying the motifs present in a sequence for the TF to bind, is to clarify the co-expression of these genes spatiotemporally to elucidate the network of regulation and the cascade of events.

To identify the motifs in the *MC3* promoter region, we selected an area of 1.5Kb upstream the ATG of the first exon. In a first approach we compared the cis elements of all Arabidopsis metacaspases to identify potentially different regulation using PlantCARE. The region upstream that was chosen for all of them was at least 1000bp. As shown in Table 3, most of the motifs identified are related to hormone signalling and stresses, either biotic or abiotic. *MC3* promoter contains the EIRE motif and the Box W1 that are associated with fungal elicitor and pathogen induced response, respectively. Although *MC1* has a role in HR, its promoter region did not show any motif related to pathogens, whereas *MC4* that is activated upon wounding, contains the WUN motif accordingly. Most of the metacaspases have predicted motifs responding to SA and JA. Interestingly, regarding responses to ABA and osmotic stress, the ABRE motif is present in *MC1*, *MC3*, *MC4*, *MC7* and *MC9* that have shown expression in the vascular tissue. Also *MC1* and *MC3* contain the GARE motif that is associated with gibberellin (GA) response and *MC3* and *MC9* share a motif that responds to auxin. At last, ARE motif that participates in anaerobic-related responses can also be found in the promoter sequence of *MC3*.

Results

Table 3: Analysis of promoter regions for all members of the metacaspase family in Arabidopsis from PlantCARE database. Motifs have been organised according to the associated function that regulate the TF binding on them.

		AtMC1	AtMC2	AtMC3	AtMC4	AtMC5	AtMC6	AtMC7	AtMC8	AtMC9
endosperm expression	Skn-1									
endosperm expression	GCN-4									
RNApol binbing site	TCT motif									
light, senescence	G-Box									
light	ACE									
heat	HSE									
light	Sp-1									
salt	TC repeats									
senescence -Li Liu et al. 2016	W box									
	Circadian									
cis elements, MBS, MBSI, MRE	MYB TFs									
pathogen	Box W1									
wound respons. Element	WUN motif									
Giberellic Acid	GARE									
Ethylene	ERE									
Absisic Acid response, osmotic stress	ABRE									
Giberellin	P-Box									
Auxin	AuxRR									
Auxin	TGA Box									
SA response	TCA element									
MeJA response	CGTCA motif									
MeJA response	TGACG motif									
Anaerobic induction	ARE									
Zein metabolism regulation	O ₂ site									
elicitor responsive	EIRE									

To confirm that the motifs were identified correctly we performed another promoter analysis for *MC3* using AGRIS. *In silico* analysis can often provide different results in every individual run, so the comparison of all the results can help to have more robust predictions. In Table 4 all the motifs found are displayed with the exact binding site (BS) in *MC3* promoter and the family of TFs that binds to them. Those related to abiotic stress responses are highlighted in yellow and in blue are those related to pathogens. For the family of bHLH, which is one of them, it was recently shown that participated in plant responses to stress conditions, mostly drought, salt and cold (Sun et al., 2018). Another osmotic stress-related family is bZIP and more specifically the group ATB2 that binds to the ACTCAT sequence (Sato et al., 2004). The MYB family is quite diverse and has been related with development as well as abiotic stresses. In the promoter of *MC3* a motif where the MYB4 TF could potentially bind was found. The MYB4

Chapter 3

loss-of-function mutant shows UV-B tolerance due to increased accumulation of hydroxycinnamate esters, and on the contrary, MYB4 overexpression caused a reduction in UV-B absorbing compounds, resulting in UV-B hypersensitivity (Jin et al., 2000). Finally multiple binding sites were detected for HSE (Heat Shock Element) TFs, which are responsible for heat signalling (Nover et al., 2001). For the rest of the motifs, not all the TFs that can bind are characterized or they have a more general function.

Results

Table 4: Analysis of promoter region motifs for MC3 with AGRIS database.

BS Name	BS Genome Start	BS Genome End	Binding Site Sequence	Binding Site Family/TF	Publication	Reference
AtMYC2 BS in RD22	25712470	25712475	cacatg	BHLH	Role of Arabidopsis MYC and MYB homologs in drought- and abscisic acid-regulated gene expression.	Plant Cell 9:1859-1868 (1997)
ATB2/AtbZIP53/AtbZIP44/GBF5 BS in ProDH	25711367	25711372	actcat	bZIP	A Novel Subgroup of bZIP Proteins Functions as Transcriptional Activators in Hyposmolality-Responsive Expression of the ProDH gene in Arabidopsis	Plant Cell Physiol. 45(3):300-317. (2004)
W-box promoter motif	25712133, 25712284, 25711804	25712138, 25712289, 25711809	ttgacc	WRKY	Evidence for an important role of WRKY DNA binding proteins in the regulation of NPR1 gene expression	Plant Cell 13: 1527-1540 (2001).
ATHB2 binding site motif	25712703	25712711	taataatta	HB	ATHB2 is a negative regulator of germination in Arabidopsis thaliana seeds	SCI REP 11.1: 9688-9692 (2021)
CCA1 binding site motif	25712139	25712146	aaaaatct	MYB-related	A myb-related transcription factor is involved in the phytochrome regulation of an Arabidopsis Lhcb gene	Plant cell 9:491-507 (1997)
DPBF1&2 binding site motif	25711160, 25712119	25711166, 25712125	acacaag	bZIP	Negatively regulates drought and salt tolerance, promote flowering and defence responses to virus.	MOL BIOL REP 47, 3585-3592 (2020), Planta 243, 623-633 (2016), PlosOne E 9(3): e90734
HSEs binding site motif	25711312, 25712291, 25712290, 25711311	25711321, 25712300, 25712299, 25711320	agaaatttct	HSF	Arabidopsis and the heat stress transcription factor world: how many heat stress transcription factors do we need?	Cell Stress Chaperones. 2001 Jul;6(3):177-89. Review.
MYB4 binding site motif	25712750	25712756	accaacc	MYB	Expression profile matrix of Arabidopsis transcription factor genes suggests their putative functions in response to environmental stresses.	Plant Cell. 2002 Mar;14(3):559-74.
RAV1-A binding site motif	25711852, 25711898, 25712165, 25712835, 25711947, 25711384	25711856, 25711902, 25712169, 25712839, 25711951, 25711388	caaca	ABI3VP1	Arabidopsis RAV1 transcription factor, phosphorylated by SnRK2 kinases, regulates the expression of ABI3,ABI4, and ABI5 during seed germination and early seedling development	The Plant Journal 80,4: 654-668 (2014)
BoxII promoter motif	25712443	25712448	gggtaa	...	Transcriptional activation by Arabidopsis GT-1 may be through interaction with TFIIA-TBP-TATA complex	Plant J. 1999 Jun;18(6):663-8.
GATA promoter motif [LRE]	25711154, 25711399, 25711416, 25711827, 25712551, 25712625, 25712683	25711159, 25711404, 25711421, 25711832, 25712556, 25712630, 25712727, 25712688	tgataa	...	Arabidopsis thaliana GATA factors: organisation, expression and DNA-binding characteristics	Plant Mol Biol. 2002 Sep;50(1):43-57.
Ibox promoter motif	25711828, 25712723	25711833, 25712728	gataag	...	An evolutionarily conserved protein binding sequence upstream of a plant light-regulated gene	Proc Natl Acad Sci USA 85:7089-7093 (1988)

The analysis was performed using two different platforms: PlantCARE and AGRIS. AGRIS currently contains two databases, AtcisDB (Arabidopsis thaliana cis-regulatory database) and AtTFDB (Arabidopsis thaliana transcription factor database). These are databases of cis-elements on the promoters of all genes in the Arabidopsis genome. The results have not been verified experimentally and are based on simply presence of the putative regulatory cis element. These putative promoter sequences are somewhat different from those from TAIR cis element motif tool because AGRIS has incorporated the information of full-length cDNA sequences from RIKEN and SALK.

Overall, we noticed that in both independent analysis of the promoter sequence and the binding motifs present, many of the TF sets that appeared are related with abiotic stresses and most of them are more specific for osmotic stress and ABA signalling, which is consistent with our proteomics data hinting towards a function of MC3 in these processes. Also there are W-box motifs that are an indication of biotic responses.

MC3 function upon Abiotic Stresses

Heat stress

Temperature is a factor that can vary during different seasons but also during the day and plants have evolved mechanisms to cope with these fluctuations. In a cellular level, upon heat stress, proteins are not folding properly and proteostasis is challenged. Effects on the rhythm of protein synthesis, folding and degradation lead to aggregate formation. This phenomenon affects the stability and the proper function of protein complexes. As a defence mechanism cells activate chaperone proteins that will contribute to the aggregate clearance and restore the balance. Prolonged elevated temperatures can lead the plant to activate PCD, but short heat shock waves can actually enhance the “memory” against the stress factor and provide tolerance.

We wanted to test how MC3 behaves upon heat stress. First, 7-day-old seedlings were kept at 45°C for 45min, then they were left for 1 hour to recover

Results

and placed again at 37°C for 1 hour. We analysed the seedlings after fixation with confocal microscopy, using Proteostat Aggregosome Detection, a dye that binds to aggregate and misfolded proteins and gives fluorescence. In Figure 3.1A and B, different parts of the seedling root are shown after the second incubation at 37°C. From the root tip to the upper differentiation zone the aggregate accumulation of MC3 is evident, although the aggregates do not seem to co-localize with those stained by Proteostat. We also tested if the aggregates disappear upon recovery of the seedling. Heat shock was performed for 1h at 37°C and seedlings were observed with confocal microscopy. All the expression of the protein was observed in masses all over the root (Fig 3.1C) but upon recovery of 1hour at 22°C the aggregates are reduced and the ubiquitous pattern of expression is getting slowly restored all over the root.

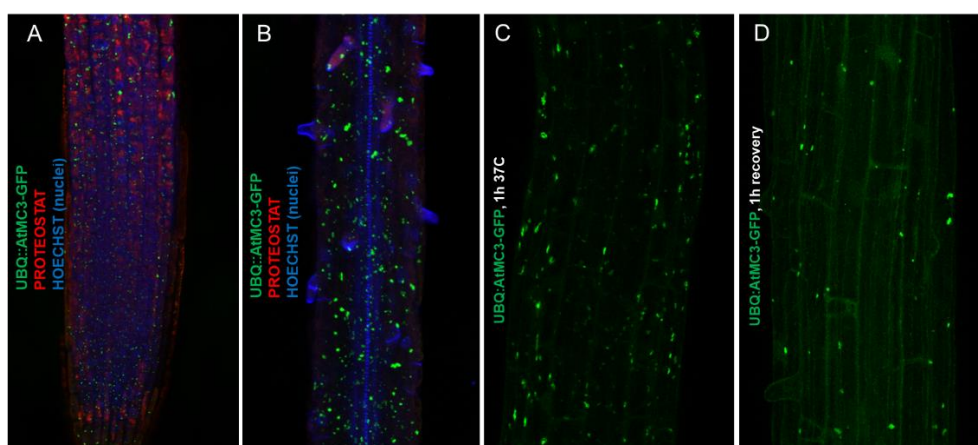


Figure 3.1: Formation of aggregates of MC3 upon heat stress. The construct UBQ:MC3-GFP was detected using confocal microscopy. Hoechst to stain the nuclei is visualized as blue and Proteostat dye is visualized as red. (A) Representative picture of the root tip (A) and differentiation zone (B) from 7d old seedlings. Seeds were vernalized for 2 days at 4°C, grown at LD/22°C conditions for 7 days and placed at 45°C for 45min. They were left at 22°C to recover for 1h before placed again at 37°C for 1h. They were fixed and stained with Proteostat Aggregosome Detection kit and imaged with confocal microscopy. Representative picture from the differentiation zone of the root of 7d old seedlings, grown at LD/22°C conditions for 7 days and placed at 37°C for 1h (C) and after 1h of recovery at /22°C (D).

Chapter 3

Thermo- and photo- morphogenesis is the effect that temperature and light respectively, have on plant development (Erwin et al., 1989; Franklin and Quail, 2010). Many physiological traits are altered as plants perceive signals from their environment of multiple temperatures or light intensities. Regarding temperature, the most common feature is the elongation of hypocotyl and the different size of plant organs such as cotyledons and leaves (Quint et al., 2016). The molecular mechanism behind the response of shoots to ambient temperatures is well studied but for the root responses little is known. Recently a connection between root and shoot thermomorphogenesis was discovered, which was proposed to be mediated by auxin as major regulator (Gaillochet et al., 2020). During photomorphogenesis, high light intensity inhibits growth in the hypocotyl, but increases growth and development in cotyledons and emerging true leaves, as well as in roots. The fact that different tissues can respond individually to the environmental signal relies on the type and the amount of photoreceptors promoting or inhibiting growth in different plant organs (phytochromes and cryptochromes) (Montgomery 2016).

MC3 showed promoter regions that could potentially bind factors that are related to heat stress. Furthermore, in the proteome analysis performed, there were proteins in higher abundance in the overexpressor that are related with responses to heat stress. In order to address how ambient temperature in combination with light modulate shoot and root development in the different mutant backgrounds of *MC3*, we used low and high light growth conditions in chambers with 22 and 28°C. Seeds of wild-type, overexpressor and mutant plants were vernalized for 2 days at 4°C, placed for 3 days under LD conditions (16h:8h) in order to have simultaneous germination and then the 3-day-old seedlings were transferred to four different conditions. The growth chambers used were: 1) 22 °C and 40 $\mu\text{mol}/\text{m}^2/\text{s}$, 2) 22 °C and 170 $\mu\text{mol}/\text{m}^2/\text{s}$, 3) 28 °C and 40 $\mu\text{mol}/\text{m}^2/\text{s}$, 4) 28 °C and 170 $\mu\text{mol}/\text{m}^2/\text{s}$. Roots were measured in all the different conditions as shown in Figure 3.2B, with no significant difference observed between the genotypes in none of the conditions. Hypocotyl length was also calculated in 22 °C and 28 °C, under low light conditions when elongation defects are more evident. In that case significant differences were observed. At 28°C, mutant plants

Results

lacking MC3 did not elongate their hypocotyl more than 7mm whereas wild-type and overexpressor plants could reach the 9mm length (Fig 3.2A). That could mean that temperature could affect the mutant line but since the changes are minor, the phenotype cannot be translated into a major influence of MC3 in plant responses to heat.

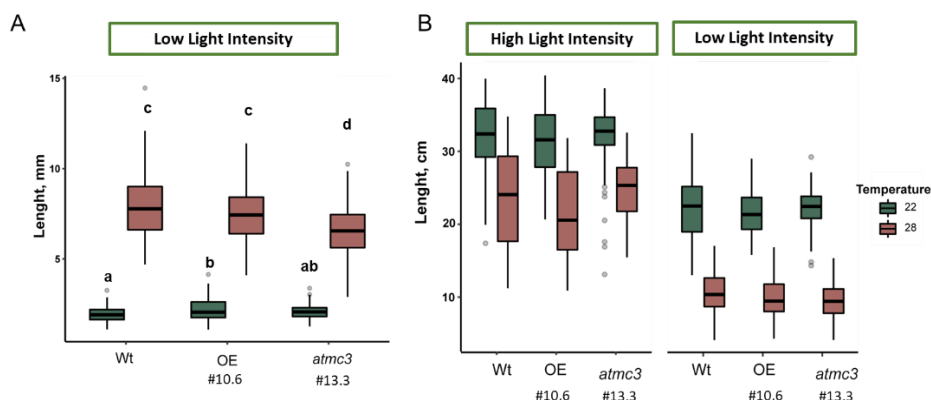


Figure 3.2 Effect of light and temperature on root and hypocotyl length of *mc3* mutants. (A) Hypocotyl growth (28°C (green)/22°C (pink)) in wild-type, overexpressor and *mc3* mutants under low light intensity growth conditions-170 $\mu\text{mol}/\text{m}^2/\text{s}$. (B) Root growth (28°C/22°C) in wild type, overexpressor and *mc3* under low and high light intensity (40 and 170 $\mu\text{mol}/\text{m}^2/\text{s}$ respectively) growth conditions. Statistics: one-way ANOVA, Tukey HSD test $p\text{-value} < 0.05$ is represented in the graphs and was calculated separately for each condition.

Hypoxia

Hypoxia stress in plants is the lack of molecular oxygen and can occur usually under flooding conditions. It can appear as soil saturation with water or plant submergence. Upon lack of O_2 plant cells activate a metabolic reprogramming and the whole organism adopts morphological changes that enables tolerance mechanisms to counter the stress. The most devastating effects of hypoxia are the limitation of ATP production due to the lack of oxygen that leads to a decrease in energy production, the acidification of cytoplasm by malfunction of $\text{H}^+\text{-ATPase}$ and organic acid production (Perata and Alpi 1993).

Chapter 3

The mechanism of sensing primary hypoxic signals has been studied the past years with hormone signals being crucial in activating downstream signalling pathways. JA, ABA, gibberellins (GA) and ethylene are crucial hormones for the LOES (Low Oxygen Escape Syndrome) response by promoting or inhibiting growth, formation of aerenchyma structures and increasing fitness. The family of ERF VII (Ethylene Response Factors VII) TFs has been shown to receive the initial stress signal and modulate the expression of hypoxia-related genes (Bui et al., 2015; Weits et al., 2014). These TFs contain a specific N-terminal residue and removal of the first Met allows them to become modified by PCOs (Plant Cysteine Oxidases). With this process, which is called N-end rule or N-degron pathway, the N-terminal Cysteine changes to a Cys-sulfinic acid and passes through a lot of modifications. Recently reviewed were these so called “core-hypoxia genes” and the importance of the Cys N-degron pathway, which is the conserved complex pathway in higher plants to transduce signal upon limited oxygen conditions (Gibbs et al., 2011; Gibbs and Holdsworth 2020; Hsu and Shih 2013).

Roots and shoots can differ in their responses to hypoxia. Root tissue activates signalling that can be characterized as autonomous, whereas shoot tissue mostly relies on systemic signalling that comes from the lower parts of the plant. Ethylene and ABA were shown to be involved in this long distance communication establishment between aerial and root parts of the plant. In particular, ABA biosynthesis was increased in the shoots and completely the opposite in the roots and helps the plant recovery (Bui et al., 2020; Hsu et al., 2011). If ethylene and ABA are acting in an antagonistic manner still is unclear and can be different depending on the species studied. Furthermore, analysis of metabolic pattern between the root and shoot tissues showed distinct accumulation patterns of C% and N% but also starch and sugar metabolites upon stress. This fact was explained by the altered phloem sugar transportation which was observed after analysis of the different phloem sap in the tissues (Lothier et al., 2020).

Results

From public available data, *MC3* showed an upregulation upon hypoxic stress and according to the promoter region analysis, ARE motif is related to anaerobic conditions. We wanted to test how the survival was affected in the different *MC3* backgrounds. Nowadays, most of the studies regarding hypoxia use either roots or whole seedlings kept in darkness in a N_2 atmosphere or under submergence. In the experiments conducted for this study a desiccator (hypoxia chamber) was used. Nitrogen was introduced at a flow rate of 4L/min in the dark, for 4hrs at which the oxygen in the desiccator was at approx. 0.5% at the end of the experiment. Our control for this experiment were seedlings in a similar desiccator with light excluded but in still air (conditions of normoxia). Before and after the treatment, plants were grown in LD conditions in plates. Root tip survival was scored after 3 days of recovery. Extension of primary root tips beyond the marked point was scored as root tip survival for each seedling. Survival threshold was determined following this procedure. Root tip survival is measured by scoring the seedlings whose primary root has grown below marked point as survival and those that did not grow as dead (Fig 3.3B). All seedlings survived at 98-100% in normoxia hence the data is not shown here. As expected, the root tips of the positive control *prt6-1* survived better in hypoxia than wild type (Fig 3.3C). Interestingly, root tips of the overexpressor line survived significantly better than wild-type seedlings, with statistically significant results. Another unexpected result was the higher survival rate shown by the mutant line, which displayed better performance than wild-type, although not as strong as the overexpressor.

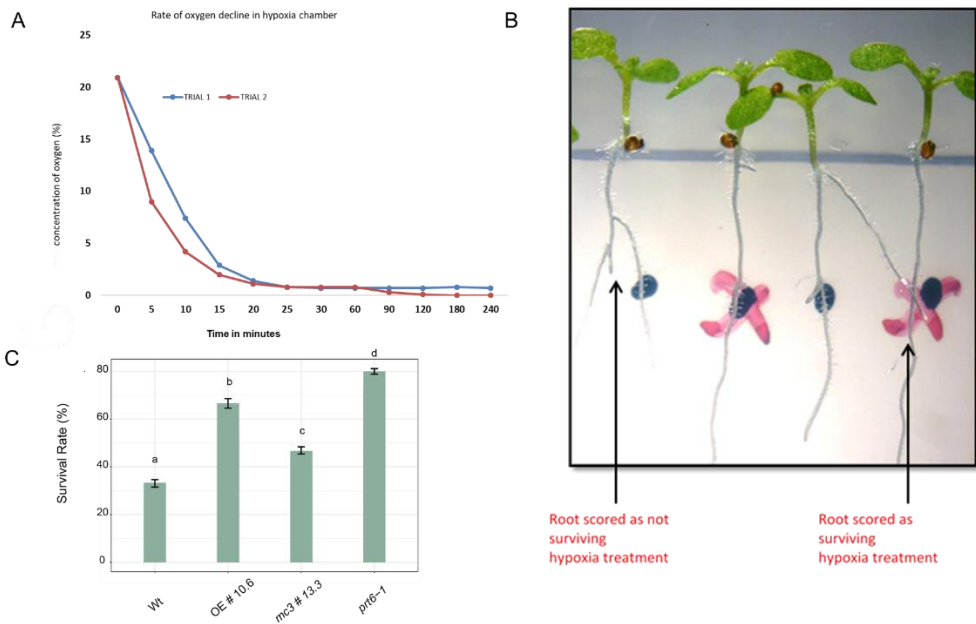


Figure 3.3: MC3 is involved in seedling survival upon hypoxia stress. (A) Rate of oxygen decline in the hypoxia chamber used for the treatments. (B) Root tip survival was measured by scoring the seedlings whose primary root (PR) grew below marked point after 3 days of recovery from the hypoxic stress. (C) Plant survival rates after 3 days of recovery in LD/22°C conditions in normal oxygen rate. Averages of three independent biological replicates (\pm SE), ($n > 80$). Statistics: one-way ANOVA, Tukey HSD post-hoc test $P < 0.05$ is represented in the graphs.

In order to determine which genes and pathway mediated the higher tolerance to low oxygen availability observed in plants with altered MC3 levels, we analysed expression of some of the main “core hypoxia genes”. Seedlings were grown in MS plates under normal conditions for 7 days before roots and shoots were collected separately to analyse the expression pattern of *ACO1* (ACC Oxidase 1), *SUS4* (Sucrose Synthase 4), *PCO1* (Plant Cysteine Oxidase 1), *PCO2* (Plant Cysteine Oxidase 2), *ADH* (Alcohol dehydrogenase 1) and *AHb* (Arabidopsis Haemoglobin). *ACO1* is an ethylene biosynthesis gene, *SUS4* increases sucrose levels for anaerobic catabolism, *PCO1* and 2 are enzymes which oxidize the cysteine of ERF VII TFs by using oxygen as a co-substrate in

Results

the N- degron pathway, *ADH* is responsible for fermentation and *AHb* also is a typical up regulated gene is hypoxic conditions.

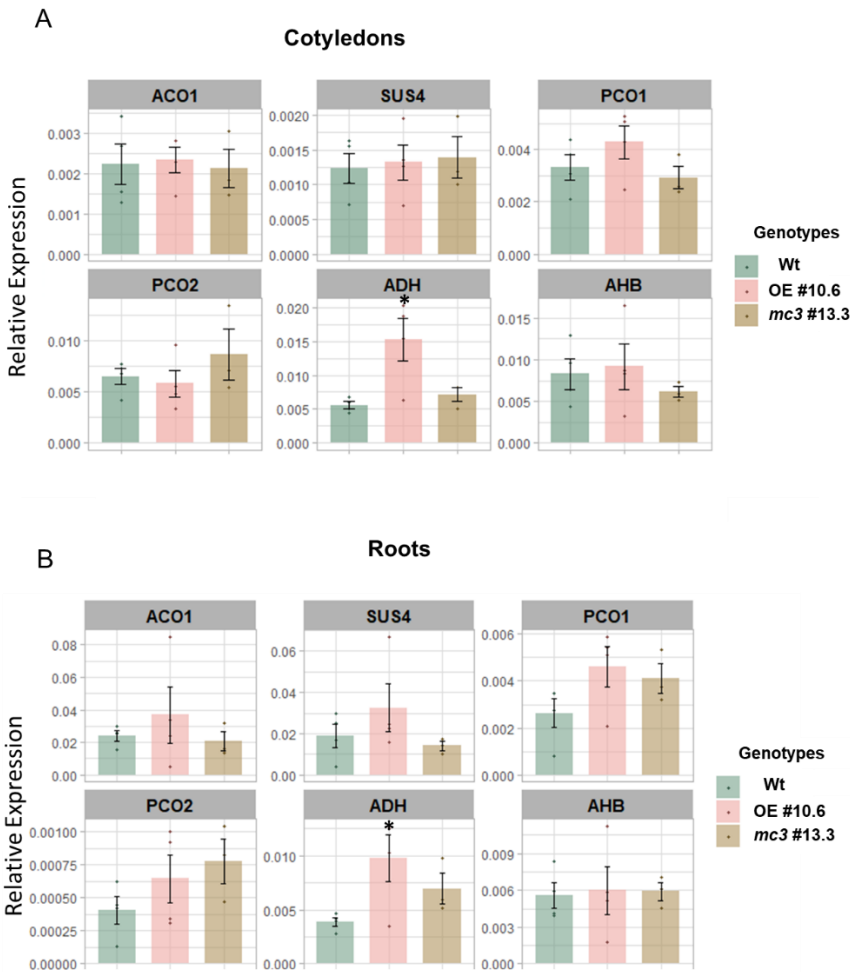


Figure 3.4: Expression analysis for six hypoxia related genes. Quantitative RT-PCR was performed on 7-day-old shoots (A) and roots (B) of seedlings grown under normoxic conditions. Wild-type plants are compared with overexpressor of MC3 and *mc3*. Total RNA was extracted and used for cDNA synthesis. *EIF4a* gene was used as a housekeeping gene, to normalize the expression of the genes analysed. Statistics: Student T-test was performed to detect significant difference in expression (* p- value < 0.05).

From the analysis performed in separated root and shoot samples, only *ADH* showed significant upregulation in the overexpressor plants. *ADH* is the last gene in the pathway of the reversible transformation of acetaldehyde to alcohol by oxidizing NAD^+ to NADH. This fermentation process is upregulated in hypoxic conditions but also upon hypoxic events during development such as seed development and germination (Ventura et al., 2020). In general, plants with higher amount of ADH show enhanced tolerance to hypoxia and that could be an indication for the higher survival of overexpressor of MC3 plants (Fig 3.4). The rest of the genes tested did not show any differential expression upon normal conditions, thus we cannot exclude the possibility that differences appeared under stress conditions only.

Drought

Water is one of the most crucial elements for plant growth. Thus, when the availability of water decreases, plant development is limited. Drought is an emerging environmental stress due to climate change which is becoming increasingly prevalent. Crop yields all over the world are affected severely from limited precipitation and extensive water loss, with the reduction of crop yield to be estimated at 40% annually. Since plants are sessile organisms and they cannot run away from the stress, they developed during evolution mechanisms to cope with it. Drought “resistance” is a very general term used to describe the ability of the plant to survive during prolonged drought stress with two main mechanisms, drought tolerance and drought avoidance. Tolerance can be translated to drought escape or hardness and the plant is able to complete its life cycle before the severe stress thus do not experience drought. At an organism level, plants reduce their root growth, leaf size, seed production and promote early flowering and develop morphological traits that enable them to escape. On the other hand, in drought avoidance the plant is able to endure the stress by altering evapotranspiration, reduce soil water uptake, accumulate osmoprotectant molecules such as proline, raffinose, trehalose etc. in its tissues and protect the osmotic balance in their cells (Basu et al., 2016).

Results

Photosynthesis is the major parameter to identify the plant productivity hence water deficit impairs photosynthetic rate and transpiration. Upon mild drought the CO₂ levels are significantly reduced mainly due to stomata closure and damaged plastids but upon severe drought stress the factor that leads to CO₂ limitation is the direct reduction of gas diffusion that afterwards results in reduction of stomata and photosynthetic capacity in mesophyll (Flexas et al., 2008). Light import and usage balance is compromised, which leads to overproduction of reactive oxygen species and oxidative burst and finally decline the effectivity of photosystem II. As a response, plant cells trigger expression of genes related to chloroplast metabolism and peroxidase enzymes to maintain redox homeostasis.

The responses of a plant to drought stress start shortly after the first signal transduction for water limitation. Hormonal pathways are activated including abscisic acid (ABA), ethylene, gibberellic acid (GA), jasmonic acid, auxin and brassinosteroids. The complex crosstalk of these hormones regulate the adaptation to stress. ABA is synthesized *de novo* in root tissue and translocated to the aerial parts, leading to stomata closure, while auxin regulates negatively the plant responses to the stress. GA and ethylene have an important role in balancing the yield when water is limited (Basu et al., 2016). The mechanisms that the plants deploy to deal with the stress can vary depending on the species studied and the availability of water in the environment. For example, root architecture plasticity is an important trait for the adaptation. Roots are the first tissue that senses the stress but behave differently in completely dry and slightly moisture soil. Arabidopsis showed root growth inhibition, reduced lateral root formation through ABA and auxin signalling when osmotic stress was tested in plates but many plants develop longer and thinner roots for maximum exploitation of water when tested in completely dry surface soil with moisture in further depth (Deak & Malamy, 2005; Dinneny, 2019).

Given the stress-related proteins that are differentially expressed in the overexpressor line, we wanted to test the possible role of MC3 in osmotic stress by exposing adult plants in severe drought stress. Plants were grown for 3 weeks in individual pots and water was withheld for 8-9 days. All genotypes showed

to be affected by the stress. Then, plants were re-watered and survival rate was calculated. We observed that two independent overexpressor lines tested showed increased drought tolerance than the wild-type plants, reaching a 15% higher survival rate (Fig 3.5B). Furthermore, both *mc3* mutants were less able to survive when at very low water levels. As expected, in the complementation line of the *mc3* knock out mutant with the *MC3* under the control of its endogenous promoter (*mc3 pMC3:MC3-GFP*), the ability to withstand drought was recovered similar to wild-type levels (Fig 3.5A, B). Most of drought tolerant phenotypes are usually due to growth arrest when plants lose less water because of their leaf surface and growth is compromised in order to favour abiotic stress tolerance. Neither overexpressor or *mc3* mutant are exhibiting visible growth phenotypes, so we wanted to test their behaviour in a time course of drought stress. To ensure that all the plants are in the same stress level conditions, we weighted daily the pots and calculated for each one individually the field capacity. The overexpressor plants along with the complementation line took 7-8 days to arrive to 10% field capacity (water availability) whereas wild-type and mutant plants needed only 6-7 days which could indicate less water losses through evapotranspiration (Fig 3.5C).

Results

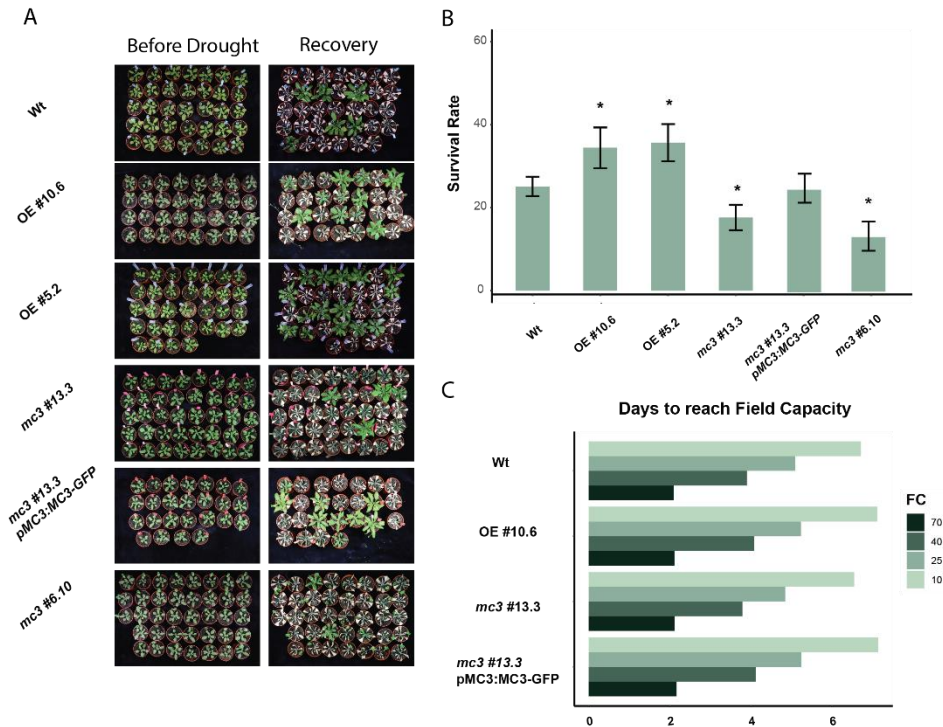


Figure 3.5: MC3 is involved in drought tolerance. (A) Phenotypes from plants before drought stress in well-watered conditions (left column) and post-stress, after 5 days of re-watering and recovery (right column). From top to bottom 3-week-old rosettes of Wt, overexpressor lines #10.6 and #5.2, *mc3* #13.3, complementation line of the mutant and *mc3* #6.10 are shown. (B) Plant survival rates after 5 days of re-watering. Averages of six independent biological replicates (\pm SE) ($n > 200$). Asterisks indicate significant differences (p -value < 0.05) in a chi-squared test for survival ratios compared to wild-type. (C) Results for the days needed to reach different percentages of the field capacity for wild-type, overexpressor, knock-out mutant and complemented line are shown in bar plots for five independent replicates ($n > 70$).

Plant water content was measured as an indicator for the water status upon specific soil water contents. Relative water content (RWC) did not show significant differences as drought progresses between the different lines but in well-watered conditions – field capacity 100%, the overexpressor and the complementation line contained already more water than the wild-type plants (Fig 3.6). The maximum quantum yield of photosynthesis (F_v/F_m) is often used as a

stress indicator and is related to the maximum capacity of photosynthesis since the electron transport is not active. On the other hand, the operating efficiency of PSII is measured after a light pulse has activated the photosynthetic centre which is an indication of the actual light used from the plant to perform photosynthesis (Murchie and Lawson 2013). The overexpressor seemed to maintain higher photosynthetic activity upon severe drought stress both upon dark adaptation and without. Fv/Fm ratio was similar for all the lines upon watered conditions but when the stress was present the overexpressor was able to perform photosynthesis better than the wild-type plants. In comparison to the other two lines, there is a tendency from the overexpressor and the complemen-

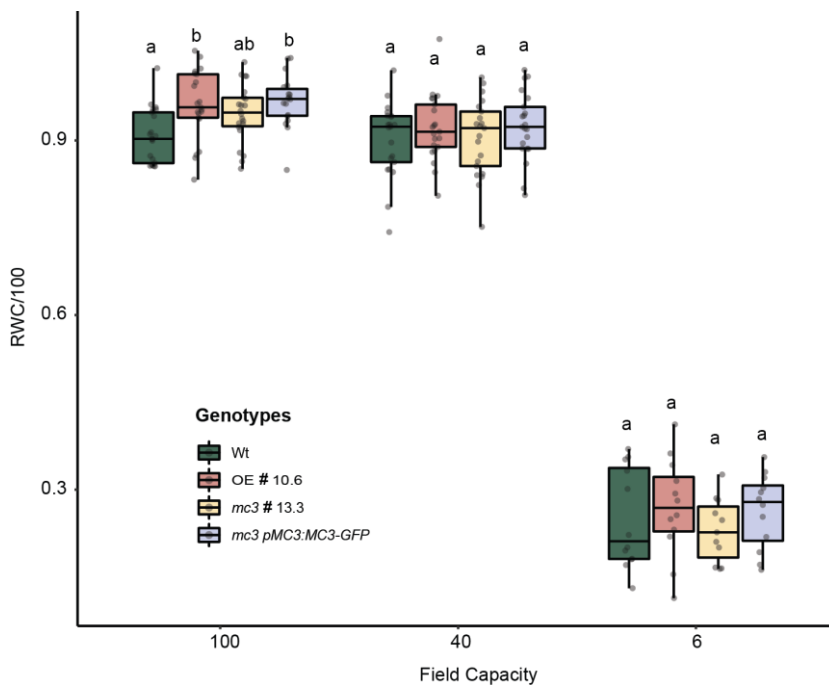


Figure 3.6: Relative water content (RWC) measurements upon drought stress. For RWC experiments, mature rosettes were collected at 100%, 40% and 6% field capacity. Experiments were repeated four times ($n > 16$). Different letters depict significant differences within each genotype calculated for each FC separately with one-way ANOVA plus a Tukey's HSD test.

Results

-ted to perform better than the mutant but these differences were not statistically significant (Fig 3.7A). On the contrary, wild-type plants showed a better actual photosynthetic capacity under basal conditions, which became reduced upon stress. At 6% FC the mutants appeared more stressed than the rest of the lines, agreeing with the survival rates from the drought experiments (Fig 3.7B).

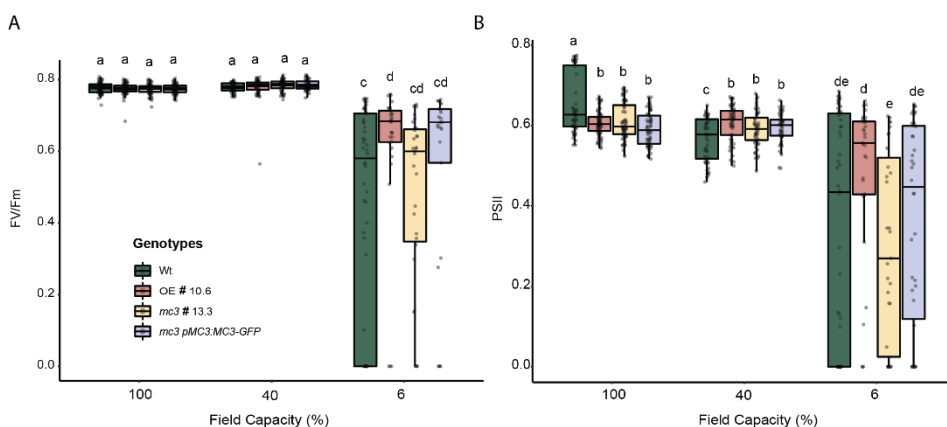


Figure 3.7: Photochemical parameters upon drought stress are affected. (A) Maximum Quantum Yield of photosynthesis (Fv/Fm) ratio for Wt, overexpressor, *mc3* mutant and complemented line at different percentages of field capacity. (B) Operating efficiency of PSII for Wt, overexpressor, *mc3* mutant and complemented line at different percentages of field capacity. Experiments were repeated four times ($n > 16$). In (A) and (B) different letters depict significant differences within each genotype with one-way ANOVA plus a Tukey's HSD test.

ABA sensitivity is reduced in *mc3* knock out plants

As mentioned above, abscisic acid holds an important role in responses to water stress conditions, regulates water status to protect cell systems and induces genes that express dehydration-tolerant proteins. It also mediates drought responses and activates tolerant mechanisms by regulating stomatal closure. When the stress appears, ABA biosynthesis and accumulation is enhanced mainly in the vasculature of the leaves because almost all biosynthesis

Chapter 3

enzymes and membrane transporters are expressed in vascular tissues (Kuromori et al., 2018; Vishwakarma et al., 2017). ABA was recently shown to promote xylem differentiation in a similar way as osmotic stress does, by activating VASCULAR-RELATED NAC DOMAIN (VND) transcription factors and to facilitate vascular plasticity to improve water transport (Ramachandran et al., 2021). The vasculature is important for the distribution of the hormone, since it has also developmental roles in the plant growth apart from the stress responses. It regulates plant transpiration, seed maturation and germination time, embryo development and inhibits shoot and root growth (Planes et al., 2015; Raz et al., 2001; Sun et al., 2018; Yoshida et al., 2019). It is also important for senescence, since internal ABA signals can regulate the onset of the process by upregulation of early senescence related genes (Song et al., 2016).

From the proteome data obtained in the root tissue from seedlings, proteins related to ABA were found to be differentially abundant in the overexpressor compared to wild-type and mutant line. Taking into account the involvement of MC3 in drought stress we wanted to test if the function of the protease is ABA-dependent. We performed several experiments to determine the responsiveness of the different genetic backgrounds of MC3 to the hormone. First, we germinated overexpressor and *mc3* mutant seeds together with wild-type and complementation line seeds on plates containing three different concentrations of ABA: 0 (control), 1, or 2 μM . After 8 days of growth we observed that the germination rates of the *mc3* mutants were the only significantly higher than the rest of the genotypes when seeds were germinated on media containing ABA, in comparison to control plates that did not show any difference (Fig 3.8 A, B). When root growth inhibition was checked, seedlings were grown firstly on MS-media for 3 days to ensure equal germination and after were transferred to MS media containing 0 (control), 0.3, 3 or 30 μM ABA for 7 more days. The root growth of all the lines was almost similarly inhibited at 3 and 30 μM of ABA (Fig 3.8 C, D). Although some of the differences observed appeared statistically significant, the values were not dramatically different, so that the hormone can be considered as having a strong effect on root growth. At 0.3 μM ABA the overexpressor roots seem to be even more elongated than control conditions and

Results

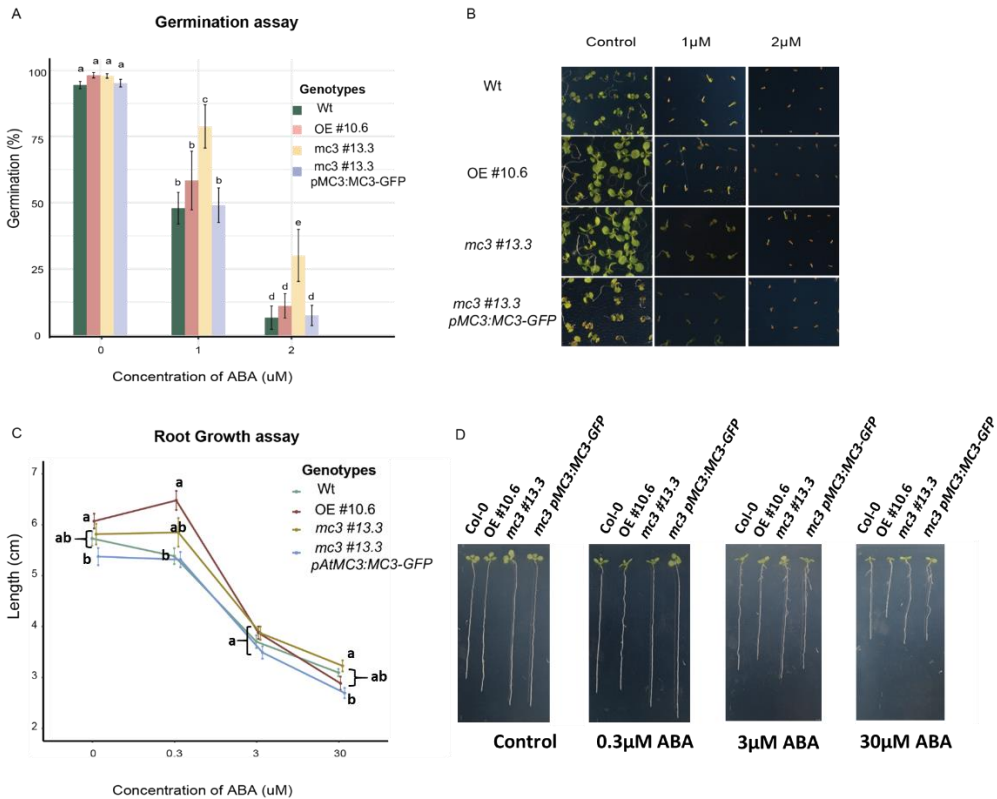


Figure 3.8: Analysis of germination rate and root growth inhibition upon ABA treatment. (A) and (B) Germination assays of wild-type, overexpressor, *mc3* mutant and complemented plants of MC3 with and without ABA treatment. Seeds were germinated on MS- medium plates supplemented with 0 (control), 1 or 2 μM ABA solution and grew for 8 days before pictures were taken (A) and germination rate was calculated (B). Bar plots in (B) are means (\pm SE) for five biological replicates ($n > 90$ per replicate/per genotype). Statistics: one-way ANOVA plus a Tukey's HSD test were performed to detect differences between the lines used. (C) and (D) Effects of ABA treatment on root growth of wild-type, overexpressor, *mc3* mutant and complemented plants of MC3. Seeds were first germinated on MS- medium plates for 3 days, then seedlings were transferred to new plates supplemented with 0 (control), 0.3, 3 and 30 μM ABA, and left to vertically grow for further 7 days before images were taken (D) and root length was calculated (C). Data are means (\pm SE) for five biological replicates ($n > 15$ per replicate/per genotype). Significant differences from Wt were determined by Student's t-test and letters are representing differences calculated for each conditions separately.

show a significant difference compared to the rest of lines. It was recently demonstrated that indeed, low ABA concentrations ($<1\mu\text{M}$) can actually promote primary root growth. Phosphatases PP2Cs are positive regulators of ABA signalling pathway and when they get activated, they interact with AHA2, a plasma membrane (PM) H⁺-dependent adenosine triphosphatase (ATPase), to dephosphorylate it and hence, growth is compromised. In the presence of low ABA concentrations, cytosolic ABA receptors bind to PP2Cs to relieve AHA2, therefore, the phosphorylation state does not change and roots grow normally (Miao et al., 2021). Overall, this result shows that the overexpressor line is responding to ABA treatment.

As mentioned, ABA is able to promote senescence in detached organs (Song et al., 2016; Wang et al., 2018) so we hypothesized that *mc3* leaves may show a delay in senescence compared to the wild-type or overexpressor plants upon ABA treatment. To test this hypothesis, we grew plants for 5 weeks and we treated detached rosette leaves with 50 μM ABA for 3 days under LD conditions. To be able to quantify the level of senescence, we extracted chlorophyll and measured the respective absorbance for chlorophyll a and b. Interestingly, we found that the leaves of the *mc3* mutants contained higher levels of the chlorophyll a in comparison to wild-type and complemented plants, and the overexpressor line showed similar results. The levels of chlorophyll b were the same for all the lines tested, in control conditions and upon ABA treatment respectively (Fig 3.8). Chl a and Chl b are the main pigments for the photosynthesis and absorb the sunlight at different wavelengths (Chl a mainly absorbs red-orange light and Chl b blue-purple light). Chl a is the primary pigment present in all photosynthetic centres and Chl b is considered an additional helping molecule. The total amount of leaf chlorophyll content (Chl a+b) directly influences the photosynthetic activity of plants. In Figure 3.10 Chl a+b is calculated relativized to the tissue weight. No significant differences were detected between the lines, for neither control or ABA treated conditions, although the *mc3* mutant seemed to have a tendency towards higher Chl levels when compared to the rest of the lines.

Results

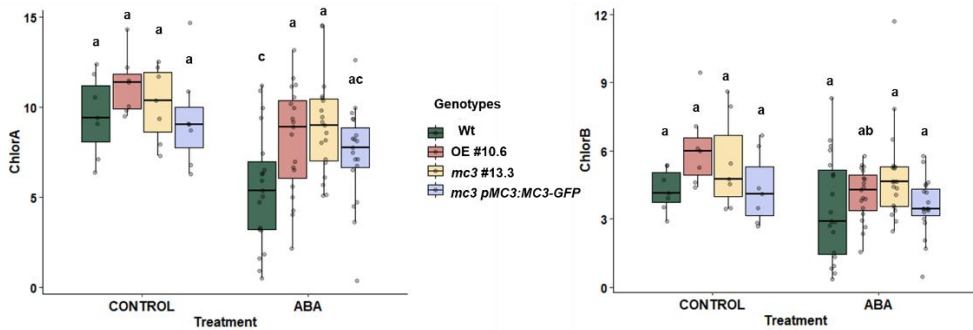


Figure 3.9: Quantification of chlorophyll a and b. Detached leaves from 5-week-old Col-0, overexpressor line, *mc3* mutant, and MC3 complementation line were incubated without (control) or with 50 μ M ABA for 3 days upon LD conditions. Leaves were weighted individually and chlorophyll was extracted. Absorbance was measured at 663 nm and 646 nm for chlorophyll a and b, respectively. Statistics: One way anova plus Tukey's HSD test was performed to detect significant differences (p -value < 0.05).

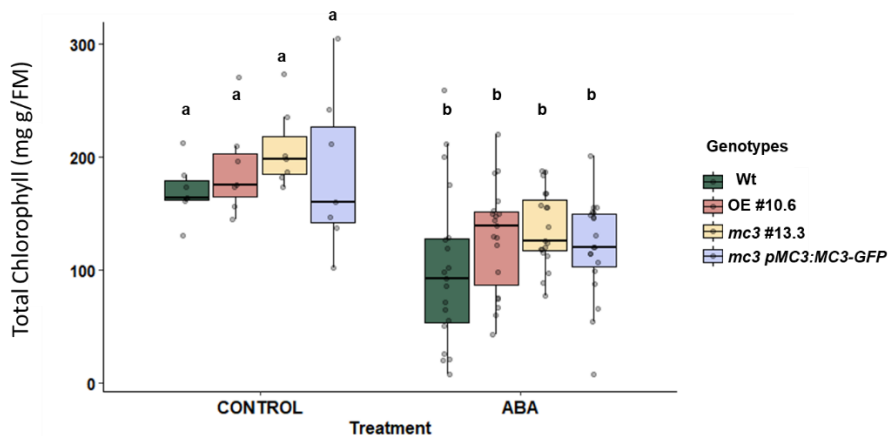


Figure 3.10: Quantification of total chlorophyll. Detached leaves from 5-week-old Col-0, overexpressor line, *mc3* mutant, and MC3 complementation line were incubated without (control) or with 50 μ M ABA for 3 days upon LD conditions. Leaves were weighted individually and chlorophyll was extracted. Absorbance was measured at 663 nm and 646 nm for chlorophyll a and b, respectively. Total amount of chlorophyll was estimated as a sum of the amount for chlorophylls a and b, divided by the weight of each sample. Statistics: One way anova plus Tukey's HSD test was performed to detect significant differences (p -value < 0.05).

Chapter 3

Finally, another parameter to study ABA sensitivity is the stomatal movement since it promotes stomatal closure when the hormonal concentration increases. For this experiment cotyledon leaves were treated with a buffer that opens the stomata for three hours before starting hormone treatment. Fifty μM ABA were added to the buffer and stomata aperture was measured at 30 min afterwards. We observed a statistical difference of $1\mu\text{m}$ in the width of *mc3* mutant guard cells in comparison with the rest of the genotypes (Fig 3.11). If stomata are not closed properly and show reduced sensitivity to ABA, when ABA increases

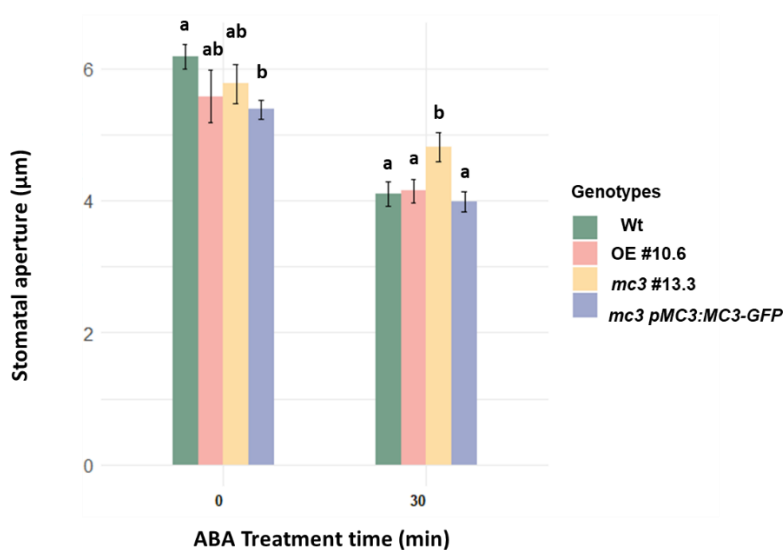


Figure 3.11: Stomata Closure upon ABA treatment. Cotyledons from 10 day-old seedlings were incubated with opening buffer for stomata for 3 h before $50\mu\text{M}$ of ABA was added to the buffer. Changes in stomatal aperture in *Wt*, overexpressor, *mc3* mutants and complemented lines were observed and photographed after 30 min of ABA treatment under microscope. In parallel, control samples were not treated and were kept with the initial buffer for 30 min. Stomatal aperture was measured with Image J and is represented in the graph. Data are means ($\pm\text{SE}$) for three biological replicates; for each genotype, 25 guard cells in total from 3 different plants were examined in each of the three replicates. Significant differences were calculated with Tukey's HSD test for multiple comparison between the genotypes, separately in each time point.

Results

upon drought stress, the mutants will lose more water, which could explain the reduced survival rate that they demonstrate and the shorter time that they need to reach the 6% FC compared to the other lines tested.

Overall, the *mc3* mutants showed less sensitivity to ABA, although we cannot claim that they do not respond to the hormone. These results could give a plausible explanation for the drought phenotype observed for these lines, although they do not explain the higher survival rate of the overexpressor line. In most of the experiments performed with ABA, the sensitivity of the overexpressor line was comparable to the wild-type and complementation line.

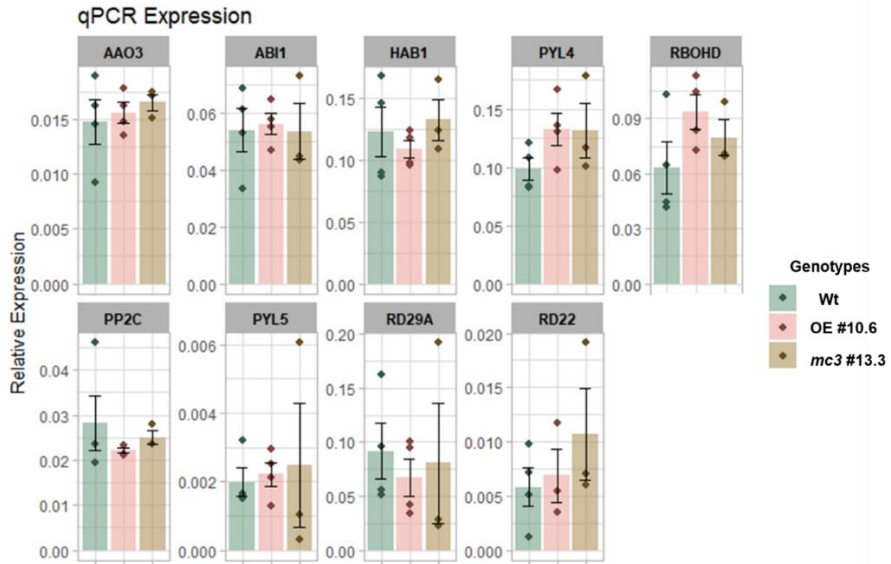
To analyse if ABA synthesis/ degradation or downstream signalling was altered in the *mc3* mutant background, we decided to analyse the expression of some of the genes involved in these pathways (*ABI1*, *HAB1*, *PYL5*, *PYL4*, *AAO3*, *RBOHD*, *PP2C* and *RD29A*, *RD22*). We separated root from cotyledons and analysed in each tissue the expression levels upon no treatment (Fig 3.12). Two negative regulators of the hormone, *ABI1* and *HAB1* did not show any change in expression between the lines. Also *AAO3*, which codes for an aldehyde oxidase responsible for the biosynthesis of the hormone was not altered. Positive regulators of downstream signalling (*PYL4*, *PYL5*, *RBOHD*, *PP2C*) behaved the same in all the samples. Regarding signalling, some of the genes tested are receptors and some are responsible for activation of cascade signals downstream. If there is a connection between ABA and MC3, the fact that no change was observed in terms of gene expression could be attributed to these factors acting upstream of MC3 so, no effect from the absence of the protease can be observed, or that without treatment the differences are not visible.

Two dehydration-responsive genes related to ABA responsiveness were also tested (Tuteja 2007). *RD29A* has an DRE motif in the promoter and is highly induced by ABA to maintain the osmotic balance in the cell. Interestingly, in root samples there was significantly less expression of the gene in the mutant background. Furthermore, water deficit and ABA induce expression of some

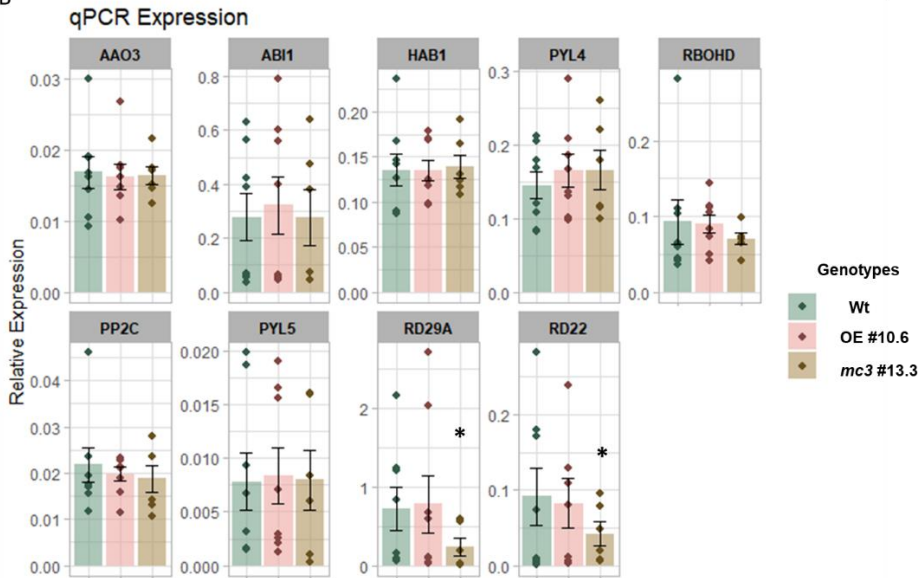
Chapter 3

RD22 proteins. Same pattern was observed, with *mc3* mutant roots to show less

A



B



Results

Figure 3.12: Expression analysis for nine ABA related genes. Quantitative RT-PCR in 7-day-old shoots (A) and roots (B) of seedling grown in normoxia conditions. Wt plants are compared with overexpressor of MC3 and *mc3*. Total RNA was extracted and used for cDNA synthesis. *EIF4a* gene was used as a housekeeping gene, to normalize the expression of the genes analysed. Statistics: Student T-test was performed to detect significant difference in expression (* p-value < 0.05).

expression (Fig 3.12B). The phenomenon of differentially expressed genes in roots and shoots is quite common for hormone-responsive genes and is not unexpected. The results from this analysis did not show any direct connection between ABA and MC3 in terms of changes in regulatory pathways gene expression. In contrast, the observed reduced expression in the root of two dehydration responsive genes could be an additive explanation for the worse performance of *mc3* mutants upon drought.

Next, we performed hormone quantification analysis to determine if altering MC3 levels had an effect on the overall hormone levels of the plant. Samples were collected from wild-type, overexpressor and *mc3* mutant plants, grown for three weeks in LD conditions in growth chambers. The analysis included main hormones such as ABA, SA, auxin (IAA), JA, Gibberellic Acid 4 and 7 but also the JA precursors OPDA and ZR and finally the hormonal molecules melatonin, Zeatin, ACC and IPA. We did not observe any significant difference in the main hormone or precursor molecules that were tested upon normal growth conditions. (Fig 3.13).

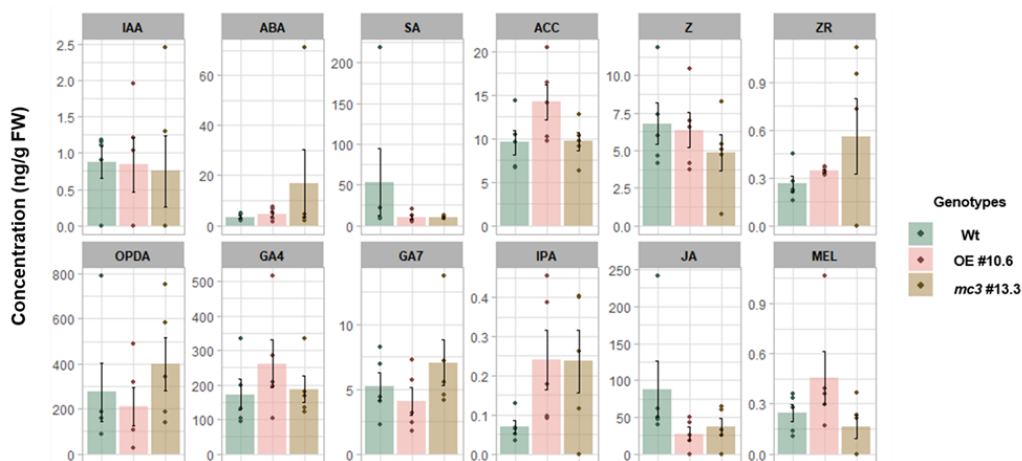


Figure 3.13: Hormone Levels Quantification. Three week old wild-type plants are compared with overexpressor of MC3 and *mc3* mutants. Data are means (\pm SE) for four biological replicates; Statistics: Student T-test was performed to detect significant difference in expression (* p-value<0.05).

Stress Responses related to ABA

Apart from seed germination, development of seedlings, stomata closure, senescence and responses to drought, ABA has an important role in the general responses of the plants to osmotic stress, which can be caused from increased salinity or cold environment. These three stresses (drought, increased salinity and cold) share a quite common pathway of downstream signalling genes since they all affect the osmotic balance of the cells. ABA is considered the endogenous messenger of water availability and it has been characterized mainly as a stress hormone. The moment that the plant is challenged by an abiotic stress factor, ABA is *de novo* synthesized and starts accumulating. Downstream from the hormone signalling many genes alter their expression to activate the cellular defence responses (Chen et al., 2020). Upon salt stress, Na⁺ ions are increased in the plant tissues and negatively regulate root growth, formation of lateral roots, flowering time and finally reduce plant survival (Neuman, 1995; Duan et al., 2013;

Results

Shu et al., 2018). Ion balance is impaired in the cells and increased oxidative damage takes place from ABA-derived ROS accumulation (Shabala et al., 2016).

Since *mc3* mutants showed reduced sensitivity to ABA we wanted to test whether salinity conditions had an impact on the different lines. Salinity causes inhibition of root growth and osmotic imbalance, similar to the responses caused by drought stress. Since MC3 overexpressor plants were more tolerant to osmotic stress caused by water deficit, it was interesting to determine whether they also showed increased tolerance upon salt stress. We tested both primary root (PR) root length and LR number upon different concentrations of NaCl. Seeds were placed in MS media to germinate for 3 days prior their transfer to 50, 100 mM NaCl and control plates respectively for 7 additional days. Since salt stress can inhibit germination, we wanted to exclude the fact that the reduced root size was due to delayed germination. The primary root length of 10-day-old seedlings was measured and we observed that the root length of overexpressor and mutant lines in control conditions was significantly higher than the wild-type and complemented line as expected. This difference though, was preserved upon higher salt concentrations. In both 50 and 100 mM NaCl the genotypes are grouped similar to the normal conditions and no significant differences were detected (Fig 3.14).

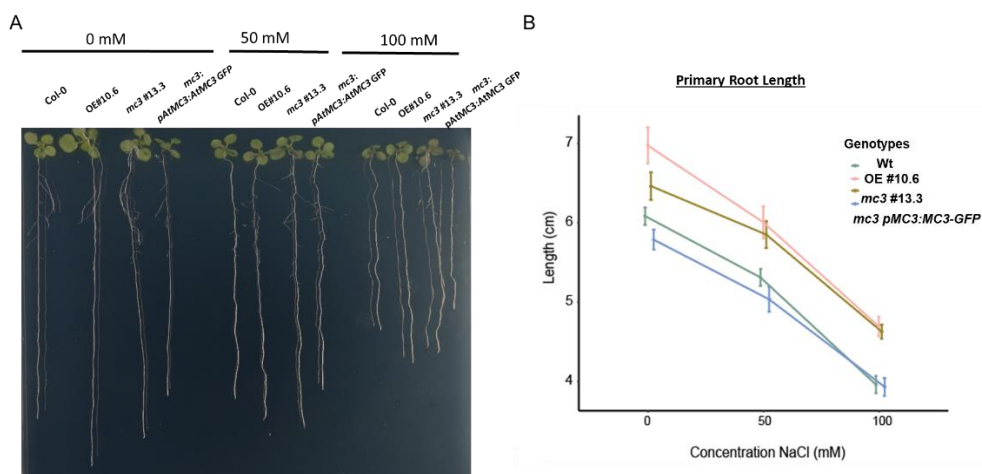


Figure 3.14: Primary root growth upon salt stress was not affected. (A) and (B) Effects of salt treatment on primary root growth of wild-type, overexpressor, *mc3* mutant and complemented plants of MC3. Seeds were first germinated on MS medium plates for 3 days, then seedlings were transferred to new plates supplemented with 0 (control), 50 and 100 mM NaCl, and left to vertically grow for further 7days before images were taken (A) and root length was calculated (B).

The measurements of lateral roots took place also at 10 days-old seedlings. We counted the visible lateral roots using a stereoscope through all the extension of the primary root. The number of LRs detected upon control conditions did not show any significant difference between the genotypes but both in lower (50mM) and higher (100mM) concentrations of NaCl the overexpressor showed an increased number of visible LRs in comparison to the rest of lines. Wild-type, *mc3* mutant and complementation line had the same number of LRs in all conditions tested (Fig 3.15).

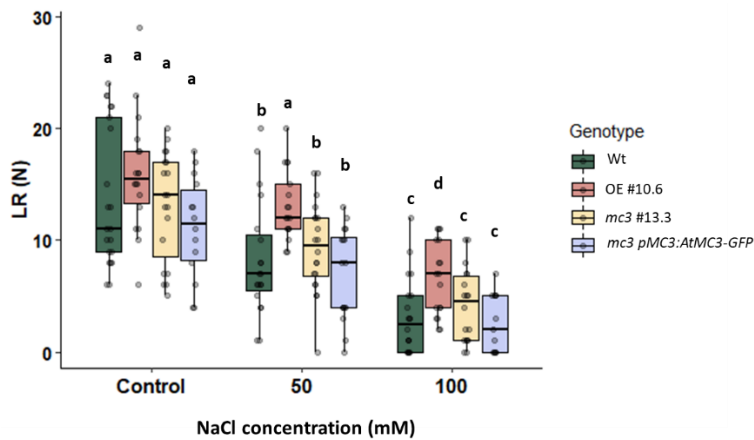


Figure 3.15: Overexpressor of MC3 shows increased number of lateral roots upon salt stress. Effects of salt treatment on lateral root emergence of wild-type, overexpressor, *mc3* mutant and complemented plants of MC3. Seeds were first germinated on MS medium plates for 3 days, then seedlings were transferred to new plates supplemented with 0 (control), 50 and 100 mM NaCl, and left to vertically grow for further 7days before microscopy analysis in order to count the LRs. Statistics: One-way ANOVA with Tukey HSD test was performed to detect significant difference in expression (p -value < 0.05).

Results

ABA has been demonstrated to regulate responses also upon biotic stresses although its implication is more complex. It can act as a defence mechanism by closing the stomata thus blocking the entrance of the pathogens and also by enhancing the callose deposition in the cells in order to limit the spread of the pathogens (Ton and Mauch-Mani 2004). On the other hand, there are evidences that it can compromise the plant defence. It has been suggested that the crosstalk of ABA with other hormones such as SA and JA, which are the main regulators of the plant responses to biotic factors, is based on antagonistic relationships (Anderson et al., 2004; Moeder et al., 2010). ABA can suppress the expression of defence genes and facilitates the infection. For example, the pathogenic bacterium *Pseudomonas syringe* has developed a strategy that is based on disturbing the homeostasis of the hormone, inducing NCED and ABI1 genes in the host upon infection, increasing ABA biosynthesis which leads finally to higher bacteria multiplication (De Torres-Zabala et al., 2007). However, ABA can show positive or negative effects on the susceptibility of the host to a pathogen depending on the pathosystem studied (Lievens et al., 2017).

Ralstonia solanacearum is a soil-borne vascular pathogen that cause severe bacterial wilting disease to the host and leads to huge economical losses in the field. It enters in the plant-host from natural formed openings or wounded tissue and passes from cortex to endodermal layer until it reaches the xylem tissue where it can colonize and multiply. It moves through the vascular tissue to the aerial parts, starting to produce exopolysaccharide, which blocks the vessels and leads to plant death by reprogramming many virulence genes and metabolic pathways to facilitate their establishment (Genin 2010; de Pedro-Jové et al., 2021). A recent transcriptomic analysis showed that during early infection stages, many ABA related genes are upregulated in the plant root that is the main entry point of the bacteria. Mutants deficient in ABA downstream signalling were more sensitive in *R. solanacearum* infection and wilting disease although the morphology of the root tissue was not affected when compared to the wild-type plants (Zhao et al., 2019).

Chapter 3

MC3 showed a vascular localization and we tested if the different genotypes can be more resistant or susceptible to an invasion from *R. solanacearum*. Plants were grown under controlled SD/22°C conditions for 4 weeks and then they were infected by submergence in high amounts (10^8 colony-forming units, CFU) of bacteria in order to score symptoms daily. During the infection the plants were moved to 12:12/26°C conditions that favour the growth of the bacteria. Experiments were repeated at least 4 times with similar results as shown in Figure 3.16. The scale used for the symptoms was: 0 for no wilting, 1 for 1 leaf wilted, 2 for almost half the plant wilted, 3 for some leaves not wilted and 4 for completely wilted plants. The wild-type plants and the mutants lacking MC3 had similar levels of symptoms as the disease was spreading, arriving to the total wilting after approximately 15 days post-infection (dpi). The overexpressor line had a small delay in the appearance of the symptoms since at 15 dpi the symptoms were scored around 3, which correspond to half plant wilted (Fig 3.16). The differences observed though, when statistical T-test was applied were not showing significant differences. Absence of differences between the lines shows that for the progress of the infection many factors are important, from hormones to structural layers of defence and most likely the enhanced insensitivity of the mutants to ABA is not sufficient to cause delay of the bacteria multiplication once they entered the plant.

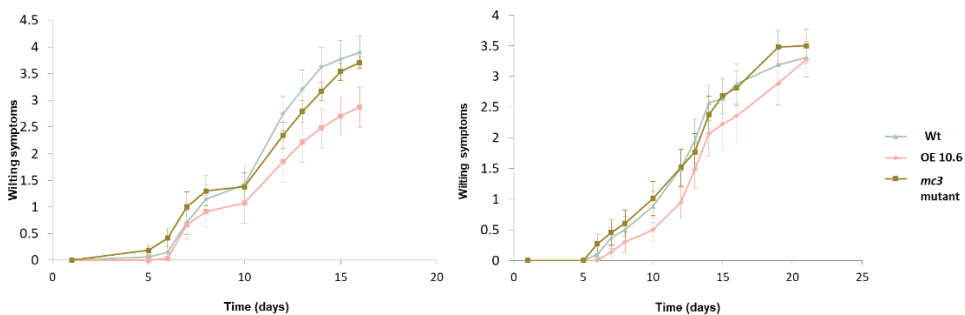


Figure 3.16: Drenching inoculation assay with *Ralstonia solanacearum*. Disease index scaled from 0 (no wilt) to 4 (whole plant death), measured daily in 4-week-old plants after drenching with 10^8 bacteria inoculum. Error bars represent standard errors of the means of results from 30 plants per genotype used in a single assay. The assay was performed at least 5 times. The results of two independent experiments are shown.

Results

Vascular formation occurs earlier upon osmotic stress in plants over-accumulating MC3

Taking into account the specific localization of MC3 and the fact that overexpression of the protease leads to enhanced drought tolerance, we wanted to test whether osmotic stress affects the developmental formation of phloem tissues. Upon osmotic stress, root cells are known to lose water content and accumulate sugars and other osmoprotectant compounds to avoid cellular damage. Notably, incubation of plants in sorbitol media for 48h to cause osmotic imbalance resulted in an arrest of the root growth. To better assess whether sorbitol affects protophloem development, sorbitol-treated roots were analysed with confocal microscopy prior Calcofluor staining. A prolonged exposition for 48h to osmotic stress appears to accelerate the differentiation of PSE, evident by the appearance of fully differentiated PSE close to the quiescence center in all the genotypes. Interestingly, overexpressor line showed as well a premature differentiation of MSE as identified from their thick cell wall (Fig 3.17). Metaphloem is the main transporting form of the phloem which replaces the protophloem tissue when the surrounding cell types have already differentiated. Although the two phloem tissues share the same precursor cell, metaphloem formation occurs in the maturation zone, approximately at 27nm upper from the QC (Mahonen et al., 2000; Rodriguez-Villalon et al., 2014). Our data showed that in the overexpressor line metaphloem is formed even before protoxylem differentiation, thus transport is mediated more efficient and that could lead to enhanced tolerance of osmotic stress.

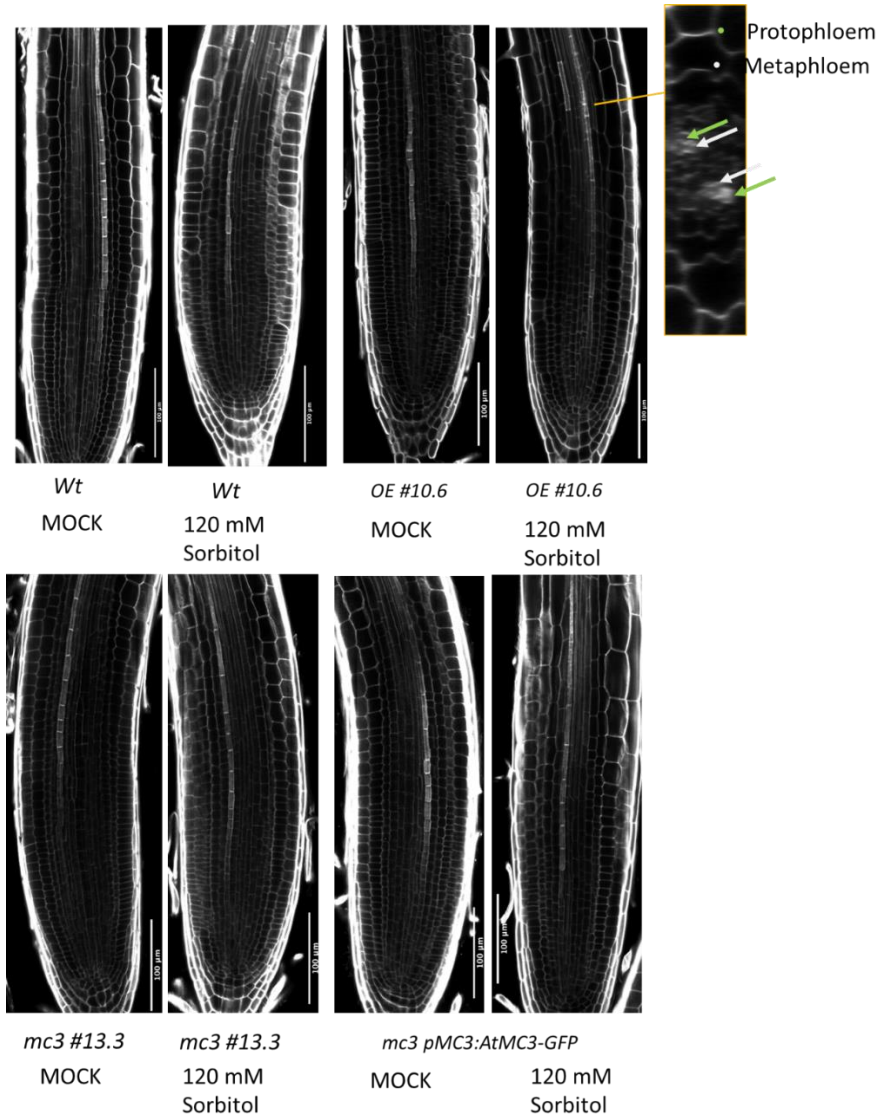


Figure 3.17: Overexpressor of MC3 shows earlier metaphloem development upon osmotic stress conditions. Confocal microscopy of 5-days-old seedlings focusing on the root tip to visualize the vascular formation. Seeds were first germinated on MS medium plates for 3 days, then transferred to new plates supplemented with 0 (mock) and 120 mM sorbitol, and left to vertically grow for further 2 days before microscopy analysis. Calcofluor staining, scale bar 100µm. Green arrow shows protophloem differentiated tissues and grey arrow shows metaphloem.

Results

Chapter 4

General Discussion

Discussion

Overview of the thesis

Since their discovery more than three decades ago, metacaspases have been linked with programmed cell death and protein homeostasis, though their mode of action and their biological role remains partly elusive. Up to date they have been shown to be involved in biotic and abiotic stress responses but also in developmental processes. Due to their miscellaneousness in protein localization, it is challenging to infer certain biological function. In the present study, we provide new insights into the contribution of metacaspases to abiotic stresses.

In [Chapter 2](#), using reverse genetic approach was shown that over-accumulation or total absence of MC3 did not result in any obvious phenotypes with regards to plant growth or vascular tissue formation. Upon normal growth conditions, N-termini based analysis did not provide any potential direct substrate of MC3. In parallel, proteome-wide analysis in seedling roots from plants lacking or over-expressing the protease pointed towards a function of MC3 in abiotic stresses, including a possible role of MC3 under water affected environments. In [Chapter 3](#), experiments performed upon severe drought conditions showed that MC3 is involved in osmotic stress responses since the abundance of the protease was concomitant with plant survival. MC3 overexpression led to enhanced vascular tissue formation which highlights the important role of phloem upon osmotic stress. Altogether, this study contributes to our understanding on metacaspase function in a tissue-specific manner and opens new avenues for future research on plant metacaspases in the context of plant adaptation to changing environmental conditions.

A metacaspase specifically localized in the phloem vascular tissue

According to multiple expression analyses, Arabidopsis metacaspases display diverse expression values during development and in different anatomical

Discussion

structures. From functional analysis performed in some of them, it has been demonstrated that they participate in various processes. Our data demonstrated that MC3, which belongs to type I metacaspases of Arabidopsis, has a very specific vascular localization both at the level of gene expression and endogenous protein accumulation (Fig 2.4-6). This result is consistent with previous studies, where promoter activity assays using transgenic plants containing the promoter region fused to GUS were used to study Arabidopsis MCs spatial expression patterns (Kwon & Hwang, 2013). Type I MCs were observed in the vascular tissue of the roots, shoots, cotyledons and leaves but also were present in flowering organs (Castillo-Olamendi et al. 2007; Kwon and Hwang 2013; Otero et al. 2021). Interestingly, MC3 was not showing expression close to the primary root tip, in accordance to our results from *pMC3:GUS* lines (Fig 2.2). In this study, to be able to follow the expression at a cellular level, constructs with *pMC3:NLS-Venus* were used in combination with high resolution microscopy. We discovered that MC3 displays a strongly active and restricted expression pattern similar to many genes related to phloem formation such as *APL*, *NAC45/86* and *CLE45* (Bonke et al., 2003; Rodriguez-Villalon et al., 2014). The MC3 expression is visible in the last three undifferentiated protophloem cells and continues to the surrounding companion cells after sieve element enucleation takes place. This pattern continues in the whole root until the hypocotyl tissue where fluorescent signal was also detected (Fig 2.4). The *pMC3:GUS* marker line indicated that the vascular expression is present in the vascular throughout the whole plant body (Fig 2.3). Another metacaspase with quite specific expression for the vascular is the type II, MC9. The expression pattern has been detected in the xylem vessels all over the plant life but also in lateral root cap tissue. Xylem undergoes a differentiation program that includes PCD as a last step. AtMC9 is helping in the *post mortem* clearance of the products coming from the cytosolic breakdown (Bollhöner et al. 2013). On the contrary, phloem upon differentiation loses its nucleus, most of the organelles and forms secondary cell wall, though it is not considered a dead cell, but terminally differentiated. The remaining organelles move close, maintain a low metabolic function, thus they depend on the surrounding companion cells for its survival and function. SE and CC are connected with plasmodesmata to facilitate the exchange of molecules. A

tempting hypothesis could be that MC3 has a similar function in the cytosolic clearance during this remarkable process of protophloem cell differentiation. Although for xylem it is not known the exact trigger of PCD initiation, many TFs and proteases that participate in PCD execution have been studied (reviewed by Cubría-Radio & Nowack, 2019; Daneva et al., 2016). Furuta et al. (2014) identified some molecular players responsible for the nuclear degradation but the mechanism driving cytosolic clearance, organelle morphological changes and sieve plate formation remain unravelled. To our knowledge our results represent the first direct demonstration of a protease with such a specific localization for the phloem tissue in *Arabidopsis*.

Using CRISPR technology we created mutated forms of the gene and we proceeded to the analysis using mutants that code either for a truncated form or do not produce the protease (Fig 2.11). Characterization of macroscopic phenotypes for overexpressor and mutant lines was performed but no obvious phenotypes were detected when plants were grown under standard growth conditions (LD and SD, 22°C) (Fig 2.15-16,18-19). In addition, we specifically tested if the vascular formation was affected. Phloem tissue is of great importance for the mobilization of nutrients and transport of signalling molecules. If these processes are affected, development of the plant would be hampered as well. The most common phenotypes associated with phloem defects are shorter primary root length, affected emergence of lateral roots, discontinuous cotyledon vein pattern and “gaps” in the protophloem strand. In our hands, *mc3* mutants or overexpressor didn't exhibit any difference from the wild-type plants that could be linked to affected vascular tissue (Fig 2.20,21). Gujas et al. in 2020 demonstrated that CCs can maintain their plasticity and trans-differentiate in PSE when is necessary in order to ensure the correct formation of the protophloem strand. By crossing marker lines for phloem vascular genes (*CVP2* for protophloem and *SUC2* for CCs) with *mc3* mutants we didn't notice any phenotype associated with cell identity, formation pattern or phloem loading (Fig 2.22).

Most of *AtMCs* haven't shown any phenotype in plant growth and development. *mc9* mutants have a delay in the clearance of the xylem vessels when tested with electron microscopy which was not translated to any visible phenotype (Bollhöner et al. 2013). One explanation could be that *MCs* have mild

Discussion

phenotypes because of redundancy. The sequence similarity for some members of the family is quite high and the function of one could be replaced by another. For this reason, we used publically available databases, online tools and transgenic lines to verify which MCs are co-expressed specifically with MC3. MC4 exhibits a high and ubiquitous expression all over the seedling root and MC1 was detected mostly in the stele. Interestingly, the expression was also visible at the root tip in the last SE before enucleation and upwards in companion cells (Fig 2.14). When transcriptional levels were tested in the *mc3* mutant background, there were no significant changes either in the rest of metacaspases or in other proteases with expression in the vascular (Fig 2.12,13). However, transcriptomic data do not always correlate with protein abundance. Proteases are regulated mostly in a post- translational level and to clarify if they act redundantly we created double mutants of *mc1mc3* and *mc3mc4* to include them in the analysis. Unfortunately, none of them showed any visible phenotype. High order mutants will be required to elucidate the real contribution of the metacaspase family in plant development and stress responses (Shen et al., 2019). Another approach would be to use experiments with higher specificity (such as electron microscopy, cell death assays etc.) to detect a molecular phenotype.

In the plant kingdom MC3 is not the only one localized in the phloem. (Suarez et al. 2004) showed that the expression of the type II metacaspase, mCII-Pa in mature embryos of *P. abies* was associated with procambial strands, the precursors of all vascular cells. Another MC localized in sieve elements is TaeMCAII which exhibited a dynamic trend in the development of SEs and its expression coincided with the nuclear DNA fragmentation, a sign of cell degradation. Since the enucleated phloem cells depend on the supporting companion cells even for protein synthesis, it was hypothesized that TaeMCAII was originally located in the CCs and then transported to SE. Indications for type I and type II MCs' expression in the stem of *Populus tremula* trees, more specifically to the secondary phloem and xylem can be found in databases for gene expression (aspwood.popgenie.org).

Subcellularly, MC3 was distributed in the cytoplasm of the companion cells and was not detected in the nuclei or the vacuole (Fig 2.5,7). This finding is in accordance with the location for most of metacaspases studied, at least in their

inactive form (Bollhöner et al. 2013; Coll et al. 2010; Hander et al. 2019). Furthermore, it is unlikely that is transported from the companion cells to the mature sieve elements since there was not fluorescent signal detected in the vascular tube, although it cannot be excluded the size limitation for the transport through the plasmodesmata. Studies have shown that peptides less than 70kD can be transported unspecifically into the vascular (Ross-Elliott et al. 2017). MC3 protein when is fused to GFP reaches the 78kD whereas the endogenous protease is 47kD, a fact that could affect the detection of movement. For plants with endogenous levels or overexpressing a version of MC3 with a mutated cysteine at the catalytic position 230, the localization was not altered (Fig 2.5,7). Therefore, the catalytic activity is not required for the protease distribution. Whereas past researchers have found that some particular metacaspases required auto-process for their activation (Coll et al. 2010; Hander et al. 2019; Tsiatsiani et al. 2013; Vercaemmen et al. 2004), the present study has shown that MC3 seems to be cleaved in more than one sites, although it might be a result of another protease performing the cleavage (Fig 2.8,9). These results raise the question for the existence of a pattern in metacaspase activation and processing, thus further investigation needs to be done to identify interactors that could regulate this process.

A new role for metacaspases in osmotic stress conditions

Characterization of macroscopic phenotypes for proteases often do not give results as discussed above. We decided to centre out attention in the proteomic changes that occur from different expression levels of MC3 in the plants. At first, a shotgun proteomic approach was performed in leaf tissue and a total of 2970 proteins were identified. By dual comparisons between the different MC3 backgrounds only a few proteins appeared to be significantly changed. From our data we observed that the majority of them can be linked with signalling transport and responses to stresses. Some proteins deregulated in the overexpressor were linked to plastids and their membrane composition or electron transport chain

Discussion

(Fig. 2.23-25). Photosynthesis is a major sensor of the environmental stimuli, thus changes in plastid proteins can help in the maintenance of energy homeostasis towards an upcoming stress. It is important though to take into account that a limitation that comes from the use of leaf tissue is that plastid proteins are highly expressed and cover the majority of the proteins detected. As a result, changes that could be caused from MC3 absence or over-accumulation could be masked. We obtained data from a similar proteomic analysis conducted with root tissue collected from cotyledons. It was interesting that many proteins related to ABA downstream signalling, osmotic stress and hypoxia stress appeared deregulated (Fig 2.27, 28). From our dataset, some peroxidases showed less expression when there is more MC3, providing information for changes in the endodermal layer of the root. In contrast, other proteins related to protection from oxidative stress such as ACX1 or DOX1 were upregulated in the overexpression lines. In addition, BGU22 and BFRUCT4 respond to ABA hormone and further responses to osmotic stress and were detected higher in the mutant but BGLU18 behaved opposite. Finally, NAI2, a component of the ER bodies structures was less in the overexpressor. The reduced expression could be an indication of increased proline accumulation which assist to responses at stresses such as drought (Kumar et al., 2015).

A significant indication that led us to the conclusion that MC3 function was involved in osmotic stresses, were the observed proteomic changes detected even upon basal growth conditions. A possible explanation could be that the increased expression of MC3 prepares the plant to respond faster and more robust towards the upcoming stress, a phenomenon called “priming” (Balmer et al., 2015; Ding et al., 2012; Leuendorf et al., 2020). The idea was further supported by the finding that MC3 overexpressor was able to withstand better drought stress (Fig 3.5). By monitoring on a daily basis the water consumption, we observed that under the same conditions, plants with higher levels of MC3 were able to cope with stress better and look healthier than wild-type and *mc3* mutants. Moreover, when plants were experiencing the severe stress photosynthetic capacity was in general better when the amount of MC3 was higher (Fig 3.7). These results could be perceived as an indirect effect from the overexpression of the metacaspase if the mutant was behaving similar to wild-

type plants. On the contrary, we observed that both mutant lines survive less when water is not available and the complementation line was restoring the survival rate. It was interesting the finding that upon well-watered conditions both overexpressor and complementation lines contain more water than the wild-type plants, showing that they could take better advantage of the water availability from the soil (Fig 3.6).

Although proteases encompass a numerous protein family, essential for many developmental, metabolic and stress related responses, our knowledge regarding their role upon osmotic stress adaptation is still fragmentary. Protein turnover, altered metabolic activities, proteolytic activation of signalling peptides and mobilization of nutrients are some of the protease activity associated especially with drought stress. In *Arabidopsis*, the aspartic protease ASPG1 is expressed in the guard cells and confers drought avoidance in an ABA dependent signalling pathway (Yao et al., 2012). Furthermore, AtSBT1.4 (SASP) a subtilase which was downregulated in our overexpressor root samples according to the proteomic data, recently was shown to interact and degrade OST1, regulating ABA signalling. *sasp* mutants exhibited significant drought tolerance whereas overexpression of another subtilase, AtSBT3.8 or its substrate PSK lead to better plant performance upon osmotic stress in *Arabidopsis* seedlings (Stührwohldt et al., 2021; Wang et al., 2018). Cysteine proteases can have controversial roles in drought responses, for example ectopic expression in *Arabidopsis* of the sweet potato SPCP3 increased drought sensitivity whereas SPCP2 was demonstrated to enhance plant tolerance (Chen et al., 2010; 2013). It has been shown that the root meristem shows PCD characteristics upon drought stress such as organelle degradation, vacuole swelling and plasma membrane disruption. This mechanism contributes to the lateral root formation in order to enhance the plant defense and facilitate recovery (Duan et al., 2010) but no mechanism of execution or more specific protease has been linked to the process up to date. Leaf senescence is an another adaptation strategy, mediated by ROS triggered PCD, essential for the plant survival (Munné-Bosch and Alegre 2004). Through sacrificing an amount of leaves, nutrients can be recycled and used from the rest of the plant but also reduce transpiratory surface to minimize further water losses.

It would be interesting to test in the future if MC3 is involved in PCD responses. Certain limitations of the study such as the specific protein localization could be addressed in future research by establishing VISUAL trans-differentiation system (Kondo et al., 2015; Tamaki et al., 2020), as discussed in the Introduction chapter, and mimicking osmotic stress conditions in order to identify the function of the protease more specifically in the vascular.

MC3 overexpression leads to pre-mature metaphloem development upon osmotic stress

Upon drought stress, photosynthesis is impaired and sucrose is accumulating in the shoot disturbing the energy balance for metabolic activity (Thalmann and Santelia 2017). Phloem is the responsible tissue for sucrose transportation, loaded primarily in leaves by SWEET11 and 12 sugar transporters from the phloem parenchyma cells to the apoplast and then from CCs to the phloem SEs by SUT transporters (Chen et al., 2012; Durand et al., 2018). Since sugars constitutes the energy source for the root development, defects in protophloem differentiation are reflected in an impaired meristematic activity, and in turn, post-embryonic root growth. Less studied is the plasticity of this tissue in response to environmental stresses. Interestingly, the protophloem-specific CLAVATA3/EMBRYO-SURROUNDING REGION-RELATED 25 (CLE25) peptide has been recently described as a mobile root-to-shoot signal promoting ABA biosynthesis in the leaves and, in turn, stomata closure upon water deficit. While is well known that exogenous CLE25 application prevents PSE differentiation, whether drought stress affects phloem formation remains unknown. (Dinneny, 2019; Takahashi et al., 2018). Protophloem strand is easier to study since it differentiates in the meristematic zone of the root before the differentiation of any other cell type. On the other hand, less studied is the metaphloem which appears in the post-meristematic zone of the root and remains functional for a longer time. Metaphloem formation either in basal conditions or upon stress conditions remains elusive. In this study, we provide evidence that upon osmotic stress,

plants that contain higher amounts of MC3 are able to form metaphloem much earlier- before protoxylem strand differentiation compared to the wild-type (Fig 3.17). Although this finding explains the higher tolerance of the overexpressor plants for drought stress, its most important contribution may be that it raises a variety of intriguing questions for the undiscovered strategies of plant roots to cope with unfavourable environments. Two very recent studies (Graeff and Hardtke 2021; Otero et al. 2021) proposed a series of molecular markers to follow the delicate metaphloem development which would be a valuable asset to delve into the mechanism that MC3 overexpression results in pre-mature tissue formation. The MC3-mediated enhanced metaphloem differentiation may be necessary to drive more sugars to the root tip and prevent water loss from protophloem and neighbouring cells to compensate osmotic pressure/unbalance.

Yet, it is not clear if the catalytic activity of the protease is necessary for the plant response. We can propose two scenarios: i) MC3 acts as protease and cleaves a substrate upon osmotic stress that gets transported through the phloem and alerts the plant, and ii) that the catalytic activity is not required and MC3 acts simply a protein homeostasis sensor. In the first case, the substrate could be directly involved in the response and in the second the protease would have an indirect role to ensure the plant fitness is not compromised (Fig 4.1). Further experiments including overexpressor lines of the catalytic inactive version (MC3 C230A) should be performed to clarify these hypotheses.

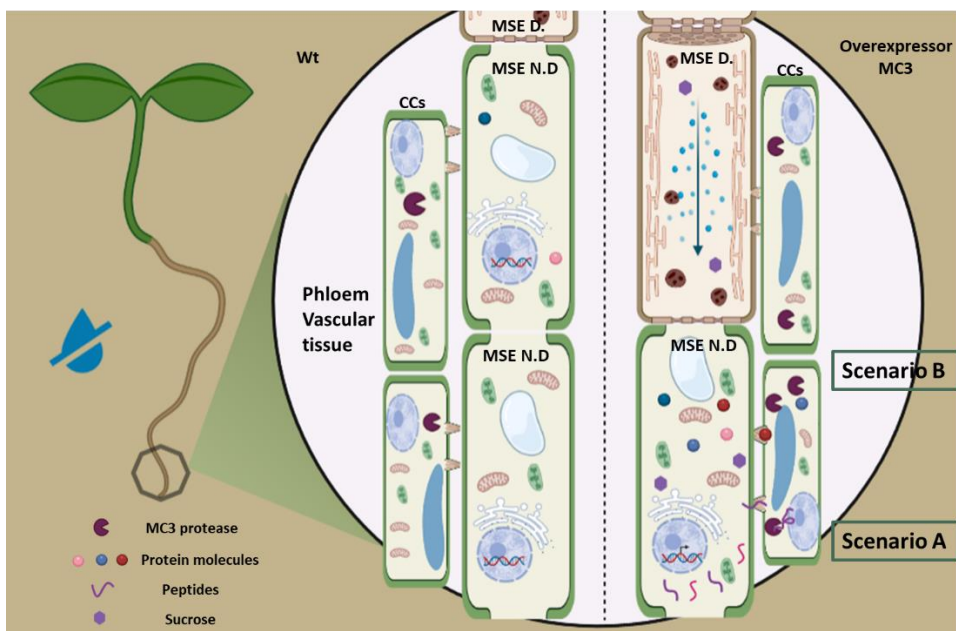


Figure 4.1: Plausible mechanisms of MC3 function upon osmotic stress conditions.

A closer look at the root tip of Arabidopsis seedlings is presented, where the phloem vascular begins to differentiate. In Scenario A, MC3 acts as a protease by cleaving a substrate. The peptides derived from the cleavage event could be transported to the non-differentiated Metaphloem Sieve elements (MSE N.D), multiply the perceived signal of upcoming stress and lead to earlier differentiation of the tissue (MSE D). In Scenario B, MC3 does not require its catalytic activity and upon water deprivation acts as a sensor of stress. Proteins related to responses become upregulated preparing the plant to face the stressful conditions. Furthermore, these affected proteins from increased MC3 levels could affect downstream the time of metaphloem maturation. The result from both plausible mechanisms is the faster formation of the vascular that facilitates the transport of nutrients, signalling molecules and hormones.

Over-accumulation of MC3 might enhance plant performance upon various stresses

Stress conditions like drought, increased salinity and freezing temperatures tend to provoke an osmotic imbalance to the plant. ABA is the main

phytohormone orchestrating responses to osmotic stresses both in root and shoot tissue (Takahashi et al., 2020). Along with auxin synthesis and transport, hormonal changes have an impact on root architecture in order to maximize water uptake while reducing losses to minimum (Karlova et al., 2021; Korver et al., 2018). From our results was shown that *mc3* mutant show reduced sensitivity to ABA which leads to less drought tolerance (Fig 3.8). Stomatal closure is an immediate response to increased ABA concentration through activation of NO and ROS. We observed that there is a delay in the response of our mutant line to the hormone (Fig 3.11). The amount of chlorophyll A upon ABA treatment was more in the mutant and overexpressor lines showing that when senescence is promoted these plants are less sensitive to the pressure that the hormone is creating for them to die (Fig 3.9). Since ABA is transported through the vascular system through long distances we wanted to test if there is a connection between ABA and MC3 or the reduced sensitivity was caused by vascular formation defects. The biosynthesis of the hormone was not affected since all hormones levels were tested upon basal conditions and didn't exhibit any difference (Fig 3.13). Moreover, the expression of biosynthesis genes was not altered either in root or shoot tissue as well as receptors and regulators of downstream signalling. We found interesting that the levels of RD22 and RD29A were reduced only in the root samples of *mc3* mutant (Fig 3.12) which was consistent with the upregulated expression in the root observed for RD29A upon cold temperatures (Prerostova et al. 2021). Msanne et al. (2011) shown that RD29A is highly induced by salt stress and possibly act like a warning signal for the upcoming stress. RD22 also responds to ABA specifically upon drought stress and not cold or salt treatments (Kazuko). More experiments are needed to clarify if the downstream signalling is affected because of direct MC3 implication to the pathway or indirect effects.






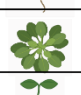

Saline soils show less water potential, making the osmosis for water uptake a challenging process for the plant. Increased salt ions block the function of enzymes in translocation and availability of nutrients (Van Zelm et al., 2020). It has been shown that there is a different response of the primary root (PR) and the lateral roots (LR) in response to salt stress, downstream ABA signalling. PR shows growth inhibition upon concentration of 100 mM NaCl, but is not as

Discussion

affected as the LR post-emergence formation. Endodermis is the crucial cell type layer that controls the LR formation and the latter appear to be hypersensitive to ABA accumulation (Duan et al., 2013). Although MC3 PR length was not affected, the number of LRs was increased in the overexpressor compared to the rest of the genotypes both in mild and increased salt stress implying that the protease function could be linked to stresses causing osmotic unbalance in general (Fig 3.14,15). On the other hand, there was no difference in the progress of the wilting disease caused by *R. solanacearum*, a pathogen moving in the plant mostly through xylem vessels (Fig 3.16). It would be interesting to test more vascular pathogens, such as *Xylella fastidiosa* to investigate if MC3 has a role in defence. Furthermore, light and elevated temperature didn't give a strong phenotype to the plant when MC3 is overexpressed or missing (Fig 3.2). Upon strong heat stress MC3 forms aggregates similar to MC1 (Ruiz et al., unpublished data) but there is no evidence that it affects the plant survival so far.

Finally, indications from public transcriptomic data pointed us to hypoxic stress. Overexpression of MC3 showed higher survival in seedling stage upon lack of oxygen but to our surprise *mc3* mutant has also higher survival compared to the wild-type (Fig 3.3). The higher tolerance to hypoxic stress could be explained by the increased ADH expression that was detected in roots and shoots of MC3 overexpressor even in basal conditions (Fig 3.4). *ADH* codes for an alcohol dehydrogenase which apart from hypoxic stress as discussed in Chapter 3, has also a role in responses to multiple stresses (Shi et al., 2017). Consistent with our findings, this study demonstrated that plants overexpressing ADH had increased expression of ABA related genes such as RD22, RD29A and KIN1. Another factor that can induce ADH expression is the sucrose catabolism that occurs during stress (Loreti et al., 2018). Taken together, our findings indicate MC3 overexpression can be linked to ABA signalling and therefore stress tolerance when the stress involves water availability, either excess or lack of it, since lately more and more evidences come to light that connect ABA and hypoxic responses as well (reviewed by González-Guzmán et al., 2021).

Table 5: Overview of the phenotypes observed in the overexpressor and mutant lines of MC3 in every environmental condition tested. Right side: Indication of the developmental stage of the Arabidopsis plant when the experiments were performed.

Environmental Conditions	Phenotypes observed compared to Wt			
	Characteristic/ Genotype	Overexpressor	Mutant	
Standard Growth	Rosette Leaf Area	Similar	Similar	
	Rosette Fresh Weight	Similar	Similar	
	Shoot Length	Similar	Similar	
	Inflorescence tissue formation	Similar	Similar	
	Flowering Time	Similar	Similar	
	Root Length	Longer	Longer	
	Hypocotyl Length SD	Similar	Similar	
	Cotyledon Vein Pattern	Similar	Similar	
	Meristem Size	Larger	Larger	
	Vascular formation	Similar	Similar	
Lateral Root Number	Similar	Similar		
Drought	Survival	Higher	Lower	
	RWC	Similar	Similar	
	Photosynthesis	Similar	Lower	
	Vascular formation	Earlier Metaphloem	Similar	
Salinity	Primary Root Growth	Similar	Similar	
	Lateral Root Number	Increased	Similar	
Hypoxia	Survival	Higher	Higher	
Pathogens	Disease progress	Similar	Similar	
Heat	Aggregate formation	YES		
	Root Length	Similar	Similar	
	Hypocotyl Length	Similar	Shorter	

In summary, the present research is a first step towards the integration of three different topics of research: metacaspases, vascular formation and osmotic stress responses that have not been linked before. It would be useful to broaden our knowledge regarding the variety of ways plants use to cope with stresses and especially the role of the vascular since is the most important connection for the signal transduction. Moreover, another question that comes up is the way a plant can respond to a combination of stresses. Dissecting tissue specific responses is a necessity in order to study and fully understand complex stresses like drought. A step further would be the use of that knowledge and its translation to crops in order to improve plant traits for the reinforcement of agriculture.

Discussion

CONCLUSIONS

For the main goals of this work, we arrived to the following conclusions:

Determine MC3 gene expression pattern and localize the MC3 protein

- *MC3* gene is specifically expressed in the phloem vascular tissue.
- MC3 protein follows a similar pattern of highly specialized expression in companion cells. The catalytic activity of the protease is not necessary for the proper localization. Subcellularly, MC3 is evenly distributed in the cytoplasm.
- In plants overexpressing MC3, the localization was present in all the tissues with an enhanced signal in the protophloem strand and stele in general.
- The levels of expression of the protein with endogenous promoter are very low detected. Between wild-type and predicted catalytic inactive version (C230A) there was no difference in the cleavage events indicating that the protein is not self-cleaved.

Identify potential MC3 proteolytic substrates and changes occurring in the proteome caused by altered MC3 levels.

- Leaf and root total proteome analysis of MC3 overexpressor and mutant lines compared to wild-type plants indicate that MC3 is possibly involved in osmotic and hypoxic stress responses.
- N-termini analysis didn't provide evidence for direct proteolytic events from MC3 function.

To investigate the role of MC3 during development of the plant by phenotypical analysis of the effects caused by altered MC3 levels.

- Upon basal growth conditions *mc3* mutants do not have any striking phenotype on the plant growth and development.
- Deletion of MC3 does not affect phloem formation upon basal conditions.

- Vascular proteases´ or metacaspases´ expression was not affected from the absence of MC3. No visible phenotype was detected for *mc1mc3*, *mc3mc4* double mutants upon basal growth conditions.

To investigate the role of MC3 in stress responses by phenotypical analysis of the effects caused by altered MC3 levels when plants are challenged with a stress factor.

- Promoter sequence analysis revealed the presence of possible motifs for TFs related to mostly abiotic but also biotic stress responses.
- Light and temperature doesn´t affect MC3 function. Furthermore, upon infection with *Ralstonia solanacearum*, a vascular pathogen, the disease progressed similarly for all the backgrounds of MC3.
- MC3 overexpressor and *mc3* mutant lines have higher survival rate compared to wild-type plants under hypoxic conditions. In the overexpressor line, the hypoxia “core gene” *ADH* was found upregulated upon basal conditions.
- Under severe drought stress, protein levels of MC3 were concomitant with the survival rate. At low water availability, MC3 overexpressor plants maintained a better photosynthetic activity.
- Knock-out mutants of MC3 show less sensitivity to ABA.
- Expression of *RD22* and *RD29A*, genes which are responding downstream to the ABA, was downregulated in the *mc3* mutant upon basal growth conditions.
- The quantity of basic hormones is not altered upon basal conditions.
- MC3 overexpression leads to enhanced metaphloem development under osmotic stress conditions.
- Upon increased salinity conditions MC3 overexpressor was generating more lateral roots, an indication for higher stress tolerance.

Materials and Methods

Materials and Methods

Generation of Genetic tools

1. Plant material

Arabidopsis thaliana (L.) Heynh wild-type (Col-0) and *Nicotiana benthamiana* were used in the experiments performed in this study. Besides the transgenic and mutant lines generated as part of this work, marker lines obtained from other laboratories are indicated in Table 1 and 2.

Table 1: Mutant lines used in this study

Name of the line	Gene	Order	Reference
<i>mc3</i> CRISPR #13.3	<i>At5g64240</i>	Single	In this work
<i>mc3</i> CRISPR #6.10	<i>At5g64240</i>	Single	In this work
<i>mc3</i> G175E TILLING	<i>At5g64240</i>	Single	In this work
<i>mc1</i> GABI_096A10	<i>At1g02170</i>	Single	GABI-Kat Resource
<i>mc4</i> SAIL_856_D05	<i>At1g79340</i>	Single	SAIL mutant
<i>mc3</i> CRISPR X <i>mc1</i>		Double	In this work
<i>mc3</i> CRISPR X <i>mc4</i>		Double	In this work

Table 2: Transgenic lines used in this study

Name of the line	Genetic Background	Description	Reference
<i>pMC3: GUS</i>	Col-0	Marker line	Van Breusegem Lab
<i>pMC3: NLS-3XVenus</i>	Col-0	Marker line	Rodriguez-Villalon Lab
<i>pCVP2:NLS-3XVenus</i>	Col-0	Marker line	(Rodriguez-Villalon et al. 2014)
<i>pSUC2:GFP</i>	Col-0	Marker line	(Rodriguez-Villalon et al. 2014)
<i>pNAKR1:NLS-Venus</i>	Col-0	Marker line	(Gujas et al. 2020)
<i>pAtMC1:MC1-GFP</i>	<i>mc1</i> GABI_096A10	Complemented line	(Salguero-Linares et al., unpublished)
<i>UBQ10:MC3-GFP</i>	Col-0	MC3 Overexpressor	In this work
<i>UBQ10:MC3C230A-GFP</i>	Col-0	MC3 Catalytic Inactive Overexpressor	In this work
<i>UBQ10:MC3-GFP</i>	<i>mc3</i> CRISPR#13.3	MC3 Overexpressor	In this work

Materials and Methods

<i>UBQ10:MC3C230A-GFP</i>	<i>mc3</i> CRISPR #13.3	MC3 Catalytic Inactive Overexpressor	In this work
<i>pMC3:MC3-GFP</i>	<i>mc3</i> G175E TILLING	Complemented line	In this work
<i>pMC3:MC3-GFP</i>	<i>mc3</i> CRISPR #13.3	Complemented line	In this work
<i>pMC3:MC3 C230A-GFP</i>	<i>mc3</i> CRISPR #13.3	Complemented line	In this work
<i>pMC3:MC3 G175E-GFP</i>	<i>mc3</i> CRISPR #13.3	Complemented line	In this work
<i>pCVP2:NLS-3XVenus</i>	<i>mc3</i> CRISPR #13.3	Marker line	In this work
<i>pSUC2:GFP</i>	<i>mc3</i> CRISPR #13.3	Marker line	In this work

2. Cloning

1. Expression Constructs

For generating expression constructs, Gateway Cloning Technology (Invitrogen) and Green Gate Cloning System (Lampropoulos et al. 2013) were used. All primers used are presented in Table 3. Several independent transgenic lines were analysed, and the strongest lines of each construct were selected to continue the analysis.

For protein localization experiments, fusion of fluorescent proteins to *MC3* and *MC3-C230A* genomic or CDS sequences was performed using GREENGATE cloning strategy. Briefly, the full-length genomic of *MC3* was amplified with primers set *GG_MC3_NOSTOP_R/GG_MC3_F* and then was cloned into the entry vector *pGGC* (with gentamicin resistance). The CDS sequence of *MC3* was amplified with primer set *GG_MC3_MB_F/R* to be inserted in *pGGB* module. To create the catalytic inactive version of the gene, the Quick site mutagenesis kit (Agilent Technology) was used with *pGGC/B_MC3* module as a template (Primers indicated in Table 2). C-terminal eGFP fluorescent protein was separately cloned in both *pGGC* module and *pGGD* module to create the library of vectors (Primers indicated in Table 3). The native promoter of *MC3* was also cloned with the primers *GG_MC3_PRM_F/R* in the *pGGA* entry vector. All the entry modules as well as the construct with *UBQ10* constitutive promoter in module A, constructs with dummies in modules B and D, terminator sequence in

Materials and Methods

E and resistance for plant selection in F, are commercially available in AddGene database. For the overexpression lines *pGGA-UBQ10*, *pGGC-MC3* genomic and *pGGC- MC3 C230A* genomic, *pGGB- dummy*, *pGGD- eGFP*, *pGGE-UBQ10terminator*, *pGGF- BASTA* were combined in the *pGGZ003*-empty destination vector (with resistance to spectinomycin). The final construct possesses the BASTA cassette for transgenic plant selection. For the expression of the protein under the native promoter the constructs used, were: *pGGA-promoter MC3*, *pGGB-MC3* CDS sequence, *pGGC- eGFP*, *pN95 (RBCSt.D-F-pGGD000)*, *pGGF- Alli-YFP* (entry_ plant selection) combined in the *pGGZ003*-empty destination vector. In these constructs dummy sequences were avoided in order to obtain the maximum expression without any interference. In both cases for the final reaction 1.5 µl plasmid of each of the entry modules were mixed with 1 ml of the destination vector, 1.5 µl CutSmart Buffer (alternatively: FastDigest buffer), 1.5 µl ATP (10 mM), 1 µl T4 DNA ligase (30 u/ml) and 1 µl BsaI-HF (alternatively FastDigest Eco311) in a total volume of 15 µl. The conditions of the reaction were 50 cycles of 37 °C for 5 minutes and 16 °C for 5 minutes each, followed by 50 °C for 5 minutes and 80 °C for 5 minutes.

II. Generation of CRISPR Mutants

For generation of the CRISPR MC3 mutants the target sequence was selected using CRISPOR program (Haeussler et al. 2016). DNA backbone fragments of a total length of 500bp containing :20 bp of the target sequence that neighbouring the PAM (3bp Protospacer Adjacent Motif) sequence, overhang *attB* sequences for Gateway cloning, *tracrRNA* sequence (which will bind the Cas-9 enzyme), U6 promoter sequence and restriction sites for the cloning were ordered as gBlocks® from IDT. All the sequences of the gBlocks used are mentioned in the Appendix Part 1. In order to create effectively a deletion in the gene, three different gRNAs were designed targeting the sequence in the beginning of the transcription, in the end just before the stop codon and close to the triplet that codes for the catalytic cysteine residue of MC3. For the generation of point mutations in the catalytic centre only one gRNA was designed targeting the 20bp including the catalytic triplet. 3 µl (50ng/µl) of the gBlock sequence was introduced to 1µl (150ng/µl) of pDONR207 (with resistance to Gentamycin) with BP reaction using 1µl of BP

Materials and Methods

clonase II enzyme (Thermo Fisher Scientific). For the combination of the three gRNAs in one vector we digested the vectors including the individual gRNAs with the restriction enzymes that they contained (BamHI/PstI/Sall). The *pDONR207* vector containing the triple gRNAs sequences and the single gRNA sequence were then transferred into the *pDe-CAS9-DsRED* vector (Morineau et al. 2017) via LR reaction (Thermo Fisher Scientific) following the manufacture's protocol. The resulting construct was transformed into wild-type plants. Transformed plants were obtained by dsRED selection. T2 seeds from single insertion lines were germinated on MS agar plates without antibiotics. Cas9-free mutants were counter selected from the T2 population by dsRED and sequenced using the primers listed in Table 4 as *DET_delICP1_F/R* and *DET_delIT_F2/R2*.

Table 3: Primers used for cloning strategies

<u>NAME</u>	<u>SEQUENCE</u>
<i>GG_MC3_PRM_F</i>	AACAGGTCTCAACCTGAAGATGGCGGTTTATGGAT
<i>GG_MC3_PRM_R</i>	AACAGGTCTCATGTTATTGAGCTTTGTTTTGGTTTTT
<i>GG_MC3_F</i>	AACAGGTCTCAGGCTCAATGGCTAGTCGGAGAGAAGTAC
<i>GG_MC3_Full_R</i>	AACAGGTCTCTCTGATCAGAGTACAACTTTGTGCGCGTA
<i>GG_eGFP_D_F</i>	AACAGGTCTCATCAGGTATGGTGAGCAAGGGCGAGGA
<i>GG_eGFP_D_R</i>	AACAGGTCTCTGCAGTCACTTGTACTGTCCATGCC
<i>GG_eGFP_C_F</i>	AACAGGTCTCAGGCTCAACAGTATGGTGAGCAAGGGCGAGGA
<i>GG_eGFP_C_R</i>	AACAGGTCTCTCTGATCACTTGTACTGTCCATGCC
<i>GG_MC3_MB_F</i>	AACAGGTCTCAAACAATGGCTAGTCGGAGAGAAGTACGG
<i>GG_MC3_MB_R</i>	AACAGGTCTCTAGCCGAGTACAACTTTGTGCGGTACACG
<i>AtMC3_C230A_F_2</i>	CGCTGTCATCGACGCCGCTAACAGCGGGACTGTC
<i>AtMC3_C230A_R_2</i>	GACAGTCCCCTGTTAGCGGCGTCGATGACAGCG

3. Transient expression

Transient *Agrobacterium tumefaciens*- mediated transformation of *Nicotiana benthamiana* was performed as previously described in (Coll et al. 2010). Whole *N. benthamiana* leaves (c. 300 mg each) transiently expressing the constructs to test together with the anti-silencing vector p19 (Voinnet et al., 2003)–UBQ10::MC3-GFP + 35S::p19 (OD600 0.4 + 0.1), UBQ10::MC3C230-GFP +

Materials and Methods

35S::p19 (OD600 0.4 + 0.1), – were collected 3 days after the infiltration and frozen in liquid nitrogen before further processing for protein extraction. For microscopic imaging leaf discs were collected from the infiltrated leaves 3 days after the infiltration.

4. Stable Transformation of Arabidopsis transgenic lines

All constructs created in the cloning section were transformed in the *Agrobacterium* strain GV3101 (pMP90) by the electroporation method and plated in selective Luria- Bertani (LB) plates. Plants were transformed with the floral dip method as previously described in (Zhang et al., 2006). Homozygous transgenic lines were selected on MS media supplemented with 20 $\mu\text{g ml}^{-1}$ Basta (glufosinate- ammonium). Mature T1 seeds of CRISPR transformed and transgenic lines with the construct driven by the endogenous promoter, were selected by fluorescent signal under an Olympus DP71 stereomicroscope (Olympus, Centre Valley, PA, USA).

5. Obtention of tilling lines

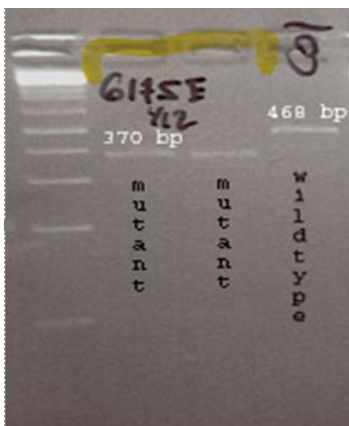
To get Col-0 plants with point mutations in the *MC3 (At5g64240)* gene, seeds were ordered from Seattle Tilling Project, created as described in the webpage http://tilling.ucdavis.edu/index.php/Arabidopsis_TILLING. The mutations could appear in homo- or hetero- zygosity. From the list of mutations available from the TILLING- Davis database (for details in Appendix Part 2), those that carrying an amino acid substitution were selected to continue with. Homozygosity was successfully obtained with the lines G175E, G183E and A269T that carry the respective amino acid alterations in the protein sequence. Plants were backcrossed 7 times with Wt Col-0 plants to eliminate potential background mutations. A269T line did not show any phenotype hence it was not analysed further. G175E was transformed with *pMC3:MC3-GFP* construct to be complemented.

DNA and RNA Analysis

1. DNA extraction and genotyping

Plant genomic DNA was extracted for genotyping purposes. Leaf discs from cotyledon or rosette leaves were collected in a 1.5 ml Eppendorf tube with 200 μ l of 2X CTAB Extraction Buffer (CTAB 2%, 100mM Tris-HCl (pH 8.0), 20mM EDTA (pH 8.0), 1M NaCl, 1% PVP). Tissue was homogenized using a mechanical pestle and an additional 200 μ l of 2X CTAB were added. Suspension was incubated at 65°C for 1 h. Then, 400 μ l of chloroform were added and the samples were centrifuged at 16.000xg for 5 min. Supernatant was transferred in a new 1.5 ml Eppendorf tube and 100 μ l of isopropanol were added for DNA precipitation. Incubation on ice for 30 min took place. The suspension was centrifuged at 16000xg for 15 min at 4°C followed by the removal of the supernatant to obtain pelleted DNA. Pellet was washed with 100 μ l of 80% EtOH and spun down again for 5 min. Supernatant was discarded and pellet was dried at 65°C and resuspended in 40 μ l double distilled water containing RNase 0.4 μ g/ml.

Genotyping for the TILLING mutant plants was conducted by PCR using *MC3-1F/MC3-1R* primers (Table 3). A DNA fragment was first amplified (468 bp) and then the PCR product was digested at 37°C overnight with the restriction enzyme BspHI (5 μ l PCR Product, 2 μ l Restriction Buffer, 1 μ l BspHI, 12 μ l water). Digestion reaction was heat-inactivated and the products were separated using gel electrophoresis. Resulting bands showing either an undigested fragment for wild-type (468 bp) or the digestion products of the mutant fragment (370 bp and 98 bp) as indicated in the following picture. The heterozygous genotype would include all three theoretical fragments.



For the CRISPR line that contain the deletion of the gene a PCR was conducted with the primer set *DET_delT_F/R*. In the wild-type background the size of the band would be 1645bp whereas in the transgenic homozygous plant would be 903bp. For the CRISPR line containing the point mutation, PCR was conducted with the primer set *DET_delCP1_F/R* and the amplified band was 498bp. To identify the existence of the mutation, bands were cut from the gel, purified with the NZYGelPure kit from NZYTech and sequenced. For the generation of double mutants *mc1mc3* and *mc3mc4*, homozygous single mutant plants were crossed in pairs to obtain *mc1mc3* and *mc3mc4*. Primers used to genotype the plants are indicated in Table 4.

Table 4: Primers for Genotyping

<u>NAME</u>	<u>FORWARD PRIMER</u>	<u>REVERSE PRIMER</u>
<i>MC3_1F/R</i>	CGCAGAGAATACCCACGAAG	AAGCTGCTCCACCATCTGTT
<i>DET_delCP1_F</i>	GTGATGCTAAGTCCATGAGATCTT	TACCTCTCCATCCTGCAAATGAAG
<i>DET_delT_F2</i>	CGTGGACAAATCAACATTCCACAT	TATTGCTCGTAAGAAGAGAGAGGC
<i>AtMC1_F3/R3</i>	GCGTCACCTTCTCATCAACA	ACGGTACCACTATGGCAAGCT
<i>Gabi_Kat/Lb3.1</i>	ATATTGACCATCATACTCATTGC	ATTTTGCCGATTTGCGGAAC
<i>EL1526/Lb3.1</i>	TGTTGATGACCCTTTTGTCTTGGA	ATTTTGCCGATTTGCGGAAC
<i>EL1617/EL1618</i>	AGGCGGTGCTTATTGGGATCA	TCCAATGTGAAACCCTCGAGA

2. RNA Extraction and qPCR analysis

For quantitative gene expression analysis, tissue was collected separately from roots and cotyledons of 7 days old seedlings. Root tissue was collected from approximately 300 seedlings and cotyledons from 50 seedlings. In the case that the analysis took place in grown plants, leaves were collected from 3 week-old rosette leaves from fully grown plants. RNA was extracted with the Maxwell RCS Plant Kit (Promega) according to manufacturer's instructions with an included DNase I treatment during the washing steps. cDNA was synthesized with 2 µg RNA template in 20 µl reaction by using the High Capacity cDNA Reverse Transcriptase Kit (Applied Biosystems). For the qPCR reaction mixture KAPA SYBR FAST Master Mix (2x) Universal (Kapa Biosystems) was used with a final concentration of 10 ng template cDNA. Measurements of CT values took place on a LightCycler 480 (Roche Applied Science). The thermal cycle conditions were: an initial denaturation at 95°C for 3 min, followed by 45 cycles starting with denaturation at 95°C for 10 s, annealing at 60°C for 30 s and elongation at 72°C for 30s. The qPCR primers performance was checked by efficiency and melting curve (Applied Biosystems 2004). *ACT2* (*AT3G18780*) and *EIF4a* (*AT4G18040*) were used as the reference housekeeping genes and calculations of the relative transcription level were done with the comparative 2-CT -method (Livak and Schmittgen 2001). Used primers are found in Table 5.

Table 5: Primers used in qPCR analysis

<u>GENE</u>	<u>FORWARD PRIMER</u>	<u>REVERSE PRIMER</u>
<i>ADH</i>	TTCTCAGGATCAACACCGAGCG	GAACGTGGAAGTCCCAAGGAAA
<i>ACO1</i>	GTCCTGAGCTTATGAGAGGGCTG	TAAAGAACTCAAGACCAGGCACCTT
<i>AHB1</i>	TGAGGAAAACAGGGAAAGTTACGG	ACCTCAAAGTGTTTCGTCAACGAC
<i>SUS4</i>	TTTTCTTGCCAGTTCACGGCTG	CTCATATTGACCAACAGTGTCTCT
<i>PCO1</i>	TGATGATGACGTGGCGACGGAA	ACCACCATTAGAGAACAACCTTCCT
<i>PCO2</i>	GTAGATTCCGACTTTACCGCACC	AATAACATCAAGAACCGCGCAAG
<i>AAO3</i>	CTTGTGGTGCAACAAGGCA	CCGCAAAGAGACTTCACCAC
<i>ABI1</i>	TTCCTGGAATGCGCATTGTG	TGTTACTCTCATTCTTCTCTCGTCG
<i>HAB1</i>	AGTGCTCATACTAGCCAGTGACG	GCTTGGCAAGCTGGATCTATTCC

Materials and Methods

PYL4	CGTCGTTGATGTTCTCCAGGC	GCTCTCAGCCGCAGTATTCTCG
RBOHD	ATTACAAGCACCAAACCAG	TGCCAAGCCATAACATCA
PP2C	ACCTCTGCTCTTGTCAAACACAT	ACTGTACATCTGCTCACAAACGG
PYL5	ACTTCATCAGACAGTGCCGTAT	CAAGATCTCGAGCCTCTCGGT
OST1	GTTGCTGACCCTGCAAAGAGGA	CTATGCTTTGGCCCGTTGATCC
RD22	GGTTCGGAAGAAGCGGAG	GAAACAGCCCTGACGTGATAT
RD29A	GGCGTAACAGGTAACCTAGAG	TCCGATGTAAACGTCTGCTCC
KIN1	AACAAGAATGCCTTCCAAGC	CGCATCCGATACACTCTTTCC
MC1	GATCACGTCTACGGGTGCTATG	GGTGCGCATAGAATTCAGAAGG
MC2	CGTGGACGATGAGATCAATGC	CGGTACCACTATGACAAGCGT
MC3	CACCAACCGCAACATCATGAAC	CTGCTCTCTCTTCCCAAACGG
MC4	TTATGCTGGTGGATCAAGAGGT	CATCAGCAGAGGTCTGATCGG
MC5	ATGTCGTGAACAAATCTCTGCCT	ACACATTGAAAAGGGTTGGTCTG
MC6	AGCTTAGCGACGATGTGAAACC	GGGCTTGCGTCTGAAGAAGTTT
MC7	CTGCGTCAATGACGTCCATAGA	TCCTGTGGGTTGAGTGTAAGAT
MC8	GGCTTTCCTCGATCTGCTCCTT	TGGGACTCTTGTCATAGTGGTGG
MC9	CGACATTGAGGTGCTAACGGAC	CGGCTTGAGCTTTATCCACCAT
At4g33490	CGGCTTGAGCTTTATCCACCAT	CCTCCACCTAAACTGCTTAGGC
PP2	AGGGACTCATTACTCGGTTTACG	CTTGGTAGCTACTTTCCCCACAA
At5g59090	AATCTGCAGCTTCATCTGCTTG	CTCGGACCACCACACTAAAAT
At3g45310	TGTCATGGTGGACTTCTTCTCA	TTTGCAGCCACCGTCTTTTCCG

Protein Analysis

1. Protein Extraction

To isolate proteins from Arabidopsis, tissue was collected from leaves of 3 week-old plants or 7 day-old seedlings depending of the experiment and frozen immediately with liquid nitrogen which was used for the grinding of the tissue as well. Three volumes of extraction buffer (20 mM Tris, pH 7.5, 150 mM NaCl, 1mM EDTA, Glycerol, 1% Triton X-100, 0,1% SDS and 5mM DTT) supplemented with a 1:100 dilution of plant protease inhibitor cocktail (Roche)- were added on the tube. Protein extract was centrifuged 20 minutes at 6.000xg at 4°C. The supernatant was collected, transferred in a new Eppendorf tube and centrifuged again at 11.000xg 4°C. Supernatant was transferred in a new tube and protein concentration was measured with Bradford (BIORAD) assay.

Materials and Methods

To isolate protein from leaves of *N. bethamiana* plants, the extraction protocol was as described above with the exception of the extraction buffer used, which was based on HEPES (HEPES, Sodium Salt, ULTROL® Grade - CAS 75277-39-3 – Calbiochem). The extraction buffer was made with 1 X HEPES, 1mM EDTA and 5mM DTT, supplemented with 1:100 dilution of plant protease inhibitor cocktail (Roche).

2. Western Blot Analysis

Protein electrophoresis SDS-PAGE was performed with 10% or 12% acrylamide gel for the separation part and 5% for the stacking. Protein samples were run at 120V for 30 min and 150V for 1.5- 2h depending on the molecular weight of the protein of interest. Protein samples were transferred in a nitrocellulose membrane by blotting at 25V for 30 min in a Trans- Blot Turbo device (BioRad). Blocking solution of 3% milk in TBS-T buffer (TBS with 0,1% Tween) was added to the membrane for 1-hour incubation at room temperature. Three washing steps were following with TBST buffer. Primary conjugated antibody was incubated overnight in 0.1% milk in TBST. Membrane was rinsed with TBST 3 times (10-15 min each wash step) before incubation with secondary antibody whenever necessary. All secondary antibodies were incubated in 0,1% milk with TBST buffer for 1 hour with the membrane at room temperature. Finally, membranes were washed 3 times with TBST before protein detection. ECL Prime Peroxide Solution and ECL Prime Luminol Enhancer Solution (Amersham) were added to the membrane and proteins were detected in ChemiDoc Imaging System (Biorad) device.

Primary antibodies dilutions: anti- GFP 1/1000 (Sigma), anti- GFP HRP 1/1000 (Roche)

Secondary antibodies dilutions: anti- mouse monoclonal 1/5000 (Sigma)

3. Protein Tertiary Structure Modelling

The online-based tool SWISS-MODEL (Biasini et al. 2014) was queried with the native protein sequence of the *MC3* gene and the mutant allelic sequence of *MC3* mutant with the single amino acid substitution at G175E.

Proteomics analysis

Root tissue

Approximately 0.6 g of root tissue was collected from each of the three genotypes used in the experiment: Wt Col-0, *mc3* CRISPR mutant and overexpressing line (*UBQ: MC3-GFP*). Seedlings grew for 7 days in MS plates under LD conditions. Samples were collected and ground in a fine powder with liquid nitrogen. 1 ml of Guanidine hydrochloride extraction buffer (6M GuaHCl, HEPES 1 M, EDTA: 5 Mm, adjust to pH 7.5) supplemented with protease inhibitor cocktail (Roche), was added in the tube. Samples were then centrifuged at 600 xg for 7min at 4°C and the supernatant was passed through Miracloth to get rid of the cell debris. At this step, protein concentration was measured with Bradford Assay. Proteins in the supernatant were purified by chloroform/methanol precipitation (Wessel and Flügge, 1984) and re-solubilized in 6 M GuaHCl, 100 mM HEPES pH 7.5. Protein concentration was estimated using the BCA assay (Bio-Rad) and frozen and -80°C until further processing.

Leaf tissue

Same approach as described above was followed for samples collected from 3-week old plants. Rosette leafs were selected and 3 different plants were pooled for each replicate. After the step of precipitation, protein concentration was estimated using the BCA assay kit (Thermo Fisher Scientific). The mean concentration of the samples was about 1.2 µg/µl. Samples were treated with 1µg Benzoylase and incubated for 30mins at 37°C under constant shaking (700rpm). For all following steps low bind tubes (Eppendorf) were used. Samples were reduced with 10 mM dithiothreitol (DTT) at 37°C under constant shaking (700 rpm) for 30mins. The samples were cooled down to RT, then alkylated with 50 mM chloroacetamide in the darkness for 30 min. The reaction was quenched by additional 50 mM DTT at RT for 30 min.

1. Shotgun proteome analysis

For the label-free proteome analysis of leaf samples, 20µg proteome were purified using single-pot solid-phase (SP3) beads (Hughes et al. 2019). For binding the proteins to the beads, HPLC-grade EtOH was added to a concentration of 80% and incubated for 15mins at RT. The beads were separated

Materials and Methods

on a magnetic stand and washed with 90% HPLC-grade ACN. The proteins were resuspended in 30 μ L Trypsin digestion buffer (100 mM HEPES, 2.5 mM CaCl₂, pH7.5) and digested with 0.2 μ g Trypsin (SERVA, proteome: enzyme ratio 100:1) at 37 °C under constant shaking (700 rpm) overnight. Digestion was stopped by addition of formic acid to pH < 3.

2. HUNTER N-terminome analysis

For HUNTER N-terminome analysis of leave proteomes, 100 μ g proteome were used per condition and replicate essentially as described (Samuel S.H. Weng et al. 2019). For root proteins, the whole sample was used (approximately 1mg of protein sample). Briefly, samples were purified using SP3 beads as above, followed by solubilisation in 6M GuHCl, 100mM HEPES, pH7.5 and subsequent differential isotope labelling with 30 mM formaldehyde (CH₂O) and 30 mM sodium cyanoborohydride (NaBH₃CN) as “light” label for wild-type, 30 mM deuterated formaldehyde (CD₂O) and 30 mM NaBH₃CN as “medium” label for the overexpression line, and 30 mM deuterated/carbon-13-labeled formaldehyde (¹³CD₂O) and 30 mM deuterated sodium cyanoborohydride (NaBD₃CN) as “heavy” label for the *mc3* mutant line. Samples were incubated at 37°C for 1h, an equal amount of fresh reagents added and incubated for another 1h. The reaction was quenched by addition of final 500mM Tris-HCl (pH 6.8) and incubation for 30 min at 37°C. The differently labelled samples were combined for each replicate (final 300 μ g proteome for each replicate), followed by SP3-cleanup as described above, resuspension in 150 μ l trypsin digestion buffer (to final protein conc. 2 μ g/ μ L) and digested with 3 μ g trypsin overnight at 37°C under constant shaking (700 rpm) overnight. Then, 20 μ g of the peptides were withdrawn as “preHUNTER” sample, which allows assessing dimethylation efficiency and determine protein abundance. The remaining majority of the HUNTER-samples were incubated for 1h at 37°C under constant shaking (700rpm) with 150 mM undecanal and 30mM sodium cyanoborohydride in 40% EtOH. Subsequently the reaction was applied to a HRX-RP cartridge (Macherey and Nagel), which retains undecanal-tagged internal and C-terminal tryptic peptides, while N-terminal peptides were collected in the flow through.

All peptide samples were desalted using self-made triple-layer C18 STAGE-tips as described (Rappsilber et al., 2007), dried in a vacuum concentrator (Christ) and resuspended in 15 µl 0.1% FA. For each sample, an estimated 1 µg of the peptides was analysed on a nano-LC-high resolution QToF system. The HPLC (Ultimate 3000 RSLCnano, Thermo, Germany) was operated in two-column setup (µPAC C18 trap and a 50 cm µPAC C18 analytical column, PharmaFluidics) online coupled to an high resolution Q-TOF mass spectrometer (Impact II, Bruker, Germany) via a CaptiveSpray nano ESI source with NanoBooster (Bruker, Germany) as described (Beck et al. 2015).

3. Mass spectrometry data analysis

MaxQuant (Tyanova et al., 2016) was used to identify peptide sequence by matching spectra to the UniProt *Arabidopsis thaliana* protein database (downloaded 2019-04) with appended common contaminant protein sequences and reverse decoy entries at estimated FDR<0.01 at PSM and protein level. Additional parameters were set as follows: For shotgun proteome analysis, trypsin was set as digestion enzyme (specific), and variable N-terminal acetylation and Met oxidation. The function “match between runs” was enabled and iBAQ values calculated. A minimum of 2 ratio counts for one quantification was set valid. For preHUNTER analysis, digestion enzyme was set to “ArgC” (since trypsin does not cleave at dimethylated Lys residues) with 2 missed cleavages, and isotope labels at Lys residues were considered. For HUNTER datasets, the digestion enzyme was set to “semi-ArgC” with variable N-terminus, appropriate combination of dimethylation at N-termini and Lys residues was set as labels, and variable N-terminal modification by acetylation and pyro-Glu formation from Glu and Gln were considered. All queries considered Cys carbamidomethylation as fixed and Met oxidation as variable modification.

4. Data analysis

Shotgun and preHUNTER proteome data were analysed by Perseus (Tyanova, Temu, Sinitcyn, et al. 2016) v 1.6.14.0. N-terminome datasets were processed using MANTI (Demir et al., 2021).

Imaging

1. Histological Techniques

To visualize the promoter activity GUS staining was performed. In vitro grown seedlings or samples taken from soil-grown plants were fixed in 90% acetone for 1 hour at -20°C. Two washes with sodium phosphate buffer (PBS, pH 7.0) took place before the samples were immersed in the GUS staining solution containing 1 mM X-Gluc, 2.5 mM K₃Fe(CN)₆, 2.5 mM K₄Fe(CN)₆ and 0.1% Triton x-100 in 100 mM sodium phosphate buffer (Na₂HPO₄/NaH₂PO₄, pH 7.0) for 2h till overnight at 37°C depending on the tissue. Reactions were stopped with 70% ethanol.

To analyse the protein expression lines and the crossed plants with promoter fusion constructs, 6 or 7 day-old roots were stained with 10 mg/ml propidium iodide staining (PI, Sigma) and visualized as fresh tissue in the confocal microscope. For fixation of the samples, 4% paraformaldehyde was used for 1 h, afterwards Clear-See was added following the protocol as described in (Kurihara et al., 2015) and further stained with Calcofluor White M2R dye (Sigma) for 1h before confocal microscopy visualization.

2. Confocal Microscopy

Confocal laser scanning microscopy was mostly performed on a Leica SP2 AOBS inverted confocal microscope (Leica Microsystems, Wetzlar, Germany). eGFP fusion was excited with a 488 nm Argon laser and detected using a 505–530 band pass emission filter. PI staining was excited using a 561 nm He-Ne laser and detected using a custom 595–620 nm band pass emission filter. Calcofluor-stained samples were excited at 405 nm and at 425-475 nm was the emission. Different Z stacks and transverse optical sections from microscopy images were analysed using Image J software (<https://imagej.nih.gov/ij/>).

For the detection of aggregates with ProteoStat Aggresome detection kit (Enzo Life Sciences), seedlings were stained according to the manufacturer's instructions. Briefly, seedlings were collected and were fixed in 4% formaldehyde solution for 30 min at room temperature. Formaldehyde solution was removed and seedlings were washed with 1X PBS twice followed by an incubation with

Materials and Methods

permeabilizing solution (0.5% Triton X-100, 3 mM EDTA, pH 8.0) with gently shaking for 30 min at 4°C. Washes were repeated with 1X PBS. Finally, plants were incubated with 1X PBS supplemented with 1 µl/ml of ProteoStat and 1 µl/ml Hoechst 33342 (for nuclear staining) for 30 min at room temperature before mounting them on a slide for microscopic analysis.

3. Other Imaging Techniques

For root and hypocotyl length measurements, square plates plants were photographed with a NIKON D7000 digital camera. Pictures were later analysed by using ImageJ- Fiji (Schindelin et al. 2009). For the phenotypical characterization of the whole plants and different organs, plants were photographed with a NIKON D7000 digital camera. Whenever higher resolution was needed, specific plant tissues were placed under an Olympus DP71 stereomicroscope (Olympus, Center Valley, PA, U.S.A.). Digital picture acquisition for histochemical detection of GUS activity and hypocotyl analysis took place on a Leica DM6 epifluorescence microscope (Leica, Wetzlar, Germany).

Phenotyping Under Normal Conditions

1. Growth Conditions

All seeds were surface sterilized in a solution containing 35% sodium hypochlorite and 100% ethanol under agitation for 10 minutes followed by 2 washing steps with 70% ethanol and 1 step with 100% ethanol. Seeds were dried in a filter paper under a laminar flow hood before use. To synchronize seed germination, seeds were vernalized at 4°C for 48-72h. *In vitro* plants were germinated on square plates containing 1X MS media (Murashige and Skoog) salt without sucrose and 5 mM MES including vitamins (Duchefa Biochemie) at pH 5,7 previous to agar addition 8g/L. For all experiment described, plants were grown in controlled ARALAB growth chambers under different photoperiodic light/dark cycles (LD 16:8 light/dark, SD 8:16 light/dark, 12:12 light/dark) and 60% relative humidity unless is indicated different in the experiment. Light intensity in the growth chambers was set at 120 µmol/m²/s of LED light bulbs.

Nicotiana benthamiana was grown under long day conditions (16 h light: 8 h darkness, 26°C: 22°C, 60% humidity).

2. Cotyledon vein pattern

To analyse vein pattern, the cotyledons were removed from 6 day-old seedlings and submerged for 1h in a 3:1 95% ethanol: acetic acid solution at room temperature. Subsequently, they were washed twice 30 min with 70% ethanol and the cotyledons were incubated overnight at 4°C with 100% ethanol. 10% NaOH was added for 1 h and the samples were left at 37°C before Clear-See was added as a final step.

3. Macroscopic analysis

For macroscopic analysis of the entire plant, inflorescences were harvested and opened to reveal carpel and stamen. Siliques upwards to the flowering buds were successively collected for displaying a brief developmental snapshot. Siliques were immobilized by sticking them on double sided tape to open them with a razor blade and tweezers to reveal the content.

For flowering time experiments, seedlings were grown for 7 days after germination in MS- plates and then were transplanted in pots filled with soil (8 substrate: 1 perlite: 1 vermiculite). 15 seeds per genotype were used and experiments were performed on soil-grown plants three times with similar results (LD photoperiod). Days needed for the plants to bolt and flower and number of rosette leaves respectively were determined. Days to bolting was the number of days from germination until an inflorescence shoot was visible at the centre of a rosette. Days to flower was the number of days from germination until the first bud was formed and ready to open and become a flower. To measure rosette leaf area, whole rosettes from 3-week-old plants were used. Plants were photographed with a NIKON D7000 digital camera and images were analysed with Adobe Photoshop. Images were processed in order to detect only the green colour of the leaf and exclude the background. The same scale was set for all the pictures and images were analysed with RGB colour tool. Pixels were calculated and mean value of rosette leaf area was estimated per plant.

Phenotyping Under Stress Conditions

1. Infection Assays with the Vascular Pathogen *Ralstonia solanacearum*

For the pathogenicity assays the vascular pathogen *Ralstonia solanacearum* GMI1000 was used. Bacteria were grown at 28°C in solid or liquid rich Φ medium (1% Bacto peptone, 0.1% yeast extract, and 0.1% casamino acids, all from Becton, Dickinson and Co. [Franklin Lakes, NJ, U.S.A.]), adding the appropriate antibiotic for the resistance. Experiments were carried out with the soil-drench method with small modifications (Monteiro et al., 2012). Briefly, Arabidopsis was grown for 4 weeks on Jiffy pots (Jiffy Group, Lorain, OH, U.S.A.) in a controlled chamber at 22°C, 60% humidity and SD photoperiod. Jiffys were transferred 3-4 before the infection to 12:12 photoperiod, 28°C, 60% humidity to acclimate. The day of the infection, the jiffys were pinched with toothpick at 4 spots in order to damage the roots of the plant and were immediately submerged O/N into a culture solution of *R. solanacearum* adjusted to $OD_{600} = 0.1$ with distilled water, corresponding to 10^8 colony-forming units (CFU) ml^{-1} (30 ml of bacterial solution were calculated per plant). Then, inoculated plants were transferred to trays containing a thin layer of soil drenched with the same *R. solanacearum* solution and were kept back in the growth chamber. Plant wilting symptoms were recorded every day and were calculated according to a disease index scale (0 = no wilting, 1 = 25% wilted leaves, 2 = 50%, 3 = 75%, and 4 = death). At least 35 plants were used in each assay, performed in at least three independent replicates.

For in vitro infection assays with *R. solanacearum*, experiments were carried out as described before (Lu et al. 2018). At 3-days post-infection (dpi), plants were analysed under ChemiDoc Imaging System device, to detect the presence of the bacteria and the progress of the infection. For root-hair evaluation, pictures were taken 3 dpi with an Olympus DP71 stereomicroscope (Olympus, Center Valley, PA, U.S.A.). Root length of infected seedlings was recorded over time.

2. Osmotic stress assays

Seeds were sown on MS- medium, cold treated for 2 days and grown for 3 days in growth chamber. Then, they were transferred to different MS plates containing increasing NaCl concentration for 7 additional days. Primary root length was measured at 10days after germination with Image J software. Number of visible lateral roots was counted under Olympus DP71 stereomicroscope.

Experiments of sorbitol treatment were performed by Dr. Antia's Rodriguez-Villalon group of Plant Vascular Development, at the Swiss Federal Institute of Technology (ETH) Zurich, in Switzerland

For observation of vascular tissue upon osmotic stress, seeds were sown on half-strength (1/2) MS- medium, stratified for 2 days at 4°C and grown for 3 days in growth chamber with continuous light at 110 $\mu\text{mol}/\text{ms}^2$. Then, they were transferred to MS plates containing 120 mM sorbitol for 3 additional days before confocal microscopy analysis. Seedlings were stained with Calcofluor before confocal microscopy as described above (Histological techniques section).

3. Hypoxia Treatments

Experiments with hypoxia were performed by Dr. Michael Holdsworth at the School of Biosciences, in the University of Nottingham, United Kingdom.

Seeds were sown in MS- plates and were cold- treated for 5days before transferred to growth chamber (SD, 20°C, light intensity= 110 $\mu\text{mol}/\text{ms}^2$). At day 4 the plates were transferred to the hypoxia chamber with lids taken off. Experiments were set up in a desiccator (hypoxia chamber) with nitrogen being introduced at a flow rate of 4L/min in the dark, for 4h at which the oxygen in the desiccator was at approx. 0.5% at the end of the experiment. Control samples were placed in a similar desiccator upon dark conditions but with air introduced (normoxia). After 4h, plates were taken out and sealed with micropore tape to allow gas exchange and root tips were marked with a marker pen and transferred back to growth room with short daylight conditions for recovery. Root tip survival was scored after 3 days of recovery. Extension of primary root tips beyond the marked point was scored as root tip survival for each seedling. Seedlings whose

primary root has not been able to grown below marked point were considered dead.

4. Thermophotomorphogenesis

Seeds were placed in MS- plates, cold- treated for 3 days and grown for 3 days in growth chamber (LD, 22°C, 60% humidity) to synchronize the emergence of the root. On the third day, some plants were shifted at 28°C and grown for 4 additional days at 22°C or 28°C and at light intensities 40 and 170 $\mu\text{mol}/\text{m}^2/\text{s}$. Roots and hypocotyls were measured from 7 days old seedlings with Image J software.

5. Drought stress

Scoring Survival Rate

Seeds were placed in MS- plates, cold-treated for 3 days and grown for 1 week in growth chamber. One-week-old seedlings were transferred individually to pots containing 30 ± 0.5 g of substrate (plus 1:8 v/v vermiculite and 1:8 v/v perlite). Three-week-old plants were subjected to severe drought stress by withholding water for 8-9 days followed by re-watering. After the 5-day recovery period, the surviving plants were photographed and counted.

Physiological Parameters and Chlorophyll fluorescence

Seedlings grown in MS agar plates were transferred after 7 days to individual to pots containing 30 ± 0.5 g of substrate (plus 1:8 v/v vermiculite and 1:8 v/v perlite). Plants were grown in LD conditions for 3 weeks before subjected to drought stress. Pots were weighed daily during the experiment. Well-watered control plants were grown in 100% field capacity (0% of water loss). Relative Water Content (RWC, %) was calculated according to the formula: $(FW-DW)/(TW-DW)$. Fresh weight (FW) was obtained by harvesting and weighing freshly detached rosettes. Turgid weight (TW) was obtained by putting cut rosettes into a tube with de-ionized water for 16 hours at room temperature, removing excess water by wiping with absorbent paper and weighing plant material. Rosette dry weight (DW) was recorded after an overnight incubation at 80 °C in a dry oven. The time

Materials and Methods

course drought stress assay was started by withholding the nutrient solution until reaching 30%, 60%, 75%, and 90% water loss.

Photosynthesis efficiency was measured in control (well-watered) and drought plants in 100%, 40% and 6% field capacity. After 30 min of dark adaptation, the kinetics of chlorophyll fluorescence in whole rosettes were monitored using Imaging Pulse Amplitude Modulation (PAM) Fluorometry M-series, MAXI version device, by measuring F_0 in the dark and F_m with initial saturation pulse. F_v/F_m and F_v'/F_m' ratio for the maximum quantum efficiency upon dark and light conditions was calculated according to the manufacturer's instructions (Walz, Effeltrich, Germany).

6. Absisic Acid sensitivity

Germination rate and Root growth

Around 100 seeds per replicate were sown on MS medium plates supplemented without (control) or with ABA (Sigma) at concentrations of 1 or 2 μM . After a 2-day period of cold stratification at 4 °C, seeds were transferred to a growth chamber for additional 8 days and the germination rates were determined. For root growth assay, seeds were germinated on MS medium plates for 3d, and then the seedlings were transferred to new plates containing 0 (control), 0.3, 3, or 30 μM ABA, and left to vertically grow for further 7d. Images were then taken when seedlings were 10 day old and root length was measured for each genotype with Image J software.

Stomatal Aperture

For measurement of stomatal aperture following ABA treatment, cotyledons were sampled from 10-day-old seedlings and immediately were immersed in a stomata-opening buffer with 10 mM KCl, 0.2 mM CaCl_2 , and 10 mM Mes-KOH (pH 6.15) for 2^{1/2} h under continuous white light at 22 °C (Du et al., 2013). ABA was then added into the same buffer to reach a final concentration of 10 μM and the cotyledons were collected after 30 and 90 min. Guard cells were photographed with a LEICA DM6 microscope, and stomatal lengths and widths were measured with Image J software.

Senescence induction

Detached 5-week-old cauline leaves from examined lines were soaked in distilled water without or with 50 μ M ABA under light conditions for 3 days prior to observations of leaf senescence. Chlorophyll was extracted and homogenized in 1 ml of 80% acetone then maintained on ice for overnight treatment. OD662 nm and OD647 nm were measured using a UV spectrophotometer. The concentration of chlorophylls a and b, as well as the total amount of chlorophyll, were calculated as described by (Lichtenthaler 1987).

Hormone Quantification

Hormone extraction and measurements were performed by Dr. Sergi Munné at the Department of Evolutionary Biology, Ecology and Environmental Sciences, Faculty of Biology, Universitat de Barcelona, in Spain.

Approximately 100 mg of leaf material from 3 week-old plants grown in LD/22°C conditions were harvested and ground to a fine powder in liquid nitrogen. IAA, ABA, SA, JA, GA4, GA7, Zeatin, ACC, ZR, OPDA, IPA and Melatonin were quantified as described previously (Müller and Munné-bosch 2011).

Statistical Analysis

For most of the experiments performed, data were compared with T-test significance (p value < 0.05) or with one-way ANOVA plus Tukey HD test (p value < 0.05) to be considered significant, with R studio packages. In every experiment is indicated the degree of significance and the method used. For scoring plant survival upon drought, we compared the results of each genotype with chi-square test with the expected values from the wild type plants.

For the proteomic data, we evaluated in every experiment the log₂ Fold change ratio between dual comparisons which was the average of the fold changes between the four replicates. According to the values of peptides reads- iBAQs, T-test was performed for the root data and multiple ANOVA for the leaf data (Shotgun experiment and HUNTER).

Resumen en castellano

Las metacaspasas son una familia de cisteína proteasas que se encuentran en eucariotas inferiores y plantas. Se consideran parientes lejanos de las caspasas, presentes solo en animales. El rol de las metacaspasas es bastante diverso, desde los procesos de desarrollo involucrados en la formación de tejidos, hasta las respuestas contra patógenos y otras tensiones ambientales. Para algunos miembros de la familia se está investigando su función y posibles sustratos y para otros no se han caracterizado.

En este estudio intentamos analizar funcionalmente *Arabidopsis thaliana* metacaspase 3 (MC3), una metacaspasa no caracterizada presente en el tejido vascular. Consideramos que la mejor manera de abordar este desafío era utilizar un enfoque de genética inversa en combinación con el análisis proteómico. En el Capítulo 2, identificamos específicamente la localización exacta de la transcripción y la proteína en planta, generamos plantas mutantes utilizando la tecnología CRISPR / Cas9 y analizamos su crecimiento en condiciones basales. Además, realizamos un análisis de proteoma completo para diferentes tejidos e intentamos identificar sustratos candidatos mediante análisis de péptidos N-terminales. En el Capítulo 3, profundizamos en múltiples estreses mostrando cómo las plantas con sobreacumulación o falta de MC3 respondieron a las condiciones de estrés, ya que del estudio proteómico surgieron múltiples proteínas relacionadas con las respuestas al estrés.

En el Capítulo 2 generamos líneas reporteras para especificar la localización exacta de la expresión génica. Se encontró que *MC3* se expresaba específicamente en el tejido vascular del floema. Además, la fusión traslacional a proteínas fluorescentes verificó el mismo patrón para la localización de proteínas. Utilizando múltiples líneas mutantes, realizamos un análisis de los fenotipos causados por la ausencia, mal funcionamiento o sobreexpresión de la supuesta proteasa en el desarrollo de la planta. El crecimiento general y la formación del tejido vascular en particular no se vieron afectados cuando las plantas se cultivaron en condiciones de crecimiento estándar. A partir de estudios anteriores, las líneas reporteras de *MC1* mostraron expresión en la estela en casi

todas las etapas del desarrollo y *MC4* tiene una expresión alta y ubicua en la mayoría de los tejidos. Se generaron mutantes dobles con el fin de excluir la posibilidad de redundancia funcional y mostramos que en condiciones normales el crecimiento general de estas plantas se mantuvo similar al de las plantas de tipo salvaje. Finalmente, comprobamos el proteoma total de las plantas para comparar las proteínas diferencialmente abundantes en diferentes fondos genéticos. En general, el análisis demostró que el tejido de la raíz de las líneas sobreexpresoras de *MC3* muestran una acumulación diferencial de proteínas relacionadas con el estrés, específicamente relacionadas con el osmótico y la hipoxia.

Se ha demostrado que las metacaspasas participan, entre otras cosas, en las respuestas de las plantas al estrés biótico y abiótico. En el Capítulo 3 analizamos si *MC3* tuvo un papel en las respuestas a diferentes tensiones ambientales. Encontramos que la función de *MC3* está asociada con el estrés por sequía, ya que las plantas que sobreacumulan *MC3* pudieron sobrevivir más y funcionar mejor en condiciones de baja disponibilidad de agua. Además, en comparación con las plantas de tipo salvaje, el mutante *mc3* parecía menos sensible a ABA, que es una de las hormonas que orquestan las respuestas a la sequía. Teniendo en cuenta que la vasculatura juega un papel muy importante en la facilitación de la señalización de ABA, investigamos la formación vascular tras el estrés osmótico en plantas con niveles alterados de *MC3*. Las líneas sobreexpresoras mostraron una formación más rápida del tejido vascular en condiciones de estrés osmótico que las plantas de tipo salvaje. Finalmente, observamos que en condiciones de bajas concentraciones de oxígeno, la cantidad excesiva de *MC3* también puede ser beneficiosa para la supervivencia de las plantas. Se probaron tensiones adicionales para detectar si la función de *MC3* era específica de los desequilibrios osmóticos. Las plantas no se vieron afectadas por la presencia o ausencia de *MC3* por condiciones de luz y temperatura alteradas, ni por infección con un patógeno vascular. En conclusión, reportamos que la metacaspasa 3 es una metacaspasa específica del floema que contribuye a la tolerancia a la sequía posiblemente debido a la diferenciación vascular mejorada del metafloema en condiciones de estrés osmótico.

References

- Abe, Mitsutomo, Hidetaka Kaya, Ayako Watanabe-Taneda, Mio Shibuta, Ayako Yamaguchi, Tomoaki Sakamoto, Tetsuya Kurata, Israel Ausín, Takashi Araki, and Carlos Alonso-Blanco. 2015. "FE, a Phloem-Specific Myb-Related Protein, Promotes Flowering through Transcriptional Activation of FLOWERING LOCUS T and FLOWERING LOCUS T INTERACTING PROTEIN 1." *Plant Journal* 83(6):1059–68.
- Ahmad, Rafiq, Yasmine Zuily-Fodil, Chantal Passaquet, Olivier Bethenod, Romain Roche, and Anne Repellin. 2012. "Ozone and Aging Up-Regulate Type II Metacaspase Gene Expression and Global Metacaspase Activity in the Leaves of Field-Grown Maize (*Zea Mays* L.) Plants." *Chemosphere* 87(7):789–95.
- Ahn, Young Ock, Bun Ichi Shimizu, Kanzo Sakata, Dashzeveg Gantulga, Zhanghe Zhou, David R. Bevan, and Asim Esen. 2010. "Scopolin-Hydrolyzing β -Glucosidases in Roots of Arabidopsis." *Plant and Cell Physiology* 51(1):132–43.
- Amasino, Richard. 2010. "Seasonal and Developmental Timing of Flowering." *Plant Journal* 61(6):1001–13.
- Anderson, Jonathan P., Ellet Badruzsaufari, Peer M. Schenk, John M. Manners, Olivia J. Desmond, Christina Ehlert, Donald J. Maclean, Paul R. Ebert, and Kemal Kazan. 2004. "Antagonistic Interaction between Abscisic Acid and Jasmonate-Ethylene Signaling Pathways Modulates Defense Gene Expression and Disease Resistance in Arabidopsis." *Plant Cell* 16(12):3460–79.
- Andrade Bueno, Rafael, Roman Hudecek, and Moritz K. Nowack. 2019. *The Roles of Proteases during Developmental Programmed Cell Death in Plants*.
- Anne, Pauline, Marianne Azzopardi, Lionel Gissot, Sébastien Beaubiat, Kian Hématy, and Jean Christophe Palauqui. 2015. "OCTOPUS Negatively Regulates BIN2 to Control Phloem Differentiation in Arabidopsis Thaliana." *Current Biology* 25(19):2584–90.
- Anne, Pauline and Christian S. Hardtke. 2018. "Phloem Function and Development — Biophysics Meets Genetics." *Current Opinion in Plant Biology* 43:22–28.
- Ari Pekka Mahonen,¹ Martin Bonke,¹ Leila Kauppinen,¹ Marjukka Riikonen,¹ Philip N. Benfey,² and Yka Helariutta^{1, 3} 1Plant. 2000. "A Novel Two-Component Hybrid Molecule Regulates Vascular Morphogenesis of the Arabidopsis Root." *Genes & Development* (14):2938–43.
- Arizumi, Tohru, Kenji Higuchi, Shoko Arakaki, Tsunenori Sano, Erika Asamizu, and Hiroshi Ezura. 2011. "Genetic Suppression Analysis in Novel Vacuolar Processing

References

- Enzymes Reveals Their Roles in Controlling Sugar Accumulation in Tomato Fruits.” *Journal of Experimental Botany* 62(8):2773–86.
- Avci, Utku, H. Earl Petzold, Ihab O. Ismail, Eric P. Beers, and Candace H. Haigler. 2008. “Cysteine Proteases XCP1 and XCP2 Aid Micro-Autolysis within the Intact Central Vacuole during Xylogenesis in Arabidopsis Roots.” *Plant Journal* 56(2):303–15.
- Balakireva, Anastasia V. and Andrey A. Zamyatnin. 2019. “Cutting out the Gaps between Proteases and Programmed Cell Death.” *Frontiers in Plant Science* 10(June):1–7.
- Balmer, Andrea, Victoria Pastor, Jordi Gamir, Victor Flors, and Brigitte Mauch-Mani. 2015. “The ‘Prime-Ome’: Towards a Holistic Approach to Priming.” *Trends in Plant Science* 20(7):443–52.
- Barrett, A. J. 1994. “Classification of Peptidases.” *Methods in Enzymology* 244:1–15.
- Basu, Supratim, Venkategowda Ramegowda, Anuj Kumar, and Andy Pereira. 2016. “Plant Adaptation to Drought Stress [Version 1; Referees: 3 Approved].” *F1000Research* 5:1–10.
- Beck, Scarlet, Annette Michalski, Oliver Raether, Markus Lubeck, Stephanie Kaspar, Niels Goedecke, Carsten Baessmann, Daniel Hornburg, Florian Meier, Igor Paron, Nils A. Kulak, Juergen Cox, and Matthias Mann. 2015. “The Impact II, a Very High-Resolution Quadrupole Time-of-Flight Instrument (QTOF) for Deep Shotgun Proteomics.” *Molecular and Cellular Proteomics* 14(7):2014–29.
- Beers, Eric P. 1997. “Programmed Cell Death during Plant Growth and Development.” *Cell Death and Differentiation* 4(8):649–61.
- Van Bel, A. J. E. 2003. “The Phloem, a Miracle of Ingenuity.” *Plant, Cell and Environment* 26(1):125–49.
- Benfey, Philip N. and Ben Scheres. 2000. “Root Development.” *Current Biology* 10(22):813–15.
- Bhuiyan, Nazmul H., Elden Rowland, Giulia Friso, Lalit Ponnala, Elena J. S. Michel, and Klaas J. Va. Wijk. 2020. “Autocatalytic Processing and Substrate Specificity of Arabidopsis Chloroplast Glutamyl Peptidase1[OPEN].” *Plant Physiology* 184(1):110–29.
- Biasini, Marco, Stefan Bienert, Andrew Waterhouse, Konstantin Arnold, Gabriel Studer, Tobias Schmidt, Florian Kiefer, Tiziano Gallo Cassarino, Martino Bertoni, Lorenza Bordoli, and Torsten Schwede. 2014. “SWISS-MODEL: Modelling Protein Tertiary and Quaternary Structure Using Evolutionary Information.” *Nucleic Acids Research* 42(W1):252–58.
- Bishopp, Anthony, Hanna Help, Sedeer El-Showk, Dolf Weijers, Ben Scheres, Jiří Friml, Eva Benková, Ari Pekka Mähönen, and Ykä Helariutta. 2011. “A Mutually Inhibitory

References

- Interaction between Auxin and Cytokinin Specifies Vascular Pattern in Roots.” *Current Biology* 21(11):917–26.
- Bollhöner, Benjamin, Soile Jokipii-Lukkari, Joakim Bygdell, Simon Stael, Mathilda Adriasola, Luis Muñiz, Frank Van Breusegem, Inés Ezcurra, Gunnar Wingsle, and Hannele Tuominen. 2018. “The Function of Two Type II Metacaspases in Woody Tissues of Populus Trees.” *New Phytologist* 217(4):1551–65.
- Bollhöner, Benjamin, Jakob Prestele, and Hannele Tuominen. 2012. “Xylem Cell Death: Emerging Understanding of Regulation and Function.” *Journal of Experimental Botany* 63(3):1081–94.
- Bollhöner, Benjamin, Bo Zhang, Simon Stael, Nicolas Denancé, Kirk Overmyer, Deborah Goffner, Frank Van Breusegem, and Hannele Tuominen. 2013. “Post Mortem Function of AtMC9 in Xylem Vessel Elements.” *New Phytologist* 200(2):498–510.
- Bonke, Martin, Siripong Thitamadee, Ari Pekka Mähönen, Marie Theres Hauser, and Ykä Helariutta. 2003. “APL Regulates Vascular Tissue Identity in Arabidopsis.” *Nature* 426(6963):181–86.
- Bosch, Maurice and Noni V. E. Franklin-Tong. 2018. “The Stigma of Death.” *Nature Plants* 4(6):323–24.
- Bouquin, Thomas, Carsten Meier, Randy Foster, Mads Eggert Nielsen, and John Mundy. 2015. “Control of Specific Gene Expression by Gibberellin and Brassinosteroid 1.” *Plant Physiology* 127:450-458.
- Bozhkov, P. V., M. F. Suarez, L. H. Filonova, G. Daniel, A. A. Zamyatnin, S. Rodriguez-Nieto, B. Zhivotovsky, and A. Smertenko. 2005. “Cysteine Protease MclI-Pa Executes Programmed Cell Death during Plant Embryogenesis.” *Proceedings of the National Academy of Sciences* 102(40):14463–68.
- Brady, Siobhan M., David A. Orlando, Ji-Young Lee, Jean Y. Wang, Jeremy Koch, José R. Dinneny, Daniel Mace, Uwe Ohler, and Philip N. Benfey. 2007. “A High Resolution Root Spatiotemporal Map Reveals Dominant Expression Patterns.” *Science* (318):801–6.
- Breda, Alice S., Ora Hazak, and Christian S. Hardtke. 2017. “Phosphosite Charge Rather than Shootward Localization Determines OCTOPUS Activity in Root Protophloem.” *Proceedings of the National Academy of Sciences of the United States of America* 114(28):E5721–30.
- Bryan, Philip N. 2002. “Prodomains and Protein Folding Catalysis.” *Chemical Reviews* 102(12):4805–15.
- Bui, Liem T., Beatrice Giuntoli, Monika Kosmacz, Sandro Parlanti, and Francesco Licausi. 2015. “Constitutively Expressed ERF-VII Transcription Factors Redundantly

References

- Activate the Core Anaerobic Response in Arabidopsis Thaliana." *Plant Science* 236:37–43.
- Bui, Liem T., Vinay Shukla, Federico M. Giorgi, Alice Trivellini, Pierdomenico Perata, Francesco Licausi, and Beatrice Giuntoli. 2020. "Differential Submergence Tolerance between Juvenile and Adult Arabidopsis Plants Involves the ANAC017 Transcription Factor." *Plant Journal* 104(4):979–94.
- Campbell, Liam, Simon Turner, and Peter Etchells. 2016. "Regulation of Vascular Cell Division." *Journal of Experimental Botany* 68(1):27–43.
- Canbay, Vahap and Ulrich auf dem Keller. 2021. "New Strategies to Identify Protease Substrates." *Current Opinion in Chemical Biology* 60:89–96.
- Carella, Philip, Daniel C. Wilson, Christine J. Kempthorne, and Robin K. Cameron. 2016. "Vascular Sap Proteomics: Providing Insight into Long-Distance Signaling during Stress." *Frontiers in Plant Science* 7(MAY2016):1–8.
- Castillo-Olamendi, Luis, Armando Bravo-García, Julio Morán, Mario Rocha-Sosa, and Helena Porta. 2007. "AtMCP1b, a Chloroplast-Localised Metacaspase, Is Induced in Vascular Tissue after Wounding or Pathogen Infection." *Functional Plant Biology* 34(12):1061–71.
- Chang, Howard Y. and Xiaolu Yang. 2000. "Proteases for Cell Suicide: Functions and Regulation of Caspases." *Microbiology and Molecular Biology Reviews* 64(4):821–46.
- Chen, Hsien Jung, Cheng Ting Su, Chia Hung Lin, Guan Jhong Huang, and Yaw Huei Lin. 2010. "Expression of Sweet Potato Cysteine Protease SPCP2 Altered Developmental Characteristics and Stress Responses in Transgenic Arabidopsis Plants." *Journal of Plant Physiology* 167(10):838–47.
- Chen, Hsien Jung, Yi Jing Tsai, Che Yu Shen, Ting No Tsai, Guan Jhong Huang, and Yaw Huei Lin. 2013. "Ectopic Expression of Sweet Potato Cysteine Protease SPCP3 Alters Phenotypic Traits and Enhances Drought Stress Sensitivity in Transgenic Arabidopsis Plants." *Journal of Plant Growth Regulation* 32(1):108–21.
- Chen, Kong, Guo Jun Li, Ray A. Bressan, Chun Peng Song, Jian Kang Zhu, and Yang Zhao. 2020. "Abscisic Acid Dynamics, Signaling, and Functions in Plants." *Journal of Integrative Plant Biology* 62(1):25–54.
- Chen, Li Qing, Xiao Qing Qu, Bi Huei Hou, Davide Sosso, Sonia Osorio, Alisdair R. Fernie, and Wolf B. Frommer. 2012. "Sucrose Efflux Mediated by SWEET Proteins as a Key Step for Phloem Transport." *Science* 335(6065):207–11.
- Chen, Su Fen, Ke Liang, Dong Mei Yin, Di An Ni, Zhi Guo Zhang, and Yong Ling Ruan. 2016. "Ectopic Expression of a Tobacco Vacuolar Invertase Inhibitor in Guard Cells

References

- Confers Drought Tolerance in Arabidopsis." *Journal of Enzyme Inhibition and Medicinal Chemistry* 31(6):1381–85.
- Cho, Kwang Moon, Ha Thi Kim Nguyen, Soo Youn Kim, Jin Seok Shin, Dong Hwa Cho, Seung Beom Hong, Jeong Sheop Shin, and Sung Han Ok. 2016. "CML10, a Variant of Calmodulin, Modulates Ascorbic Acid Synthesis." *New Phytologist* 209(2):664–78.
- Choi, C. J. and J. A. Berges. 2013. "New Types of Metacaspases in Phytoplankton Reveal Diverse Origins of Cell Death Proteases." *Cell Death and Disease* 4(2):e490-7.
- Chung, Ho Yong, Shozo Fujioka, Sunghwa Choe, Soyoun Lee, Youn Hyung Lee, Nam In Baek, and In Sik Chung. 2010. "Simultaneous Suppression of Three Genes Related to Brassinosteroid (BR) Biosynthesis Altered Campesterol and BR Contents, and Led to a Dwarf Phenotype in Arabidopsis Thaliana." *Plant Cell Reports* 29(4):397–402.
- Claassen, Manfred, Lukas Reiter, Michael O. Hengartner, Joachim M. Buhmann, and Ruedi Aebersold. 2012. "Generic Comparison of Protein Inference Engines." *Molecular and Cellular Proteomics* 11(4):1–11.
- Coll, N. S., A. Smidler, M. Puigvert, C. Popa, M. Valls, and J. L. Dangl. 2014. "The Plant Metacaspase AtMC1 in Pathogen-Triggered Programmed Cell Death and Aging: Functional Linkage with Autophagy." *Cell Death and Differentiation* 21(9):1399–1408.
- Coll, Nuria S., Dominique Vercammen, Andrea Smidler, Charles Clover, Frank Van Breusegem, Jeffery L. Dangl, and Petra Epple. 2010. "Arabidopsis Type I Metacaspases Control Cell Death." *Science* 330(6009):1393–97.
- Cubría-Radio, Marta and Moritz K. Nowack. 2019. "Transcriptional Networks Orchestrating Programmed Cell Death during Plant Development." Pp. 161–84 in *Current Topics in Developmental Biology*. Vol. 131. Academic Press Inc.
- Cui, Man, Mengjun Gu, Yaru Lu, Yue Zhang, Chunlin Chen, Hong Qing Ling, and Huilan Wu. 2020. "Glutamate Synthase 1 Is Involved in Iron-Deficiency Response and Long-Distance Transportation in Arabidopsis." *Journal of Integrative Plant Biology* 62(12):1925–41.
- Daneva, Anna, Zhen Gao, Matthias Van Durme, and Moritz K. Nowack. 2016. "Functions and Regulation of Programmed Cell Death in Plant Development." *Annual Review of Cell and Developmental Biology* 32(1):441–68.
- Deak, Karen I., Jocelyn Malamy, and Molecular Genetics. 2005. "Osmotic Regulation of Root System Architecture." *The Plant Journal* 43:17–28.
- Demir, Fatih, Jayachandran N. Kizhakkedathu, Markus M. Rinschen, and Pitter F.

References

- Huesgen. 2021. "MANTI: Automated Annotation of Protein N-Termini for Rapid Interpretation of N-Terminome Data Sets." *Analytical Chemistry* 93(13):5596–5605.
- Depuydt, Stephen, Antia Rodriguez-Villalon, Luca Santuari, Céline Wyser-Rmili, Laura Ragni, and Christian S. Hardtke. 2013. "Suppression of Arabidopsis Protophloem Differentiation and Root Meristem Growth by CLE45 Requires the Receptor-like Kinase BAM3." *Proceedings of the National Academy of Sciences of the United States of America* 110(17):7074–79.
- DeWitt, N. D. and M. R. Sussman. 1995. "Immunocytological Localization of an Epitope-Tagged Plasma Membrane Proton Pump (H⁺-ATPase) in Phloem Companion Cells." *Plant Cell* 7(12):2053–67.
- Ding, Yong, Michael Fromm, and Zoya Avramova. 2012. "Multiple Exposures to Drought 'train' Transcriptional Responses in Arabidopsis." *Nature Communications* 3.
- Dinneny, José R. 2019. "Developmental Responses to Water and Salinity in Root Systems." *Annual Review of Cell and Developmental Biology* 35:239–57.
- Dolan, L., K. Janmaat, V. Willemsen, P. Linstead, S. Poethig, K. Roberts, and B. Scheres. 1993. "Cellular Organisation of the Arabidopsis Thaliana Root." *Development* 119(1):71–84.
- DomÃ-nguez, Fernando and Francisco J. Cejudo. 2014. "Programmed Cell Death (PCD): An Essential Process of Cereal Seed Development and Germination." *Frontiers in Plant Science* 5(July):1–11.
- Van Doorn, W. G., E. P. Beers, J. L. Dangl, V. E. Franklin-Tong, P. Gallois, I. Hara-Nishimura, A. M. Jones, M. Kawai-Yamada, E. Lam, J. Mundy, L. A. J. Mur, M. Petersen, A. Smertenko, M. Taliany, F. Van Breusegem, T. Wolpert, E. Woltering, B. Zhivotovsky, and P. V. Bozhkov. 2011. "Morphological Classification of Plant Cell Deaths." *Cell Death and Differentiation* 18(8):1241–46.
- Duan, Lina, Daniela Dietrich, Chong Han Ng, Penny Mei Yeen Chan, Rishikesh Bhalerao, Malcolm J. Bennett, and José R. Dinneny. 2013. "Endodermal ABA Signaling Promotes Lateral Root Quiescence during Salt Stress in Arabidopsis Seedlings." *Plant Cell* 25(1):324–41.
- Duan, Yunfeng, Wensheng Zhang, Bao Li, Youning Wang, Kexue Li, T. Sodmergen, Chunyu Han, Yizhang Zhang, and Xia Li. 2010. "An Endoplasmic Reticulum Response Pathway Mediates Programmed Cell Death of Root Tip Induced by Water Stress in Arabidopsis." *New Phytologist* 186(3):681–95.
- Durand, Mickaël, Dany Mainson, Benoît Porcheron, Laurence Maurousset, Rémi Lemoine, and Nathalie Pourtau. 2018. "Carbon Source–Sink Relationship in Arabidopsis Thaliana: The Role of Sucrose Transporters." *Planta* 247(3):587–611.

References

- Earnshaw, William 1, Martins,Luis M. 2 and Scott Kaufmann. 1999. "MAMMALIAN CASPASES: STRUCTURE, ACTIVATION, SUBSTRATES, AND FUNCTIONS DURING APOPTOSIS." *Annual Review of Biochemistry* 68(February):383–424.
- Ebeed, Heba T., Sean R. Stevenson, Andrew C. Cuming, and Alison Baker. 2018. "Conserved and Differential Transcriptional Responses of Peroxisome Associated Pathways to Drought, Dehydration and ABA." *Journal of Experimental Botany* 69(20):4971–85.
- Endo, Motomu, Hanako Shimizu, Maria A. Nohales, Takashi Araki, and Steve A. Kay. 2014. "Tissue-Specific Clocks in Arabidopsis Show Asymmetric Coupling." *Nature* 515(7527):419–22.
- Erwin, John E., Royal D. Heins, and Meriam G. Karlsson. 1989. "Thermomorphogenesis in *Lilium Longiflorum*." *Amer. J. Bot.* 76(1):47–52.
- Escamez, Sacha, Dominique André, Bo Zhang, Benjamin Bollhöner, Edouard Pesquet, and Hannele Tuominen. 2016. "METACASPASE9 Modulates Autophagy to Confine Cell Death to the Target Cells during Arabidopsis Vascular Xylem Differentiation ." *Biology Open* 5(2):122–29.
- Escamez, Sacha, Simon Stael, Julia P. Vainonen, Patrick Willems, Huiting Jin, Sachie Kimura, Frank Van Breusegem, Kris Gevaert, Michael Wrzaczek, and Hannele Tuominen. 2019. "Extracellular Peptide Kratos Restricts Cell Death during Vascular Development and Stress in Arabidopsis." *Journal of Experimental Botany* 70(7): 2199–2210.
- Escamez, Sacha and Hannele Tuominen. 2014. "Programmes of Cell Death and Autolysis in Tracheary Elements: When a Suicidal Cell Arranges Its Own Corpse Removal." *Journal of Experimental Botany* 65(5):1313–21.
- Fàbregas, Norma, Na Li, Sjeff Boeren, Tara E. Nash, Michael B. Goshe, Steven D. Clouse, Sacco de Vries, and Ana I. Caño-Delgado. 2013. "The BRASSINOSTEROID INSENSITIVE1-LIKE3 Signalosome Complex Regulates Arabidopsis Root Development." *Plant Cell* 25(9):3377–88.
- Farage-Barhom, Sarit, Shaul Burd, Lilian Sonogo, Rafael Perl-Treves, and Amnon Lers. 2008. "Expression Analysis of the BFN1 Nuclease Gene Promoter during Senescence, Abscission, and Programmed Cell Death-Related Processes." *Journal of Experimental Botany* 59(12):3247–58.
- Fausser, Friedrich, Simon Schiml, and Holger Puchta. 2014. "Both CRISPR/Cas-Based Nucleases and Nickases Can Be Used Efficiently for Genome Engineering in Arabidopsis Thaliana." *Plant Journal* 79(2):348–59.
- Fendrych, Matyáš, Tom Van Hautegeem, Matthias Van Durme, Yadira Olvera-Carrillo,

References

- Marlies Huysmans, Mansour Karimi, Saskia Lippens, Christopher J. Guérin, Melanie Krebs, Karin Schumacher, and Moritz K. Nowack. 2014. "Programmed Cell Death Controlled by ANAC033/SOMBRERO Determines Root Cap Organ Size in Arabidopsis." *Current Biology* 24(9):931–40.
- Fernández-Trijuque, Juan, Antonio Jesús Serrato, and Mariam Sahrawy. 2019. "Proteomic Analyses of Thioredoxins f and m Arabidopsis Thaliana Mutants Indicate Specific Functions for These Proteins in Plants." *Antioxidants* 8(3).
- Flexas, Jaume, Miquel Ribas-Carbó, Antonio Diaz-Espejo, Jeroni Galmés, and Hipólito Medrano. 2008. "Mesophyll Conductance to CO₂: Current Knowledge and Future Prospects." *Plant, Cell and Environment* 31(5):602–21.
- Franklin, Keara A. and Peter H. Quail. 2010. "Phytochrome Functions in Arabidopsis Development." *Journal of Experimental Botany* 61(1):11–24.
- Furuta, Kaori Miyashima, Shri Ram Yadav, Satu Lehesranta, Ilya Belevich, Shunsuke Miyashima, Jung ok Heo, Anne Vatén, Ove Lindgren, Bert De Rybel, Gert Van Isterdael, Panu Somervuo, Raffael Lichtenberger, Raquel Rocha, Siripong Thitamadee, Sari Tähtiharju, Petri Auvinen, Tom Beeckman, Eija Jokitalo, and Ykä Helariutta. 2014. "Plant Development. Arabidopsis NAC45/86 Direct Sieve Element Morphogenesis Culminating in Enucleation." *Science (New York, N.Y.)* 345(6199):933–37.
- Gaillochet, Christophe, Yogev Burko, Matthieu Pierre Platre, Zhang Ling, Simura Jan, Vinod Kumar, Ljung Karin, Joanne Chory, and Wolfgang Busch. 2020. "Shoot and Root Thermomorphogenesis Are Linked by a Developmental Trade-Of." *BioRxiv* <https://doi.org/10.1101/2020.05.07.083246>.
- Galluzzi, Lorenzo, Ilio Vitale, Stuart A. Aaronson, John M. Abrams, Dieter Adam, Patrizia Agostinis, Emad S. Alnemri, Lucia Altucci, Ivano Amelio, David W. Andrews, Margherita Annicchiarico-Petruzzelli, Alexey V Antonov, Eli Arama, Eric H. Baehrecke, Nickolai A. Barlev, Nicolas G. Bazan, Francesca Bernassola, Mathieu J. M. Bertrand, Katuscia Bianchi, Mikhail V Blagosklonny, Klas Blomgren, Christoph Borner, Patricia Boya, Catherine Brenner, Michelangelo Campanella, Eleonora Candi, Didac Carmona-Gutierrez, Francesco Cecconi, Francis K. M. Chan, Navdeep S. Chandel, Emily H. Cheng, Jerry E. Chipuk, John A. Cidlowski, Aaron Ciechanover, Gerald M. Cohen, Marcus Conrad, Juan R. Cubillos-Ruiz, Peter E. Czabotar, Vincenzo D'Angiolella, Ted M. Dawson, Valina L. Dawson, Vincenzo De Laurenzi, Ruggero De Maria, Klaus-Michael Debatin, Ralph J. DeBerardinis, Mohanish Deshmukh, Nicola Di Daniele, Francesco Di Virgilio, Vishva M. Dixit, Scott J. Dixon, Colin S. Duckett, Brian D. Dynlacht, Wafik S. El-Deiry, John W. Elrod, Gian

References

- Maria Fimia, Simone Fulda, Ana J. García-Sáez, Abhishek D. Garg, Carmen Garrido, Evripidis Gavathiotis, Pierre Golstein, Eyal Gottlieb, Douglas R. Green, Lloyd A. Greene, Hinrich Gronemeyer, Atan Gross, Gyorgy Hajnoczky, J. Marie Hardwick, Isaac S. Harris, Michael O. Hengartner, Claudio Hetz, Hidenori Ichijo, Marja Jäättelä, Bertrand Joseph, Philipp J. Jost, Philippe P. Juin, William J. Kaiser, Michael Karin, Thomas Kaufmann, Oliver Kepp, Adi Kimchi, Richard N. Kitsis, Daniel J. Klionsky, Richard A. Knight, Sharad Kumar, Sam W. Lee, John J. Lemasters, Beth Levine, Andreas Linkermann, Stuart A. Lipton, Richard A. Lockshin, Carlos López-Otín, Scott W. Lowe, Tom Luedde, Enrico Lugli, Marion MacFarlane, Frank Madeo, Michal Malewicz, Walter Malorni, Gwenola Manic, Jean-Christophe Marine, Seamus J. Martin, Jean-Claude Martinou, Jan Paul Medema, Patrick Mehlen, Pascal Meier, Sonia Melino, Edward A. Miao, Jeffery D. Molkentin, Ute M. Moll, Cristina Muñoz-Pinedo, Shigekazu Nagata, Gabriel Nuñez, Andrew Oberst, Moshe Oren, Michael Overholtzer, Michele Pagano, Theocharis Panaretakis, Manolis Pasparakis, Josef M. Penninger, David M. Pereira, Shazib Pervaiz, Marcus E. Peter, Mauro Piacentini, Paolo Pinton, Jochen H. M. Prehn, Hamsa Puthalakath, Gabriel A. Rabinovich, Markus Rehm, Rosario Rizzuto, Cecilia M. P. Rodrigues, David C. Rubinsztein, Thomas Rudel, Kevin M. Ryan, Emre Sayan, Luca Scorrano, Feng Shao, Yufang Shi, John Silke, Hans-Uwe Simon, Antonella Sistigu, Brent R. Stockwell, Andreas Strasser, Gyorgy Szabadkai, Stephen W. G. Tait, Daolin Tang, Nektarios Tavernarakis, Andrew Thorburn, Yoshihide Tsujimoto, Boris Turk, Tom Vanden Berghe, Peter Vandenabeele, Matthew G. Vander Heiden, Andreas Villunger, Herbert W. Virgin, Karen H. Vousden, Domagoj Vucic, Erwin F. Wagner, Henning Walczak, David Wallach, Ying Wang, James A. Wells, Will Wood, Junying Yuan, Zahra Zakeri, Boris Zhivotovsky, Laurence Zitvogel, Gerry Melino, and Guido Kroemer. 2018. "Molecular Mechanisms of Cell Death: Recommendations of the Nomenclature Committee on Cell Death 2018." *Cell Death and Differentiation* 25(3):486–541.
- Geldner, Niko. 2014. "Making Phloem - A near-Death Experience." *Science* 345(6199):875–76.
- Genin, Stéphane. 2010. "Molecular Traits Controlling Host Range and Adaptation to Plants in *Ralstonia Solanacearum*." *New Phytologist* 187(4):920–28.
- Gibbs, Daniel J. and Michael J. Holdsworth. 2020. "Every Breath You Take: New Insights into Plant and Animal Oxygen Sensing." *Cell* 180(1):22–24.
- Gibbs, Daniel J., Seung Cho Lee, Nurulhikma Md Isa, Silvia Gramuglia, Takeshi Fukao, George W. Bassel, Cristina Sousa Correia, Françoise Corbineau, Frederica L.

References

- Theodoulou, Julia Bailey-Serres, and Michael J. Holdsworth. 2011. "Homeostatic Response to Hypoxia Is Regulated by the N-End Rule Pathway in Plants." *Nature* 479(7373):415–18.
- Gong, Peijie, Michael Riemann, Duan Dong, Nadja Stoeffler, Bernadette Gross, Armin Markel, and Peter Nick. 2019. "Two Grapevine Metacaspase Genes Mediate ETI-like Cell Death in Grapevine Defence against Infection of *Plasmopara Viticola*." *Protoplasma* 256(4):951–69.
- González-Guzmán, Miguel, Aurelio Gómez-Cadenas, and Vicent Arbona. 2021. "Abscisic Acid as an Emerging Modulator of the Responses of Plants to Low Oxygen Conditions." *Frontiers in Plant Science* 12(April).
- Gottwald, Jennifer R., Patrick J. Krysan, Jeffery C. Young, Ray F. Evert, and Michael R. Sussman. 2000. "Genetic Evidence for the in Planta Role of Phloem-Specific Plasma Membrane Sucrose Transporters." *Proceedings of the National Academy of Sciences of the United States of America* 97(25):13979–84.
- Graeff, Moritz and Christian S. Hardtke. 2021. "Metaphloem Development in the Arabidopsis Root Tip." *BioRxiv* <https://doi.org/10.1101/2021.04.30.442082> .
- Graeff, Moritz, Surbhi Rana, Petra Marhava, Bernard Moret, and Christian S. Hardtke. 2020. "Local and Systemic Effects of Brassinosteroid Perception in Developing Phloem." *Current Biology* 1–13.
- Graeff, Moritz, Surbhi Rana, Jos R. Wendrich, Julien Dorier, Thomas Eekhout, Ana Cecilia Aliaga Fandino, Nicolas Guex, George W. Bassel, Bert De Rybel, and Christian S. Hardtke. 2021. "A Morpho-Transcriptomic Map of Brassinosteroid Action in the Arabidopsis Root." *BioRxiv* <https://doi.org/10.1101/2021.03.30.437656>.
- Graff van Creveld, Shiri, Shifra Ben-Dor, Avia Mizrachi, Uria Alcolombri, Amanda Hopes, Thomas Mock, Shilo Rosenwasser, and Assaf Vardi. 2018. "A Redox-Regulated Type III Metacaspase Controls Cell Death in a Marine Diatom." *BioRxiv* <https://doi.org/10.1101/444109>.
- Gray, W. M. 2004. "Hormonal Regulation of Plant Growth and Development." *PLoS Biology* 2(9).
- Guan, Miao, Thomas C. de Bang, Carsten Pedersen, and Jan K. Schjoerring. 2016. "Cytosolic Glutamine Synthetase Gln1;2 Is the Main Isozyme Contributing to GS1 Activity and Can Be up-Regulated to Relieve Ammonium Toxicity." *Plant Physiology* 171(3):1921–33.
- Guaragnella, Nicoletta, Antonella Bobba, Salvatore Passarella, Ersilia Marra, and Sergio Giannattasio. 2010. "Yeast Acetic Acid-Induced Programmed Cell Death Can Occur without Cytochrome c Release Which Requires Metacaspase YCA1." *FEBS Letters*

References

- 584(1):224–28.
- Gujas, Bojan, Tiago M. D. Cruz, Elizabeth Kastanaki, Joop E. M. Vermeer, Teun Munnik, and Antia Rodriguez-Villalon. 2017. “Perturbing Phosphoinositide Homeostasis Oppositely Affects Vascular Differentiation in Arabidopsis Thaliana Roots.” *Development (Cambridge)* 144(19):3578–89.
- Gujas, Bojan, Elizabeth Kastanaki, Alessandra Sturchler, Tiago M. D. Cruz, M. Aguila Ruiz-Sola, Rene Dreos, Simona Eicke, Elisabeth Truernit, and Antia Rodriguez-Villalon. 2020. “A Reservoir of Pluripotent Phloem Cells Safeguards the Linear Developmental Trajectory of Protophloem Sieve Elements.” *Current Biology* 30(5):755-766.e4.
- Gunawardena, Arunika H. L. A. N. 2008. “Programmed Cell Death and Tissue Remodelling in Plants.” *Journal of Experimental Botany* 59(3):445–51.
- Haeussler, Maximilian, Kai Schönig, Hélène Eckert, Alexis Eschstruth, Joffrey Mianné, Jean Baptiste Renaud, Sylvie Schneider-Maunoury, Alena Shkumatava, Lydia Teboul, Jim Kent, Jean Stephane Joly, and Jean Paul Concordet. 2016. “Evaluation of Off-Target and on-Target Scoring Algorithms and Integration into the Guide RNA Selection Tool CRISPOR.” *Genome Biology* 17(1):1–12.
- Han, Jingyi, Hui Li, Bin Yin, Yongzhuo Zhang, Yadi Liu, Ziyi Cheng, Di Liu, and Hai Lu. 2019. “The Papain-like Cysteine Protease CEP1 Is Involved in Programmed Cell Death and Secondary Wall Thickening during Xylem Development in Arabidopsis.” *Journal of Experimental Botany* 70(1):205–15.
- Hander, Tim, Álvaro D. Fernández-Fernández, Robert P. Kumpf, Patrick Willems, Hendrik Schatowitz, Debbie Rombaut, An Staes, Jonah Nolf, Robin Pottie, Panfeng Yao, Amanda Gonçalves, Benjamin Pavie, Thomas Boller, Kris Gevaert, Frank Van Breusegem, Sebastian Bartels, and Simon Stael. 2019. “Damage on Plants Activates Ca²⁺-Dependent Metacaspases for Release of Immunomodulatory Peptides.” *Science* 363(6433):eaar7486.
- Hao, L., P. H. Goodwin, and T. Hsiang. 2007. “Expression of a Metacaspase Gene of Nicotiana Benthamiana after Inoculation with Colletotrichum Destructivum or Pseudomonas Syringae Pv. Tomato, and the Effect of Silencing the Gene on the Host Response.” *Plant Cell Reports* 26(10):1879–88.
- Hara-Nishimura, I. and N. Hatsugai. 2011. “The Role of Vacuole in Plant Cell Death.” *Cell Death and Differentiation* 18(8):1298–1304.
- Hara-Nishimura, Ikuko, Noriyuki Hatsugai, Satoru Nakaune, Miwa Kuroyanagi, and Mikio Nishimura. 2005. “Vacuolar Processing Enzyme: An Executor of Plant Cell Death.” *Current Opinion in Plant Biology* 8(4):404–8.

References

- He, Mei, Cheng Qiang He, and Nai Zheng Ding. 2018. "Abiotic Stresses: General Defenses of Land Plants and Chances for Engineering Multistress Tolerance." *Frontiers in Plant Science* 871(December):1–18.
- He, Rui, Georgina E. Drury, Vitalie I. Rotari, Anna Gordon, Martin Willer, Tabasum Farzaneh, Ernst J. Woltering, and Patrick Gallois. 2008. "Metacaspase-8 Modulates Programmed Cell Death Induced by Ultraviolet Light and H₂O₂ in Arabidopsis." *Journal of Biological Chemistry* 283(2):774–83.
- Heo, Jung ok, Bernhard Blob, and Ykä Helariutta. 2017. "Differentiation of Conductive Cells: A Matter of Life and Death." *Current Opinion in Plant Biology* 35:23–29.
- Hirakawa, Yuki, Yuki Kondo, and Hiroo Fukuda. 2010. "Regulation of Vascular Development by CLE Peptide-Receptor Systems." *Journal of Integrative Plant Biology* 52(1):8–16.
- Hirakawa, Yuki, Yuki Kondo, and Hiroo Fukuda. 2011. "Establishment and Maintenance of Vascular Cell Communities through Local Signaling." *Current Opinion in Plant Biology* 14(1):17–23.
- Hoerberichts, Frank A., Arjen Ten Have, and Ernst J. Woltering. 2003. "A Tomato Metacaspase Gene Is Upregulated during Programmed Cell Death in Botrytis Cinerea-Infected Leaves." *Planta* 217(3):517–22.
- Van Der Hoorn, Renier A. L. 2008. "Plant Proteases: From Phenotypes to Molecular Mechanisms." *Annual Review of Plant Biology* 59:191–223.
- Hsu, Fu Chiun, Mei Yi Chou, Hsiao Ping Peng, Shu Jen Chou, and Ming Che Shih. 2011. "Insights into Hypoxic Systemic Responses Based on Analyses of Transcriptional Regulation in Arabidopsis." *PLoS ONE* 6(12):14–16.
- Hsu, Fu Chiun and Ming Che Shih. 2013. "Plant Defense after Flooding." *Plant Signaling and Behavior* 8(11).
- Huete-Pérez, Jorge A., Juan C. Engel, Linda S. Brinen, Jeremy C. Mottram, and James H. McKerrow. 1999. "Protease Trafficking in Two Primitive Eukaryotes Is Mediated by a Prodomain Protein Motif." *Journal of Biological Chemistry* 274(23):16249–56.
- Hughes, Christopher S., Sophie Moggridge, Torsten Müller, Poul H. Sorensen, Gregg B. Morin, and Jeroen Krijgsveld. 2019. "Single-Pot, Solid-Phase-Enhanced Sample Preparation for Proteomics Experiments." *Nature Protocols* 14(1):68–85.
- Huysmans, Marlies, Saul Lema A, Nuria S. Coll, and Moritz K. Nowack. 2017. "Dying Two Deaths — Programmed Cell Death Regulation in Development and Disease." *Current Opinion in Plant Biology* 35:37–44.
- Ingram, Paul, Jan Dettmer, Yrjo Helariutta, and Jocelyn E. Malamy. 2011. "Arabidopsis Lateral Root Development 3 Is Essential for Early Phloem Development and

References

- Function, and Hence for Normal Root System Development." *Plant Journal* 68(3):455–67.
- Dello Ioio, Raffaele, Francisco Scaglia Linhares, Emanuele Scacchi, Eva Casamitjana-Martinez, Renze Heidstra, Paolo Costantino, and Sabrina Sabatini. 2007. "Cytokinins Determine Arabidopsis Root-Meristem Size by Controlling Cell Differentiation." *Current Biology* 17(8):678–82.
- Ishikawa, H. and M. L. Evans. 1995. "Specialized Zones of Development in Roots." *Plant Physiology* 109(3):725–27.
- Jaeger, Katja E. and Philip A. Wigge. 2007. "FT Protein Acts as a Long-Range Signal in Arabidopsis." *Current Biology* 17(12):1050–54.
- Jan Dettmer, Robertas Ursache, Ana Campilho, Shunsuke Miyashima, Ilya Belevich, Seana O'Regan, Daniel Leroy Mullendore, Shri Ram Yadav, Christa Lanz, Luca Beverina, Antonio Papagni, Korbinian Schneeberger, Detlef Weigel, York-Dieter Stierhof, Thomas Morit, Eija and Eija Jokitalo Yka" Helariutta. 2014. "CHOLINE TRANSPORTER-LIKE1 Is Required for Sieve Plate Development to Mediate Long-Distance Cell-to-Cell Communication." *Nature Communications* 5(4276).
- Jerala, Roman, Eva Zerovnik, Jurka Kidric, and Vito Turk. 1998. "PH-Induced Conformational Transitions of the Propeptide of Human Cathepsin L." *Journal of Biological Chemistry* 273(19):11498–504.
- Jin, H., Eleonora Cominelli, Paul Bailey, Adrian Parr, Frank Mehrtens, Jonathon Jones, Chiara Tonelli, and Bernd and Cathie Marti Weisshaar. 2000. "Transcriptional Repression by AtMYB4 Controls Production of UV-Protecting Sunscreens in Arabidopsis." *The EMBO Journal* 19(22):6150–61.
- Kang, Yeon Hee, Alice Breda, and Christian S. Hardtke. 2017. "Brassinosteroid Signaling Directs Formative Cell Divisions and Protophloem Differentiation in Arabidopsis Root Meristems." *Development (Cambridge)* 144(2):272–80.
- Karlova, Romyana, Damian Boer, Scott Hayes, and Christa Testerink. 2021. "Root Plasticity under Abiotic Stress." *Plant Physiology* 1–14.
- Kim, Ji Yun, Efthymia Symeonidi, Tin Yau Pang, Tom Denyer, Diana Weidauer, Margaret Bezruczyk, Manuel Miras, Nora Zöllner, Thomas Hartwig, Michael M. Wudick, Martin Lercher, Li Qing Chen, Marja C. P. Timmermans, and Wolf B. Frommer. 2021. "Distinct Identities of Leaf Phloem Cells Revealed by Single Cell Transcriptomics." *The Plant Cell* 33(3):511–30.
- Kim, Jin Sun, Hyun Ju Jung, Hwa Jung Lee, Kyung Ae Kim, Chang Hyo Goh, Youngmin Woo, Seung Han Oh, Yeon Soo Han, and Hunseung Kang. 2008. "Glycine-Rich RNA-Binding Protein7 Affects Abiotic Stress Responses by Regulating Stomata

References

- Opening and Closing in *Arabidopsis Thaliana*." *Plant Journal* 55(3):455–66.
- Kim, Su Min, Chungyun Bae, Sang Keun Oh, and Doil Choi. 2013. "A Pepper (*Capsicum Annuum* L.) Metacaspase 9 (Camc9) Plays a Role in Pathogen-Induced Cell Death in Plants." *Molecular Plant Pathology* 14(6):557–66.
- Kleifeld, Oded, Alain Doucet, Ulrich Auf Dem Keller, Anna Prudova, Oliver Schilling, Rajesh K. Kainthan, Amanda E. Starr, Leonard J. Foster, Jayachandran N. Kizhakkedathu, and Christopher M. Overall. 2010. "Isotopic Labeling of Terminal Amines in Complex Samples Identifies Protein N-Termini and Protease Cleavage Products." *Nature Biotechnology* 28(3):281–88.
- Klemenčič, Marina and Christiane Funk. 2018a. "Structural and Functional Diversity of Caspase Homologues in Non-Metazoan Organisms." *Protoplasma* 255(1):387–97.
- Klemenčič, Marina and Christiane Funk. 2018b. "Type III Metacaspases: Calcium-Dependent Activity Proposes New Function for the P10 Domain." *New Phytologist* 218(3):1179–91.
- Klemenčič, Marina and Christiane Funk. 2019. "Evolution and Structural Diversity of Metacaspases." *Journal of Experimental Botany* 70(7):2039–47.
- Kondo, Yuki, Takashi Fujita, Munetaka Sugiyama, and Hiroo Fukuda. 2015. "A Novel System for Xylem Cell Differentiation in *Arabidopsis Thaliana*." *Molecular Plant* 8(4):612–21.
- Kondo, Yuki, Alif Meem Nurani, Chieko Saito, Yasunori Ichihashi, Masato Saito, Kyoko Yamazaki, Nobutaka Mitsuda, Masaru Ohme-Takagi, and Hiroo Fukuda. 2016. "Vascular Cell Induction Culture System Using *Arabidopsis* Leaves (VISUAL) Reveals the Sequential Differentiation of Sieve Element-like Cells." *Plant Cell* 28(6):1250–62.
- Korver, Ruud A., Iko T. Koevoets, and Christa Testerink. 2018. "Out of Shape During Stress: A Key Role for Auxin." *Trends in Plant Science* 23(9):783–93.
- Kumar, M. Nagaraj, Yi Fang Hsieh, and Paul E. Verslues. 2015. "At14a-Like1 Participates in Membrane-Associated Mechanisms Promoting Growth during Drought in *Arabidopsis Thaliana*." *Proceedings of the National Academy of Sciences of the United States of America* 112(33):10545–50.
- Kumpf, Robert P. and Moritz K. Nowack. 2015. "The Root Cap: A Short Story of Life and Death." *Journal of Experimental Botany* 66(19):5651–62.
- Kunikowska, A., A. Byczkowska, M. Doniak, and A. Kaźmierczak. 2013. "Cytokinins Résumé: Their Signaling and Role in Programmed Cell Death in Plants." *Plant Cell Reports* 32(6):771–80.
- Kurihara, Daisuke, Yoko Mizuta, Yoshikatsu Sato, and Tetsuya Higashiyama. 2015.

References

- “ClearSee: A Rapid Optical Clearing Reagent for Whole-Plant Fluorescence Imaging.” *Development (Cambridge)* 142(23):4168–79.
- Kurkela, Sirpa and Marianne Borg-franck. 1992. “Structure and Expression of Kin2, One of Two Cold- and ABA-Induced Genes of Arabidopsis Thaliana.” *Plant Molecular Biology* 19:689–92.
- Kuroha, Takeshi, Asako Okuda, Masahiro Arai, Yuta Komatsu, Shusei Sato, Tomohiko Kato, Satoshi Tabata, and Shinobu Satoh. 2009. “Identification of Arabidopsis Subtilisin-like Serine Protease Specifically Expressed in Root Stele by Gene Trapping.” *Physiologia Plantarum* 137(3):281–88.
- Kuromori, Takashi, Mitsunori Seo, and Kazuo Shinozaki. 2018. “ABA Transport and Plant Water Stress Responses.” *Trends in Plant Science* 23(6):513–22.
- Kwon, Soon Il and Duk Ju Hwang. 2013. “Expression Analysis of the Metacaspase Gene Family in Arabidopsis.” *Journal of Plant Biology* 56(6):391–98.
- Lampropoulos, Athanasios, Zoran Sutikovic, Christian Wenzl, Ira Maegele, Jan U. Lohmann, and Joachim Forner. 2013. “GreenGate - A Novel, Versatile, and Efficient Cloning System for Plant Transgenesis.” *PLoS ONE* 8(12).
- Lee, Kwang Hee, Hai Lan Piao, Ho Youn Kim, Sang Mi Choi, Fan Jiang, Wolfram Hartung, Ildoo Hwang, June M. Kwak, In Jung Lee, and Inhwan Hwang. 2006. “Activation of Glucosidase via Stress-Induced Polymerization Rapidly Increases Active Pools of Abscisic Acid.” *Cell* 126(6):1109–20.
- Lee, Robin E. C., Steve Brunette, Lawrence G. Puente, and Lynn A. Megeney. 2010. “Metacaspase Yca1 Is Required for Clearance of Insoluble Protein Aggregates.” *Proceedings of the National Academy of Sciences of the United States of America* 107(30):13348–53.
- Lehesranta, Satu J., Raffael Lichtenberger, and Ykä Helariutta. 2010. “Cell-to-Cell Communication in Vascular Morphogenesis.” *Current Opinion in Plant Biology* 13(1):59–65.
- Lema Asqui, Saul, Dominique Vercammen, Irene Serrano, Marc Valls, Susana Rivas, Frank Van Breusegem, Frank L. Conlon, Jeffery L. Dangl, and Núria S. Coll. 2018. “AtSERPIN1 Is an Inhibitor of the Metacaspase AtMC1-Mediated Cell Death and Autocatalytic Processing in Planta.” *New Phytologist* 218(3): 1156-1166.
- De León, Inés Ponce, Ana Sanz, Mats Hamberg, and Carmen Castresana. 2002. “Involvement of the Arabidopsis α -DOX1 Fatty Acid Dioxygenase in Protection against Oxidative Stress and Cell Death.” *Plant Journal* 29(1):61–72.
- Leuendorf, Jan Erik, Manuel Frank, and Thomas Schmülling. 2020. “Acclimation, Priming and Memory in the Response of Arabidopsis Thaliana Seedlings to Cold Stress.”

References

- Scientific Reports* 10(1):1–11.
- Lichtenthaler, Hartmut K. 1987. "Chlorophylls and Carotenoids: Pigments of Photosynthetic Biomembranes." *Methods in Enzymology* 148(C):350–82.
- Lievens, Laurens, Jacob Pollier, Alain Goossens, Rudi Beyaert, and Jens Staal. 2017. "Abscisic Acid as Pathogen Effector and Immune Regulator." *Frontiers in Plant Science* 8(April):1–15.
- Liu, Huijuan, Menghui Hu, Qi Wang, Lin Cheng, and Zaibao Zhang. 2018. "Role of Papain-Like Cysteine Proteases in Plant Development." *Frontiers in Plant Science* 9(December):1–10.
- Liu, Liang and Xiu duo Fan. 2013. "Tapetum: Regulation and Role in Sporopollenin Biosynthesis in Arabidopsis." *Plant Molecular Biology* 83(3):165–75.
- Liu, Lu, Chang Liu, Xingliang Hou, Wanyan Xi, Lisha Shen, Zhen Tao, Yue Wang, and Hao Yu. 2012. "FTIP1 Is an Essential Regulator Required for Florigen Transport." *PLoS Biology* 10(4).
- Livak, Kenneth J. and Thomas D. Schmittgen. 2001. "Analysis of Relative Gene Expression Data Using Real-Time Quantitative PCR and the 2- $\Delta\Delta$ CT Method." *Methods* 25(4):402–8.
- Loreti, Elena, Maria Cristina Valeri, Giacomo Novi, and Pierdomenico Perata. 2018. "Gene Regulation and Survival under Hypoxia Requires Starch Availability and Metabolism." *Plant Physiology* 176(2):1286–98.
- Lothier, Jérémy, Houssein Diab, Caroline Cukier, Anis M. Limami, and Guillaume Tcherkez. 2020. "Metabolic Responses to Waterlogging Differ between Roots and Shoots and Reflect Phloem Transport Alteration in *Medicago truncatula*." *Plants* 9(10):1–20.
- Lothier, Jérémy, Laure Gaufichon, Rodnay Sormani, Thomas Lemaître, Marianne Azzopardi, Halima Morin, Fabien Chardon, Michle Reisdorf-Cren, Jean Christophe Avice, and Céline Masclaux-Daubresse. 2011. "The Cytosolic Glutamine Synthetase GLN1;2 Plays a Role in the Control of Plant Growth and Ammonium Homeostasis in Arabidopsis Rosettes When Nitrate Supply Is Not Limiting." *Journal of Experimental Botany* 62(4):1375–90.
- Lu, Haibin, Saul A. Lema, Marc Planas-Marquès, Alejandro Alonso-Díaz, Marc Valls, and Núria S. Coll. 2018. "Type III Secretion-Dependent and-Independent Phenotypes Caused by *Ralstonia solanacearum* in Arabidopsis Roots." *Molecular Plant-Microbe Interactions* 31(1):175–84.
- Luan, Qing Ling, Yu Xiu Zhu, Shijun Ma, Yang Sun, Xiao Ying Liu, Mengjie Liu, Peter J. Balint-Kurti, and Guan Feng Wang. 2021. "Maize Metacaspases Modulate the

References

- Defense Response Mediated by the NLR Protein Rp1-D21 Likely by Affecting Its Subcellular Localization." *Plant Journal* 105(1):151–66.
- Lucas, William J., Andrew Groover, Raffael Lichtenberger, Kaori Furuta, Shri Ram Yadav, Ykä Helariutta, Xin Qiang He, Hiroo Fukuda, Julie Kang, Siobhan M. Brady, John W. Patrick, John Sperry, Akiko Yoshida, Ana Flor López-Millán, Michael A. Grusak, and Pradeep Kachroo. 2013. "The Plant Vascular System: Evolution, Development and Functions." *Journal of Integrative Plant Biology* 55(4):294–388.
- Madeo, Frank, Eva Herker, Corinna Maldener, Silke Wissing, Stephan Lächelt, Mark Herlan, Markus Fehr, Kirsten Lauber, Stephan J. Sigrist, Sebastian Wesselborg, and Kai Uwe Fröhlich. 2002. "A Caspase-Related Protease Regulates Apoptosis in Yeast." *Molecular Cell* 9(4):911–17.
- McLuskey, Karen and Jeremy C. Mottram. 2015. "Comparative Structural Analysis of the Caspase Family with Other Clan CD Cysteine Peptidases." *Biochemical Journal* 466:219–32.
- Meyer, Jesse G., Natalie M. Niemi, David J. Pagliarini, and Joshua J. Coon. 2020. "Quantitative Shotgun Proteome Analysis by Direct Infusion." *Nature Methods* 17(12):1222–28.
- Meyer, Michael, Sebastian Leptihn, Max Welz, and Andreas Schaller. 2016. "Functional Characterization of Propeptides in Plant Subtilases as Intramolecular Chaperones and Inhibitors of the Mature Protease." *Journal of Biological Chemistry* 291(37):19449–61.
- Miao, Rui, Wei Yuan, Yue Wang, Irene Garcia-Maquilon, Xiaolin Dang, Ying Li, Jianhua Zhang, Yiyong Zhu, Pedro L. Rodriguez, and Weifeng Xu. 2021. "Low ABA Concentration Promotes Root Growth and Hydrotropism through Relief of ABA INSENSITIVE 1-Mediated Inhibition of Plasma Membrane H⁺-ATPase 2." *Science Advances* 7(12):1–15.
- Milhinhos, Ana and Célia M. Miguel. 2013. "Hormone Interactions in Xylem Development: A Matter of Signals." *Plant Cell Reports* 32(6):867–83.
- Minina, E. A., N. S. Coll, H. Tuominen, and P. V. Bozhkov. 2017. "Metacaspases versus Caspases in Development and Cell Fate Regulation." *Cell Death and Differentiation* 24(8):1314–25.
- Minina, Elena A., Lada H. Filonova, Kazutake Fukada, Eugene I. Savenkov, Vladimir Gogvadze, David Clapham, Victoria Sanchez-Vera, Maria F. Suarez, Boris Zhivotovsky, Geoffrey Daniel, Andrei Smertenko, and Peter V. Bozhkov. 2013. "Autophagy and Metacaspase Determine the Mode of Cell Death in Plants." *Journal of Cell Biology* 203(6):917–27.

References

- Minina, Elena A., Jens Staal, Vanina E. Alvarez, John A. Berges, Ilana Berman-Frank, Rudi Beyaert, Kay D. Bidle, Frédéric Bornancin, Magali Casanova, Juan J. Cazzulo, Chang Jae Choi, Nuria S. Coll, Vishva M. Dixit, Marko Dolinar, Nicolas Fasel, Christiane Funk, Patrick Gallois, Kris Gevaert, Emilio Gutierrez-Beltran, Stephan Hailfinger, Marina Klemenčič, Eugene V. Koonin, Daniel Krappmann, Anna Linusson, Maurício F. M. Machado, Frank Madeo, Lynn A. Megeney, Panagiotis N. Moschou, Jeremy C. Mottram, Thomas Nyström, Heinz D. Osiewacz, Christopher M. Overall, Kailash C. Pandey, Jürgen Ruland, Guy S. Salvesen, Yigong Shi, Andrei Smertenko, Simon Stael, Jerry Ståhlberg, María Fernanda Suárez, Margot Thome, Hannele Tuominen, Frank Van Breusegem, Renier A. L. van der Hoorn, Assaf Vardi, Boris Zhivotovsky, Eric Lam, and Peter V. Bozhkov. 2020. "Classification and Nomenclature of Metacaspases and Paracaspases: No More Confusion with Caspases." *Molecular Cell* 77(5):927–29.
- Miyashima, Shunsuke, Jose Sebastian, Ji Young Lee, and Yka Helariutta. 2013. "Stem Cell Function during Plant Vascular Development." *EMBO Journal* 32(2):178–93.
- Moeder, Wolfgang, Huoi Ung, Stephen Mosher, and Keiko Yoshioka. 2010. "SA-ABA Antagonism in Defense Responses." *Plant Signaling and Behavior* 5(10):1231–33.
- Monteiro, Freddy, Montserrat Solé, Irene Van Dijk, and Marc Valls. 2012. "A Chromosomal Insertion Toolbox for Promoter Probing, Mutant Complementation, and Pathogenicity Studies in *Ralstonia Solanacearum*." *Molecular Plant-Microbe Interactions* 25(4):557–68.
- Montgomery, Beronda L. 2016. "Spatiotemporal Phytochrome Signaling during Photomorphogenesis: From Physiology to Molecular Mechanisms and Back." *Frontiers in Plant Science* 7(APR2016):1–8.
- Morineau, Céline, Yannick Bellec, Frédérique Tellier, Lionel Gissot, Zsolt Kelemen, Fabien Nogué, and Jean Denis Faure. 2017. "Selective Gene Dosage by CRISPR-Cas9 Genome Editing in Hexaploid *Camelina Sativa*." *Plant Biotechnology Journal* 15(6):729–39.
- Mouchel, Céline F., Karen S. Osmont, and Christian S. Hardtke. 2006. "BRX Mediates Feedback between Brassinosteroid Levels and Auxin Signalling in Root Growth." *Nature* 443(7110):458–61.
- Msanne, Joseph, Jiusheng Lin, Julie M. Stone, and Tala Awada. 2011. "Characterization of Abiotic Stress-Responsive Arabidopsis Thaliana RD29A and RD29B Genes and Evaluation of Transgenes." *Planta* 234(1):97–107.
- Müller, Maren and Sergi Munné-bosch. 2011. "Rapid and Sensitive Hormonal Profiling of Complex Plant Samples by Liquid Chromatography Coupled to Electrospray

References

- Ionization Tandem Mass Spectrometry." *Plant Methods* 1–11.
- Munné-Bosch, Sergi and Leonor Alegre. 2004. "Die and Let Live: Leaf Senescence Contributes to Plant Survival under Drought Stress." *Functional Plant Biology* 31(3):203–16.
- Murchie, E. H. and T. Lawson. 2013. "Chlorophyll Fluorescence Analysis : A Guide to Good Practice and Understanding Some New Applications." *Journal of Experimental Botany* 64(13):3983–98.
- Nakaune, S. 2005. "A Vacuolar Processing Enzyme, VPE, Is Involved in Seed Coat Formation at the Early Stage of Seed Development." *The Plant Cell Online* 17(3):876–87.
- Nguyen, Hong Hanh, Myoung Hui Lee, Kyungyoung Song, Gyeongik Ahn, Jihyeong Lee, and Inhwan Hwang. 2018. "The A / ENTH Domain-Containing Protein AtECA4 Is an Adaptor Protein Involved in Cargo Recycling from the Trans -Golgi Network / Early Endosome to the Plasma Membrane." *Molecular Plant* 11(4):568–83.
- Ni, Jun and Steven E. Clark. 2006. "Evidence for Functional Conservation, Sufficiency, and Proteolytic Processing of the CLAVATA3 CLE Domain." *Plant Physiology* 140(2):726–33.
- Niklas, Karl J. and Stuart A. Newman. 2013. "The Origins of Multicellular Organisms." *Evolution and Development* 15(1):41–52.
- Nover, L., K. Bharti, P. Döring, S. K. Mishra, A. Ganguli, and K. D. Scharf. 2001. "Arabidopsis and the Heat Stress Transcription Factor World: How Many Heat Stress Transcription Factors Do We Need?" *Cell Stress and Chaperones* 6(3):177–89.
- Oparka, K. J., C. M. Duckett, D. A. M. Prior, and D. B. Fisher. 1994. "Real-time Imaging of Phloem Unloading in the Root Tip of Arabidopsis." *The Plant Journal* 6(5):759–66.
- Oparka, Karl J. and Robert Turgeon. 1999. "Sieve Elements and Companion Cells - Traffic Control Centers of the Phloem." *Plant Cell* 11(4):739–50.
- Otero, Sofia, Ykä Helariutta, and Simon Turner. 2016. "Companion Cells: A Diamond in the Rough." *Journal of Experimental Botany* 68(1):71–78.
- Otero, Sofia, Iris Sevilem, Pawel Roszak, Yipeng Lu, Valerio Di Vittori, Lothar Kalmbach, Bernhard Blob, Jung-ok Heo, and Federico Peruzzo. 2021. "An Arabidopsis Root Phloem Pole Cell Atlas Reveals PINEAPPLE Genes as Transitioners to Autotrophy." *BioRxiv* <https://doi.org/10.1101/2021.08.31.458411>
- Overall, Christopher M. and Carl P. Blobel. 2007. "In Search of Partners: Linking Extracellular Proteases to Substrates." *Nature Reviews Molecular Cell Biology* 8(3):245–57.
- Paulus, Judith K. and Renier A. L. Van der Hoorn. 2019. "Do Proteolytic Cascades Exist

References

- in Plants?" *Journal of Experimental Botany*.
- de Pedro-Jové, R., M. Puigvert, P. Sebastià, A. P. Macho, J. S. Monteiro, N. S. Coll, J. C. Setúbal, and M. Valls. 2021. "Dynamic Expression of *Ralstonia Solanacearum* Virulence Factors and Metabolism-Controlling Genes during Plant Infection." *BMC Genomics* 22(1):1–18.
- Perata, Pierdomenico and Amedeo Alpi. 1993. "Plant Responses to Anaerobiosis." *Plant Science* 93(1–2):1–17.
- Perrar, Andreas, Nico Dissmeyer, and Pitter F. Huesgen. 2019. "New Beginnings and New Ends: Methods for Large-Scale Characterization of Protein Termini and Their Use in Plant Biology." *Journal of Experimental Botany* 70(7):2021–38.
- Phee, Bong-kwan, Jeong-il Kim, Dong Ho Shin, Jihye Yoo, Kyoung-jin Park, Yun-jeong Han, and Yong-kook Kwon. 2008. "A Novel Protein Phosphatase Indirectly Regulates Phytochrome-Interacting Factor 3 via Phytochrome." *Biochem. J* 255:247–55.
- Pittermann, J. 2010. "The Evolution of Water Transport in Plants: An Integrated Approach." *Geobiology* 8(2):112–39.
- Planas M., 2014. TFG tesis "Caracterització de la metacaspasa-3 (AtMC3) en els processos de desenvolupament i resposta a patogen", University of Barcelona, Grau de Biotecnologia.
- Planes, María D., Regina Niñoles, Lourdes Rubio, Gaetano Bissoli, Eduardo Bueso, María J. García-, José A. Fernández, and Ramón Serrano. 2015. "A Mechanism of Growth Inhibition by Abscisic Acid in Germinating Seeds of *Arabidopsis Thaliana* Based on Inhibition of Plasma Membrane H⁺-ATPase and Decreased Cytosolic PH_o, K⁺, and Anions." *Journal of Experimental Botany* 66(3):813–25.
- Prerostova, Sylva, Martin Černý, Petre I. Dobrev, Vaclav Motyka, Lucia Hluskova, Barbara Zupkova, Alena Gaudinova, Vojtech Knirsch, Tibor Janda, Bretislav Brzobohatý, and Radomira Vankova. 2021. "Light Regulates the Cytokinin-Dependent Cold Stress Responses in *Arabidopsis*." *Frontiers in Plant Science* 11(February):1–21.
- Putterill, Jo, Rebecca Laurie, and Richard Macknight. 2004. "It's Time to Flower: The Genetic Control of Flowering Time." *BioEssays* 26(4):363–73.
- Quint, Marcel, Carolin Delker, Keara A. Franklin, Philip A. Wigge, Karen J. Halliday, and Martijn Van Zanten. 2016. "Molecular and Genetic Control of Plant Thermomorphogenesis." *Nature Plants* 2(January):1–9.
- Ramachandran, Prashanth, Frauke Augstein, Shamik Mazumdar, Thanh Van Nguyen, Elena A. Minina, Charles W. Melnyk, and Annelie Carlsbecker. 2021. "Abscisic Acid Signaling Activates Distinct VND Transcription Factors to Promote Xylem

References

- Differentiation in Arabidopsis." *Current Biology* 31(14):3153-3161.e5.
- Rappsilber, Juri, Matthias Mann, and Yasushi Ishihama. 2007. "Protocol for Micro-Purification, Enrichment, Pre-Fractionation and Storage of Peptides for Proteomics Using StageTips." *Nature Protocols* 2(8):1896–1906.
- Ratajczak, Rafael. 2000. "Structure, Function and Regulation of the Plant Vacuolar H⁺-Translocating ATPase." *Biochimica et Biophysica Acta - Biomembranes* 1465(1–2):17–36.
- Rautengarten, Carsten, Dirk Steinhauser, Dirk Büssis, Annick Stintzi, Andreas Schaller, Joachim Kopka, and Thomas Altmann. 2005. "Inferring Hypotheses on Functional Relationships of Genes: Analysis of the Arabidopsis Thaliana Subtilase Gene Family." *PLoS Computational Biology* 1(4):0297–0312.
- Raven, J. A. 2003. "Long-Distance Transport in Non-Vascular Plants." *Plant, Cell and Environment* 26: 73–85
- Rawlings, Neil D., Alan J. Barrett, Paul D. Thomas, Xiaosong Huang, Alex Bateman, and Robert D. Finn. 2018. "The MEROPS Database of Proteolytic Enzymes, Their Substrates and Inhibitors in 2017 and a Comparison with Peptidases in the PANTHER Database." *Nucleic Acids Research* 46(D1):D624–32.
- Raz, Vered, Jan H. W. Bergervoet, and Maarten Koornneef. 2001. "Sequential Steps for Developmental Arrest in Arabidopsis Seeds." 252:243–52.
- Rodriguez-Villalon, Antia, Bojan Gujas, Yeon Hee Kang, Alice S. Breda, Pietro Cattaneo, Stephen Depuydt, and Christian S. Hardtke. 2014. "Molecular Genetic Framework for Protophloem Formation." *Proceedings of the National Academy of Sciences of the United States of America* 111(31):11551–56.
- Rodriguez-Villalon, Antia, Bojan Gujas, Ringo van Wijk, Teun Munnik, and Christian S. Hardtke. 2015. "Primary Root Protophloem Differentiation Requires Balanced Phosphatidylinositol-4,5-Biphosphate Levels and Systemically Affects Root Branching." *Development (Cambridge)* 142(8):1437–46.
- Rogers, Hilary J. 2006. "Programmed Cell Death in Floral Organs: How and Why Do Flowers Die?" *Annals of Botany* 97(3):309–15.
- Rojas-Murcia, Nelson, Kian Hématy, Yuree Lee, Aurélie Emonet, Robertas Ursache, Satoshi Fujita, Damien de Bellis, and Niko Geldner. 2020. "High-Order Mutants Reveal an Essential Requirement for Peroxidases but Not Laccases in Casparian Strip Lignification." *Proceedings of the National Academy of Sciences of the United States of America* 117(46):29166–77.
- Ross-Elliott, Timothy J., Kaare H. Jensen, Katrine S. Haaning, Brittney M. Wager, Jan Knoblauch, Alexander H. Howell, Daniel L. Mullendore, Alexander G. Monteith,

References

- Danae Paultre, Dawei Yan, Sofia Otero, Matthieu Bourdon, Ross Sager, Jung Youn Lee, Ykä Helariutta, Michael Knoblauch, and Karl J. Oparka. 2017. "Phloem Unloading in Arabidopsis Roots Is Convective and Regulated by the Phloempole Pericycle." *ELife* 6:1–31.
- Rozsak, Pawel, Jung-ok Heo, Bernhard Blob, Koichi Toyokura, Maria Angels de Luis Balaguer, Winnie Lau, Fiona Hamey, Jacopo Cirrone, Xin Wang, Robertas Ursache, Hugo Tavares, Kevin Verstaen, Jos Wendrich, Charles Melnyk, Dennis Shasha, Sebastian E. Ahnert, Yvan Saeys, Bert De Rybel, Heidstra Renze, Ben Scheres, Ari Pekka Mähönen, Berthold Göttgens, Rosangela Sozzani, Kenneth Birnbaum, and Yrjö Helariutta. 2021. "Analysis of Phloem Trajectory Links Tissue Maturation to Cell Specialization." *BioRxiv* 1–38.
- Ruiz Sola, M. Aguila, Mario Coiro, Simona Crivelli, Samuel C. Zeeman, Signe Schmidt Kjølner Hansen, and Elisabeth Truernit. 2017. "OCTOPUS-LIKE 2, a Novel Player in Arabidopsis Root and Vascular Development, Reveals a Key Role for OCTOPUS Family Genes in Root Metaphloem Sieve Tube Differentiation." *New Phytologist* 216(4):1191–1204.
- De Rybel, Bert, Ari Pekka Mähönen, Yrjö Helariutta, and Dolf Weijers. 2016. "Plant Vascular Development: From Early Specification to Differentiation." *Nature Reviews Molecular Cell Biology* 17(1):30–40.
- Ryu, Kook Hui, Ling Huang, Hyun Min Kang, and John Schiefelbein. 2019. "Single-Cell RNA Sequencing Resolves Molecular Relationships among Individual Plant Cells." *Plant Physiology* 179(4):1444–56.
- Saito, Masato, Yuki Kondo, and Hiroo Fukuda. 2018. "BES1 and BZR1 Redundantly Promote Phloem and Xylem Differentiation." *Plant and Cell Physiology* 59(3):590–600.
- Salguero-Linares, Jose and Núria S. Coll. 2019. "Plant Proteases in the Control of the Hypersensitive Response." *Journal of Experimental Botany* 70(7):2087–95.
- Salvesen, Guy S., Anne Hempel, and Nuria S. Coll. 2016. "Protease Signaling in Animal and Plant-Regulated Cell Death." *FEBS Journal* 2577–98.
- Satoh, Rie, Yasunari Fujita, Kazuo Nakashima, Kazuo Shinozaki, and Kazuko Yamaguchi-Shinozaki. 2004. "A Novel Subgroup of BZIP Proteins Functions as Transcriptional Activators in Hypoosmolarity-Responsive Expression of the ProDH Gene in Arabidopsis." *Plant and Cell Physiology* 45(3):309–17.
- Savickas, Simonas, Philipp Kastl, and Ulrich auf dem Keller. 2020. "Combinatorial Degradomics: Precision Tools to Unveil Proteolytic Processes in Biological Systems." *Biochimica et Biophysica Acta - Proteins and Proteomics*

References

- 1868(6):140392.
- Scacchi, Emanuele, Karen S. Osmont, Julien Beuchat, Paula Salinas, Marisa Navarrete-Gómez, Marina Trigueros, Cristina Ferrándiz, and Christian S. Hardtke. 2009. "Dynamic, Auxin-Responsive Plasma Membrane-to-Nucleus Movement of Arabidopsis BRX." *Development* 136(12):2059–67.
- Schachtman, Daniel P., Julian I. Schroeder, William J. Lucas, Julie A. Anderson, and Richard F. Gaber. 1992. "Expression of an Inward-Rectifying Potassium Channel by the Arabidopsis KAT1 CDNA." *Science* 258(5088):1654–58.
- Schaeffer, A., R. Bronner, P. Benveniste, and H. Schaller. 2001. "The Ratio of Campesterol to Sitosterol That Modulates Growth in Arabidopsis Is Controlled by STEROL METHYLTRANSFERASE 2;l." *Plant Journal* 25(6):605–15.
- Schardon, Katharina, Mathias Hohl, Lucile Graff, Jens Pfannstiel, Waltraud Sculze, Annick Stintzi, and Andreas Schaller. 2016. "Precursor Processing for Plant Peptide Hormone Maturation by Subtilisin-like Serine Proteinases." *Science* 8550(December):1–9.
- Schindelin, Johannes, Ignacio Arganda-Carrera, Erwin Frise, Kaynig Verena, Longair Mark, Pietzsch Tobias, Preibisch Stephan, Rueden Curtis, Saalfeld Stephan, Schmid Benjamin, Tinevez Jean-Yves, James White Daniel, Hartenstein Volker, Eliceiri Kevin, Tomancak Pavel, and Cardona Albert. 2009. "Fiji - an Open Platform for Biological Image Analysis." *Nature Methods* 9(7).
- Sedbrook, John C., Kathleen L. Carroll, Kai F. Hung, Patrick H. Masson, and Chris R. Somerville. 2002. "The Arabidopsis SKU5 Gene Encodes an Extracellular Glycosyl Phosphatidylinositol-Anchored Glycoprotein Involved in Directional Root Growth." *Plant Cell* 14(7):1635–48.
- Shabala, Sergey, Jayakumar Bose, Anja Thoe Fuglsang, and Igor Pottosin. 2016. "On a Quest for Stress Tolerance Genes: Membrane Transporters in Sensing and Adapting to Hostile Soils." *Journal of Experimental Botany* 67(4):1015–31.
- Shen, Wenzhong, Jiuer Liu, and Jian Feng Li. 2019. "Type-II Metacaspases Mediate the Processing of Plant Elicitor Peptides in Arabidopsis." *Molecular Plant* 12(11):1524–33.
- Shi, Haitao, Wen Liu, Yue Yao, Yunxie Wei, and Zhulong Chan. 2017. "Alcohol Dehydrogenase 1 (ADH1) Confers Both Abiotic and Biotic Stress Resistance in Arabidopsis." *Plant Science* 262:24–31.
- Shim, Jae Sung, Akane Kubota, and Takato Imaizumi. 2017. "Circadian Clock and Photoperiodic Flowering in Arabidopsis: CONSTANS Is a Hub for Signal Integration." *Plant Physiology* 173(1):5–15.

References

- Shimizu, Hanako, Kana Katayama, Tomoko Koto, Kotaro Torii, Takashi Araki, and Motomu Endo. 2015. "Decentralized Circadian Clocks Process Thermal and Photoperiodic Cues in Specific Tissues." *Nature Plants* 1(November):1–6.
- Shu, Kai, Xiaofeng Luo, Yongjie Meng, and Wenyu Yang. 2018. "Toward a Molecular Understanding of Abscisic Acid Actions in Floral Transition." *Plant and Cell Physiology* 59(2):215–21.
- Shulse, Christine N., Benjamin J. Cole, Doina Ciobanu, Junyan Lin, Yuko Yoshinaga, Mona Gouran, Gina M. Turco, Yiwen Zhu, Ronan C. O'Malley, Siobhan M. Brady, and Diane E. Dickel. 2019. "High-Throughput Single-Cell Transcriptome Profiling of Plant Cell Types." *Cell Reports* 27(7):2241-2247.e4.
- Sjölund, Richard D. 1997. "The Phloem Sieve Element: A River Runs through It." *Plant Cell* 9(7):1137–46.
- Smertenko, A. and V. E. Franklin-Tong. 2011. "Organisation and Regulation of the Cytoskeleton in Plant Programmed Cell Death." *Cell Death and Differentiation* 18(8):1263–70.
- Smertenko, Andrei and Peter V. Bozhkov. 2014. "Somatic Embryogenesis: Life and Death Processes during Apical-Basal Patterning." *Journal of Experimental Botany* 65(5):1343–60.
- Smit, Margot E., Cristina I. Llavata-Peris, Mark Roosjen, Henriette van Beijnum, Daria Novikova, Victor Levitsky, Iris Sevilem, Pawel Roszak, Daniel Slane, Gerd Jürgens, Victoria Mironova, Siobhan M. Brady, and Dolf Weijers. 2020. "Specification and Regulation of Vascular Tissue Identity in the Arabidopsis Embryo." *Development (Cambridge)* 147(8).
- Song, Young Hun, Jae Sung Shim, Hannah A. Kinmonth-Schultz, and Takato Imaizumi. 2015. "Photoperiodic Flowering: Time Measurement Mechanisms in Leaves." *Annual Review of Plant Biology* 66:441–64.
- Song, Yuwei, Fuyou Xiang, Guozeng Zhang, Yuchen Miao, and Chen Miao. 2016. "Abscisic Acid as an Internal Integrator of Multiple Physiological Processes Modulates Leaf Senescence Onset in Arabidopsis Thaliana." *Frontiers in Plant Science* 7:1–16.
- Staes, An, Petra Van Damme, Kenny Helsens, Hans Demol, Joël Vandekerckhove, and Kris Gevaert. 2008. "Improved Recovery of Proteome-Informative, Protein N-Terminal Peptides by Combined Fractional Diagonal Chromatography (COFRADIC)." *Proteomics* 8(7):1362–70.
- Stührwohldt, Nils, Eric Bühler, Margret Sauter, and Andreas Schaller. 2021. "Phytosulfokine (PSK) Precursor Processing by Subtilase SBT3.8 and PSK

References

- Signaling Improve Drought Stress Tolerance in Arabidopsis." *Journal of Experimental Botany* 72(9):3427–3440.
- Suarez, Maria F., Lada H. Filonova, Andrei Smertenko, Eugene I. Savenkov, David H. Clapham, Sara von Arnold, Boris Zhivotovsky, and Peter V. Bozhkov. 2004. "Metacaspase-Dependent Programmed Cell Death Is Essential for Plant Embryogenesis." *Current Biology* 14(9):R339–40.
- Sun, Li Rong, Yi Bin Wang, Shi Bin He, Fu Shun Hao, Li Rong Sun, Yi Bin Wang, Shi Bin He, and Fu Shun Hao. 2018. "Mechanisms for Abscisic Acid Inhibition of Primary Root Growth Mechanisms for Abscisic Acid Inhibition of Primary Root Growth." *Plant Signaling & Behavior* 13(9):1–4.
- Sun, Xi, Yu Wang, and Na Sui. 2018. "Transcriptional Regulation of BHLH during Plant Response to Stress." *Biochemical and Biophysical Research Communications* 503(2):397–401.
- Takahashi, Fuminori, Takehiro Suzuki, Yuriko Osakabe, Shigeyuki Betsuyaku, Yuki Kondo, Naoshi Dohmae, Hiroo Fukuda, Kazuko Yamaguchi-Shinozaki, and Kazuo Shinozaki. 2018. "A Small Peptide Modulates Stomatal Control via Abscisic Acid in Long-Distance Signaling." *Nature* 556(7700):235–38.
- Takahashi, Yohei, Jingbo Zhang, Po Kai Hsu, Paulo H. O. Ceciliato, Li Zhang, Guillaume Dubeaux, Shintaro Munemasa, Chennan Ge, Yunde Zhao, Felix Hauser, and Julian I. Schroeder. 2020. "MAP3Kinase-Dependent SnRK2-Kinase Activation Is Required for Abscisic Acid Signal Transduction and Rapid Osmotic Stress Response." *Nature Communications* 11(1).
- Tamaki, Takayuki, Satoyo Oya, Makiko Naito, Yasuko Ozawa, Tomoyuki Furuya, Masato Saito, Mayuko Sato, Mayumi Wakazaki, Kiminori Toyooka, Hiroo Fukuda, Ykä Helariutta, and Yuki Kondo. 2020. "VISUAL-CC System Uncovers the Role of GSK3 as an Orchestrator of Vascular Cell Type Ratio in Plants." *Communications Biology* 3(1):1–9.
- Tang, Yulin, Rong He, Jian Zhao, Guangli Nie, Lina Xu, and Baoshan Xing. 2016. "Oxidative Stress-Induced Toxicity of CuO Nanoparticles and Related Toxicogenomic Responses in Arabidopsis Thaliana." *Environmental Pollution* 212:605–14.
- Thalman, Matthias and Diana Santelia. 2017. "Starch as a Determinant of Plant Fitness under Abiotic Stress." *New Phytologist* 214(3):943–51.
- Till, Bradley J., Steven H. Reynolds, Elizabeth A. Greene, Christine A. Codomo, Linda C. Enns, Jessica E. Johnson, Chris Burtler, Anthony R. Odden, Kim Young, Nicholas E. Taylor, Jorja G. Henikoff, Luca Comai, and Steven Henikoff. 2003. "Large-Scale

References

- Discovery of Induced Point Mutations with High-Throughput TILLING." *Genome Research* 13(3):524–30.
- Ton, Jurriaan and Brigitte Mauch-Mani. 2004. "β-Amino-Butyric Acid-Induced Resistance against Necrotrophic Pathogens Is Based on ABA-Dependent Priming for Callose." *Plant Journal* 38(1):119–30.
- De Torres-Zabala, Marta, William Truman, Mark H. Bennett, Guillaume Lafforgue, John W. Mansfield, Pedro Rodriguez Egea, Laszlo Bögre, and Murray Grant. 2007. "Pseudomonas Syringae Pv. Tomato Hijacks the Arabidopsis Abscisic Acid Signalling Pathway to Cause Disease." *EMBO Journal* 26(5):1434–43.
- Trobacher, Christopher P. 2009. "Ethylene and Programmed Cell Death in Plants." *Botany* 87(8):757–69.
- Truernit, Elisabeth, H el ene Bauby, Katia Belcram, Julien Barth el emy, and Jean Christophe Palauqui. 2012. "OCTOPUS, a Polarly Localised Membrane-Associated Protein, Regulates Phloem Differentiation Entry in Arabidopsis Thaliana." *Development* 139(7):1306–15.
- Tsiatsiani, L., F. Van Breusegem, P. Gallois, A. Zavalov, E. Lam, and P. V. Bozhkov. 2011. "Metacaspases." *Cell Death and Differentiation* 18(8):1279–88.
- Tsiatsiani, L., E. Timmerman, P. J. De Bock, D. Vercammen, S. Stael, B. van de Cotte, A. Staes, M. Goethals, T. Beunens, P. Van Damme, K. Gevaert, and F. Van Breusegem. 2013. "The Arabidopsis METACASPASE9 Degrads." *The Plant Cell* 25(8):2831–47.
- Tsuwamoto, Ryo and Takeo Harada. 2011. "The Arabidopsis COR13 Promoter Contains Two Cis-Acting Regulatory Regions Required for Transcriptional Activity in Companion Cells." *Plant Cell Reports* 30(9):1723–33.
- Tuteja, Narendra. 2007. "Abscisic Acid and Abiotic Stress Signaling." *Plant Signaling and Behavior* 2(3):135–38.
- Tyanova, Stefka, Tikira Temu, and Juergen Cox. 2016. "The MaxQuant Computational Platform for Mass Spectrometry-Based Shotgun Proteomics." *Nature Protocols* 11(12):2301–19.
- Tyanova, Stefka, Tikira Temu, Pavel Sinitcyn, Arthur Carlson, Marco Y. Hein, Tamar Geiger, Matthias Mann, and J urgen Cox. 2016. "The Perseus Computational Platform for Comprehensive Analysis of (Prote)Omics Data." *Nature Methods* 13(9):731–40.
- Ueda, Yoshiaki, Shahid Siddique, and Michael Frei. 2015. "A Novel Gene, OZONE-RESPONSIVE APOPLASTIC PROTEIN1, Enhances Cell Death in Ozone Stress in Rice." *Plant Physiology* 169(1):873–89.

References

- Uren, Anthony G., Karen O'Rourke, L. Aravind, M. Teresa Pisabarro, Somasekar Seshagiri, Eugene V. Koonin, and Vishva M. Dixit. 2000. "Identification of Paracaspases and Metacaspases: Two Ancient Families of Caspase-like Proteins, One of Which Plays a Key Role in MALT Lymphoma." *Molecular Cell* 6(4):961–67.
- Ventura, Irene, Luca Brunello, Sergio Iacopino, Maria Cristina Valeri, Giacomo Novi, Tino Dornbusch, Pierdomenico Perata, and Elena Loreti. 2020. "Arabidopsis Phenotyping Reveals the Importance of Alcohol Dehydrogenase and Pyruvate Decarboxylase for Aerobic Plant Growth." *Scientific Reports* 10(1):1–14.
- Vercammen, Dominique, Brigitte Van De Cotte, Geert De Jaeger, Dominique Eeckhout, Peter Casteels, Klaas Vandepoele, Isabel Vandenberghe, Jozef Van Beeumen, Dirk Inzé, and Frank Van Breusegem. 2004. "Type II Metacaspases Atmc4 and Atmc9 of Arabidopsis Thaliana Cleave Substrates after Arginine and Lysine." *Journal of Biological Chemistry* 279(44):45329–36.
- Vishwakarma, Kanchan, Neha Upadhyay, Nitin Kumar, Gaurav Yadav, Jaspreet Singh, Rohit K. Mishra, Vivek Kumar, Rishi Verma, R. G. Upadhyay, Mayank Pandey, and Shivesh Sharma. 2017. "Abscisic Acid Signaling and Abiotic Stress Tolerance in Plants: A Review on Current Knowledge and Future Prospects." *Frontiers in Plant Science* 8:1–12.
- Voinnet, Olivier, Susana Rivas, Pere Mestre, and David Baulcombe. 2003. "An Enhanced Transient Expression System in Plants Based on Suppression of Gene Silencing by the P19 Protein of Tomato Bushy Stunt Virus." *The Plant Journal* 949–56.
- Wallner, Eva Sophie, Vadir López-Salmerón, Ilya Belevich, Gernot Poschet, Ilona Jung, Karin Grünwald, Iris Sevillem, Eija Jokitalo, Rüdiger Hell, Yrjö Helariutta, Javier Agustí, Ivan Lebovka, and Thomas Greb. 2017. "Strigolactone- and Karrikin-Independent SMXL Proteins Are Central Regulators of Phloem Formation." *Current Biology* 27(8):1241–47.
- Wang, Qianqian, Qianli Guo, Yuanyuan Guo, Jieshu Yang, Min Wang, Xiaoke Duan, Jiayu Niu, Shuai Liu, Jianzhen Zhang, Yanke Lu, Zhi Hou, Wei Miao, Xiangyu Wang, Weiwen Kong, Xiaoming Xu, Yufeng Wu, Qi Rui, and Honggui La. 2018. "Arabidopsis Subtilase SASP Is Involved in the Regulation of ABA Signaling and Drought Tolerance by Interacting with OPEN STOMATA 1." *Journal of Experimental Botany* 69(18):4403–17.
- Wang, Xiaodong, Xiaojie Wang, Hao Feng, Chunlei Tang, Pengfei Bai, Guorong Wei, Lili Huang, and Zhensheng Kang. 2012. "TaMCA4, a Novel Wheat Metacaspase Gene Functions in Programmed Cell Death Induced by the Fungal Pathogen Puccinia Striiformis f. Sp. Triticum." *MPMI* 25(6):755–64.

References

- Watanabe, Naohide and Eric Lam. 2005. "Two Arabidopsis Metacaspases AtMCP1b and AtMCP2b Are Arginine/Lysine- Specific Cysteine Proteases and Activate Apoptosis-like Cell Death in Yeast." *Journal of Biological Chemistry* 280(15):14691–99.
- Watanabe, Naohide and Eric Lam. 2011. "Arabidopsis Metacaspase 2d Is a Positive Mediator of Cell Death Induced during Biotic and Abiotic Stresses." *Plant Journal* 66(6):969–82.
- Weichert, Annett, Christopher Brinkmann, Nataliya Y. Komarova, Kathrin Thor, Stefan Meier, Marianne Suter Grottemeyer, Doris. 2012. "AtPTR4 and AtPTR6 Are Differentially Expressed, Tonoplast-Localized Members of the Peptide Transporter/Transporter 1 (PTR/NRT) family." *Planta* 235(2):311–23.
- Weigel, Detlef and Gerd Jürgens. 2002. "Stem Cells That Make Stems." *Nature* 415(6873):751–54.
- Weits, Daan A., Beatrice Giuntoli, Monika Kosmacz, Sandro Parlanti, Hans Michael Hubberten, Heike Riegler, Rainer Hoefgen, Pierdomenico Perata, Joost T. Van Dongen, and Francesco Licausi. 2014. "Plant Cysteine Oxidases Control the Oxygen-Dependent Branch of the N-End-Rule Pathway." *Nature Communications* 5.
- Wendrich, Jos R., Bao Jun Yang, Niels Vandamme, Kevin Verstaen, Wouter Smet, Celien Van de Velde, Max Minne, Brecht Wybouw, Eliana Mor, Helena E. Arents, Jonah Nolf, Julie van Duyse, Gert van Isterdael, Steven Maere, Yvan Saeys, and Bert De Rybel. 2020. "Vascular Transcription Factors Guide Plant Epidermal Responses to Limiting Phosphate Conditions." *Science* 370(6518).
- Weng, Samuel S.H., Fatih Demir, Enes K. Ergin, Sabrina Dirnberger, Anuli Uzozie, Domenic Tuscher, Lorenz Nierves, Janice Tsui, Pitter F. Huesgen, and Philipp F. Lange. 2019. "Sensitive Determination of Proteolytic Proteoforms in Limited Microscale Proteome Samples." *Molecular and Cellular Proteomics* 18(11):2335–47.
- Wessel, D. and U. I. Flügge. 1984. "A Method for the Quantitative Recovery of Protein in Dilute Solution in the Presence of Detergents and Lipids." *Analytical Biochemistry* 138(1):141–43.
- Wilkins, Katie A., Maurice Bosch, Tamanna Haque, Nianjun Teng, Natalie S. Poulter, and Veronica E. Franklin-Tong. 2015. "Self-Incompatibility-Induced Programmed Cell Death in Field Poppy Pollen Involves Dramatic Acidification of the Incompatible Pollen Tube Cytosol." *Plant Physiology* 167(3):766–79.
- Wrzaczek, M., J. P. Vainonen, S. Stael, L. Tsiatsiani, H. Help-Rinta-Rahko, A. Gauthier, D. Kaufholdt, B. Bollhoner, A. Lamminmaki, A. Staes, K. Gevaert, H. Tuominen, F.

References

- Van Breusegem, Y., Helariutta, and J. Kangasjarvi. 2014. "GRIM REAPER Peptide Binds to Receptor Kinase PRK5 to Trigger Cell Death in Arabidopsis." *The EMBO Journal* 34(1):55–66.
- Wu, Xiaomeng, Zhu Qiao, Huiping Liu, Biswa R. Acharya, Chunlong Li, and Wei Zhang. 2017. "CML20, an Arabidopsis Calmodulin-like Protein, Negatively Regulates Guard Cell ABA Signaling and Drought Stress Tolerance." *Frontiers in Plant Science* 8(May):1–12.
- Xie, Bo, Xiaomin Wang, Maosheng Zhu, Zhongming Zhang, and Zonglie Hong. 2011. "CalS7 Encodes a Callose Synthase Responsible for Callose Deposition in the Phloem." *Plant Journal* (1):1–14.
- Yang, Jianyi, Renxiang Yan, Ambrish Roy, Dong Xu, Jonathan Poisson, and Yang Zhang. 2015. "Correspondence The I-TASSER Suite: Protein Structure and Function Prediction A." *Nature Publishing Group* 12(1):7–8.
- Yao, Xuan, Wei Xiong, Tiantian Ye, and Yan Wu. 2012. "Overexpression of the Aspartic Protease ASPG1 Gene Confers Drought Avoidance in Arabidopsis." *Journal of Experimental Botany* 63(7):2579–93.
- Yoo, Soo Cheul, Cheng Chen, Maria Rojas, Yasufumi Daimon, Byung Kook Ham, Takashi Araki, and William J. Lucas. 2013. "Phloem Long-Distance Delivery of FLOWERING LOCUS T (FT) to the Apex." *Plant Journal* 75(3):456–68.
- Yoshida, Takuya, Toshihiro Obata, Regina Feil, John E. Lunn, Yasunari Fujita, Kazuko Yamaguchi-Shinozaki, and Alisdair R. Fernie. 2019. "The Role of Abscisic Acid Signaling in Maintaining the Metabolic Balance Required for Arabidopsis Growth under Nonstress Conditions." *Plant Cell* 31(1):84–105.
- Zauner, Florian B., Brigitta Elsässer, Elfriede Dall, Chiara Cabrele, and Hans Brandstetter. 2018. "Structural Analyses of Arabidopsis Thaliana Legumain Reveal Differential Recognition and Processing of Proteolysis and Ligation Substrates." *Journal of Biological Chemistry* 293(23):8934–46.
- Van Zelm, Eva, Yanxia Zhang, and Christa Testerink. 2020. "Salt Tolerance Mechanisms of Plants." *Annual Review of Plant Biology* 71:403–33.
- Zhang, Changqing, Roger A. Barthelson, Georgina M. Lambert, and David W. Galbraith. 2008. "Global Characterization of Cell-Specific Gene Expression through Fluorescence-Activated Sorting of Nuclei." *Plant Physiology* 147(1):30–40.
- Zhang, Dandan, Di Liu, Xiaomeng Lv, Ying Wang, Zhili Xun, Zhixiong Liu, Fenglan Li, and Hai Lu. 2014. "The Cysteine Protease CEP1, a Key Executor Involved in Tapetal Programmed Cell Death, Regulates Pollen Development in Arabidopsis." *Plant Cell* 26(7):2939–61.

References

- Zhang, Lizhi, Qiumin Tan, Raymond Lee, Alexander Trethewy, Yong Hwa Lee, and Mechthild Tegeder. 2010. "Altered Xylem-Phloem Transfer of Amino Acids Affects Metabolism and Leads to Increased Seed Yield and Oil Content in Arabidopsis." *Plant Cell* 22(11):3603–20.
- Zhang, Tian Qi, Zhou Geng Xu, Guan Dong Shang, and Jia Wei Wang. 2019. "A Single-Cell RNA Sequencing Profiles the Developmental Landscape of Arabidopsis Root." *Molecular Plant* 12(5):648–60.
- Zhang, Xiuren, Rossana Henriques, Shih Shun Lin, Qi Wen Niu, and Nam Hai Chua. 2006. "Agrobacterium-Mediated Transformation of Arabidopsis Thaliana Using the Floral Dip Method." *Nature Protocols* 1(2):641–46.
- Zhang, Yi and Eric Lam. 2011. "Sheathing the Swords of Death: Post-Translational Modulation of Plant Metacaspases." *Plant Signaling and Behavior* 6(12):2051–56.
- Zhang, Zhihui, Yani Lv, Zhuqing Zhou, Fangzhu Mei, and Likai Wang. 2017. "Type II Metacaspase Protein Localization and Gene Transcription during Programmed Cell Semi-Death of Sieve Elements in Developing Caryopsis of *Tritium Aestivum*." *Biologia (Poland)* 72(4):398–406.
- Zhao, Chengsong, Johanna C. Craig, H. Earl Petzold, Allan W. Dickerman, and Eric P. Beers. 2005. "The Xylem and Phloem Transcriptomes from Secondary Tissues of the Arabidopsis Root-Hypocotyl." *Plant Physiology* 138(2):803–18.
- Zhao, Cuizhu, Huijuan Wang, Yao Lu, Jinxue Hu, Ling Qu, Zheqing Li, Dongdong Wang, Yizhe He, Marc Valls, Núria S. Coll, Qin Chen, and Haibin Lu. 2019. "Deep Sequencing Reveals Early Reprogramming of Arabidopsis Root Transcriptomes upon *Ralstonia Solanacearum* Infection." *Molecular Plant-Microbe Interactions* 31(7):813–27.
- Zhou, Liang Zi, Timo Höwing, Benedikt Müller, Ulrich Z. Hammes, Christine Gietl, and Thomas Dresselhaus. 2016. "Expression Analysis of KDEL-CysEPs Programmed Cell Death Markers during Reproduction in Arabidopsis." *Plant Reproduction* 29(3):265–72.
- Zhu, Ping, Xiao Hong Yu, Cheng Wang, Qingfang Zhang, Wu Liu, Sean McSweeney, John Shanklin, Eric Lam, and Qun Liu. 2020. "Structural Basis for Ca²⁺-Dependent Activation of a Plant Metacaspase." *Nature Communications* 11(1):1–9.
- Zhu, Yang, Lu Liu, Lisha Shen, and Hao Yu. 2016. "NaKR1 Regulates Long-Distance Movement of FLOWERING LOCUS T in Arabidopsis." *Nature Plants* 2, 16075 .

ANNEX

PART 1

At-gRNA-U6 backbone#1 seq

attB (1 to 31), U6 promoter (38 to 350), N20 sequence (351 to 370) tracrRNA (371 to 463), attB (470 to 499). Target sequence in the gene is in bold letters, BamH1 site at position 32, Sal1 site at position 464.

```
ggggacaagttgtacaaaaaagcaggcttcGGATCCTTTTCTTCTTTTTAACTTTCCATT
CGGAGTTTTTGTATCTTGTTTCATAGTTTGTCCCAGGATTAGAATGATTAGG
CATCGAACCTTCAAGAATTTGATTGAATAAAACATCTTCATTCTTAAGATAT
GAAGATAATCTTCAAAAGGCCCTGGGAATCTGAAAGAAGAGAAGCAGGC
CCATTTATATGGGAAAGAACAATAGTATTTCTTATATAGGCCCATTTAAGTT
GAAAACAATCTTCAAAAGTCCCACATCGCTTAGATAAGAAAACGAAGCTGA
GTTTATATACAGCTAGAGTCGAAGTAGTGATTgGGCTAGTCGGAGAGAAGT
AGTTTAAGAGCTATGCTGGAAACAGCATAGCAAGTTTAAATAAGGCTAGTC
CGTTATCAACTTGAAAAAGTGGCACCGAGTCGGTGCTTTTTTTGTGCGACgac
ccagcttctgtacaaagtgtgtcccc
```

At-gRNA-U6 backbone#2 seq

attB (1 to 31), U6 promoter (32 to 344), N20 sequence (345 to 364) tracrRNA (365 to 457), attB (464 to 493). Target sequence in the gene is in bold letters, BamH1 site at position 458.

```
ggggacaagttgtacaaaaaagcaggcttcTTTTCTTCTTTTTAACTTTCCATTCCGGAGT
TTTTGTATCTTGTTTCATAGTTTGTCCCAGGATTAGAATGATTAGGCATCGA
ACCTTCAAGAATTTGATTGAATAAAACATCTTCATTCTTAAGATATGAAGATA
ATCTTCAAAAGGCCCTGGGAATCTGAAAGAAGAGAAGCAGGCCCATTTAT
ATGGGAAAGAACAATAGTATTTCTTATATAGGCCCATTTAAGTTGAAAACAA
TCTTCAAAAGTCCCACATCGCTTAGATAAGAAAACGAAGCTGAGTTTATATA
CAGCTAGAGTCGAAGTAGTGATTgTGTTCTTCCCCGTGAACACGTTAAGA
GCTATGCTGGAAACAGCATAGCAAGTTTAAATAAGGCTAGTCCGTTATCAA
CTTGAAAAAGTGGCACCGAGTCGGTGCTTTTTTTGGATCCgaccagcttctgtga
caaagtgtgtcccc
```

At-gRNA-U6 backbone#2 seq

attB (1 to 31), U6 promoter (38 to 350), N20 sequence (351 to 370) tracrRNA (371 to 463), attB (464 to 493). Target sequence in the gene is in bold letters, Sal1 site at position 32.

ggggacaagttgtacaaaaagcaggcttcGTCGACTTTTCTTCTTTTTAACTTTCCATT
CGGAGTTTTGTATCTTGTTTCATAGTTTGTCCCAGGATTAGAATGATTAGG
CATCGAACCTTCAAGAATTTGATTGAATAAAACATCTTCATTCTTAAGATAT
GAAGATAATCTTCAAAAGGCCCTGGGAATCTGAAAGAAGAGAAGCAGGC
CCATTTATATGGGAAAGAACAATAGTATTTCTTATATAGGCCCATTTAAGTT
GAAAACAATCTTCAAAAGTCCCACATCGCTTAGATAAGAAAACGAAGCTGA
GTTTATATACAGCTAGAGTCGAAGTAGTGATTg**TCATCGACGCCTGTAACA**
GGTTTAAGAGCTATGCTGGAAACAGCATAGCAAGTTTAAATAAGGCTAGTC
CGTTATCAACTTGAAAAAGTGGCACCGAGTCGGTGCTTTTTTTgaccagctttct
tgtacaaagtgggtcccc

PART 2

List of mutation for AtMC3 obtained in the TILLING UC-Davis project:

Individual Stock	Sequence Obtain Stock	Effect	SIFT (IC)	Zygosity
i175E2 12012	g744r ABRC Stock CS92923	G175E	0.00 (3.05)	Hetero
i179C6 12318	g1119r ABRC Stock CS93223	S273N	0.01 (3.04)	Hetero
i180H7 12411	g1106r ABRC Stock CS93309	A269T	0.06 (3.05)	Hetero
i185A6 9800	c983y ABRC Stock CS92063	Intron		Hetero
i187C6 14089	g768r ABRC Stock CS93645	G183E	0.00 (3.05)	Hetero
i187D2 14013	c1001y ABRC Stock CS93614	Intron		Hetero
i189F7 14441	g1359r ABRC Stock CS93802	R324Q	0.03 (3.05)	Hetero
i201F5 17039	c785m ABRC Stock CS94675	Q189K	0.03 (3.05)	Hetero
i201H6 17050	c533y ABRC Stock CS94685	L134=		Hetero
i207B5 17482	g744a ABRC Stock CS95066	G175E		Homo
i208A7 17565	c925y ABRC Stock CS95146	V235=		Hetero
i209F2 17596	c841y ABRC Stock CS95176	D207=		Hetero

Cell Death in Plant Immunity

Eugenia Pitsili,¹ Ujjal J. Phukan,¹ and Nuria S. Coll

Centre for Research in Agricultural Genomics (CRAG), CSIC-IRTA-UAB-UB, Bellaterra 08193, Barcelona, Spain

Correspondence: nuria.sanchez-coll@cragenomica.es



Pathogen recognition by the plant immune system leads to defense responses that are often accompanied by a form of regulated cell death known as the hypersensitive response (HR). HR shares some features with regulated necrosis observed in animals. Genetically, HR can be uncoupled from local defense responses at the site of infection and its role in immunity may be to activate systemic responses in distal parts of the organism. Recent advances in the field reveal conserved cell death-specific signaling modules that are assembled by immune receptors in response to pathogen-derived effectors. The structural elucidation of the plant resistosome—an inflammasome-like structure that may attach to the plasma membrane on activation—opens the possibility that HR cell death is mediated by the formation of pores at the plasma membrane. Necrotrophic pathogens that feed on dead tissue have evolved strategies to trigger the HR cell death pathway as a survival strategy. Ectopic activation of immunomodulators during autoimmune reactions can also promote HR cell death. In this perspective, we discuss the role and regulation of HR in these different contexts.

To detect potential invaders and respond appropriately, plants have evolved a complex and fine-tuned immune system. Current models have both extracellular and intracellular plant immune receptors initiating signaling cascades in response to invasion (Cook et al. 2015). In turn, potential invaders have developed diverse virulence strategies to evade or subvert plant immunity.

A form of regulated cell death known as the hypersensitive response (HR) is a frequent consequence of pathogen recognition by the plant immune system. The term hypersensitivity stems from the abnormally rapid death of plant cells encountering biotrophic pathogens, which rely on plant living tissue for their survival (Stakman 1915). HR can be manipulated genet-

ically and is under tight control to avoid runaway cell death beyond the site of infection. HR cell death resembles forms of regulated necrosis in mammals, such as necroptosis and pyroptosis, but it also features some apoptosis-like traits (Vanden et al. 2014; Dickman et al. 2017; Galluzzi et al. 2018; Salguero-Linares and Coll 2019). Cell contents leaked during HR cell death may alert other cells to a potential invasion.

HR cell death has been studied mostly in the context of plant defense against biotrophic pathogens or hemibiotrophic pathogens, the latter having an initial biotrophic phase followed by a necrotrophic phase. However, necrotrophic pathogens that feed on dead or dying tissue can hijack HR cell death for their own benefit. Here, we provide a perspective on HR cell death

¹These authors contributed equally to this work.

Editors: Kim Newton, James M. Murphy, and Edward A. Miao

Additional Perspectives on Cell Survival and Cell Death available at www.cshperspectives.org

Copyright © 2019 Cold Spring Harbor Laboratory Press; all rights reserved

Advanced Online Article. Cite this article as *Cold Spring Harb Perspect Biol* doi: 10.1101/cshperspect.a036483

E. Pitsili et al.

signaling based on recent advances in the molecular interactions between plant and pathogens, plus we discuss autoimmunity as a trigger of HR cell death in the context of certain mutations or during hybrid necrosis.

IMMUNE HR CELL DEATH AS A CONSEQUENCE OF PATHOGEN RECOGNITION

The plant immune system is constantly evolving to detect invasive microbes or their effects on the plant. Initially, plasma membrane pattern-recognition receptors (PRRs) were thought to recognize conserved microbe-associated molecular patterns, whereas cytoplasmic NLRs (nucleotide-binding domain leucine-rich repeat (LRR)-containing gene family) sensed pathogenic virulence factors or their perturbations to the cell (Jones and Dangl 2006). However, as our knowledge of plant immunity has advanced, it has become evident that PRRs also respond to virulence effectors. NLRs may also “guard” conserved molecules that act as rheostats in plant immune responses (Cook et al. 2015).

In terms of domain architecture, plant NLRs resemble animal NLRs, with a variable amino-terminal domain, a central nucleotide-binding domain, and a highly polymorphic carboxy-terminal leucine-rich domain (Fig. 1). Plant NLRs are classified according to their amino-terminal domains as Toll/interleukin-1 receptor (TIR) domain NLRs (also known as TNLs) or coiled-coil (CC) domain NLRs (or CNLs) (Cui et al. 2014; Zhang et al. 2017). NLRs recognize effector molecules deployed by pathogens, either directly or indirectly, and then initiate signaling cascades that culminate in the expression of genes mediating host defense (Cui et al. 2014). An emerging model in plant immunity is that NLRs work in functionally specialized pairs or even more complex networks, with sensor NLRs perceiving pathogen effectors and helper NLRs initiating downstream signaling (Bonardi et al. 2012; Wu et al. 2017).

Recognition of adapted biotrophic or hemibiotrophic pathogens by the plant immune system often leads to HR cell death. Thus, HR cell death is frequently described as an immune

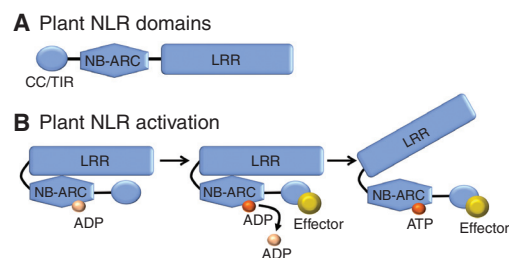


Figure 1. Plant NLRs (nucleotide-binding domain leucine-rich repeat (LRR)-containing gene family). (A) Schematic representation of a plant NLR protein. The amino-terminal region usually contains a Toll/interleukin-1 receptor (TIR) homology or a coiled-coil (CC) domain. The central region is composed of a nucleotide-binding APAF-1, R proteins, and CED-4 (NB-ARC) domain. The carboxy-terminal region contains an LRR domain. (B) NLR activation. In the inactive, closed state, ADP is bound to the NB-ARC domain. Direct or indirect effector recognition, results in ADP release and ATP binding. This results in a conformational change that renders an open, active NLR.

strategy to block pathogen colonization. However, this is not always the case, because there are numerous examples of HR cell death and inhibition of pathogen growth being genetically uncoupled (Yu et al. 1998; Greenberg et al. 2000; Balagué et al. 2003; Jurkowski et al. 2004; Coll et al. 2010; Sheikh et al. 2014; Menna et al. 2015; Lapin et al. 2019). As shown in Figure 2, HR cell death at the site of infection is crucial to initiate systemic signals that activate immunity in distal parts of the plant and eventually lead to resistance. This phenomenon is known as systemic acquired resistance (SAR) (Fu and Dong 2013; Shine et al. 2019).

Although we are far from an integrated view of HR signaling, research in the last 30 years has substantially increased our understanding of the molecular mechanisms controlling HR. Downstream from NLR activation, HR involves a series of events that include calcium influxes, oxidative bursts originating in different cellular compartments, hormone signaling, mitogen-activated protein kinases, and transcriptional reprogramming (Adachi and Tsuda 2019). Most of these elements are shared between PRR and NLR signaling, and HR cell death has often been

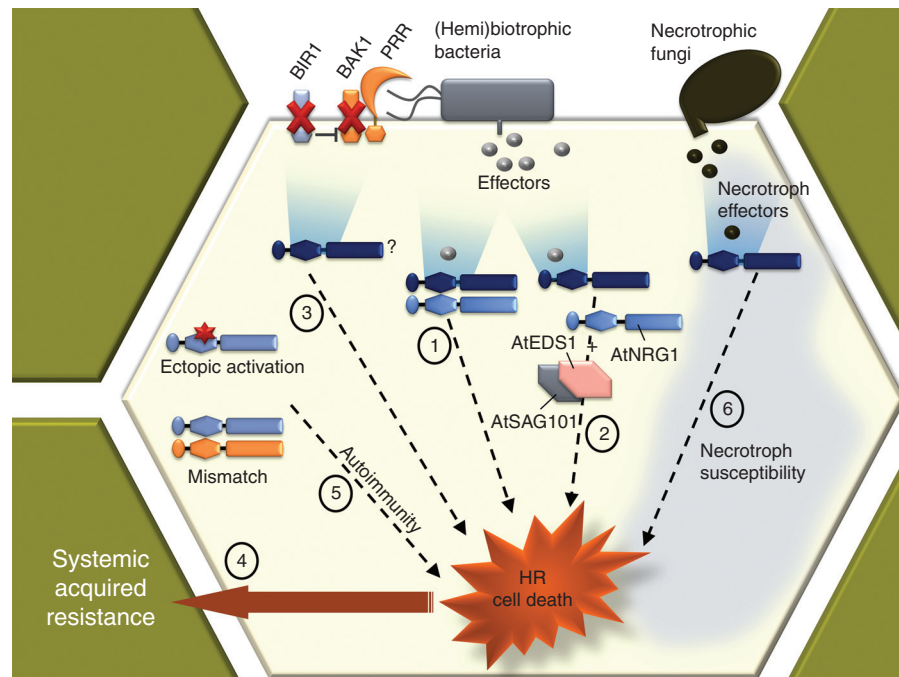


Figure 2. Pathways leading to hypersensitive response (HR) cell death in plant immunity. (1) HR can be triggered on recognition of a biotrophic or hemibiotrophic pathogen via direct or indirect effector recognition by NLR (nucleotide-binding domain leucine-rich repeat-containing gene family) immune receptors, often operating in pairs (sensor NLR + helper NLR). (2) Cell death-specific modules have been identified, which translate the signal generated by effector perception via Toll/interleukin-1 receptor domain NLR (TIR-NLR) activation, into HR cell death. (3) Pattern-recognition receptors (PRRs) signaling at the plasma membrane may be monitored by NLRs, with PRR signaling disturbance leading to HR cell death. (4) HR cell death can be genetically uncoupled from local defense responses, but may have a role in activating systemic resistance responses. (5) HR can occur as a result of autoimmune reactions, owing to the ectopic activation of NLRs or other defense signaling modulators or an NLR mismatch. (6) Necrotrophic fungi can cause disease by hijacking the host HR cell death. A common strategy is activation of NLR receptors by toxins secreted by the fungi into the plant cytoplasm.

regarded as a consequence of surpassing certain signaling thresholds, rather than as a highly regulated phenomenon. However, this view is challenged by recent findings that shed light on HR-specific signaling.

Cell Death Signaling Hubs and the Resistosome

Recent work indicates the importance of signaling hubs downstream from NLR activation, which may partition cell death and immune responses (Wu et al. 2016, 2017; Qi et al. 2018; Castel et al. 2019; Lapin et al. 2019). The lipase-like protein ENHANCED DISEASE

SUSCEPTIBILITY1 (AtEDS1) mediates all resistance outputs downstream from activated TNLs (Wiermer et al. 2005). As shown in Figure 2, AtEDS1 interacts with SENESCENCE-ASSOCIATED GENE101 (AtSAG101), and this heterodimer functions together with the helper CNL family member N Requirement Gene 1 (AtNRG1) to form a cell death signaling module in *Arabidopsis thaliana* that can be transferred to unrelated plant species. In parallel, transcriptional reprogramming to enhance the basal defense response is mediated by the interaction of EDS1 with PHYTOALEXIN-DEFICIENT 4 (AtPAD4) and a different helper CNL, ACCELERATED DISEASE RESISTANCE 1 (AtADR1) (Lapin et

E. Pitsili et al.

al. 2019). Helper NLRs have a high degree of redundancy in plant genomes, which may allow functional diversification and expansion of their corresponding sensor NLRs. For example, functionally redundant members of the helper NLR family NRC (NLR required for cell death) may contribute to immunity against different types of pathogens via their interactions with particular sensor NLRs (Wu et al. 2017). Studying interactions and outputs between the components of all these signaling modules is complex because they vary between plant species and according to the pathogen under study. In fact, we still do not know how the signals emanating from these modules execute cell death.

Clues were provided earlier this year by the reconstitution of an NLR supramolecular struc-

ture termed the resistosome (Wang et al. 2019a, b). The resistosome has been hypothesized to directly induce HR by forming pores in the plasma membrane, an exciting idea that awaits testing. This immune complex, with stunning structural and mechanistic similarities to mammalian inflammasomes, is composed of the NLR HOPZ-ACTIVATED RESISTANCE 1 (ZAR1) and two receptor-like cytoplasmic kinases (RLCKs) (Fig. 3). In its resting state, ZAR1 is bound to ADP and the RLCK RESISTANCE-RELATED KINASE 1 (RKS1). RKS1 (RLCK XII) is a pseudokinase that interacts with the LRR domain of ZAR1 (Roux et al. 2014). The bacterial pathogen *Xanthomonas campestris* uses a type III secretion system to deliver the bacterial effector AvrAC into the

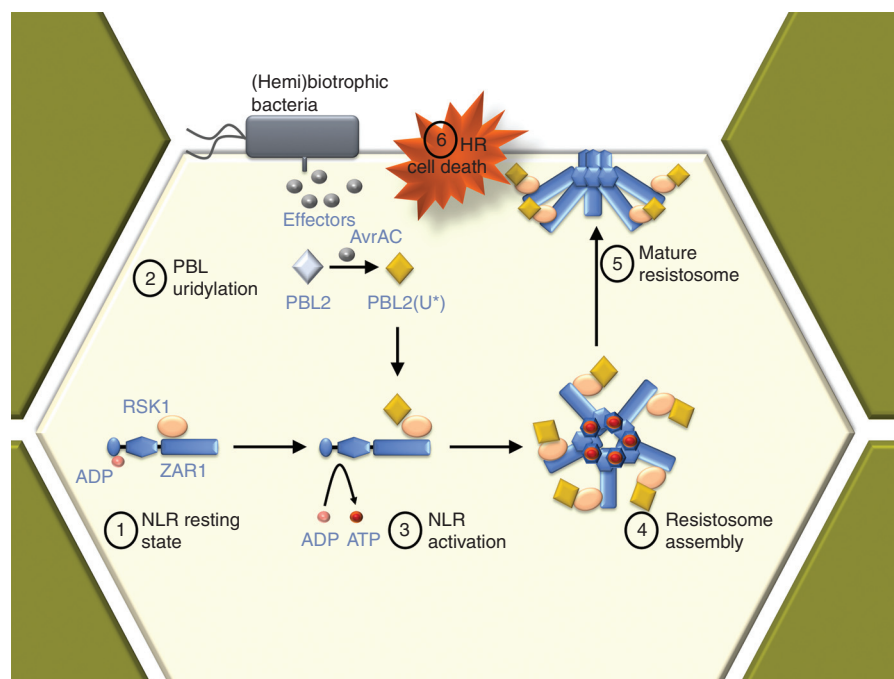


Figure 3. Mechanism of resistosome activation. (1) In its resting state, the NLR HOPZ-ACTIVATED RESISTANCE 1 (ZAR1) is bound to ADP and the RLCK RESISTANCE-RELATED KINASE 1 (RKS1). (2) *Xanthomonas campestris* secretes the effector AvrAC into the host plant cells, which uridylylates the RLCK PBS1-LIKE PROTEIN 2 (PBL2). (3) Uridylylated PBL2 binds to RKS1, causing conformational changes to the ZAR1-RKS1 dimer that release ADP and prime the complex for activation. (4) Subsequent ATP binding results in formation of the resistosome via pentamerization of the ZAR1-RKS1-PBL2 complex. (5) Conformational changes expose a funnel-like structure essential for accumulation of the complex in the plasma membrane, bacterial resistance, and (6) cell death, which has been hypothesized to be mediated by pore formation at the plasma membrane on insertion of the resistosome.



plant cytoplasm, where it uridylylates a decoy RLCK, PBS1-LIKE PROTEIN 2 (PBL2) (Wang et al. 2015a). Unlike RKS1, PBL2 is an active kinase, but its catalytic activity appears dispensable for immune defense. Instead, modified PBL2 (RLCK VII) binds to RKS1 in the ZAR1-RKS1 dimer, causing conformational changes that release ADP and prime the complex for activation. Subsequent ATP binding drives formation of the resistosome via pentamerization of the ZAR1-RKS1-PBL2 complex. Intriguingly, formation of the resistosome exposes a funnel-like structure that is essential both for resistance to bacteria and for accumulation of the complex in the plasma membrane (Fig. 3). This “death-fold switch” may act in an analogous manner to the membrane pores and ion channels formed by mixed lineage kinase domain-like (MLKL) or gasdermins in mammals, or during NLR activation in fungi, potentially suggesting a common evolutionary origin of NLRs from plants and animals (Adachi et al. 2019).

Rather than being the direct cause of cell death, these potential pores could mediate specific ion influxes that activate HR-specific downstream signaling, such as activation of cell death executioner proteases (Dangl and Jones 2019; Feng and Tang 2019). For example, the metacaspase AtMC4 is rapidly activated by calcium that enters the cell on loss of membrane integrity (Huang et al. 2018; Hander et al. 2019). Activation of AtMC4 results in cleavage of the precursor protein PROPEP1, which releases the danger peptide Pep1 to trigger wound-induced defense signaling. This program shares many components with pathogen-induced defense responses. Whether AtMC4 or other proteases are activated by resistosome pores will certainly be worth analyzing in the coming years.

PRR Perturbation as an HR Trigger

Plasma membrane signaling may have a very important role in HR signaling. When PRRs in the plasma membrane sense certain microbial molecular patterns, they team up with coreceptors in specific nanodomains that initiate signaling cascades (Bücherl et al. 2017). For example, knocking out or overexpressing *AtBAK1* (*BRAS-*

SINOSTEROID INSENSITIVE1-ASSOCIATED RECEPTOR KINASE1), a coreceptor of several different PRRs, leads to a potent HR cell death response and enhanced resistance to hemibiotrophic pathogens (Kemmerling et al. 2007; Domínguez-Ferreras et al. 2015). The fact that overexpression or elimination of a required element for PRR signaling leads to the same HR phenotype may indicate that perturbation or damage to components of PRR signaling is also monitored (Tang and Zhou 2016). This strategy would allow plant cells to defend against pathogen-mediated inhibition of PRR pathways. Accordingly, inactivation of another PRR regulator, the plasma membrane receptor-like kinase AtBIR1, also results in HR cell death (Liu et al. 2016a).

Proteolytic Pathways Associated with HR

Signaling downstream from NLRs may impact finely tuned proteolytic pathways, including (selective?) autophagy and the concerted action of several proteases (Hofius et al. 2017; Salguero-Linares and Coll 2019). Various proteases in the cytoplasm (metacaspases, phytaspase, or the proteasome subunit PBA1), in the vacuole (vacuolar processing enzyme [VPE]), and those secreted to the extracellular space (cathepsin B, saspase, Rcr3, Pip1) have been shown to be essential for HR cell death (Salguero-Linares and Coll 2019). In fact, they need to be tightly controlled to limit cell death beyond the HR site. Hence, the multiple levels of negative regulation exerted on, for example, the HR cell death protease METACASPASE1 (AtMC1) by the protease inhibitor SERPIN1, the scaffold protein LESION SIMULATING DISEASE 1 (AtLSD1), and the metacaspase AtMC2 (Coll et al. 2010; Lema Asqui et al. 2018). Moreover, AtMC1 has been shown to act additively to autophagy in controlling HR cell death (Coll et al. 2014). Although it is clear that autophagy promotes HR cell death, the mechanism and precise function (trigger or executioner?) remain unknown (Hofius et al. 2009; Coll et al. 2014; Munch et al. 2014). Intriguingly, to date, no canonical proteolytic cascade has ever been characterized in plants (Paulus and Van der Hoorn 2019). The

E. Pitsili et al.

coming years will hopefully provide a deeper insight into this HR-related proteolysis as the study of plant autophagy in plant–pathogen interactions has witnessed a tremendous expansion in the last few years (Avin-Wittenberg et al. 2018) and plant proteostasis is becoming a fully-fledged field of study.

Local versus Peripheral Regulation of HR

It will be important to pay closer attention to the spatiotemporal magnitude of HR in the coming years. This aspect has often been disregarded, with many studies of infected tissue not discriminating between HR versus non-HR cells. There are several examples of differential or antagonistic signaling between the cells undergoing HR and those in the surrounding area. This is true for the metacaspases AtMC1 and AtMC2, which antagonistically regulate HR cell death, and are expressed at the site of HR (AtMC1) or in the cells surrounding the HR zone (AtMC2) (Coll et al. 2010). The transcription factor AtMYB30, which mediates HR cell death and immune responses, has also been shown to be differentially regulated within HR and non-HR zones (Raffaele and Rivas 2013). Finally, signaling pathways downstream from the defense hormones salicylic acid and jasmonic acid are activated in spatially different domains during HR, with salicylic acid in the cell death zone and jasmonic acid in the surrounding area (Betsuyaku et al. 2018). Thus, it will be extremely important to define spatiotemporal markers of HR cell death, so that in the future we can time and characterize the events leading to HR cell death. These markers will help discriminate cells undergoing HR cell death from the surrounding tissue, which needs to activate protective mechanisms to survive, while integrating and transmitting danger/immune signals from dying cells to protect the organism against invasion.

MANIPULATION OF IMMUNE HR CELL DEATH BY NECROTROPHS AS A VIRULENCE STRATEGY

Necrotrophic pathogens have been regarded as generalists, but it is now evident that their inter-

action with the plant host is complex and highly regulated. Necrotrophs secrete toxins that kill plant cells and leave remnants from which the pathogen can feed. These pathogens have evolved very sophisticated strategies to trigger cell death. The most common strategy seems to be hijacking HR cell death pathways by subverting components of the plant immune system.

Secreted toxins, also known as necrotroph effectors (NEs), are recognized by the so-called NE-sensitive genes and trigger HR cell death (Fig. 2). Several NE-sensitive genes possess classical nucleotide-binding and LRR domains, and they often have roles in defense against biotrophic or hemibiotrophic pathogens (Lorang et al. 2007, 2012; Faris et al. 2010). Thus, NE genes appear to be a double-edged sword, being effective at eliciting an HR response to contain biotrophic pathogens, but able to be hijacked by NEs to confer plant susceptibility. A classic example is LOV1 (LONG VEGETATIVE PHASE1), an NLR from *A. thaliana* that confers susceptibility to *Cochliobolus victoriae* (Lorang et al. 2007). This necrotrophic fungus secretes the effector victorin, which activates LOV1 and triggers a resistance-like response that culminates in HR cell death and proliferation of the pathogen (Lorang et al. 2012).

The intricate mechanisms regulating necrotroph–host interactions have also been showcased by the study of *Sclerotinia sclerotiorum*. This necrotrophic fungus triggers HR by secreting oxalic acid into plant cells (Kim et al. 2008). During the initial phases of the infection, oxalic acid reduces levels of reactive oxygen species and creates a reducing environment that favors pathogen proliferation. At the same time, host defenses are dampened and the infection progresses unnoticed. At later stages, and once the infection is well established, oxalic acid triggers an increase in reactive oxygen species that causes cell death (Williams et al. 2011). Oxalic acid has also been shown to inhibit autophagy-mediated cell death, which could provide an additional mechanism to camouflage infection and prevent activation of defense responses (Kabbage et al. 2013).

New NEs and their plant susceptibility targets are emerging from the interaction between



wheat and the necrotrophic fungus *Parastagonospora nodorum*. For example, the effector ToxA is recognized indirectly by the NLR Tsn1 from wheat, which results in HR cell death and disease (Faris et al. 2010). Another *P. nodorum* effector, Tox1, remains in the extracellular space and is proposed to have a dual role in infection. It binds to chitin in the fungal cell wall to protect it from degradation by host chitinases, while also inducing an HR-like response via its recognition by Snn1, a wall-associated receptor kinase (Liu et al. 2016b; Shi et al. 2016). Adding to the complexity, the susceptibility triggered by an NE can vary depending on the genetic backgrounds of the host and pathogen (Peters Haugrud et al. 2019). The identification of new susceptibility gene candidates in the host holds great potential for the generation of plants that are more resistant to necrotrophic fungi, which are a serious threat to agriculture. Understanding precisely how NE genes interact with their corresponding plant susceptibility genes may allow engineering of new plant protein targets that evade the effectors without compromising plant fitness and yield.

HR CELL DEATH AS A CONSEQUENCE OF AUTOIMMUNITY

HR cell death can also be observed in plants in the absence of pathogens. This autoimmunity leads to ectopic defense activation and spontaneous cell death in the form of macroscopic disease-like lesions (Chakraborty et al. 2018). Plant autoimmunity can be triggered by gain or loss-of-function of plant immune modulators (NLRs and non-NLRs), autophagy, and impaired metabolic processes. In the 1990s, lesion mimic mutants (LMMs), which are plants with spontaneous or mutagenesis-induced mutations showing HR-like cell death in the absence of pathogen, emerged as a promising tool to characterize HR cell death. Characterization of these genes, mostly in *A. thaliana* and rice, has highlighted the importance of several cellular compartments and pathways in HR signaling, including chloroplasts and light energy, sphingolipids and fatty acids, ROS and ion fluxes, autophagy, and plasma membrane signal perception (Brugge-

man et al. 2015). Forward genetic screens targeting LMM revertants have identified additional components of defense signaling pathways, which has led to the idea that LMM phenotypes can be caused by loss of a pathogen effector target that is guarded by an NLR. Subsequent activation of the NLR promotes HR cell death (Rodriguez et al. 2016; Lolle et al. 2017).

The study of autoactive NLR alleles has also been informative. For example, the *snc1-1* (Suppressor of NPR1, Constitutive 1) mutant is a constitutively active variant of the SNC1 TLR that causes autoimmunity and HR cell death (Li et al. 2001). Autoactive SNC1 has been shown to activate immune responses in the nucleus, where it represses small RNAs involved in NLR silencing (Cai et al. 2018), and it associates with a transcriptional corepressor that blocks expression of negative regulators of immunity (Zhu et al. 2010). To ensure appropriate activation of SNC1-dependent immunity, multiple repression mechanisms directed toward this protein have been shown at the transcriptional level as well as posttranscriptionally (Zhu et al. 2010; Cheng et al. 2011; Huang et al. 2014; Johnson et al. 2015, 2017; Dong et al. 2016; Gou et al. 2017; Wang et al. 2017a,b, 2019c; Cai et al. 2018; Zhang et al. 2018; Niu et al. 2019). The *Rp1-D21* gene in maize, which derives from an intergenic recombination event between two NLR genes, *Rp1-D* and *Rp1-dp2*, provides another example of NLR autoactivation resulting in HR cell death (Chintamanani et al. 2010). Intramolecular interactions drive activation of *Rp1-D21*, although HR cell death requires light and temperatures below a certain threshold (Negeri et al. 2013; Wang et al. 2015b). Recently, it was shown that two key enzymes of the lignin biosynthetic pathway form complexes with this hybrid NLR and modulate its activity (Wang and Balint-Kurti 2016).

Autoimmunity leading to ectopic HR cell death can also be a consequence of hybrid necrosis, which is a common type of incompatibility found in the progeny of many crosses within and between species (Fig. 2). In contrast to hybrid vigor, hybrid incompatibility challenges plant fitness and can result from mismatched NLRs (Chen et al. 2016; Vaid and Laitinen

E. Pitsili et al.

2019). Indeed, genes causing hybrid necrosis are often associated with plant defense responses (Alcazar et al. 2009). Allelic interactions at the ACD6 (ACCELERATED CELL DEATH 6) locus in *A. thaliana* lead to hybrid necrosis and the enhanced expression of defense genes (Świadek et al. 2017). In fact, ACD6 acts as a quantitative resistance gene that balances growth and pathogen resistance in natural populations of *A. thaliana*, and it has been shown that deleterious autoimmune ACD6 alleles are modulated by natural variants of SNC1 (Zhu et al. 2018).

The hybrid necrosis hot spots in the *A. thaliana* genome are often densely populated with NLRs. These immune receptor loci act as hypermodulated complexes that recombine between natural genetic variants and cause imbalanced NLR activity (Chae et al. 2014). The Bateson–Dobzhansky–Muller model explains pairwise heteromeric interactions between distinct unlinked NLR loci that lead to hybrid necrosis and enhanced defense (Phadnis and Malik 2014). On the one hand, the polymorphic nature (high levels of sequence divergence) of these immune loci gives an advantage during the host response to pathogen challenges, while on the other hand it positively correlates to hybrid necrosis impacting plant fitness. Different NLR pairs have been involved in the hybrid necrosis phenomena (Bombliès and Weigel 2007; Tran et al. 2017; Atanasov et al. 2018). Many questions regarding hybrid necrosis remain unanswered. How is the NLR-mediated defense response propagated without pathogen challenge? What is the role of environmental factors and genetic distance in hybrid necrosis induction? How can the deleterious fitness effects be mitigated during interspecific crossing while preserving the resistance trait? Our understanding of the mechanisms regulating HR cell death triggered by autoimmunity is still very limited. A deeper understanding of NLR activation and signal transduction will help us integrate and advance the current knowledge.

CONCLUDING REMARKS

In plant immunity, HR cell death is often used to score resistance to pathogens. However, the

mechanisms regulating this complex phenomenon are far from understood. The intricate interplay between sensor and helper immune receptors is starting to emerge, and will help shed light on how cell death is triggered and executed on pathogen perception. Cell death-specific modules are being unveiled as integrators of signals emanating from activation of diverse sensor NLRs. HR cell death is an important part of the immune response to protect distal parts of the plant against future invasions.

The plant resistosome has been described as an inflammasome-like supramolecular structure that assembles on recognition of pathogenic effectors to initiate defense responses. The activated resistosome features a funnel-like structure that is required for insertion of the complex into the plasma membrane and HR cell death. It has been speculated that this structure creates pores in the membrane, which could mediate ion fluxes that activate cell death enzymes. Perturbation of the plasma membrane or its signaling components—including PRRs—may also be monitored by NLRs that can trigger HR cell death.

In addition to immunity against biotrophic and hemibiotrophic pathogens, HR cell death can also mediate susceptibility to necrotrophic pathogens. There are several examples of necrotrophic fungi secreting toxins (also known as NEs) that directly or indirectly activate specific NLRs and cause HR cell death. These NLRs were probably selected in the course of interactions between a plant and biotrophic pathogen, and then hijacked by a necrotrophic fungus for its own benefit. This is an emerging area of research with great potential, because susceptibility genes can serve as targets for genome-editing technologies aimed at increasing resistance against fungi in commercial cultivars.

The analysis of autoimmune phenotypes in plants is also providing a better understanding of the mechanisms regulating HR cell death. Autoactive or mismatched NLR alleles confer constitutive immunity and ectopic HR-like cell death phenotypes, highlighting the importance of a multilayered and finely tuned regulation of immune modulators to avoid deleterious fitness costs for the plant. The booming field of plant

immunity will surely deepen our insight into the mechanisms regulating pathogen-triggered HR cell death, helping us understand to what extent it is programmed.

ACKNOWLEDGMENTS

We thank Mary-Paz González García, Marc Valls, and Jose Salguero-Linares for comments on the manuscript. We also thank Jane Parker and Hans Thordal-Christensen for inspiring discussions on the topic. We apologize to all authors whose work has been omitted because of space limitations. This work was supported by the Spanish Ministry of Economy and Competitiveness with Grant Nos. RyC 2014-16158 and AGL2016-78002-R and through the Severo Ochoa Programme for Centres of Excellence in R&D (SEV-2015-0533). We also acknowledge financial support from the CERCA Programme/Generalitat de Catalunya.

REFERENCES

- Adachi H, Tsuda K. 2019. Convergence of cell-surface and intracellular immune receptor signalling. *New Phytol* **221**: 1676–1678. doi:10.1111/nph.15634
- Adachi H, Kamoun S, Maqbool A. 2019. A resistosome-activated “death switch.” *Nat Plants* **5**: 457–458. doi:10.1038/s41477-019-0425-9
- Alcazar R, Garcia AV, Parker JE, Reymond M. 2009. Incremental steps toward incompatibility revealed by *Arabidopsis* epistatic interactions modulating salicylic acid pathway activation. *Proc Natl Acad Sci* **106**: 334–339. doi:10.1073/pnas.0811734106
- Atanasov KE, Liu C, Erban A, Kopka J, Parker JE, Alcázar R. 2018. NLR mutations suppressing immune hybrid incompatibility and their effects on disease resistance. *Plant Physiol* **177**: 1152–1169. doi:10.1104/pp.18.00462
- Avin-Wittenberg T, Baluška F, Bozhkov P V, Elander PH, Fernie AR, Galili G, Hassan A, Hofius D, Isono E, Le Bars R, et al. 2018. Autophagy-related approaches for improving nutrient use efficiency and crop yield protection. *J Exp Bot* **69**: 1335–1353. doi:10.1093/jxb/ery069
- Balagué C, Lin B, Alcon C, Flottes G, Malmström S, Köhler C, Neuhaus G, Pelletier G, Gaymard F, Roby D. 2003. HLM1, an essential signaling component in the hypersensitive response, is a member of the cyclic nucleotide-gated channel ion channel family. *Plant Cell* **15**: 365–379.
- Betsuyaku S, Katou S, Takebayashi Y, Sakakibara H, Nomura N, Fukuda H. 2018. Salicylic acid and jasmonic acid pathways are activated in spatially different domains around the infection site during effector-triggered immunity in *Arabidopsis thaliana*. *Plant Cell Physiol* **59**: 439. doi:10.1093/pcp/pcy008
- Bomblies K, Weigel D. 2007. Hybrid necrosis: autoimmunity as a potential gene-flow barrier in plant species. *Nat Rev Genet* **8**: 382–393. doi:10.1038/nrg2082
- Bonardi V, Cherkis K, Nishimura MT, Dangl JL. 2012. A new eye on NLR proteins: focused on clarity or diffused by complexity? *Curr Opin Immunol* **24**: 41–50. doi:10.1016/j.coi.2011.12.006
- Bruggeman Q, Raynaud C, Benhamed M, Delarue M. 2015. To die or not to die? Lessons from lesion mimic mutants. *Front Plant Sci* **6**: 24. doi:10.3389/fpls.2015.00024
- Bücherl CA, Jarsch IK, Schudoma C, Segonzac C, Mbengue M, Robatzke S, MacLean D, Ott T, Zipfe C. 2017. Plant immune and growth receptors share common signalling components but localise to distinct plasma membrane nanodomains. *eLife* **6**: e25114. doi:10.7554/eLife.25114
- Cai Q, Liang C, Wang S, Hou Y, Gao L, Liu L, He W, Ma W, Mo B, Chen X. 2018. The disease resistance protein SNC1 represses the biogenesis of microRNAs and phased siRNAs. *Nat Commun* **9**: 5080. doi:10.1038/s41467-018-07516-z
- Castel B, Ngou PM, Cevik V, Redkar A, Kim DS, Yang Y, Ding P, Jones JDG. 2019. Diverse NLR immune receptors activate defence via the RPW8-NLR NRG1. *New Phytol* **222**: 966–980. doi:10.1111/nph.15659
- Chae E, Bomblies K, Kim ST, Karelina D, Zaidem M, Ossowski S, Martín-Pizarro C, Laitinen RAE, Rowan BA, Tenenboim H, et al. 2014. Species-wide genetic incompatibility analysis identifies immune genes as hot spots of deleterious epistasis. *Cell* **159**: 1341–1351. doi:10.1016/j.cell.2014.10.049
- Chakraborty J, Ghosh P, Das S. 2018. Autoimmunity in plants. *Planta* **248**: 751–767. doi:10.1007/s00425-018-2956-0
- Chen C EZ, Lin HX. 2016. Evolution and molecular control of hybrid incompatibility in plants. *Front Plant Sci* **7**: 1–10.
- Cheng YT, Li Y, Huang S, Huang Y, Dong X, Zhang Y, Li X. 2011. Stability of plant immune-receptor resistance proteins is controlled by SKP1-CULLIN1-F-box (SCF)-mediated protein degradation. *Proc Natl Acad Sci* **108**: 14694–14699. doi:10.1073/pnas.1105685108
- Chintamanani S, Hulbert SH, Johal GS, Balint-Kurti PJ. 2010. Identification of a maize locus that modulates the hypersensitive defense response, using mutant-assisted gene identification and characterization. *Genetics* **184**: 813–825. doi:10.1534/genetics.109.111880
- Coll NS, Vercammen D, Smidler A, Clover C, Van Breusegem F, Dangl JL, Epple P. 2010. *Arabidopsis* type I metacaspases control cell death. *Science* **330**: 1393–1397. doi:10.1126/science.1194980
- Coll NS, Smidler A, Puigvert M, Popa C, Valls M, Dangl JL. 2014. The plant metacaspase AtMC1 in pathogen-triggered programmed cell death and aging: functional linkage with autophagy. *Cell Death Differ* **21**: 1399–1408. doi:10.1038/cdd.2014.50
- Cook DE, Mesarich CH, Thomma BPHJ. 2015. Understanding plant immunity as a surveillance system to detect invasion. *Annu Rev Phytopathol* **53**: 541–563. doi:10.1146/annurev-phyto-080614-120114
- Cui H, Tsuda K, Parker JE. 2014. Effector-triggered immunity: from pathogen perception to robust defense. *Annu*

E. Pitsili et al.

- Rev Plant Biol* **66**: 487–511. doi:10.1146/annurev-arplant-050213-040012
- Dangl JL, Jones JDG. 2019. A pentangular plant inflammatory. *Science* **364**: 31–32. doi:10.1126/science.aax0174
- Dickman M, Williams B, Li Y, Figueiredo P, Wolpert T. 2017. Reassessing apoptosis in plants. *Nat Plants* **3**: 773–779. doi:10.1038/s41477-017-0020-x
- Domínguez-ferreras A, Kiss-papp M, Jehle AK, Felix G, Chinchilla D. 2015. An overdose of the *Arabidopsis* coreceptor BRASSINOSTEROID INSENSITIVE1-ASSOCIATED RECEPTOR KINASE1 or its ectodomain causes autoimmunity in a SUPPRESSOR OF BIR1-1-dependent manner. *Plant Physiol* **168**: 1106–1121.
- Dong OX, Meteignier LV, Plourde MB, Ahmed B, Wang M, Jensen C, Jin H, Moffett P, Li X, Germain H. 2016. *Arabidopsis* TAF15b localizes to RNA processing bodies and contributes to *snc1*-mediated autoimmunity. *Mol Plant Microbe Interact* **29**: 247–257. doi:10.1094/MPMI-11-15-0246-R
- Faris JD, Zhang Z, Lu H, Lu S, Reddy L, Cloutier S, Fellers JP, Meinhardt SW, Rasmussen JB, Xu SS, et al. 2010. A unique wheat disease resistance-like gene governs effector-triggered susceptibility to necrotrophic pathogens. *Proc Natl Acad Sci* **107**: 13544–13549. doi:10.1073/pnas.1004090107
- Feng B, Tang D. 2019. Mechanism of plant immune activation and signaling: insight from the first solved plant resistosome structure. *J Integr Plant Biol* **61**: 902–907. doi:10.1111/jipb.12814
- Fu ZQ, Dong X. 2013. Systemic acquired resistance: turning local infection into global defense. *Annu Rev Plant Biol* **64**: 839–863. doi:10.1146/annurev-arplant-042811-105606
- Galluzzi L, Vitale I, Aaronson SA, Abrams JM, Adam D, Agostinis P, Alnemri ES, Altucci L, Amelio I, Andrews DW, et al. 2018. Molecular mechanisms of cell death: recommendations of the nomenclature committee on cell death 2018. *Cell Death Differ* **25**: 486–541. doi:10.1038/s41418-017-0012-4
- Gou M, Huang Q, Qian W, Zhang Z, Jia Z, Hua J. 2017. Sumoylation E3 ligase SIZ1 modulates plant immunity partly through the immune receptor gene *SNC1* in *Arabidopsis*. *Mol Plant Microbe Interact* **30**: 334–342. doi:10.1094/MPMI-02-17-0041-R
- Greenberg JT, Silverman FP, Liang H. 2000. Uncoupling salicylic acid-dependent cell death and defense-related responses from disease resistance in the *Arabidopsis* mutant *acd5*. *Genetics* **156**: 341–350.
- Hander T, Fernández-fernández AD, Kumpf RP, Willems P, Schatowitz H, Rombaut D, Staes A, Nolf J, Pottier R, Yao P, et al. 2019. Damage on plants activates Ca²⁺-dependent metacaspases for release of immunomodulatory peptides. *Science* **363**: eaar7486. doi:10.1126/science.aar7486
- Hofius D, Schultz-Larsen T, Joensen J, Tsitsigiannis DI, Petersen NHT, Mattsson O, Jørgensen LB, Jones JDG, Mundy J, Petersen M. 2009. Autophagic components contribute to hypersensitive cell death in *Arabidopsis*. *Cell* **137**: 773–783. doi:10.1016/j.cell.2009.02.036
- Hofius D, Li L, Hafrén A, Coll NS. 2017. Autophagy as an emerging arena for plant–pathogen interactions. *Curr Opin Plant Biol* **38**: 117–123. doi:10.1016/j.pbi.2017.04.017
- Huang Y, Minaker S, Roth C, Huang S, Hieter P, Lipka V, Wiermer M, Li X. 2014. An E4 ligase facilitates polyubiquitination of plant immune receptor resistance proteins in *Arabidopsis*. *Plant Cell* **26**: 485–496. doi:10.1105/tpc.113.119057
- Huang Y, Cui Y, Hou X, Huang T. 2018. The AtMC4 regulates the stem cell homeostasis in *Arabidopsis* by catalyzing the cleavage of AtLal1 protein in response to environmental hazards. *Plant Sci* **266**: 64–75. doi:10.1016/j.plantsci.2017.10.008
- Johnson KCM, Xia S, Feng X, Li X. 2015. The chromatin remodeler SPLAYED negatively regulates SNC1-mediated immunity. *Plant Cell Physiol* **56**: 1616–1623. doi:10.1093/pcp/pcv087
- Johnson KCM, Zhao J, Wu Z, Roth C, Lipka V, Wiermer M, Li X. 2017. The putative kinase substrate MUSE7 negatively impacts the accumulation of NLR proteins. *Plant J* **89**: 1174–1183. doi:10.1111/tpj.13454
- Jones JDG, Dangl JL. 2006. The plant immune system. *Nature* **444**: 323–329. doi:10.1038/nature05286
- Jurkowski GI, Smith RK, Yu I, Ham JH, Sharma SB, Klessig DF, Fengler KA, Bent AF. 2004. *Arabidopsis* DND2, a second cyclic nucleotide-gated ion channel gene for which mutation causes the “defense, no death” phenotype. *Mol Plant Microbe Interact* **17**: 511–520. doi:10.1094/MPMI.2004.17.5.511
- Kabbage M, Williams B, Dickman MB. 2013. Cell death control: the interplay of apoptosis and autophagy in the pathogenicity of *Sclerotinia sclerotiorum*. *PLoS Pathog* **9**: e1003287. doi:10.1371/journal.ppat.1003287
- Kemmerling B, Schwedt A, Rodriguez P, Mazzotta S, Frank M, Qamar SA, Mengiste T, Betsuyaku S, Parker JE, Müssig C, et al. 2007. The BRI1-associated kinase 1, BAK1, has a brassinolide-independent role in plant cell-death control. *Curr Biol* **17**: 1116–1122. doi:10.1016/j.cub.2007.05.046
- Kim KS, Min JY, Dickman MB. 2008. Oxalic acid is an elicitor of plant programmed cell death during *Sclerotinia sclerotiorum* disease development. *Mol Plant Microbe Interact* **21**: 605–612. doi:10.1094/MPMI-21-5-0605
- Lapin D, Kovacova V, Sun X, Dongus JA, Bhandari DD, von Born P, Bautor J, Guarneri N, Rzemieniewski J, Stuttmann J, et al. 2019. A coevolved EDS1-SAG101-NRG1 module mediates cell death signaling by TIR-domain immune receptors. *Plant Cell*. doi:10.1105/tpc.19.00118
- Lema Asqui S, Vercaemmen D, Serrano I, Valls M, Rivas S, Van Breusegem F, Conlon FL, Dangl JL, Coll NS. 2018. AtSERPIN1 is an inhibitor of the metacaspase AtMC1-mediated cell death and autocatalytic processing in *planta*. *New Phytol* **218**: 1156–1166. doi:10.1111/nph.14446
- Li X, Clarke JD, Zhang Y, Dong X. 2001. Activation of an EDS1-mediated R-gene pathway in the *snc1* mutant leads to constitutive, NPR1-independent pathogen resistance. *Mol Plant Microbe Interact* **14**: 1131–1139. doi:10.1094/MPMI.2001.14.10.1131
- Liu Y, Huang X, Li M, He P, Zhang Y. 2016a. Loss-of-function of *Arabidopsis* receptor-like kinase BIR1 activates cell death and defense responses mediated by BAK1 and SOBIR1. *New Phytol* **212**: 637–645. doi:10.1111/nph.14072
- Liu Z, Gao Y, Kim YM, Faris JD, Shelver WL, de Wit PJGM, Xu SS, Friesen TL. 2016b. SnTox1, a *Parastagonospora nodorum* necrotrophic effector, is a dual-function protein



- that facilitates infection while protecting from wheat-produced chitinases. *New Phytol* **211**: 1052–1064. doi:10.1111/nph.13959
- Lolle S, Greeff C, Petersen K, Roux M, Jensen MK, Bressendorff S, Rodriguez E, Sømark K, Mundy J, Petersen M. 2017. Matching NLR immune receptors to autoimmunity in *camta3* mutants using antimorphic NLR alleles. *Cell Host Microbe* **21**: 518–529.e4. doi:10.1016/j.chom.2017.03.005
- Lorang JM, Sweat TA, Wolpert TJ. 2007. Plant disease susceptibility conferred by a “resistance” gene. *Proc Natl Acad Sci* **104**: 14861–14866. doi:10.1073/pnas.0702572104
- Lorang J, Kidarsa T, Bradford CS, Gilbert B, Curtis M, Tzeng SC, Maier CS, Wolpert TJ. 2012. Tricking the guard: exploiting plant defense for disease susceptibility. *Science* **338**: 659–662. doi:10.1126/science.1226743
- Menna A, Nguyen D, Guttman DS, Desveaux D. 2015. Elevated temperature differentially influences effector-triggered immunity outputs in *Arabidopsis*. *Front Plant Sci* **6**: 1–7. doi:10.3389/fpls.2015.00995
- Munch D, Rodriguez E, Bressendorff S, Park OK, Hofius D, Petersen M. 2014. Autophagy deficiency leads to accumulation of ubiquitinated proteins, ER stress, and cell death in *Arabidopsis*. *Autophagy* **10**: 1579–1587. doi:10.4161/aut.29406
- Negeri A, Wang GF, Benavente L, Kibiti CM, Chaikam V, Johal G, Balint-Kurti P. 2013. Characterization of temperature and light effects on the defense response phenotypes associated with the maize *Rp1-D21* autoactive resistance gene. *BMC Plant Biol* **13**: 106. doi:10.1186/1471-2229-13-106
- Niu D, Lin XL, Kong X, Qu GP, Cai B, Lee J, Jin JB. 2019. SIZ1-mediated SUMOylation of TPR1 suppresses plant immunity in *Arabidopsis*. *Mol Plant* **12**: 215–228. doi:10.1016/j.molp.2018.12.002
- Paulus JK, Van der Hoorn RAL. 2019. Do proteolytic cascades exist in plants? *J Exp Bot* **70**: 1997–2002. doi:10.1093/jxb/erz016
- Peters Haugrud AR, Zhang Z, Richards JK, Friesen TL, Faris JD. 2019. Genetics of variable disease expression conferred by inverse gene-for-gene interactions in the wheat–*Parastagonospora nodorum* pathosystem. *Plant Physiol* **180**: 420–434. doi:10.1104/pp.19.00149
- Phadnis N, Malik HS. 2014. Speciation via autoimmunity: a dangerous mix. *Cell* **159**: 1247–1249. doi:10.1016/j.cell.2014.11.028
- Qi T, Seong K, Thomazella DPT, Kim JR, Pham J, Seo E, Cho MJ, Schultink A, Staskawicz BJ. 2018. NRG1 functions downstream of EDS1 to regulate TIR-NLR-mediated plant immunity in *Nicotiana benthamiana*. *Proc Natl Acad Sci* **115**: E10979–E10987. doi:10.1073/pnas.1814856115
- Raffaele S, Rivas S. 2013. Regulate and be regulated: integration of defense and other signals by the AtMYB30 transcription factor. *Front Plant Sci* **4**: 98. doi:10.3389/fpls.2013.00098
- Rodriguez E, El Ghoul H, Mundy J, Petersen M. 2016. Making sense of plant autoimmunity and “negative regulators.” *FEBS J* **283**: 1385–1391. doi:10.1111/febs.13613
- Roux F, Noël L, Rivas S, Roby D. 2014. ZRK atypical kinases: emerging signaling components of plant immunity. *New Phytol* **203**: 713–716. doi:10.1111/nph.12841
- Salguero-Linares J, Coll NS. 2019. Plant proteases in the control of the hypersensitive response. *J Exp Bot* **70**: 2087–2095. doi:10.1093/jxb/erz030
- Sheikh AH, Raghuram B, Eschen-Lippold L, Scheel D, Lee J, Sinha AK. 2014. Agroinfiltration by cytokinin-producing *Agrobacterium* sp. strain GV3101 primes defense responses in *Nicotiana tabacum*. *Mol Plant Microbe Interact* **27**: 1175–1185. doi:10.1094/MPMI-04-14-0114-R
- Shi G, Zhang Z, Friesen TL, Raats D, Fahima T, Brueggeman RS, Lu S, Trick HN, Liu Z, Chao W, et al. 2016. The hijacking of a receptor kinase-driven pathway by a wheat fungal pathogen leads to disease. *Sci Adv* **2**: e1600822. doi:10.1126/sciadv.1600822
- Shine MB, Xiao X, Kachroo P, Kachroo A. 2019. Signaling mechanisms underlying systemic acquired resistance to microbial pathogens. *Plant Sci* **279**: 81–86. doi:10.1016/j.plantsci.2018.01.001
- Stakman EC. 1915. Relation between *Puccinia graminis* and plants highly resistant to its attack. *J Agric Res* **4**: 193–199.
- Świadek M, Proost S, Sieh D, Yu J, Todesco M, Jorzig C, Rodriguez Cubillos AE, Plötner B, Nikoloski Z, Chae E, et al. 2017. Novel allelic variants in *ACD6* cause hybrid necrosis in local collection of *Arabidopsis thaliana*. *New Phytol* **213**: 900–915. doi:10.1111/nph.14155
- Tang D, Zhou JM. 2016. PEPs spice up plant immunity. *EMBO J* **35**: 4–5. doi:10.15252/emboj.201593434
- Tran DTN, Chung EH, Habring-Müller A, Demar M, Schwab R, Dangl JL, Weigel D, Chae E. 2017. Activation of a plant NLR complex through heteromeric association with an autoimmune risk variant of another NLR. *Curr Biol* **27**: 1148–1160. doi:10.1016/j.cub.2017.03.018
- Vaid N, Laitinen RAE. 2019. Diverse paths to hybrid incompatibility in *Arabidopsis*. *Plant J* **97**: 199–213. doi:10.1111/tpj.14061
- Vanden BT, Linkermann A, Jouan-Lanhouet S, Walczak H, Vandenabeele P. 2014. Regulated necrosis: the expanding network of non-apoptotic cell death pathways. *Nat Rev Mol Cell Biol* **15**: 135–147.
- Wang GF, Balint-Kurti PJ. 2016. Maize homologs of CCoAOMT and HCT, two key enzymes in lignin biosynthesis, form complexes with the NLR Rp1 protein to modulate the defense response. *Plant Physiol* **171**: 2166–2177. doi:10.1104/pp.16.00224
- Wang G, Roux B, Feng F, Guy E, Li L, Li N, Zhang X, Lautier M, Jardinaud MF, Chabannes M, et al. 2015a. The decoy substrate of a pathogen effector and a pseudokinase specify pathogen-induced modified-self recognition and immunity in plants. *Cell Host Microbe* **18**: 285–295. doi:10.1016/j.chom.2015.08.004
- Wang GF, Ji J, El-Kasmi F, Dangl JL, Johal G, Balint-Kurti PJ. 2015b. Molecular and functional analyses of a maize autoactive NB-LRR protein identify precise structural requirements for activity. *PLoS Pathog* **11**: e1004830. doi:10.1371/journal.ppat.1004830
- Wang S, Wang S, Sun Q, Yang L, Zhu Y, Yuan Y, Hua J. 2017a. A role of cytokinin transporter in *Arabidopsis* immunity. *Mol Plant Microbe Interact* **30**: 325–333. doi:10.1094/MPMI-01-17-0011-R

E. Pitsili et al.

- Wang Z, Cui D, Liu J, Zhao J, Liu C, Xin W, Li Y, Liu N, Ren D, Tang D, et al. 2017b. *Arabidopsis* ZED1-related kinases mediate the temperature-sensitive intersection of immune response and growth homeostasis. *New Phytol* **215**: 711–724. doi:10.1111/nph.14585
- Wang J, Hu M, Wang J, Qi J, Han Z, Wang G, Qi Y, Wang HW, Zhou JM, Chai J. 2019a. Reconstitution and structure of a plant NLR resistosome conferring immunity. *Science* **364**: eaav5870. doi:10.1126/science.aav5870
- Wang J, Wang J, Hu M, Wu S, Qi J, Wang G, Han Z, Qi Y, Gao N, Wang HW, et al. 2019b. Ligand-triggered allosteric ADP release primes a plant NLR complex. *Science* **364**: eaav5868. doi:10.1126/science.aav5868
- Wang Z, Cui D, Liu C, Zhao J, Liu J, Liu N, Tang D, Hu Y. 2019c. TCP transcription factors interact with ZED1-related kinases as components of the temperature-regulated immunity. *Plant Cell Environ* **42**: 2045–2056. doi:10.1111/pce.13515
- Wiermer M, Feys BJ, Parker JE. 2005. Plant immunity: the EDS1 regulatory node. *Curr Opin Plant Biol* **8**: 383–389. doi:10.1016/j.pbi.2005.05.010
- Williams B, Kabbage M, Kim HJ, Britt R, Dickman MB. 2011. Tipping the balance: *Sclerotinia sclerotiorum* secreted oxalic acid suppresses host defenses by manipulating the host redox environment. *PLoS Pathog* **7**: e1002107. doi:10.1371/journal.ppat.1002107
- Wu CH, Belhaj K, Bozkurt TO, Kamoun S. 2016. Helper NLR proteins NRC2a/b and NRC3 but not NRC1 are required for Pto-mediated cell death and resistance in *Nicotiana benthamiana*. *New Phytol* **209**: 1344–1352. doi:10.1111/nph.13764
- Wu CH, Abd-El-Halim A, Bozkurt TO, Belhaj K, Terauchi R, Vossen JH, Kamoun S. 2017. NLR network mediates immunity to diverse plant pathogens. *Proc Natl Acad Sci* **114**: 8113–8118. doi:10.1073/pnas.1702041114
- Yu I, Parker J, Bent AF. 1998. Gene-for-gene disease resistance without the hypersensitive response in *Arabidopsis dnd1* mutant. *Proc Natl Acad Sci* **95**: 7819–7824. doi:10.1073/pnas.95.13.7819
- Zhang X, Dodds PN, Bernoux M. 2017. What do we know about NOD-like receptors in plant immunity? *Annu Rev Phytopathol* **55**: 205–229. doi:10.1146/annurev-phyto-080516-035250
- Zhang N, Wang Z, Bao Z, Yang L, Wu D, Shu X, Hua J. 2018. MOS1 functions closely with TCP transcription factors to modulate immunity and cell cycle in *Arabidopsis*. *Plant J* **93**: 66–78. doi:10.1111/tpj.13757
- Zhu Z, Xu F, Zhang Y, Cheng YT, Wiermer M, Li X, Zhang Y. 2010. *Arabidopsis* resistance protein SNC1 activates immune responses through association with a transcriptional corepressor. *Proc Natl Acad Sci* **107**: 13960–13965. doi:10.1073/pnas.1002828107
- Zhu W, Zaidem M, Van de Weyer AL, Gutaker RM, Chae E, Kim ST, Bemm F, Li L, Todisco M, Schwab R, et al. 2018. Modulation of *ACD6* dependent hyperimmunity by natural alleles of an *Arabidopsis thaliana* NLR resistance gene. *PLoS Genet* **14**: e1007628. doi:10.1371/journal.pgen.1007628





Cold Spring Harbor Perspectives in Biology

Cell Death in Plant Immunity

Eugenia Pitsili, Ujjal J. Phukan and Nuria S. Coll

Cold Spring Harb Perspect Biol published online October 15, 2019

Subject Collection

For additional articles in this collection, see <http://cshperspectives.cshlp.org/cgi/collection/>

A green advertisement banner for Gene Link. On the left is the Gene Link logo, which consists of three interlocking cubes. The text 'Gene Link™' is below the logo. To the right of the logo, the text reads 'All Modifications and Oligo Types Synthesized' in a bold, white font. Below this, a list of services is provided: 'Long Oligos • Fluorescent • Chimeric • DNA • RNA • Antisense'. On the right side of the banner, there is a stylized image of a plant stem. Overlaid on this image is the text 'Oligo Modifications?' in a cursive font, followed by 'Your wish is our command.' in a smaller, sans-serif font.

Gene Link™

All Modifications and
Oligo Types Synthesized

Long Oligos • Fluorescent • Chimeric • DNA • RNA • Antisense

Oligo Modifications?
Your wish is our command.